UNIVERSITY *of the*
WESTERN CAPE

Structure-Based Virtual Screening of Selected Malaria Box Compounds Against a Multi-Staged Protein (Falstatin) in *Plasmodium falciparum*

By

Bolu Bimbola Oladunjoye

(STUDENT NUMBER: 3919192)

A thesis submitted in fulfillment of the requirements for the degree of Master of Pharmacy, the School of Pharmacy, University of the Western Cape.

Supervisor: Dr. Samuel Egieyeh

November 2021

Declaration

I, Bolu Bimbola Oladunjoye, declare that this written submission represents my work and that it has not been submitted before for any degree or examination at any other higher education institution. Where other's ideas or words have been included, I have adequately cited and referenced the sources. I also declare that I have adhered to all ethics of academic honesty and integrity and have not misrepresented or fabricated any idea/data/source in my submission.

…….. ……..

Signed

Dedication

I dedicate this project to my darling husband Dr Joshua Olabiyi, my daughter Ifeoluwa for their love and support throughout the programme and to the African child who is affected by malaria.

Abstract

Malaria disease poses substantial health risks to many nations, especially in Africa, where it primarily affects pregnant women, children, and immunocompromised patients. However, current antimalarial drugs have limitations such as low safety profile and particularly widespread treatment failure due to the increasing resistance of Plasmodium falciparum, the major causative organism to artemisinin-based therapy (ACT) and other chemotherapeutics. In the light of this, there is a pressing need for new antimalarial drugs with novel mechanisms of action and satisfactory pharmacokinetic properties, which has led to the current study.

Furthermore, current antimalarial drugs target specific stages of the *Plasmodium* life cycle. For instance, chloroquine targets the erythrocytic stage while primaquine targets the liver stage. However, these therapies cannot achieve complete elimination of the parasite once the life cycle has been established in the body. Hence, the goal of this study is to combat resistance by finding novel compounds that can bind to a multiple-staged protein in *Plasmodium falciparum.* Based on this consideration, falstatin was chosen as the protein target for this study because it was observed to play a crucial role in the degradation of haemoglobin, rupture of erythrocytes by mature schizonts, and subsequent invasion of erythrocytes by free merozoites. Hence, the protein, falstatin can be targeted to inhibit cell growth and cause plasmodial cell death in merozoites as well as schizonts of *Plasmodium* falciparum. Therefore, it is intended that compounds that bind to falstatin could serve as novel antimalarials that target multiple stages of the *Plasmodium* life cycle.

Consequently, this study explored the structure-based virtual screening approach to identify compounds that could bind to the protein target, falstatin in *Plasmodium falciparum.* An extensive literature review identified falstatin as the multi-staged drug target for this study, while homology modelling was used to generate the three-dimensional structure of falstatin. Molecular docking was conducted to predict the binding energy of compiled antiplasmodial compounds to falstatin while druglikeness analysis was used to prioritize compounds according to their ADMET (absorption, distribution, metabolism, excretion and toxicity) properties. The top-ranked compound, based on a novel ligand scoring function, was then subjected to molecular dynamics (MD). Following this step, rescoring analysis was performed on the top 5 compounds using the Molecular Mechanics-Generalized Born Surface Area (MM-GBSA) scoring function to gain insight into their component binding energies.

Thereafter, a pharmacophore hypothesis was developed based on the 5 top-ranking compounds in order to screen other compound libraries in the future.

From the results, TCMDC 131646, TCMDC-124274, TCMDC-138266, TCMDC 123844 and TCMDC 131234 possessed good binding energies and satisfactory ADMET properties showing high ligand scores of 77.1, 75.4, 75.4, 75.4 and 73.1 respectively (on a total scale of 100). Also, the study revealed that the top-ranked compound, TCMDC 131646 had a binding energy of -6.15 KJ/mol, contained no toxicophore and conformed to Lipinski, Egan and Muegge rules of druglikeness. Findings from the MD simulation demonstrated that TCMDC 131646 strongly interacted with the protein, falstatin. Morealso, the study revealed that TCMDC 131646 is structurally diverse from chloroquine, artemisinin, artemether and lumefantrine, indicating that it may possess a distinct mechanism of action. The rescoring analysis of TCMDC-131646, TCMDC 124274, TCMDC-138266, TCMDC 123844 and TCMDC 131234 predicted negative binding energies ≤ -4.662 KJ/mol for the top compounds, further indicating that these compounds are likely to bind strongly with falstatin. Additionally, the developed pharmacophore hypothesis contained -H-N-C=O and N-H moieties which strongly suggested that the presence of electron-withdrawing groups could be vital for the inhibition of falstatin at the active site.

Overall, TCMDC 131646 was predicted to be a drug-like and safe compound that could inhibit falstatin in *Plasmodium falciparum*. Chemical-disease co-occurrence analysis in literature revealed that this compound showed *in-vitro* antiplasmodial activity at an IC_{50} of 0.226µM and has also shown in vitro activity for neuralgia, hyperalgesia and arthritis. The research recommends TCMDC 131646 as a potential antimalarial hit compound that could yield novel analogues by hit expansion. However, confirmatory in-vitro and in-vivo studies are required to substantiate these predictions.

Keywords

Malaria, Resistance, Falstatin, Structure-based, Virtual screening, *Plasmodium falciparum*, Homology modelling, Molecular docking, Molecular dynamics, Druglikeness.

Acknowledgements

I am thankful to Almighty God for giving me the strength and fortitude to complete my program at the University of the Western Cape. I am deeply grateful to my amiable supervisor Dr Samuel Egieyeh for his invaluable guidance, supervision, support, motivation and expertise while completing this project. My utmost gratitude to my parents Professor and Mrs Oladunjoye for their encouragement and support always. Many thanks to Mrs Elizabeth Egieyeh for her kindness and assistance throughout the study.

I am sincerely thankful to Samson Oselusi, Christianah Omotoso, members of Computational Pharmacology and Cheminformatics Research Group (CPCRG) and the entire staff of the school of Pharmacy, University of the Western Cape for their support and assistance all through the study. Also, I am indebted to Swiss Institute of Bioinformatics, Medicines for Malaria Ventures, and Optibrium Stardrop for their assistance during the study.

Table of Content

List of Tables

List of Figures

List of Appendices

Abbreviations

MD: Molecular Dynamics

MMV: Medicines for Malaria Ventures

SBVS: Structure-based Virtual Screening

ADME: Absorption, Distribution, Metabolism and Excretion

RMSD: Root Mean Square Deviation

RMSF: Root Mean Square Fluctuation

PCA: Principal Component Analysis

DCCM: Dynamic Cross-Correlation Matrix

CDC: Centre for Disease Control

WHO: World Health Organisation

Chapter One

Introduction

1.1 Background of the study

Malaria is an infectious and life-threatening disease transmitted by the female Anopheles mosquito and caused by parasites of the genus *Plasmodium.* The causative organisms include *Plasmodium ovale, Plasmodium knowlesi, Plasmodium vivax, Plasmodium malariae* with *Plasmodium falciparum* being the most virulent species (Nureye and Assefa, 2020; Sato, 2021). In 2020, the World Health Organization reported 229 million cases of malaria and 409 000 deaths globally, out of which 92% of morbidities and 93% of fatalities occurred in Africa. In 2019, 67% (274,000) of all malaria deaths occurred in children under 5years (WHO, 2020). Hence, malaria is a leading cause of morbidities and mortality in many countries.

Malaria occurs in several developing countries particularly in Africa where young children, pregnant women, travellers, and migrants are the most vulnerable due to little or no immunity to the disease (CDC, 2019). Transmission of malaria and resulting morbidity is highest in Africa while it is less prominent in South America and South Asia (Fig 1). Other contributing factors to this disease includes seasonal variation, scarce resources, and socio-economic instability.

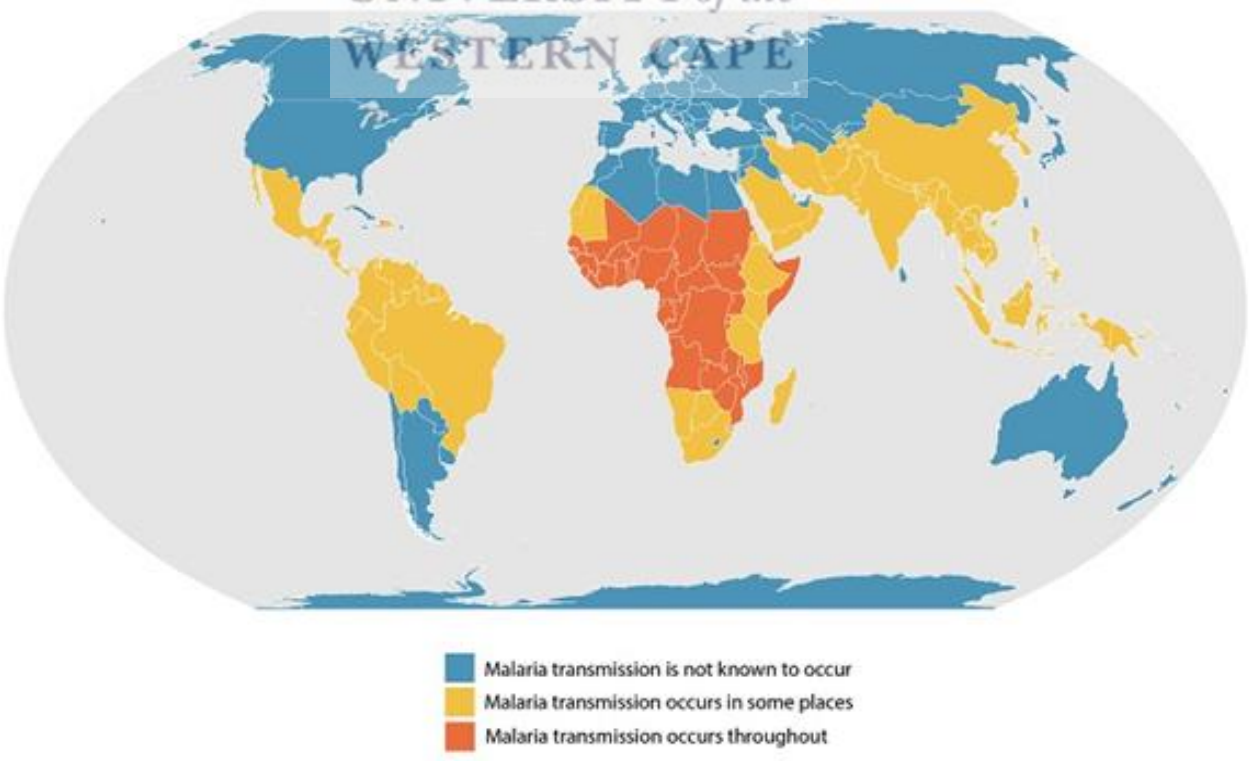

Figure 1. Map showing affected areas (CDC, 2020)

Within South Africa, malaria occurs mainly in Northern & Eastern Mpumalanga, KwaZulu-Natal and the low veld regions of Northern province (Fig 2). Malaria transmission in South Africa is seasonal due to weather conditions and marked inter-annual fluctuations (Manana et. al., 2018; Ikeda et. al., 2017). Approximately 95% of all malaria infections in South Africa are due to the parasite *Plasmodium falciparum*, the most lethal species of the *Plasmodium* genus.

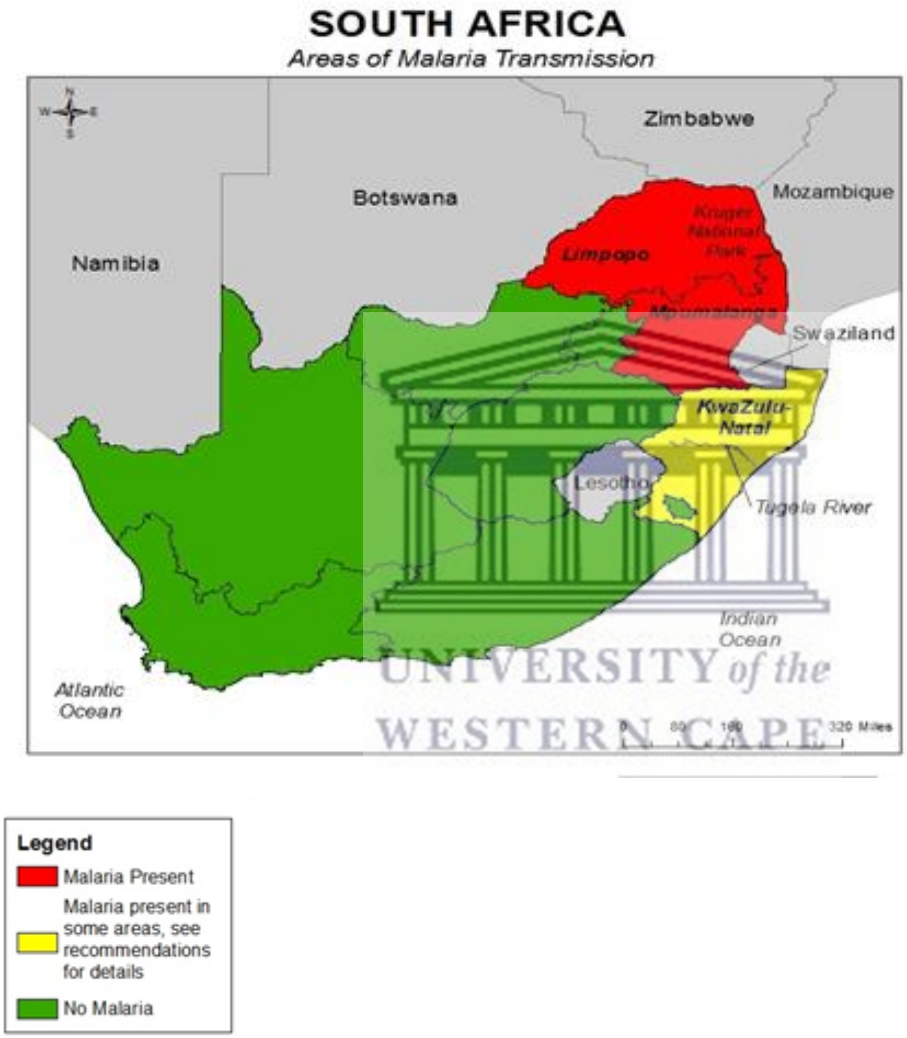

Figure 2. Map showing malaria-affected provinces in South Africa (Adapted from Warrandyte Clinic)

Several methods are currently being used to tackle the prevention and treatment of malaria. These methods include the use of insecticide-treated mosquito nets, indoor spraying with residual insecticides, and chemotherapy (WHO, 2020). Chemotherapeutics used in combating malaria include older generation drugs such as quinine, chloroquine, halofantrine, mefloquine, and newer artemisinin combination therapy (ACT's) such as artemether, arte-ether, artesunate and, lumefantrine (WHO, 2015). However, *Plasmodium falciparum* has developed increasing

resistance to these older drugs and more recently the ACT's (Huang et. al., 2021; Rosenthal et. al., 2019; Talman et. al., 2019). Therefore, there is an urgent need to search for new antimalarials with novel mechanisms of action.

In addition, most antimalarial drugs target specific stages of the *Plasmodium* life cycle. For example, chloroquine targets the erythrocytic stage while primaquine targets the liver stage (Coban et.al., 2020). However, only a few drugs target multiple stages of the *Plasmodium* life cycle. Hence, researchers have proposed that a multiple-staged protein essential for the survival of *Plasmodium* could be targeted to cause cell death and inhibit the growth of the *Plasmodium falciparum* (Tusar et. al., 2021, Mishra et. al., 2017).

Based on this consideration, falstatin has been identified as a multiple-staged protein present in merozoites and schizonts of *Plasmodium falciparum*. The protein facilitates the hydrolysis of haemoglobin, rupture of erythrocytes by mature schizonts and invasion of erythrocytes by free merozoites (Tusar et. al., 2021; Rosenthal et. al., 2014; Sunderaraj et. al., 2014; Pandey et. al., 2006). Hence, the current study seeks to identify compounds that could inhibit falstatin, these identified compounds may then be further explored for the treatment and potential elimination of malaria.

Various approaches have been used in the prevention and treatment of malaria. These approaches include the exploration of natural products and their derivatives, optimization of therapy with existing antimalarials, chemical modification of existing drugs, covalent biotherapy, drug resistance reversers, development of vaccines and development of compounds active against novel targets (Mishra et. al., 2017; Flannery et. al., 2013; Rosenthal, 2003). However, many of these approaches have various limitations such as high cost of laboratory screening and hit to lead optimization, labour intensiveness, time consumption as well as high attrition rates. Antimalarials obtained from these approaches also have some constraints such as drug toxicity, poor solubility, and notably antimalarial resistance. Hence, the in-silico approach is a strategy that can precede these expensive approaches thus limiting the cost and rate of failures from *in vitro* bio-activity testing (Maia et. al., 2020; Surabhi and Singh et. al., 2018).

The in-silico approach is beneficial because it is faster, cost-efficient, and less laborious than traditional laboratory screening and it is becoming increasingly more accurate in its predictions

(Salman et. al., 2021; Imam and Gilani, 2017). The in-silico approach involves virtual screening (VS) of chemical libraries to predict compounds that may likely bind to specific biochemical targets. It involves querying chemical databases using docking programs and algorithms that rapidly computes a vast library of compounds in order to identify promising drug candidates that can be easily optimized for clinical use. Therefore, VS reduces the time and effort involved in the preclinical development of new drugs (Meng et. al., 2011).

Furthermore, the in-silico approach lowers attrition usually encountered during clinical trials due to undesirable absorption, distribution, excretion, metabolism and toxicity (ADMET) properties (de Sousa et. al., 2020). The in-silico approach uses softwares to predict the ADMET profile of compounds; compounds with satisfactory ADMET properties are then prioritized for further experimental investigation. Thus, virtual screening reduces the drug failure rate by employing improved algorithms with greater accuracy to identify compounds with lower risk of toxicity and high potential for *in vitro* activity (Maia et. al., 2020; Chandrasekran et. al., 2018).

Virtual screening can be divided into ligand-based and structure-based methods. The ligand-based method is used when the protein target is unknown. It is based on the molecular similarity principle which relies on the search for compounds that contain chemical scaffolds that are similar to known active compounds (Vasquez et. al., 2020). The chemical library is evaluated against a reference molecule or active compounds using similarity measurements known as molecular descriptors. These descriptors are based on chemical nature and physical features of compounds such as molecular shape, volume, and pharmacophores (Chandrasekaran et. al., 2018; Varela-Rial et. al., 2021).

In contrast, the structure-based (SBVS) or target-based approach is used when the three-dimensional structure of a target protein is known, it also requires access to libraries of chemical compounds referred to as 'ligands' (Rastelli and Pinzi, 2019). SBVS predicts the interaction between ligands against a protein target and prioritizes the ligands based on their affinity to the target. SBVS also investigates the druglikeness of bioactive molecules in order to prevent attrition due to toxicity and poor ADME properties (Rudrapal and Chetia, 2020). Therefore, the SBVS helps in the identification of bioactive molecules known as hit identification and lead optimization of potential drug candidates. The leads are then optimized by improving the potency, safety, and physicochemical properties of the bioactive compounds.

Ultimately, the optimized lead undergoes experimental testing and clinical trials before approval.

Therefore, this study employs the structure-based virtual screening of antiplasmodial compounds compiled from the Medicines for Malaria Ventures database (Bathurst and Hentschel, 2006) to identify compounds that could inhibit falstatin in *Plasmodium falciparum.* The research explored the SBVS approach using computational methods involving homology modelling, molecular docking and druglikeness analysis. The homology modelling entailed building the three-dimensional structure of the target from its protein sequence falstatin based on its homologous protein, falcipain-2 which is referred to as the template (Muhamed and Aki-Yalcin, 2019). The molecular docking step involved screening chemical libraries in order to identify compounds that have a high affinity for falstatin. Following docking, compounds with high binding energy were then selected for drug-likeness profiling (Li et. al., 2019). The drug-likeness profiling prioritized hit compounds based on certain physico-chemical parameters that influence the absorption, distribution, metabolism, excretion and toxicity (ADMET) of a promising drug candidate such as partition coefficient, number of hydrogen bonds acceptors and donors, total polar surface area, molecular weight, number of rotatable bonds and molar refractivity (Gimeno et. al., 2018).

After drug-likeness profiling, the top-ranking compound known as "prioritized hit" was subjected to molecular dynamics (MD). The Molecular dynamics entailed a computer simulation of the physical movement of the modelled falstatin and the prioritized hit compound using Optimized Potentials for Liquid Simulations (OPLS-aa) forcefield which was developed for simulating proteins in liquid (Jorgensen and Tirado-Rives, 1988). The molecular dynamics step was used to study the effect of binding of the prioritized hit on the stability of the target protein, falstatin (Salmaso and Moro, 2018; Chen et. al., 2019). The trajectories obtained from the MD simulation was used to visualize, analyse and compare the stability or flexibility of the falstatin and falstatin-hit complex using tools such as hydrogen bond analysis, root mean square deviation (RMSD), root mean square fluctuation (RMSF), principal component analysis (PCA) and dynamic cross-correlation (DCCM) analyses. After ranking the compound, the top compounds were rescored to estimate their component binding energies and a pharmacophore hypothesis developed from the high-ranking ligands.

1.2 Research problem

Globally, the emergence of antimalarial resistance has become increasingly alarming due to the reduced susceptibility of *Plasmodium falciparum* to older classes of drugs which includes Cinchona alkaloids, 4-aminoquinolines, 8-aminoquinolines and antifolates (Huang et. al., 2021). More recently, a growing resistance to artemisinin-based combination therapies and other first-line therapeutics has led to increased morbidity and mortality particularly among pregnant women, children and immunocompromised patients (Miguel-Blanco et. al., 2021; Conrad and Rosenthal., 2019). Therefore, there is an urgent need to discover new classes of antimalarials with unique modes of action.

Furthermore, current antimalarial drugs target specific stages of the *Plasmodium* life cycle. For example, chloroquine targets the erythrocytic stage while primaquine targets the liver stage (Coban, 2020). However, these drugs become ineffective as the parasite transforms from one stage into another stage of its life cycle. Hence, there is a need to identify drug candidates that act on multiple stages of the parasite's life cycle (Favussa et. al., 2020; Flannery et. al., 2013). From literature search, falstatin has been identified as a multi-staged protein that can be targeted to inhibit erythrocytic invasion, rupture of schizont and degradation of haemoglobin (Tusar et. al., 2021).

In addition, the huge cost of clinical and preclinical drug development (about 2 billion dollars) as well as high failure rate during clinical trials, has been a major setback in the search for new antimalarials (Zhong et. al., 2018). Hence, it has become imperative to reduce the cost of drug discovery and to identify promising drug candidates with desirable properties such as toxicity, activity, bioavailability and efficacy as early as possible in the drug discovery process using the structure-based virtual screening approach (Neves et. al., 2018). Consequently, the current study seeks to identify promising antimalarial candidates by employing a structure-based virtual screening of selected antiplasmodial compounds against falstatin, in *Plasmodium falciparum.*

1.3 Approach

The structure-based virtual screening approach could accelerate the identification of new classes of antimalarials with novel mechanisms of action and favourable pharmacokinetic properties. The technique will screen selected compounds that are likely to have *in vitro* antiplasmodial activity against falstatin in *Plasmodium*. Subsequently, compounds with high

binding energy will be prioritized for druglikeness profiling and favourable compounds known as hits may then be considered for lead optimization and clinical trials. The study will achieve this by using computational techniques such as homology modelling, structure quality evaluation, molecular docking, molecular dynamics, rescoring analysis, structure stability analysis of the protein and protein-hit complex as well as rescoring analysis.

1.4 Significance of the study

The research study will tackle antimalarial resistance by identifying potential antimalarial candidates. This study will equip researchers with information on antimalarial hits that possess satisfactory ADMET properties that could inhibit falstatin in *Plasmodium falciparum*. The structure-based virtual screening approach could reduce the number of compounds required for high-throughput screening (HTS) and guide lead optimization in future research.

In addition, the output from this study might reduce the time, cost and effort involved in developing a new antimalarial drug. The study could also decrease the cost of synthesizing, purchasing and testing compounds in the laboratory since all the drug compounds will be analyzed and computed virtually as opposed to traditional laboratory screening that requires physical experimental testing. Further, the study will identify compounds with poor absorption, distribution, excretion, and toxicity (ADMET) properties early in the drug discovery process. Ultimately, the results obtained will reduce drug failure and lower the risk of attrition during drug development.

1.5 Aim

The aim of this study is highlighted below:

- To identify potential antimalarial candidates with favourable pharmacokinetic properties and high affinity for the plasmodial protein, falstatin in *Plasmodium falciparum* using the structure-based virtual screening approach.

1.6 Research Questions

This study is designed to use a structure-based virtual screening approach to answer the following questions.

- How can the three-dimensional structure of falstatin be computationally modelled and validated?
- What are the antiplasmodial compounds that have high affinity for falstatin, the protein target in *Plasmodium falciparum*?

- Which of the hit compounds have favourable absorption, distribution, excretion, and toxicity profile?
- Do the falstatin-ligand complex and unbound falstatin have the same structural stability when subjected to molecular dynamics and simulation?
- Is there a chemical diversity between the prioritized hit compounds and existing antimalarials drugs?

1.7 Objectives of the study

The objectives of this study include the following.

- To conduct homology modelling so as to generate the three-dimensional structure of falstatin and assess the quality of the falstatin model.
- To perform molecular docking studies on selected compounds in order to obtain the minimum binding energy for the ligand-protein complex using Molecular Operating Environment (MOE).
- To prioritize hit compounds based on favourable absorption, distribution, metabolism and toxicity (ADMET) properties using Stardrop, a software by Optibrium.
- To carry out molecular dynamics simulation to gain insight into the effect of binding on the structural stability of the modelled falstatin and lead complex.
- To compare the prioritized hit compound with chloroquine, artemisinin and artemether which are existing antimalarials with good pharmacokinetic and safety profiles.
- To conduct chemical diversity analysis of the prioritized hit with available antimalarial compounds.
- To rescore the top-ranking compounds using molecular mechanics with generalised Born and surface area solvation (MM-GBSA) scoring function.
- To develop a pharmacophore hypothesis based on the top-ranking ligands.

1.8 Scope of the Study

The research aims to identify promising antimalarial agents with potential novel mechanisms of action using the structure-based virtual screening approach. The study will also explain computational strategies such as molecular docking, druglikeness analysis, molecular dynamics simulation, structural analysis of trajectories obtained from molecular simulations and various rules of druglike compounds. Likewise, the methodology used in this study will be fully described and results from the project will be discussed exhaustively. Finally, the study will present the conclusions, limitations of the study and recommendations from the study.

1.9 Thesis outline

In this research, there are five chapters contained therein:

Chapter one describes the general overview and rationale for this study. It starts with a brief background on the epidemiology of malaria, the emergence of antimalarial resistance to currently administered drugs and the urgent need for novel drug candidates. This is followed by the statement of the problem, the significance of the study, aim, research questions, specific objectives, and outline of subsequent chapters.

Chapter two presents the literature review, it discusses the implications of malaria, strategies used in antimalarial development and the importance of structure-based virtual screening in targeting plasmodial proteases. This chapter further expands on methods and approaches of molecular docking, druglikeness profiling, molecular dynamics.

Chapter three presents the methodology. The chapter explains the specific details of methods used in homology modelling and structure validation of the modelled protein, molecular docking, druglikeness analysis, molecular dynamics simulation, structure stability analyses, rescoring analysis and development of pharmacophore hypothesis.

Chapter four presents the results and discussion. It describes actual findings from homology modelling and structure validation of falstatin, molecular docking, ADMET profiling, molecular dynamics and structure stability analyses, redocking as well as pharmacophore hypothesis generation.

Chapter five summarizes the major findings from the study and provides a recommendation for future studies. Finally, chapter 6 provides the full lists of the references, appendices and other information from this study.

Chapter Two: Strategies for Antimalarial Drug Development and Treatment

2.1 Overview

Malaria imposes serious public health concerns due to the development of drug resistance. This is exacerbated by reduced susceptibility to pesticides and indoor chemical sprays and increasing resistance to first-line chemotherapeutics leading to a pressing need for novel antimalarial compounds. Although different approaches are currently being investigated to discover new classes of antimalarials, these approaches have several limitations. Therefore, this review evaluates various strategies used in antimalarial drug development and identifies the structure-based therapy approach, particularly inhibition of multi-staged plasmodial proteins as a strategy for the total elimination of malaria in the future.

2.2 Global Impact of Malaria

Malaria is an infectious disease that causes anaemia, low birth weight and death in many countries, especially in developing countries. It accounts for 2.6% of the total disease burden worldwide and ranks fourth after pneumococcal acute respiratory disease, Human immunodeficiency virus (HIV) and tuberculosis (Mishra et. al., 2017; WHO, 2015). Poor children and pregnant women are most vulnerable to death or severe debility from malaria. In 2020, malaria reportedly caused 274 000 deaths (67%) in children under the age of five, these deaths in children could lead to reduced future population and workforce (WHO, 2020).

In addition, malaria causes permanent neurological damage such as speech and hearing disorders, blindness, cerebral palsy, epilepsy, and other learning disabilities in children. In endemic areas, malaria impedes as much as 60% of the school children's learning capacity (Riggle et. al., 2020; WHO, 2015). Also, malaria hampers children's schooling and social development through absenteeism. In some areas, malaria accounts for almost 15% of health-related absenteeism from school (Makenga et. al., 2020; WHO,2011).

Furthermore, malaria poses serious economic concerns to many countries of the world. The economic burden of malaria in Africa is estimated to cost $12 billion annually (CDC, 2021). The disease is responsible for increased health care spending which includes expenditure by the government on supply, staffing, maintenance of health care facilities and infrastructure, purchases of drugs and supplies, publicly managed vector control, health education, and research. In some countries with a heavy malaria burden, the disease accounts for

approximately 40% of public health expenditure, 30% to 50% of inpatient admissions, and up to 50% of outpatient visits (Shretta et. al., 2020; WHO, 2011).

In Sub-Saharan Africa, malaria accounts for employee absenteeism, decreases labour productivity and impedes economic growth by up to 1.3% annually (Zhao et al., 2020; Smith et. al., 2020; WHO, 2011). In endemic countries, malaria decreases the income of individuals as well as families and contributes to a vicious cycle of poverty. Households (including men and women in formal and informal employment) lose approximately 25% of their earnings to malaria due to reduced working hours associated with illness or death. Hence, malaria is referred to as a disease of poverty (Nduka et. al., 2020).

Also, malaria discourages investments and tourism in endemic areas (Rose et. al., 2020). The risk of contracting malaria can deter investment due to undeveloped tourist industry resulting from the reluctance of travellers to visit malaria-endemic areas, undeveloped markets due to traders' unwillingness to travel to and invest in endemic regions (Bagozzi and Koren, 2020; WHO, 2011).

2.3 Biology and clinical features of malaria

Malaria is transmitted by an infected female Anopheles mosquito. The life cycle of Plasmodium involves the human host and definitive host which is the mosquito (Fig 3). The mosquito bites the human and introduces sporozoites into the human blood, the sporozoites migrate to the hepatocytes and grow into schizonts which release merozoites into the blood. This stage is termed the pre-erythrocytic stage. The merozoite then reproduces asexually in the e-L0IPrythrocytes to form trophozoites which afterwards grows into schizonts (Hang et. al., 2021; Venugopal et. al., 2020). The schizonts divide into merozoites which differentiates into male and female gametes, the gametes are ingested by the mosquito during a blood meal where they undergo meiosis and fuse into a zygote or ookinete which develops into a sporozoite. The sporozoite resides in the mosquito's salivary gland and is then introduced into a new human host (Nureye and Assefa, 2020)

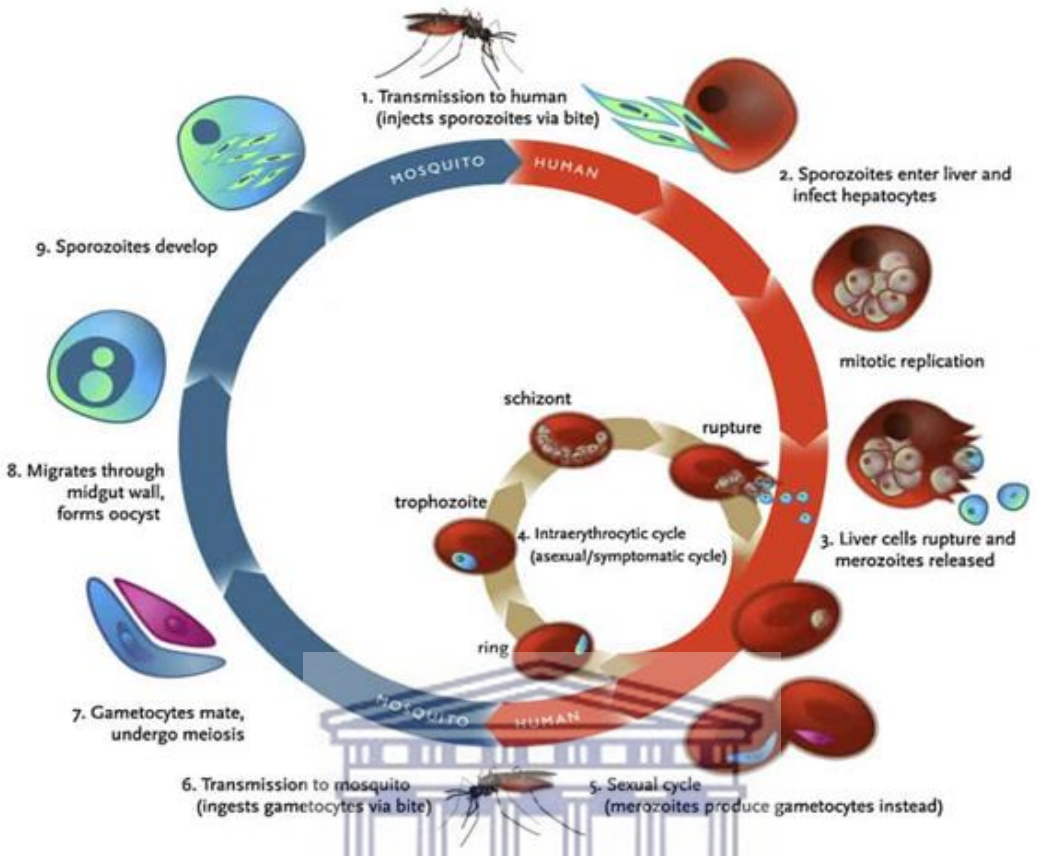

Figure 3. Life cycle of Plasmodium spp illustrating the developmental stages in the human host and mosquito (Courtesy of Centre for Disease dynamics, Economy and Policy).

Malaria is characterized by symptoms such as fever, diarrhoea, headache, fatigue, vomiting and in severe cases, seizure, paleness of eyes and skin, coma, and death (Tebben et. al., 2021). These symptoms usually begin in 10-15 days and if not properly treated, clinical recurrence may occur in about 2-3 days known as relapse or in months to years which is known as recrudescence due to reinfection by surviving parasites (Mishra et. al., 2017).

2.4 Approaches to Antimalarial Drug Development, Therapy and Prevention of Malaria

Although various strategies are being used to search for novel antimalarials, current antimalarial agents have several drawbacks such as drug resistance, toxicity, high cost and time involved in experimental screening. The most notable of these limitations is antimalarial resistance which has led to a constant need for new antimalarials. The approaches below describe the current approaches as well as prospective strategies for malaria prevention and control.

2.4.1 Exploitation of natural products and their derivatives

The search for antimalarials started as far back as the 1600's with the use of the bark extract of *Cinchona succirubra*, subsequently quinine was first isolated from the bark extract in 1820 (Achan et. al., 2011). However, quinine is only considered for treating uncomplicated malaria and as a second-line drug due to plasmodial resistance and toxicity characterized by cinchonism, tinnitus, headache, nausea, hypotension and hypoglycaemia (Belete, 2020; Fernandes-Alvero, 2016). Artemisinin, a sesquiterpene lactone was also extracted from the Chinese plant, *Artemisia annua* but its use is restricted due to neurotoxicity, low solubility, bioavailability, recrudescence and short half-life (Karri et. al., 2019). *Azadirachta indica* commonly called neem tree contains azadirachtin, quercetin, nimbin and gedunin which have in-vitro antiplasmodial activity (Tembe-Fokunang et. al., 2019). Other natural products include febrifugine and isofebrifugine isolated from *Dichroa febrifuga* and lapachol from *Tabebuia serratifolia*.

Although natural products are relatively cheap and readily available, the use of natural products is constrained due to toxicity and inadequate supply of active principles from medicinal plants. For instance, the limited supply of quinine during the second world war led to the need for synthetic derivatives of quinine (Coatney, 1963). Other notable challenges with the use of quinine include resistance and toxicity while artemisinin use is limited by resistance, poor solubility as well as chemical instability (Mishra et. al., 2017). Consequently, these limitations have necessitated the use of natural products as molecular templates for the development of analogues with improved activity and safety.

2.4.2 Development of analogues of available antimalarials

This strategy employs the chemical modification of existing antimalarials to improve their efficacy, safety, and solubility. Chloroquine, primaquine, tafenoquine and mefloquine were chemically modified from quinine (Fig 4). Chloroquine was the first-line treatment for several years because it is effective, cheap, and safe but chloroquine resistance has compelled the need for other quinine derivatives such as primaquine, tafenoquine, mefloquine and bulaquine. However, the use of mefloquine and primaquine is limited due to resistance and neurological effects (Rosenthal, 2003; Uzor et. al., 2020). Similarly, ferroquine is an organo-metallic analogue of chloroquine that has shown activity against Plasmodium. Tafenoquine also has higher liver-stage activity, longer half-life and safety than primaquine while bulaquine is an

analogue of primaquine in phase III clinical trials that prevents recrudescence in Plasmodium vivax (Mishra et. al., 2017).

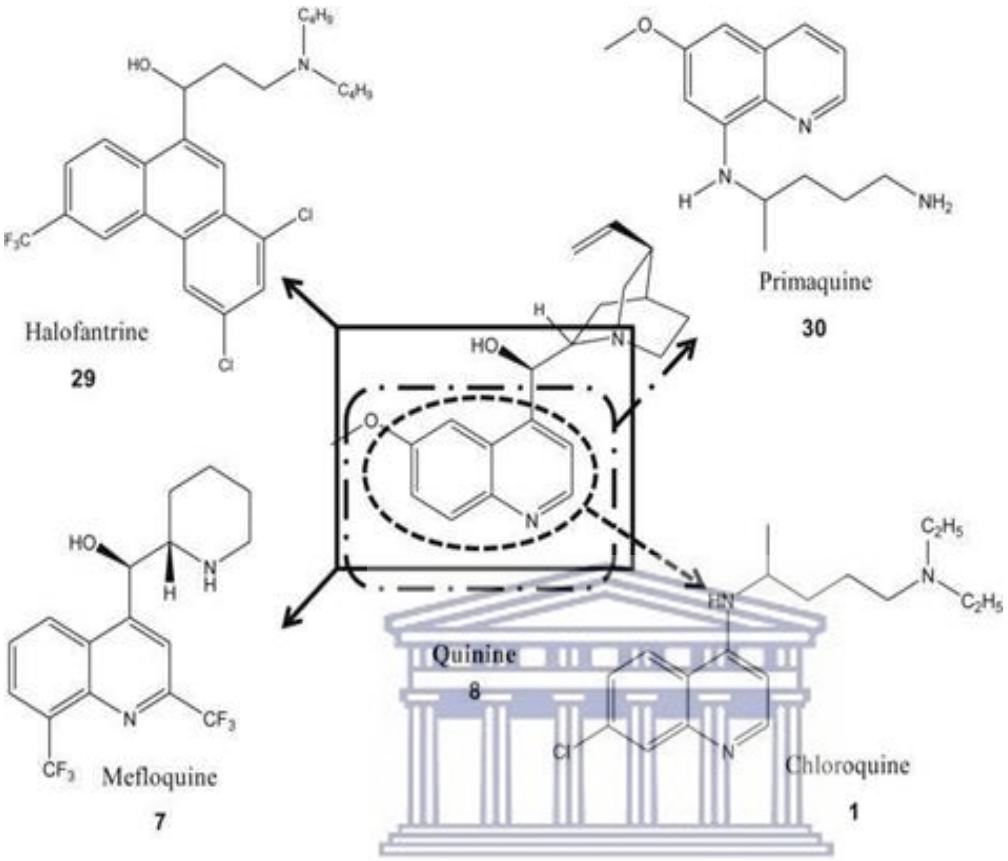

Figure 4. Chemical modification of quinine to yield other analogues

In addition, the limitations of artemisinin such as neurotoxicity, low solubility, bioavailability, recrudescence have led to its chemical modification to artesunate, artemether and arte-ether to obtain compounds with greater efficacy, stability, safety and better half-life as shown in Fig 5 (Karri et. al., 2019). Likewise, lumefantrine was developed from halofantrine because of liver and cardiac toxicity, it is commonly used in artemisinin-based combination because it is rapid-acting, has a high parasite clearance as well as good safety profile (Ishengoma et. al., 2019).

However, the high cost, time and effort involved in laboratory synthesis of compounds as well as biological assays of analogues is a major drawback to this approach. The development of resistance to most of these compounds particularly quinine and artemisinin have also been reported in many countries (Cui and Su, 2009; Rout and Mahapatra, 2019). Hence, researchers have proposed the use of combination therapy to address the limitations of this strategy.

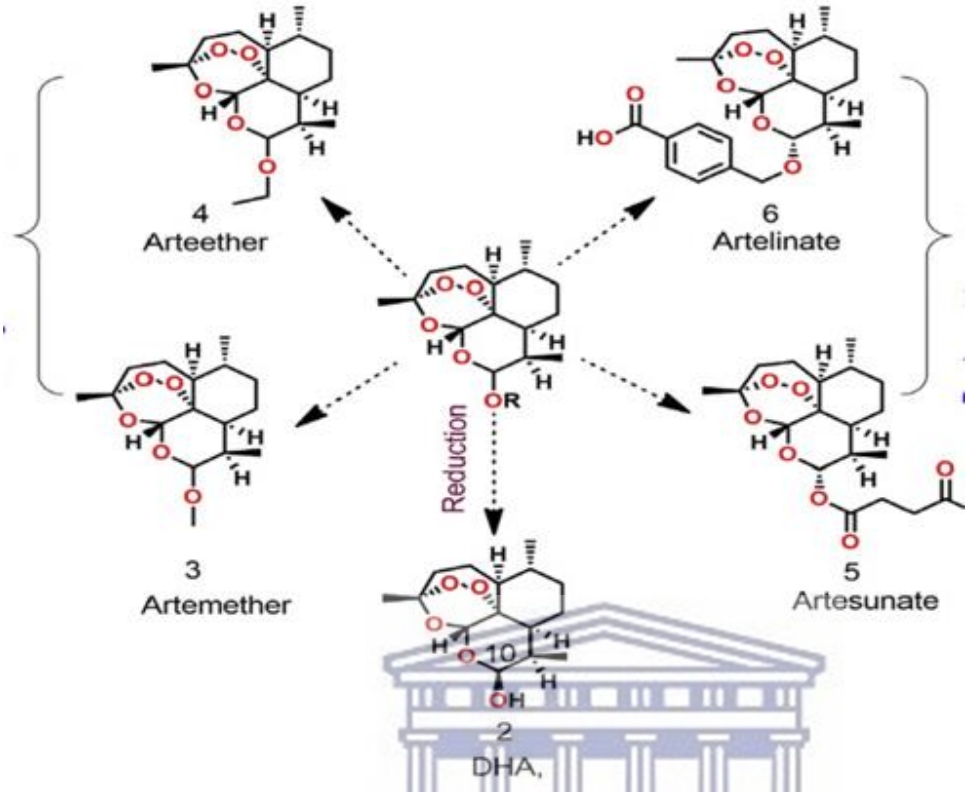

Figure 5. Structural modification of artemisinin to yield artesunate, artelinate, artemether and arte-ether.

2.4.3 Optimization of antimalarial therapy with available drugs

The optimization approach introduces new dosing regimens and formulations of existing antimalarials. The approach involves combinations of two or more drugs with different mechanisms of action and different molecular targets in the parasite (Mishra et. al., 2017). This strategy prevents recrudescence, slows down resistance, enhances safety and improves efficacy by additive or synergistic effect (Rosenthal, 2003). Following resistance to artemisinin, Chinese researchers reported that artemether and lumefantrine combinations reduced recrudescence. Thus, artemether-lumefantrine combination was first registered in China in 1992 and then registered by Novartis as Coartem in 1999 (Cui and Sui, 2009).

The optimization approach finds use in non-artemisinin-based combinations such as Proguanil-Dapsone, Quinine-Doxycycline, Amodiaquine-sulfadoxine-pyrimethamine and artemisinin-based combination therapy (ACT's) such as Dihydroartemisinin-Piperaquine (Eurartesim), Artesunate-Pyronaridine (Pyramax), Arterolane-Piperaquine (Synriam). However, plasmodial resistance to these drug combinations have been reported.

In Thailand, mefloquine and halofantrine combination was introduced in 1984 but *Plasmodium* developed resistance to the combination after a few years (Nosten and Brasseur, 2002). In 2007, resistance to artemisinin-based combinations which is the first line treatment was reported in the Greater Mekong region (GMS) in Cambodia and has since spread to other parts of the world limiting the use of this approach in malaria therapy (Ouji et. al., 2018; Tibon et. al., 2020). Also, the optimization approach is cost and time in-efficient as it requires intense laboratory assays and clinical testing. Likewise, the approach has not been effective in addressing antimalarial resistance, hence there is a need to explore other options in identifying new antimalarials.

2.4.4 Covalent biotherapy

Covalent biotherapy involves linking two different chemical moieties or pharmacophores that act on different or same biological targets through different mechanisms of action. The two distinct pharmacophores are linked through a stable covalent bond such as amide, amine or transition metals (de Sousa et. al., 2021). The two different moieties reduce susceptibility to resistance and increase antimalarial activity through a synergistic or additive effect (Capsi et. al., 2019). Examples include trioxaferroquine, chloroquine/primaquine hybrid and mefloquine/artesunate (MEFAS) hybrid which has shown schizonticidal activity against chloroquine-resistant parasites and low toxicity (Tibon et. al., 2019). Another example is trioxaquine (Fig 6) which consists of 4-aminoquinoline and 1,2,4 -trioxane (de Lima et. al., 2021). The aminoquinoline substituent inhibits haemozoin formation while the trioxane moiety alkylates haem in red blood cells. Hence, trioxaquine is active against both asexual and sexual forms of *Plasmodium* as well as chloroquine-resistant parasites (Alven and Aderibigbe, 2019; Oliveira et. al., 2015).

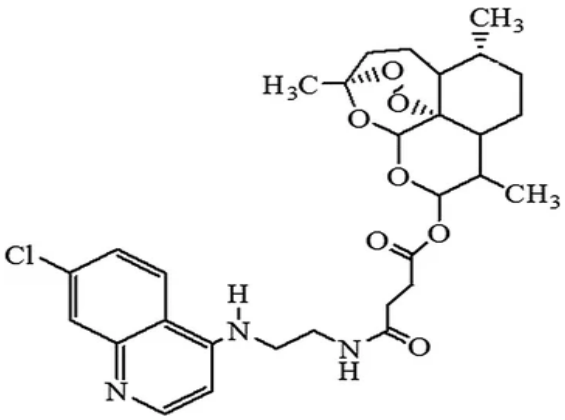

Figure 6. Chemical structure of trioxaquine

Covalent biotherapy is an improvement on the combination therapy approach, it chemically links the individual drugs instead of the physical combination of drugs in the optimization approach (Tibon et. al., 2020). Nonetheless, toxicity has also been reported in proguanil-dapsone-artesunate hybrids leading to its withdrawal from phase three clinical trials (Muregi and Ishih, 2009). Other constraints include high cost of synthesis as well as high molecular weight of hybrids leading to poor solubility and unfavourable ADMET properties (Oliveira et. al., 2015).

2.4.5 Drug Repurposing or Repositioning

Drug repurposing refers to the investigation of existing drugs as potential therapies for other diseases while drug repositioning involves using a drug effective for a specific disease as a template for synthesizing derivatives that are active against other diseases (Pushpakom et. al., 2018). This strategy entails testing commercially available drugs (used for other indications) with known pharmacokinetic and safety profiles for antimalarial activity. Examples include ritonavir, a protease inhibitor indicated for treating human immunodeficiency virus (HIV) which was confirmed to inhibit plasmepsin, a protease in *Plasmodium* while tipranavir is an antiretroviral drug that has shown gametocidal activity in *Plasmodium* (Pazhayam et. al., 2018). Folate antagonists, atorvaquone, and other antibiotics such as tetracyclines are currently being re-explored for developing new antimalarials whereas malarone containing proguanil and atorvaquone (a drug for treating *Pneumocystis*) is being marketed for the prevention and treatment of malaria (Mishra et. al., 2017).

Drug repurposing reduces the cost, time and effort required for preclinical testing and clinical trials since the pharmacokinetic properties of the drug are already known (Kiriiri et. al., 2020) Therefore, this strategy serves as a viable method that could be further explored using high-throughput screening assays.

2.4.6 Drug Resistance Reversers

This approach combines current antimalarials with compounds that ameliorate resistance leading to sustained efficacy of existing drugs. Many compounds have been shown to reverse plasmodial resistance to chloroquine, these compounds restore the use of chloroquine, a safe, rapid-acting and inexpensive drug (Achieng et. al., 2017). Resistance reversers include calcium channel blockers such as verapamil, diltiazem, tricyclic antidepressants such as imipramine, desipramine, phenothiazines such as trifluoperazine, chlorpromazine, and antihistamines such as chlorpheniramine and cyproheptadine (Gunsaru et. al., 2017).

Although the approach restores the activity of previously effective and safe compounds like chloroquine and artemisinin, high concentrations of drugs are usually required to achieve reversal of resistance, which results in adverse effects such as cardiotoxicity as seen in verapamil, as well as drowsiness as seen in chlorpheniramine and tricyclic antidepressants (Rosenthal, 2003).

2.4.7 Development of malaria vaccines

The development of effective vaccines is a promising tool in the eradication of malaria. Malaria vaccines typically targets one or more stages of the *Plasmodium* life cycle namely: pre-erythrocytic stage (sporozoite and hepatic), asexual stage (erythrocytic) and sexual stage (Shibeshi et. al., 2020). At each stage, specific proteins and antigens are targeted. Examples of pre-erythrocytic vaccine candidates are CSVAC, Chad63, PfSPZ and RTS, S. RTS, S, is a combination of circumsporozoite protein (CSp) and hepatitis B surface antigen that has shown 30-50% success rate in phase 3 clinical trials (Lozano et. al., 2021).

Erythrocyte-stage candidates target antigens on merozoites Examples include merozoite surface proteins 1, 2, 3 (MSP), apical membrane antigen (AMA), erythrocyte-binding antigen (EBA) and serine repeat antigen (SERA). Erythrocyte-stage candidates are designed to reduce parasitaemia while sexual-stage candidates stop the growth of *Plasmodium* in Anopheles mosquitoes. Sexual-stage vaccines target ookinete surface antigens such as Pfs25, Pfs28, Pvs25 and Pvs28 (Duffy and Gorres, 2020; Zheng et. al., 2019; Lyke, 2017).

The development of malaria vaccines faces various limitations such as the high cost and time involved in laboratory studies and clinical trials. Particularly, the antigenicity of *Plasmodium falciparum* is a major challenge, nonetheless, investigations into the antigenicity or immunological mechanisms that provide protection against malaria are currently ongoing. The polymorphism of *Plasmodium* which prevents antigen recognition and causes immune evasion is another constraint (Kanoi et. al., 2021; Good and Stanistic, 2021). Owing to these complexities, investigations on the structure and antigenic variation of *Plasmodium falciparum* are being intensified.

Despite these limitations, RTS, S malaria vaccine has shown good efficacy as well as safety profile and has been approved in children from 5 months upwards. However, funding, distribution and logistics of the vaccine in many countries especially in Sub-Saharan Africa

might be a challenge (WHO, 2021). Therefore, antimalarial agents remain a viable method for the prevention and treatment of malaria.

2.4.8 Structure-based or Target-based Drug Discovery Approach

This approach involves the identification and inhibition of protein targets or plasmodial proteins. These targets are indispensable proteins essential for cellular processes such as cell penetration, erythrocytic invasion, degradation of haemoglobin, immune evasion, and cell growth, inhibition of these targets cause cell death within the organism (Belete, 2020; Deu, 2017). Consequently, inhibitors of these protein targets can serve as potential antimalarial candidates. Examples of plasmodial proteins include cysteine, serine, threonine, glutamate and aspartate proteases (Shibeshi et.al., 2020). Several compounds have been shown to inhibit plasmodial proteases. These include norstatins which inhibit falcipains and plasmepsins responsible for haemoglobin degradation while imidazopyrazines inhibit plasmodium kinases essential for phospholipid biosynthesis. Similarly, P65 and P218 inhibit dihydrofolate reductase responsible for folate metabolism in *Plasmodium* while atovaquone inhibits cytochrome c-oxidoreductase which is responsible for electron transport (Mishra et. al., 2017).

The inhibition of novel drug targets could be a promising strategy in finding new antimalarials. Muregi and Ishih in 2010 stated that once a protein target has been identified and validated, it could serve as a basis for screening of compounds in order to identify novel antimalarial compounds. In another study, Favussa stated that the inhibition of novel drug targets at multiple stages of the *Plasmodium* life cycle could be a valuable approach in identifying new antimalarial leads. He also proposed that a drug regimen that acts on unique drug targets present in various life cycle stages of *Plasmodium* would be a promising drug for malaria treatment and elimination (Favussa, 2020). This proposition is based on the assertion that a drug with a novel mechanism of action would lead to a reduced possibility of resistance and mutation in *Plasmodium.* On this account, the structure-based virtual screening approach could be a useful tool in antimalarial drug discovery.

In *Plasmodium falciparum,* falstatin has been identified as a drug target that facilitates hydrolysis of haem, erythrocytic invasion by schizonts and rupture of erythrocytes by merozoites. It is a cysteine protease present in schizonts and merozoites of *Plasmodium falciparum* (Pandey et al., 2006; Sunderaraj et. al., 2014; Rosenthal et. al., 2014). Since falstatin is essential for cellular processes in *Plasmodium,* inhibition of this target can lead to cell death.

Based on this consideration, this study seeks to identify new antimalarials by employing the structure-based virtual screening of antiplasmodial compounds against falstatin, a novel and multi-staged drug target in *Plasmodium falciparum*.

In the drug discovery space, once a protein target has been identified and validated, the in-silico approach becomes a valuable and economic tool in designing inhibitory antimalarials. The in-silico approach involves the virtual screening (VS) of chemical libraries to predict compounds that could bind to a specific biochemical target in *Plasmodium falciparum* (Maia et. al., 2020). Virtual screening rapidly queries chemical databases using docking programs and algorithms that compute large numbers of compounds (10^3-10^6) within a short period of time. It filters a library of compounds to a few compounds with favourable physicochemical properties that can be easily optimized to improve efficacy and safety (Hamidovic et. al., 2021; Li and Shar, 2017). Hence, VS is a strategy that could accelerate the discovery of new antimalarials.

2.5 Virtual Screening

Virtual screening (VS) is a computational technique used in drug discovery to search large chemical libraries to identify compounds that bind to a specific target, usually a protein or enzyme (Gimeno et al., 2019). These libraries contain a huge number of compounds which are filtered to a reduced number, optimized and then tested for clinical use (Maia et. al., 2020; Kar and Roy, 2013). Virtual screening uses softwares and algorithms to predict the absorption, distribution, metabolism, excretion and toxicity (ADMET) properties of compounds (Carolina et. al., 2020). It helps to identify and prioritize active compounds known as hits and identifies compounds that require optimization called leads. Commonly used softwares include Autodock (Trott and Olsen, 2010), Schrodinger (Schrodinger, LLC, USA) and MOE (Villar et. al., 2008) while available web servers include Swissdock and Galaxy.

2.5.1 Advantages of Virtual Screening

In the past, traditional laboratory screening of compounds known as high throughput screening (HTS) was used to search for bioactive compounds, but it is expensive, exasperating and time-consuming usually about 10-15 years as many compounds have to be synthesized, purchased and tested experimentally in the laboratory (Batool et. al., 2019; Kar and Roy, 2013). However, with the introduction of virtual screening, a huge database containing several thousand compounds can be computed very rapidly. Thus, virtual screening reduces the time required for developing a new drug.

In addition, virtual screening minimizes the cost of attrition and accelerates drug development in a cost-efficient manner. In 2015, Macalino reported that the cost of bringing a new drug into the market is approximately 0.8 to 1.8 billion dollars. He stated that virtual screening lowers the cost of drug discovery and is essential for the preliminary stage of drug discovery. Likewise, VS helps to decrease the cost of synthesizing, purchasing, and testing of compounds. It also eliminates undesirable compounds and helps to reduce the initial number of compounds required for high throughput screening (Maia et. al., 2020; Croston, 2017). Using VS, compounds that are not yet available in the laboratory can be initially investigated, and then purchased or synthesized if found promising (Salman et. al., 2021; Prada-Garcia et. al., 2016). Therefore, virtual screening is a fast and cost-efficient method that could be harnessed for developing novel antimalarials.

Furthermore, virtual screening reduces the risk of attrition during drug development. VS identifies and filters out compounds with poor absorption, distribution, metabolism, excretion and toxicity (ADMET) properties using computational techniques and softwares (Carolina et. al., 2018; Chandrasekaran et. al., 2018). In 1993, it was reported that 39% of drug failures resulted from poor pharmacokinetic parameters; by 2000 drug failure rates had reduced to approximately 10% due to the introduction of early ADMET screening (Segall, 2014). Resultantly, virtual screening prevents late-stage attrition and has led to the popular "fail early, fail cheap" paradigm which means that it is better and cheaper for a drug candidate to fail early than to fail during clinical trials (Segall, 2014; Dearden, 2003; Talevi, 2018).

Similarly, virtual screening is a labour-efficient strategy in drug development. It reduces the number of compounds required for synthesis and bioassays (Surabhi, 2018; Kar and Roy, 2013). Since VS minimizes attrition, it also reduces the effort that would have been expended in clinical trials. Hence, virtual screening is a labour-efficient tool in the drug discovery process.

Because the structure-based approach lowers attrition during clinical trials and has also been proven to save the cost, time and effort required for drug discovery, it is considered an efficient approach for identifying novel antimalarial candidates. Consequently, this study explores structure-based virtual screening to identify potential antimalarial candidates.

2.5.2 Types of Virtual Screening

Virtual screening can be classified into ligand-based and structure-based methods (Fig 7). Ligand-based virtual screening (LBVS) is used when the active-ligand molecules are known while little or no structural information is available for the target (Maia et. al., 2020; Xuan-Yu, 2012). LBVS is based on the similarity property principle (SPP) which states that ligands with high structural similarity to an active compound are likely to have similar activity profiles. Thus, LBVS relies on the knowledge of the structure of active ligands to predict new chemical entities with similar behaviour (Vazquez et. al., 2020; Prada-Gracia et al., 2016).

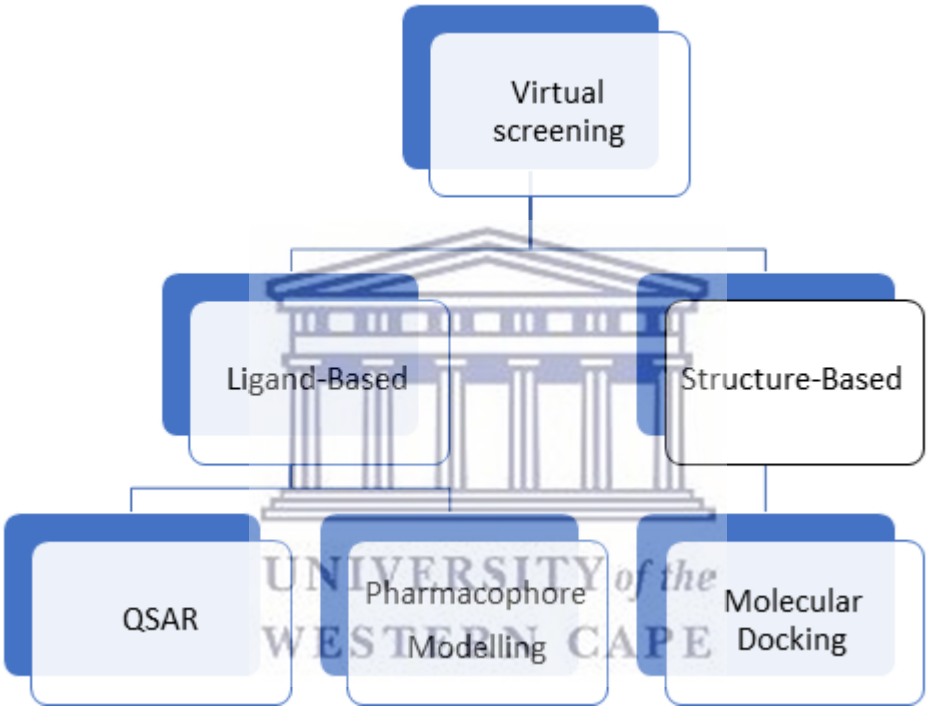

Figure 7. Schematic diagram of virtual screening

LBVS uses molecular descriptors or features such as molecular mass, partition coefficient, molar refractivity, polar surface area and atom types to compare a large library of compounds with a reference compound or set of compounds (Yang et. al., 2021). These descriptors are usually encoded as bit strings, fingerprints or structural fragments indicating the presence or absence of predefined properties (Vazquez et. al., 2020; Prada-Gracia et. al., 2016). Examples of LBVS methods include QSAR (Quantitative structure-activity relationship) and pharmacophore modelling.

Pharmacophore modelling involves the use of the two-dimensional or three-dimensional structure of a molecule to build a pharmacophore model (Kutlushina, 2018). This model describes the spatial arrangement of features essential for a compound to be biologically active,

the features include hydrogen bond donors and acceptors, aromatic rings, hydrophobic regions, acidic and basic side chains. The generated model is then used as a reference to screen large chemical databases for potential hits (Prada-Gracia et. al., 2016). Softwares used for pharmacophore modelling include LigScout (Wolber and Langer, 2005), Molecular Operating Environment (MOE) and Discovery studio (Studio, 2008).

Pharmacophore modelling, molecular docking together with other screening techniques can be combined to complement and optimize the results of in-silico screening (Macalino et. al., 2015). In combination with molecular docking, pharmacophore modelling has been used to identify a novel antimycobacterial compound ((Z)-N-(2-isopropoxyphenyl)-2-oxo-2-((3-(trifluoromethyl)-cyclohexyl)amino)acetimidic acid) which has been validated to be a potential BioA inhibitor (Macalino et. al., 2015).

The QSAR method involves the use of the QSAR model which quantifies the correlation between the molecular descriptors of a compound and a particular chemical or biological attribute (Neves et. al., 2018). To build a QSAR model, a group of compounds with desirable biological activity is first identified, then a quantitative relationship is identified between the physicochemical descriptors and the biological activity. The developed QSAR model is then used to optimize active compounds with the desired activity (Muratov et. al., 2020; Acharya et. al., 2011).

In contrast to ligand-based methods, the structure-based virtual screening (SBVS) is employed when the three-dimensional (3-D) structure of the target protein is known (Maia et. al., 2020; Meng et. al., 2012). The structure-based virtual screening approach SBVS uses the 3-D structure of target proteins (usually obtained from Nuclear Magnetic Resonance, X-ray or homology modelling) to predict the interactions between a target and chemical compound. Using a scoring function, SBVS estimates the binding energy of a ligand to a specific protein target (Guedes et. al., 2018). In SBVS, the protein is referred to as the receptor while the ligands refer to the screened compounds.

The structure-based virtual screening approach has become increasingly important in drug development. The approach has been proven to save the cost, time, resources and effort required for discovering new drug candidates (Maia et. al., 2020). SBVS also reduces attrition during clinical trials by predicting the absorption, distribution, metabolism, excretion and

toxicity (ADMET) properties of compounds (Carolina et. al., 2020). Further, SBVS minimizes the number of ligands to be synthesized, purchased, and tested for biological activity (Croston, 2017). Thus, SBVS is considered a valuable tool that could decrease the cost, time and effort required for discovering a novel antimalarial compound.

Various drugs have been developed using the SBVS approach, examples include anti-hypertensives such as aliskiren and captopril, antiretrovirals such as sasquinavir, ritonavir, indinavir and nolatrexed, an investigational drug used in the treatment of liver cancer (Maia et. al., 2020; Nunes et. al., 2019; Devi et. al., 2015). Therefore, the SBVS could accelerate the development of new antimalarials. Molecular docking is a notable example of SBVS approach which is widely used to predict the interaction between two molecules during the early stages of drug discovery.

2.5.3 Molecular Docking

Molecular docking is an important tool that has permeated all aspects of hit identification and lead optimization. Molecular docking is a method that analyzes the conformation and orientation of molecules into the binding pocket of a macromolecular target (Torres et. al., 2019). Molecular docking identifies potential ligands from a library of chemical compounds, predicts the binding mode of potential or known ligands, and uses the predicted binding pose to calculate putative binding affinities in order to identify compounds that are likely to bind to a particular target (Li et. al., 2019; Prada-Gracia et al., 2016).

Molecular docking requires a good docking target or protein receptor. A good docking target should have a deep binding pocket and have sites for specific interactions, such as charge-charge and H-bonding sites. Also, a good target must have a well-ordered side chain, with a low hydrophobic and van der Waal interaction (Bull and Doig, 2015). For this research, the protein target, falstatin possesses these attributes and was therefore selected as a docking target for this study.

Several studies have shown that molecular docking complements laboratory bioassays and facilitates antimalarial drug discovery. In a particular study by Syahri et. al., (2017), molecular docking studies revealed that chalcone derivatives showed inhibitory properties against dihydrofolate reductases–thymidylate synthase (*Pf*DHFR-TS), an enzyme essential for folate biosynthesis in *Plasmodium*, it was further confirmed that chalcones possess in-vitro

antiplasmodial activity at an IC_{50} of 0.59µM. In another study, molecular docking and in-vitro assays showed that benzimidazole derivatives could inhibit β-haematin in *Plasmodium* (Labbate et. al., 2018). In a similar report, docking studies showed that clioquinol could inhibit falcipain-2, *P. falciparum* ATPase (PfATP6) and *P. falciparum* enoyl-acyl-carrier-protein reductase (1NHW), further *in vitro* study confirmed clioquinol to be active against *Plasmodium* at an IC50 of 0.56µM (Nunes et. al., 2019). Molecular docking has also shown that remdesivir, hydroxychloroquine and simprevir could be promising in the treatment of SARS- COV2 (Uzukunova et. al., 2020; Mishra et. al., 2021).

Although, molecular docking has a major limitation which is inaccurate calculation of binding energies due to high approximations implemented by scoring functions (Prieto-Martinez and Medina-Franco, 2018). The accuracy of molecular docking can be enhanced using improved force fields, scoring functions such as consensus which combines 3 or 4 scoring functions to improve results, and algorithms that introduces water molecules or solvent in their calculations (Prieto-Martinez et. al., 2018). Similarly, molecular docking should be complemented with other experimental and computational methods such as molecular dynamics and redocking to yield better results (Ferreira et. al., 2015).

2.5.3.1 Methods of Docking

Docking methods can be described by the degree of flexibility of the molecule involved in ligand and receptor interaction. Docking methods can be classified into rigid, flexible and semi-flexible docking (Huang et. al., 2018). Rigid docking is based on the lock-and-key theory proposed by Fischer in which the ligand fits into the receptor-like a lock and key (Salmaso and Moro, 2018). In rigid docking, the ligand and protein are considered to be rigid entities, the method is suitable for large systems, such as protein-protein and protein-nucleic acid (Tao et. al., 2020; Salmaso and Moro, 2018).

For semi-flexible docking, the ligand is flexible while the protein is rigid. This is analogous to the induced-fit theory proposed by Koshland in 1892 which states that the active site of a protein is continually reshaped as the ligands interact with the protein (Salmaso et. al., 2018). The induced-fit theory suggests that the ligand and receptor should be treated as flexible during docking. Consequently, semi-flexible docking describes binding events more accurately than rigid docking (Salmaso and Moro, 2018; Meng et. al., 2011). Semi-flexible docking is suitable for the docking of small molecules and macromolecules such as proteins and nucleic acids.

Flexible docking involves both flexible protein and ligand. It is consistent with the conformational selection model which describes proteins as a pre-existing ensemble of conformational states. Flexible docking is mainly used to study the interaction between macromolecules (Tao et. al., 2020).

2.5.3.2 Approaches to Molecular Docking

Simulation Approach

In the simulation approach, the ligand binds into the groove of the target after definite times of moves. The moves involve variations to the structure of the ligand either internally (torsional angle rotation) or externally (rotations and translations). Each move in the conformational limits of the ligand generates energy known as the total energy of the system. To achieve the best-docked conformer of ligand and receptor, the ligand is allowed to fit into the receptor groove based on minimum energy consideration (Kumar and Kumar, 2019; Agarwal and Mehrotra, 2016). Simulation approach is beneficial because it considers ligand flexibility, it also assesses the molecular recognition between the ligand and target (Dar et. al., 2017). However, this approach takes a longer duration to estimate due to the large energy dissipated for each conformer (Tripathi and Misra, 2017).

Shape Complementarity Approach

This approach stems from the observation that protein surfaces are complementary to each other at the binding interface. That is, the binding interface matches the convex and concave surface of proteins (Kumar and Kumar, 2019; Li et al., 2013). Hence, the shape complementarity approach searches for a complementary groove between the ligand and the target surface. The approach is used for both rigid and flexible docking, it is a quick and robust method due to the rapid computation of ligands, finding out the possible binding properties of ligands on the target molecular surface (Agarwal and Mehrotra, 2016; Dar et al., 2017).

2.5.4 Analysis of Druglikeness

Druglikeness is a complex balance of various physical and chemical properties which determine whether a compound will behave like a drug (Gimeno et. al., 2018). These properties or descriptors include partition coefficient, number of hydrogen bonds acceptors and donors, total polar surface area, electronic distribution, molecular weight, as well as flexibility. These physico-chemical properties affect the absorption, distribution metabolism and excretion of a potential drug candidate, and thus plays a crucial role in evaluating the druglikeness of a drug

candidate (Elkwafi et. al., 2021; Medina-Franco et. al., 2015). Various physico-chemical descriptors and rules used in evaluating druglikeness are considered below.

2.5.4.1 Physico-chemical parameters in Drug-likeness Analysis

Partition Coefficient (PC)

The partition coefficient is the ratio of the un-ionized drug distributed between the organic and aqueous layers at equilibrium. It is a measure of the lipophilicity of a drug and an indication of its ability to cross the cell membrane (Isik et. al., 2019). The partition coefficient directly influences the absorption, distribution and metabolism of a compound. It characterizes the lipophilic-hydrophilic balance of a compound and determines the movement of a drug from the site of administration to the site of action (Smeralda et. al., 2019; Chmiel et. al., 2019). Positive values of log P indicate lipophilicity while low or negative values indicate hydrophilicity (Bhal, 2007). Lipophilic drugs with high partition coefficients are commonly found in the lipid bilayer while hydrophilic drugs with low partition coefficients are found in blood serum.

Hydrogen Bonding

Hydrogen bonding plays an essential role in the absorption and permeability of bioactive compounds into biological membranes (Dahlgren and Lennernas, 2019). Hydrogen bonding reflects the interaction between the H-bond (HB) acceptor target and the H-bond (HB) donor compound. It was discovered that for a compound to cross a biological membrane, the hydrogen bonds between the drug and its aqueous environment must be broken (Chandrasekaran, 2018). The number of hydrogen bonds inversely affects the degree of permeability and absorption. Morealso, the number and the strength of the hydrogen bonds between a molecule and water determines its absorption and distribution into biological membranes (Chandrasekaran, 2018). Therefore, the hydrogen bonds (including hydrophobic, salts and metallic bonds) of lead compounds can be manipulated to improve properties such as solubility while still maintaining their affinity for the protein target in an approach known as multi-parametric optimization (Baxter and Lockey, 2001; Halogen, 2007).

Topological Polar Surface Area (TPSA)

The topological polar surface area (TPSA) of a compound refers to the surface sum of all the polar surface or molecules, including oxygen, nitrogen and the hydrogen atoms attached (Prasanna and Doerksen, 2009). It characterizes the lipophilic–hydrophilic balance of a

compound and is an important parameter in assessing a compound's absorption into intestinal fluid or blood-brain barrier (Ertl et. al., 2000; Clark et. al., 2011). Molecules with a polar surface area of greater than 140 Aº are poor at permeating cell membranes while molecules that penetrate the blood-brain barrier generally have a PSA of less than 90 Aº (Prasanna and Doerksen, 2009).

Molecular Weight

The molecular weight of a compound has a significant effect on its absorption, distribution and metabolism. An increasing molecular weight usually correlates with decreased permeation into the central nervous system and intestine (Pollastri et. al., 2010; Radar et. al., 2018). Consequently, compounds with high molecular weights are less likely to be orally active due to reduced permeation through the lipid bilayer (Banks and Greig, 2019; Lipinski, 1997).

2.5.4.2 Lipinski's or Pfizer Rule of Five

In 2002, Lipinski proposed that druglike molecules or compounds with good oral bioavailability have the following properties, 5 or fewer hydrogen bond donors (including N-H and O-H bonds), 10 or fewer hydrogen bond acceptors (N-H and O-H bonds), molecular mass of fewer than 500 daltons and partition coefficient (log P) that does not exceed 5 (Chandrasekaran, 2018; Lipinski, 2002). Although there are exceptions to this rule, drug candidates that conform to this rule usually have lower attrition rates during clinical trials.

Several researchers also opined on the concept of druglikeness. For example, Veber proposed that orally active drugs commonly have 10 or fewer rotatable bonds and polar surface area not greater than 140 Aº (Sayed et. al., 2020; Veber et. al., 2002). Egan also proposed that compounds with good oral bioavailability usually have a total polar surface area of 132 Aº or below and log p of -1 to 6 (Ruswanto et. al., 2021; Egan et. al., 2002) while Ghose suggested that druglike compounds usually have a partition coefficient log P of −0.4 to +5.6 range, molar refractivity of 40 to 130, a molecular weight of between 180 to 480 and number of atoms from 20 to 70 (Oyinloye et. al., 2021; Ghose et. al., 1999).

2.5.4.3 Leadlikeness

Medicinal chemists have improved on the rule of 5, it was observed that to maintain drug-likeness during hit and lead optimization, screened compounds should have low lipophilicity and molecular weight. Therefore, the rule of 3 proposed that lead-like compounds usually have octanol-water partition coefficient log P not greater than 3, the molecular mass of fewer than

300 daltons, not more than 3 hydrogen-bond donors, not more than 3 hydrogen-bond acceptors and not more than 3 rotatable bonds (Chen et. al., 2021; Oprea and Hann, 2004).

2.5.4.4 Metabolism Analysis

Drug metabolism refers to the conversion of a drug into substances that are easily excreted from the body. Metabolism is divided into two phases namely phase I and phase II. Phase I metabolism involves the formation of new or modified functional groups through the oxidation, reduction or hydrolysis of drugs while Phase II metabolism is primarily concerned with the conjugation of drugs with endogenous substances such as glucuronic acid, glycine and sulphate (Lewis, 2003). The major enzyme system of phase I metabolism is cytochrome-P450 (CYP450), a microsomal isoenzyme system that catalyzes the oxidation of many drugs. Hence, drugs that interact with CYP450 enzymes might increase toxicity or reduce the therapeutic effects of other drugs (Kinirons and O'Mahony, 2004).

Therefore, metabolism analysis is mainly used to predict potential substrates of cytochrome (CYP) enzymes. It reduces drug failure during clinical trials by identifying compounds that are likely to have poor metabolism profiles (Kazmi et. al., 2019). Metabolism prediction is based on the structural similarity of compounds that are inhibitors of metabolizing enzymes such as CYP450, CYP3A4, CYP1A2, CYP2D6, CYP2C9. Softwares available for predicting metabolism include Stardrop, META and MetabolExpert while SwissADME is an online server (Earnshaw, 2010; Daina et. al., 2017; Tyzack and Karchmair, 2019).

2.5.4.5 Toxicity Analysis

Attrition due to toxicity is a major challenge in drug design and development, it is therefore important to identify and filter out toxic compounds before experimental as well as clinical testing. A good drug candidate must not have hepatic, hematologic, reproductive and cardiovascular toxicity. A potential drug must also be non-carcinogenic, non-mutagenic, non-teratogenic and must not have an irritating effect. Consequently, in-silico screening can be used to predict toxicity by identifying pharmacophores which are structural and physicochemical features that make a compound prone to toxicity (Tonholo et. al., 2020; Lagorce et. al., 2017).

For example, electrophilic drugs that form covalent bonds with nucleophilic sites on protein and DNA are predicted to be carcinogenic while highly lipophilic compounds have been shown to have CNS or neurotoxic effects due to their ability to permeate the blood-brain barrier. Also, certain chemical moieties predict cardiotoxic or hepatotoxic effects (Lagorce et. al., 2017).

Softwares available for predicting toxicity include Swiss ADME, Data warrior and Stardrop while commonly used programs include DEREK, ToxTree, HazardExpert, and CAESAR among others (Daina et. al., 2017; Rim, 2020).

2.6 Molecular Dynamics (MD)

Molecular dynamics is a computational technique that helps to predict and understand the properties, structure and function of molecular systems (Braun et. al., 2019). The technique considers both the ligand and protein as flexible; it studies the behaviour of molecules in different biological or chemical environments, ranging from small chemical systems to large biological molecules and material assemblies (Salmaso, 2018). Molecular dynamics compute the movement of atoms along time by the integration of Newton's equations of motions (classical mechanics) as shown in the equation,

$$F_i(t) = m_i \, d^2 r_i(t)/dt^2$$

where F_i is the force acting upon atom i at time t, m_i is the mass of atom i and $r_i(t) = (x_i(t), y_i(t), z_i(t))$. The forces between the particles and their potential energies are often calculated using interatomic potentials or molecular mechanics force fields (Salmaso and Moro, 2018; Chen et. al., 2019). The change in position of each atom per time is defined by ri(t), while the velocities vi(t) determine the kinetic energy and temperature of the system. As the atoms move their trajectories can be displayed and analysed, the dynamic motions that affect the functional properties of the system may then be traced at the atomic level. Consequently, MD simulations have been used extensively in biological systems to study the structure and dynamics of proteins in a modelled system rather than biological experiments.

In addition, MD evaluates the residue flexibility in the target binding site and explores larger conformational changes accessible to a protein. Molecular dynamics investigates, compares, analyses and visualizes chemical structures, it also gives qualitative and quantitative information about biological systems (Vlachakis, 2018). Therefore, molecular dynamics is an efficient tool for identifying receptor conformations for docking and evaluating the stability of predicted binding complexes (Pinzi and Rastelli, 2019).

Furthermore, MD simulations determine accurate and precise relative binding constants for protein systems. It analyzes biomolecular systems in different thermodynamic conditions (Dias et. al., 2008). This computational technique is usually performed using specific force fields that describe the potential energy of a system, these force fields consider forces that influence the

movement of atoms in a solvent system such as covalent bonds, dihedral angles, van der Waals and electrostatic potential. Examples of these force fields include AMBER (Wang et. al., 2004), NAMD (Phillips et. al., 2005), OPLS (Jorgensen, 1986), and GROMACS (van der Spoel et. al., 2005). Molecular dynamics simulation is highly computationally intensive hence it requires central processing units (CPU), graphic processing units (GPU), or cloud computing (Hollingsworth and Dror, 2018).

Molecular dynamics in combination with other docking methods helps to enhance virtual screening results and has been found useful in protein-ligand interactions. In a particular study, Ernsmark et. al., (2005) reported that MD simulation and in-vitro testing showed that diacylhydrazine derivatives are potent inhibitors of plasmepsin in *Plasmodium.* In another study, MD simulation, molecular docking and experimental testing was used to discover that epalrestat stabilized and inhibited aldose reductase (ALR 2), a protein implicated in the treatment of diabetic neuropathy (Ferreira et. al., 2015). MD has also been employed in host-virus interactions where hydroxychloroquine, azithromycin and ketoamide inhibitors have shown inhibitory properties for SARS-Cov-2 main protease (Zhang et. al., 2020).

Nevertheless, molecular dynamics has limitations such as the high cost of computation which could result in inaccurate sampling of conformational states. This is because MD simulations requires high-performance-computing units which are mostly unavailable and inaccessible in resource-poor countries (Ferreira et. al., 2015). Another challenge with MD is inaccurate approximations associated with the forcefields used for the simulation. To forestall this challenge, researchers have introduced quantum mechanics to refine the forcefields that characterize molecular systems (Durrant and McCammon, 2011). Despite these limitations, molecular dynamics complement molecular docking and improves the outcomes of structure-based drug design (Ferreira et. al., 2015).

2.7 Conclusions

Indeed, the structure-based virtual screening approach is a fast, labour-efficient and cost-efficient tool in drug development. The SBVS approach can accelerate the identification of new antimalarials with novel mechanisms of action and satisfactory pharmacokinetic properties. This can be achieved by using computational techniques such as molecular docking, druglikeness analysis and molecular dynamics to screen compounds with in-vitro antiplasmodial activity against falstatin, a multi-staged protein in *Plasmodium falciparum*.

Although SBVS does not replace laboratory bioassays, it complements physical laboratory screening and helps in hit identification and lead optimization of novel drug candidates. However, predictions obtained from the SBVS must be substantiated by biological assays and clinical trials.

Chapter Three: Research Methodology

This chapter presents a detailed description of the research methodology. It discusses various computational techniques used in this study such as homology modelling of falstatin, structure evaluation and validation of the built model, molecular docking, druglikeness analysis, molecular dynamics, structure stability analysis of the protein-ligand complex, redocking analysis using MM-GBSA scoring function and pharmacophore hypothesis generation.

3.1 Selection of Falstatin as Target

Falstatin is an inhibitor of cysteine proteases which have been widely reported in literature to facilitate the egress of erythrocytes, rupture of schizonts and degradation of haemoglobin (Pandey et. al., 2006; Sunderaraj et. al., 2014; Rosenthal et. al., 2014). Falstatin was selected as the target protein for this study based on the premise that the inhibition of falstatin could stop the invasion of erythrocytes and degradation of haemoglobin. Inhibition of falstatin could therefore halt the growth and lead to cellular death of the malaria parasite (Tusar et. al., 2021). In addition, falstatin was chosen as the protein target for this study because it was observed to have elicited its functions in schizonts and merozoites of *Plasmodium* life cycle (Rennenberg et. al., 2010). Therefore, it is intended that compounds that bind to falstatin could serve as novel antimalarials that target multiple stages of the life cycle of *Plasmodium*.

Furthermore, the expression data of falstatin was also obtained from PlasmoDB, a database of plasmodial proteins. The results showed that falstatin (Q81333) is closely related to chagasin and amoebasin. The protein sequence of falstatin was uploaded onto STRING webserver and interaction data is shown in Fig 8.

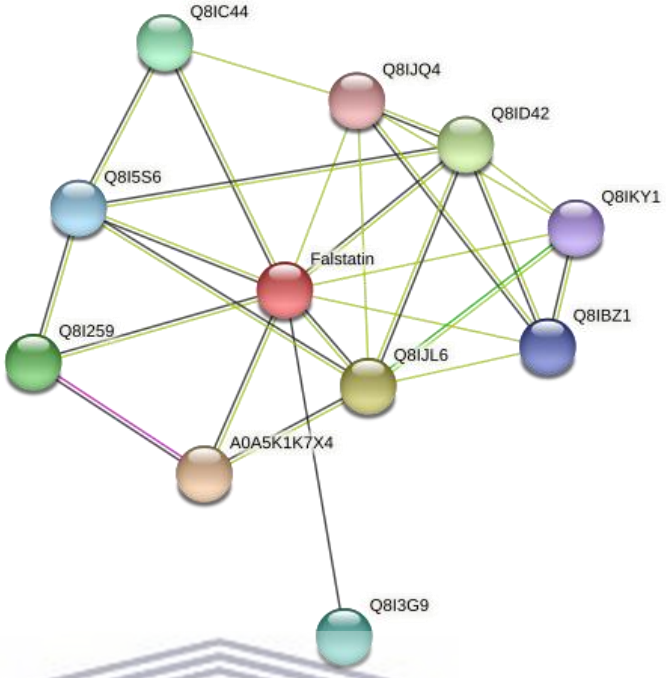

Figure 8. Protein interaction data showing proteins that falstatin interact with.

3.2 Homology Modelling of Falstatin

Homology modelling was used to generate the three-dimensional structure of falstatin due to the unavailability of the crystal structure of falstatin. The amino acid sequence of falstatin (Q8I333) was downloaded from Uniprot (Suzek et. al., 2007) and uploaded onto the Swiss Model, an open access web server, to build the three-dimensional model of the protein. The Swiss Model executed this by running a sequence similarity search using the Blast searching and HHblits algorithm to identify homologous templates (Waterhouse et. al., 2018; Camacho et. al., 2009). Potential templates were identified and ranked based on template quality as well as target-template alignment. The highest-ranking template, falcipain (3-pnr.1. B) was then selected for model construction based on sequence identity, coverage and the global model quality estimation (GMQE) score. Thereafter, the three-dimensional co-ordinates of the predicted falstatin model was built automatically based on the target-template alignment using the ProMod3 software on Swiss Model and downloaded in PDB format (Waterhouse et. al., 2018).

Homology modelling refers to building a protein model from homologous proteins which are known as templates, the templates with the highest sequence identity to the target protein are usually selected for the model construction. Homology modelling is based on the proposition that proteins with similar amino acid sequences have similar structures (Cavasotto and Phatak,

2009). It also relies on the assumption that the structural conformation of a protein is more highly conserved than its amino acid sequence, hence little changes in sequence usually result in minimal variation in the 3D structure of the protein (Vyas et. al., 2012). A template with 30% - 50% sequence identity to the target sequence can be used to build a low to medium accuracy protein structure while a template of < 15% sequence identity is considered speculative and could lead to misleading conclusions (Bishop et. al., 2008; Hillisch et. al., 2004).

However, homology modelling of protein structures has some limitations largely caused by incorrect side chain placement as well as inaccurate loop regions due to gaps in the alignment, but this can be resolved through model refinement. Model refinement optimizes the model through accurate modification of the backbone and side chains using forcefields that minimizes steric clashes in the sidechains and relaxes the backbone of the protein (Hasani and Barakat, 2017).

3.3 Prediction of Primary and Secondary Features of Falstatin

Also, the amino acid sequence of falstatin was uploaded into ProtParam (Garg et. al., 2016) and SOPMA (Geourjon and Deleage, 1995) which are online servers for predicting the primary and secondary features of proteins. The results obtained were downloaded and used for further analysis.

3.4 Structure Quality Assessment of the Predicted Falstatin Model

Structure quality assessment was used to evaluate the stereochemical quality and reliability of the predicted falstatin model. A model with good quality ensures excellent docking results and adequate inference from the protein-ligand interactions. Using the online server Pro-check facilitated by European Bioinformatics Institute (EBI) (Labarga et.al., 2007), the modelled falstatin (in PDB format) was uploaded onto the server. The Ramachandran plot (Laskowski et al., 1993), errat plot and the Z scores were then generated by the server (Wiederstein and Sippl, 2007). The Swiss Model server was also used to generate the Global Model Quality Estimate (GMQE) and Quality Model Energy Analysis (QMEAN) scores.

The Ramachandran plot was used to evaluate the quality of the modelled falstatin. The Ramachandran plot determines energetically favoured regions, torsion angles psi (ψ plot) against phi (φ) of amino acid residues present in a protein structure. Based on ϕ and ψ dihedral

angles, the Ramachandran plot analyzes the torsional angles of each amino acid residue and then classifies the residues into favourable, allowed and disallowed regions (Bhatnager et. al., 2020). The favoured and allowed regions (alpha-helical and beta-sheet) corresponds to conformations where there are no steric clashes while the disallowed regions indicate areas of protein with steric hindrance (Momen et. al., 2018).

The assessment of the modelled falstatin was performed through the ERRAT, PROVE and VERIFY3D tools. The ERRAT plot is a statistical analysis of the non-bonded atomic interaction of a protein structure, it plots the error values as a function of amino acid position (Colovos and Yeates, 1993). The PROVE program measures the degree of nativeness of a protein, it calculates the Z-score deviation of a model and compares it with Z scores of highly resolved proteins (2.0 A or more). Z-scores below 3 depicts good quality and are considered acceptable for predicted protein models (Eisenberg et. al., 1992).

The Swiss Model server produced quality assessment scores such as Qualitative Model Energy Analysis (QMEAN) and GMQE scores. The QMEAN Z-score compares a modelled protein with experimental structures of similar size. Scores above -4.0 indicates good model quality while QMEAN scores below -4 depicts low model quality (Benkart et. al., 2011). QMQE estimates the quality of a protein structure based on target-template alignment and template search method. QMQE scores are expressed as numbers between 0 to 1, where scores that are closer to 0 indicate high reliability of protein models (Benkart et. al., 2011).

3.5 Compilation of Compound Library

A total of 18, 000 antiplasmodial compounds were retrieved from the Malaria Box, the inclusion criteria of the selected compounds were based on the availability of chemical structure and biological activity against blood-stage *Plasmodium falciparum* (Bathurst and Henschel, 2006). The Malaria Box is a combination of compounds that have shown in-vitro antiplasmodial activity, It is a database generated from thorough laboratory screening of about four million compounds from GSK, Novartis, and St. Jude Children's Research Hospital library. The Malaria Box is a cross-section of chemically diverse compounds that have satisfactory oral absorption and minimal toxicity (Bathurst and Heschel, 2006). The selected compounds were collated in preparation for molecular docking.

3.6 Molecular Docking

The molecular docking was conducted to screen the compiled library in order to predict compounds with high affinity for the falstatin model. Using the Molecular Operating Environment (MOE) software, the docking procedure helped to obtain the minimum binding energy, attain optimized conformation and highest stability for the screened ligands (Vilar et. al., 2008; Dar and Mir, 2017). The docking process involved the following steps listed below,

Ligand Preparation

18, 000 compounds obtained from the Medicines for Malaria Venture (MMV) database were imported into the MOE database viewer. The selected compounds were then optimized by washing (explicit hydrogen added, protonation at PH7 and 3D structures generated), the addition of partial charges and energy minimization using Amber10: EHT force field. Thereafter, the energy minimized compounds were saved in mol2 format. The ligand preparation step was conducted for the correct assignment of stereochemistry, partial charges and ionization states of the ligands (Torres et. al., 2019).

Preparation of Protein

The modelled falstatin structure was protonated at PH7, energy minimized with Amber 10: EHT forcefield and partial charges added. Protein preparation was performed prior to molecular docking in order to specify the correct tautomerization and protonation state of the active site residues (Torres et al., 2019; Ferreira et. al., 2015).

Prediction of Active Sites

The active site of the modelled falstatin structure was predicted by using the site finder option on the MOE (Molecular Operating Environment) software. Following this, the site finder option identified possible binding pockets in the three-dimensional atomic coordinates of the protein.

Molecular Docking

Molecular docking was conducted to estimate the minimum free energy of binding of the ligands. Using the induced-fit method (Koshland, 1963) on the MOE dock module, the modelled falstatin was set as the receptor, the minimized compounds served as the ligand, and the triangle matcher was set as the ligand placement method. Thirty poses were generated for each ligand and the poses were scored based on London ΔG scoring function. The thirty poses were subjected to molecular mechanics (MM) refinement to obtain two final poses. The final docking score was evaluated with the GBVI/WSA ΔG scoring function with the Generalized Born solvation model (GBVI), the poses were then visualized using UCSF Chimera. The

minimum binding energies for each compound was generated and downloaded for further assessment.

The docking step was performed using the induced-fit method which considers both the ligand and receptor as flexible (Koshland, 1963). The Generalized Born solvation model eliminates explicit solvent water from the system, thereby speeding up the simulation process while the molecular mechanics refinement helped to obtain the lowest energy conformation of the ligands (Tsui and Case, 2000; Corbeil et. al., 2012).

3.7 ADME and Druglikeness Analysis

The druglikeness analysis was employed to identify compounds with favourable absorption, distribution, metabolism, excretion (ADME) and toxicity properties. Druglikeness analysis improves the hit rate and lowers the attrition of screened compounds by eliminating compounds with poor ADMET properties. To estimate the physicochemical properties of the ligands, the ADME, druglikeness and other chemical parameters of the compounds were predicted using Stardrop, a software developed by Optibrium (Earnshaw, 2010). Molecular descriptors of the ligands such as molecular weight, hydrogen bonds, partition coefficient between n-octanol and water, rotatable bonds, and polar surface area were estimated. These descriptors were used to assess the compounds for bioavailability, druglikeness and potential to inhibit cytochrome P450 enzymes. The compounds assessed were assigned values between 0 and 1 based on the rules of druglikeness and leadlikeness which include Lipinski's (Lipinski, 2002), Ghose's (Ghose et al., 2012), Veber's (Pollastri, 2010), Egan's (Egan, 2010), Muegge's rules (Muegge, 2002), and Pan assay interference compounds (PAIN) ((Baell et al., 2013; Brenk et al., 2008). Values closer to 1 suggest satisfactory ADME properties while values closer to 0 suggest poor ADME parameters.

Furthermore, OSIRIS DataWarrior software (Sander et. al., 2015) was used to predict the compounds carcinogenic, mutagenic, irritant, and reproductive properties based on correlation rules programmed into the software. The reproductive, tumorigenic, mutagenic and irritant effects of compounds were categorized as none, low, or high. Subsequently, ligands with lower risks of adverse effects were identified.

3.8 Prioritization of compounds and Generation of Ligand Score

The compounds were ranked based on their binding affinity, ADME properties and Toxicity properties. This was achieved by generating a ligand score for compounds with high binding energy and favourable physicochemical parameters.

Ligand score = (50% x Binding score %) + (20% x ADME score) + (30% x Toxicity score)

Where Binding score (%) = Binding energy of ligand/Maximum Binding Energy × 100

The compound with the highest ligand score was selected as the prioritized hit compound and was subjected to molecular dynamics and structure stability analyses.

3.9 Protein-Ligand Interaction Profiling

The protein-ligand (falstatin-TCMDC 131646) complex was uploaded onto the Protein-Ligand Interaction Profiler server (Salentin et. al., 2015) to gain insight into the protein-ligand interaction at the falstatin binding pocket. TCMDC 131646 was selected for the profiling because it is the highest-ranking compound (see 3.8). The server generated the interactions such as hydrophobic bonds, hydrophilic bonds, hydrogen bond donors as well as hydrogen bond acceptors between TCMDC 131646 and the modelled falstatin structure.

3.10 Molecular Dynamics Simulation

Molecular dynamics was conducted to study the stability of falstatin in the presence and absence of TCMDC 131646. The highest-ranking ligand, TCMDC 131646 was selected for the simulation because it has high affinity for falstatin (-6.28kcal/mol) and satisfactory ADMET properties. The unbound falstatin and falstatin-ligand complex ((N-methyl-2-[(2-naphthalen-1-yloxyacetyl)amino]acetamide) were separately subjected to molecular dynamics simulations using the Simulation module in Molecular Operating Environment (MOE 2019.01). The falstatin-ligand complex and falstatin receptor were protonated and energy minimized with the OPLS-aa force field (Kaminski et. al., 2001) to get the stable conformer of the unbound protein and protein complex in a vacuum (molecular system). Thereafter, each molecular system was parameterized by solvating in a TIP3P water-box (with 10A distance between the edges of the box) and "Optimized Potentials for Liquid Simulations" (OPLS-aa) forcefield which is suitable for proteins in solvents. Molecular dynamics simulations were carried out by heating each molecular system to 310 K (37 0C). Then, each molecule system was equilibrated at 310K (37 0C) for 10 nanoseconds. Following this, the simulation step was used to generate the trajectory of the molecular system at 310 K using the Nose–Poincare–Andersen algorithm (Sturgeon and Laird, 2000) for 100 nanoseconds (the time step of each simulation was set to 0.02

picoseconds). VMD software (Humphrey et. al., 1996) was then used to visualize the data while the trajectories obtained from each system (unbound falstatin and falstatin-ligand complex) were downloaded for further analysis.

The energy minimization step was conducted to fully relax the system (Ndagi et. al., 2017). The number of energy minimization steps was employed so that the systems could reach convergence and to prevent steric hindrance during the simulation (Roccatano, 2020; Cygan and Kubicki, 2018). The molecular system was heated to 310K in order to mimic the normal temperature of the body while the equilibration ensured that the system attains steady temperature and pressure resulting in thermodynamic stability (Lemkul, 2018). The Nose–Poincare–Andersen (NPA) algorithm for isothermal-isobaric simulations is particularly useful in achieving improved stability for long-term simulations (Sturgeon and Laird, 2000) while the Optimized Potentials for Liquid Simulations (OPLS-aa) forcefield appropriate for proteins in solvent systems was used to parameterize and calculate the potential energy of the system (Jorgensen and Tirado-Rives, 1988).

3.11 Structure Stability Analysis of the Protein and Protein-ligand Complex

The trajectories of the unbound falstatin and falstatin-TCMDC 131646 complex were evaluated for structural stability and flexibility. The trajectories obtained from molecular dynamics were uploaded into Usegalaxy.eu server (Afgan et. al., 2016). Following this, root mean square deviation (RMSD), root mean square fluctuation (RMSF), principal component (PC), hydrogen bond and dynamic cross-correlation matrix (DCCM) analyses were carried out on the trajectories. The graphs obtained were evaluated for structural stability and flexibility.

The RMSD calculates the average displacement of atoms or residues over time (Elfiky, 2021). The RMSD helped to measure changes in the conformation of falstatin and falstatin-hit complex over the simulation period, lower RMSD depicts higher stability while higher RMSD depicts lower stability. The RMSF shows the average fluctuation of an atoms or residue over time (Muralidharan, 2021). Lower RMSF depicts higher stability while higher fluctuations suggest lower stability of the molecular system. The principal component analysis determines the relationship between statistically meaningful conformations or motions sampled during a trajectory. The PC analysis converts a set of correlated observations (movement of selected atoms in the protein) to a set of principal components (PCs) that are linearly independent or uncorrelated (Islam et. al., 2020).

The DCCM is a three-dimensional matrix representation that analyzes time-correlated motion between the residues of the proteins in a molecular system (Ndagi et. al., 2017). The DCCM residue-based correlation data can be interpreted using visual pattern recognition. Highly positive regions represent strongly correlated motions while negative regions depict anti-correlating movements (Zhang et. al., 2018; Abseher and Nilges, 1998). The hydrogen bonding analysis calculated the number and occupancy of the hydrogen bonds during the simulation period.

3.12 Analysis of Chemical Diversity

The chemical diversity analysis was conducted to investigate the structural similarity or distinction between the prioritized hit TCMDC 131646 and selected antimalarial compounds such as chloroquine, lumefantrine, artemether and artemisinin. The analysis is based on the assertion that the chemical diversity of a compound suggests a unique mechanism of action (Egieyeh et. al., 2009). OSIRIS DataWarrior (Sander et al., 2015) was used to explore the chemical space occupied by chloroquine, lumefantrine, artemether and the best scoring ligand, TCMDC 131646. The output was then visualized on a 3D scatter plot in the software.

3.13 Rescoring Analysis of the Top-ranked Compounds

Rescoring of the top-scoring ligands was done using the Molecular Mechanics-Generalized Born Surface Area (MM-GBSA) scoring function to gain insight into the component energies of the ligand-protein binding. Using Schrodinger Maestro, the top-scoring compounds were redocked and post-processed with the MM-GBSA scoring function to estimate the free energy of binding of selected compounds with the highest ligand scores (see method 3.8). The SMILES structure of the top 5 compounds was uploaded into Schrodinger Maestro and minimized using the OPLS force field incorporating implicit water, solvation and convergence conditions. The protein was prepared for the docking step using the protein preparation wizard on Schrodinger, minimized with the OPLS force field and binding site predicted using Site map on the Maestro. The molecular docking module on Schrodinger was then used to examine and rescore the binding interaction between the modelled falstatin and the top-scoring compounds. The free energy of binding was determined based on the equation below.

$$\Delta Gbind = \Delta H - T\Delta S \approx \Delta E_{MM} + \Delta Gsolv - T\Delta S,$$

$$\text{where } \Delta EMM = \Delta E \text{ (internal)} + \Delta E \text{ (electrostatic)} + \Delta E \text{ (vdw)},$$

$$\text{and } \Delta Gsolv = \Delta G_{PB/GB} + \Delta G_{SA}$$

where ΔEMM, ΔGsol and -TΔS represent changes of the gas phase molecular mechanics energy, the solvation free energy, and the conformational entropy upon binding, respectively. ΔEMM includes ΔEinternal (bond, angle, and dihedral energies), ΔEelectrostatic (electrostatic), and ΔEvdw (van der Waals) energies. ΔGsolv is the sum of electrostatic solvation energy (polar contribution), ΔGPB/GB is the nonelectrostatic solvation component (nonpolar contribution), ΔGSA. The polar contribution is calculated using the Generalized Born model, while the nonpolar energy is determined from solvent accessible surface area (Hou et. al., 2011).

The OPLS force field was used for energy minimization because it incorporates solvation energy, hence it is considered appropriate for proteins in solvents (Damm et. al., 1997). The MM-GBSA scoring function is useful for rescoring, conformer stability and protein-ligand interaction (Genheden and Ryde, 2015). Thus, the MM-GBSA scoring function was used because it is computationally efficient and suitable for accurate ranking of inhibitors in virtual screenings (Wang et. al., 2019; Hou et. al., 2011; Sun et. al., 2014).

3.14 Development of Pharmacophore Hypothesis Based on Top-scoring Compounds

The goal of the pharmacophore hypothesis was to develop a pharmacophore model based on the top-scoring compounds which can then be used as a reference to screen other libraries in the future. To extract the common chemical features from 3D structures of the top-ranking compounds, the PHASE (Dixon et. al., 2006) module of Schrödinger suite was used to develop pharmacophore models for the top-ranked compounds. Six built-in features in PHASE are hydrogen bond donor (D), hydrogen bond acceptor (A), hydrophobic group (H), negatively charged group (N), positively charged group (P), and aromatic ring (R). The "Develop pharmacophore hypothesis" module integrated into PHASE was used to create pharmacophore models using the top-ranked compounds obtained from method 3.8. All the ligands were then prepared with the LigPrep module (Schrödinger Release 2018-2: LigPrep). After this step, the active ligands were aligned to find their best alignment and common features, the number of features in the hypothesis was chosen as four and hypothesis feature tolerance was set at 2.0 Å. Maximum and minimum number of acceptors (A), donors (D), hydrophobic (H), negative ionic (N), positive ionic (P), and aromatic rings (R) allowed are 0 and 3, respectively. Hypothesis matching criteria was set to match at least 75% of the active ligands. Also, the ranking of the compounds and hypotheses was completed using the PHASE hypo scoring function. Phase

scored and ranked possible feature combinations to produce common pharmacophores through the calculation of vector, volume, site scores, survival scores, and survival activities.

A pharmacophore model is defined as an ensemble of steric and electronic features that is necessary to ensure optimum interactions with a specific biological target (Yang, 2010). The pharmacophore hypothesis was established by aligning the top-scoring ligands and extracting common physicochemical descriptors from 3D structures of top-scoring ligands representative of essential interactions between the ligands and the falstatin model (Yang, 2010). The pharmacophore hypothesis was based on physicochemical descriptors such as HBA − Hydrogen Bond Acceptor; HPh − Hydrophobic; HBD − Hydrogen Bond Donor; PI − Positive Ionisable; HBAl − Hydrogen Bond Acceptor Lipid; RA − Ring Aromatic.

3.15 Summary of Methodology

The general scheme of this study is represented in the workflow below (Fig 9).

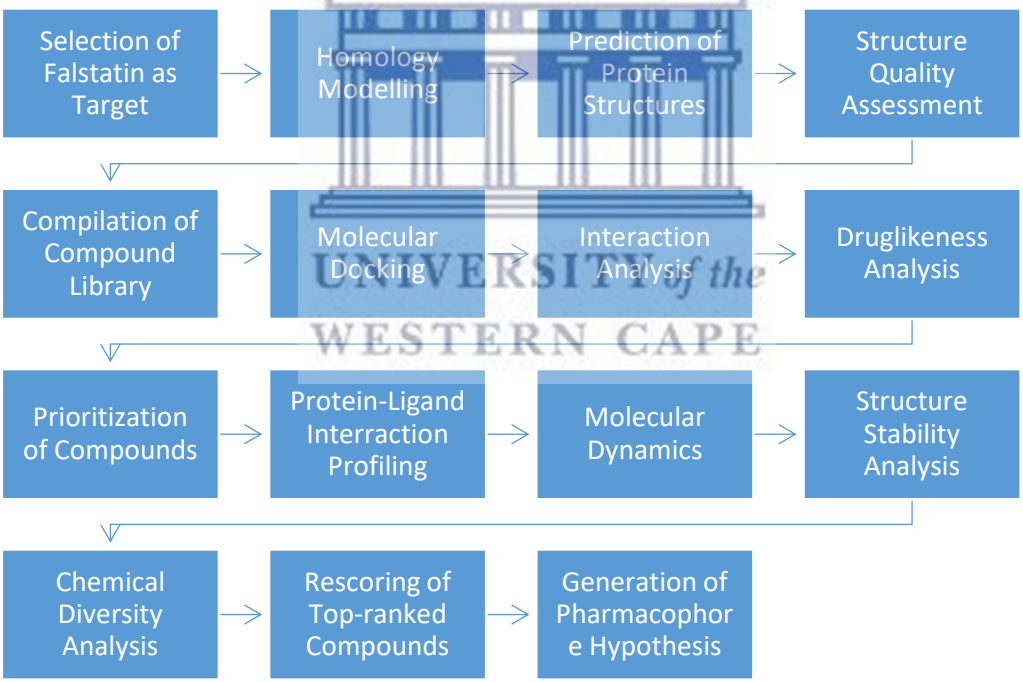

Figure 9. Workflow showing the methods used in this study

Initially, falstatin was selected as the target protein based on its ability to facilitate degradation of haemoglobin, erythrocytic egress and rupture of schizonts by free merozoites while the crystal structure of the selected target, falstatin (Q8133) was constructed using the Swiss Model server (Schwede et. al., 2003). The primary and secondary features of the modelled falstatin was predicted using the SOPMA and protParam webservers while the modelled falstatin structure was assessed through PROCHECK server (Laskowski et. al., 1993) using Errat,

Ramachandran and Z-scores as well as QMEAN and QMQE scores automatically generated from Swiss Model. Antiplasmodial compounds compiled from the Medicines for Malaria Venture database were docked against falstatin using the MOE virtual screening software. After docking, a binding energy of −6.1 KJ/mol was selected as the cut-off and ligands with binding affinities above this cut-off were exported onto Optibrium Stardrop for druglikeness analysis. The druglikeness analysis excluded compounds with poor oral bioavailability based on Lipinski's rule of 5, Veber and Egan's rules of druglikeness. Datawarrior was further used to predict the tumorigenic, mutagenic, reproductive, and irritant effects of the compounds and the compounds were ranked according to their binding energies, ADME and toxicity scores. After this step, the highest-ranking compound was subjected to protein-ligand interaction profiling using the PLIP server, chemical diversity analysis and molecular dynamics. Rescoring analysis was then performed on the 5 topmost compounds using the Schrodinger suite and a pharmacophore hypothesis was developed based on the top-scoring compounds.

Chapter Four: Results and Discussion

This chapter presents a detailed result of the structure-based virtual screening of antiplasmodial compounds against falstatin in *Plasmodium falciparum.* It describes the findings obtained from homology modelling, structure quality evaluation of the predicted falstatin model, molecular docking, druglikeness analysis, protein-ligand interaction profiling and chemical diversity analysis. The chapter further highlights the results of the molecular dynamics simulation, structure stability analysis of trajectories obtained from the simulation, rescoring analysis, development of pharmacophore hypothesis followed by a summary of the major findings from the study.

4.1 Homology Modelling

Homology modelling relies on the assumption that structurally related proteins have similar sequences and similar protein structures, thus detectable levels of sequence similarity imply significant levels of structural similarity. It also based on the proposition that the structural conformation of a protein is more highly conserved than its amino acid sequence, thus small or medium changes in the sequence only results in little changes in the 3D structure (Muhamed and Aki-Yalcin, 2019; Hasani and Barakat, 2017). A QMQE score close to 1 and a sequence identity of 30 - 50% is generally considered acceptable for building a model while a sequence similarity of less than 30% is considered speculative and inappropriate for protein modelling due to alignment errors, incorrect side chain packing and loop modelling (Idris et. al., 2020).

Based on sequence identity, coverage and GMQE score, the sequence alignment (Fig 10) revealed that falcipain-2 (3 pnr. 1.B) is the most identical homologue of falstatin, thus falcipain-2 was selected as the template for building the predicted falstatin structure. From the results, falcipain presented the highest sequence identity of 41.98%, coverage of 0.39, GMQE of 0.25 and a resolution of 2.6 Å relative to other templates. The results indicate that falcipain-2 has a sequence identity of 41.98% which falls within the acceptable value of 30% - 50%, and a resolution greater than 2Å. Therefore, falcipain-2 is appropriate and reliable for building the falstatin model (Fig 11).

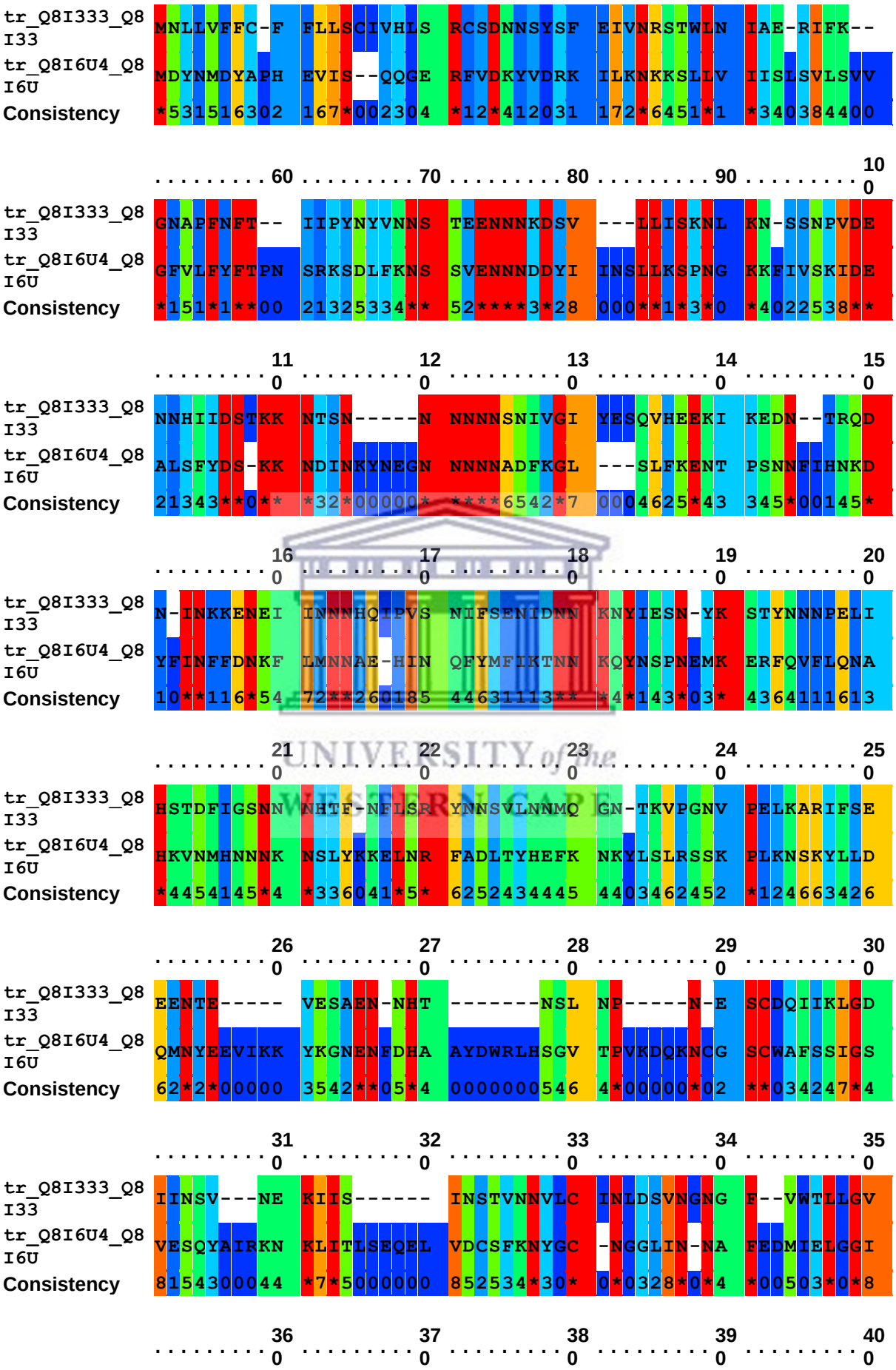

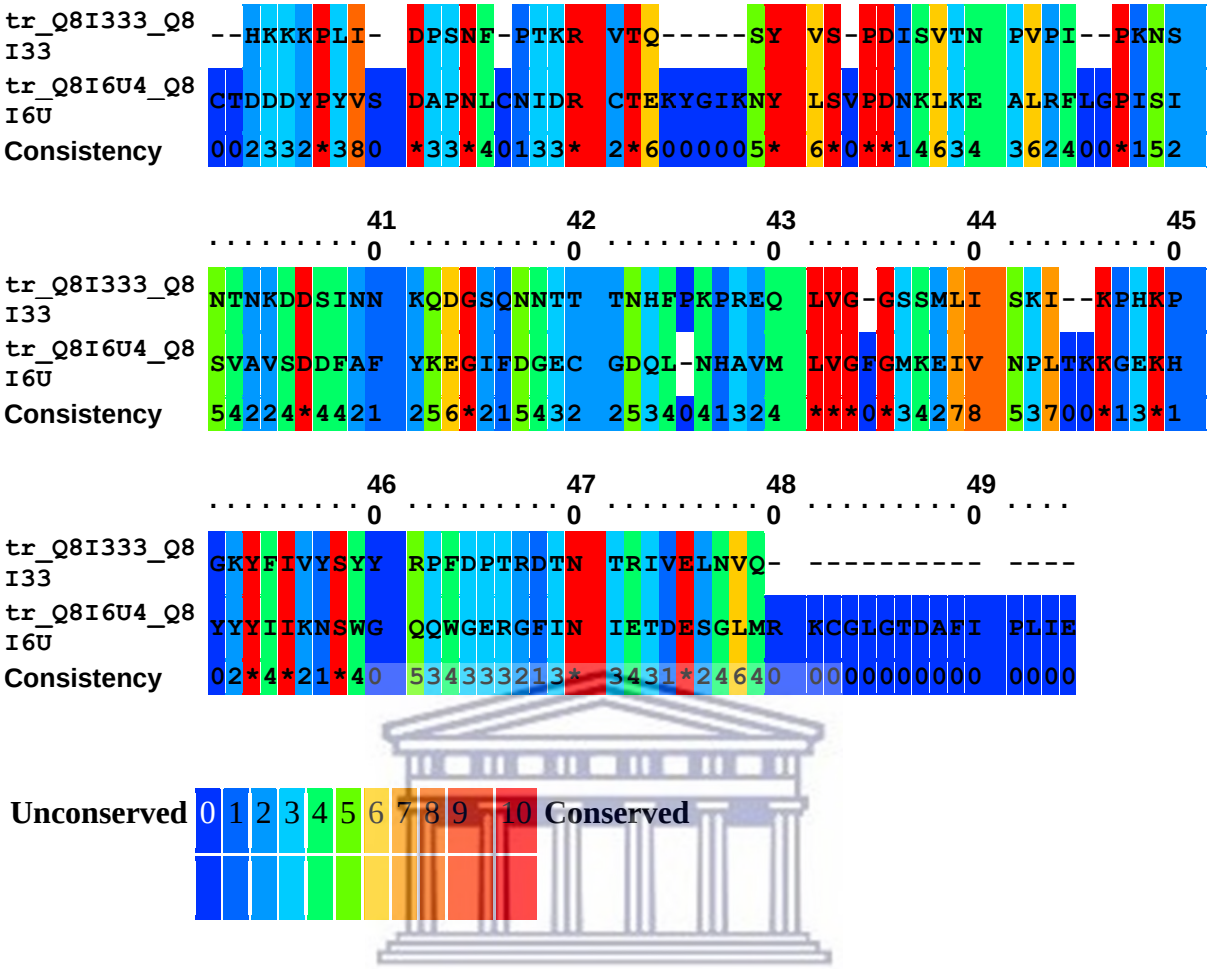

The colours are assigned from blue to red and the scoring scheme works from 0 for the least conserved alignment position, up to 10 for the most conserved alignment position.

Figure 10. Target template alignment of falstatin (Q81333) and falcipain-2 (Q8I6u4)

Figure 11. Model of falstatin built from the fasta sequence on Swiss Model.

Furthermore, the primary and secondary structural features of falstatin was calculated by ProtParam and SOPMA respectively which revealed that falstatin is composed of 16.95% alpha helix and 49.15 % random coils along with 26.39 % extended strands, 7.15 % beta turns. The N-terminal of the sequence considered is methionine. The abundance of coiled region indicates higher conservation and stability of the modelled falstatin.

4.2 Structure Quality Assessment of the Falstatin Structure

Structure quality assessment was conducted to examine the reliability of the predicted falstatin structure. The process helps to infer adequate interactions between the ligands and the predicted falstatin structure (Paramashivam et. al., 2021). The structure quality analysis is important because the quality of a protein model determines the success of the molecular docking process. As such, a good quality model will yield excellent docking results and vice versa. Therefore, the protein model was evaluated using the following methods.

4.2.1 ERRAT Plot

Using ProCHECK, the ERRAT plot analysis of the falstatin structure (Fig 12) showed an overall quality factor (OQF) of 84.46% which is greatly higher than the generally accepted score of 50% or more (Soni et. al., 2017; Colovos and Yeates, 1993). Careful observation of the falstatin model showed that the few regions that were not properly folded are not in the binding site. The high-quality factor of 84.46% showed that the residues of the falstatin model are properly folded and have low error rate. Hence, the result indicates that the model is reliable and suitable for molecular docking. Nonetheless, the few regions that are not properly folded will be refined by energy minimization before docking.

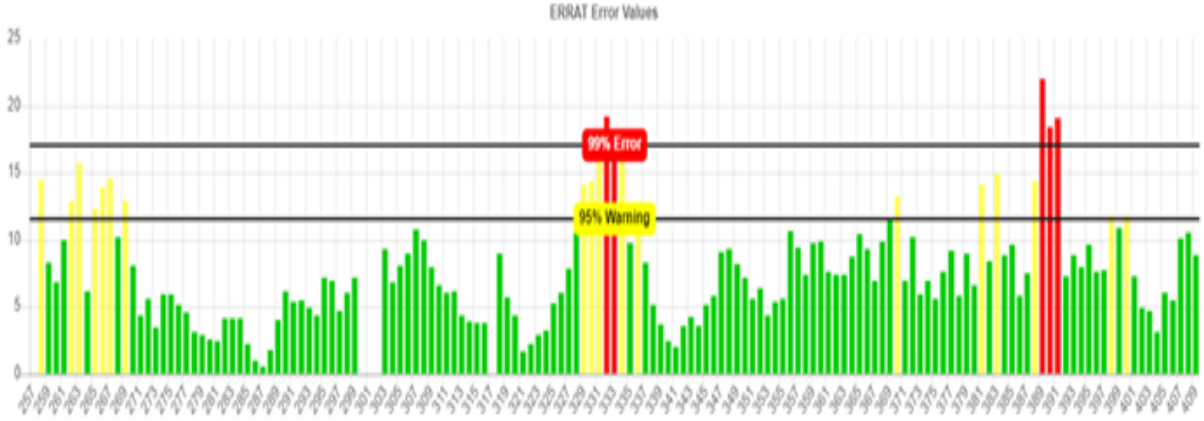

Figure 12. Errat plot of predicted falstatin model. The green bars indicate properly folded regions, yellow bars represent less properly folded regions at 95% confidence level and red bars are improperly folded regions at 99% confidence level.

4.2.2 Ramachandran Plot

The Ramachandran plot evaluated the quality of the protein structure by analyzing the main torsion angles Phi, Psi (φ, ψ) of amino acid residues present in the predicted falstatin model. The Ramachandran plot (Fig 13) showed that 99.3% of the residues in the predicted model are in the allowed regions with 87.0% in the most favoured regions (red), 12.3% in the allowed region (yellow) and 0.7% in the disallowed regions (white). The results obtained indicates that the generated falstatin model has good stereochemical quality and can be used for the docking studies. The disallowed region which depicts areas with bad angles were further resolved by energy minimization.

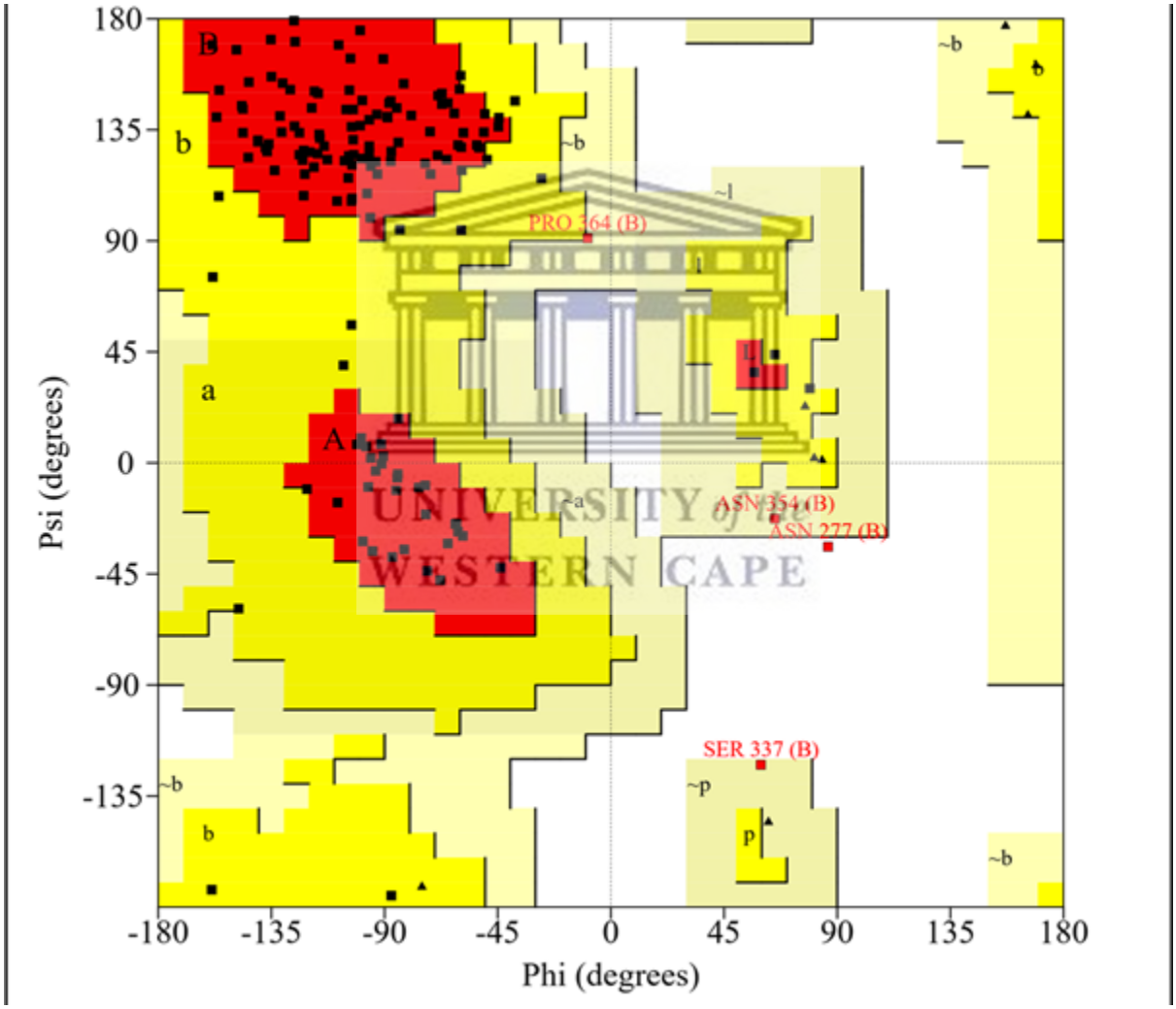

Figure 13. Ramachandran plot analysis of predicted falstatin structure showing 87.0%, 12.3% and 0.7% residues in favoured (red), allowed (yellow) and disallowed (white) region.

4.2.3 Z-Score and Local Energy Profile

The Protein Sequence Analysis Tool (PROSA) generated a Z-score of -5.27 (Fig 14) which is below 3, the score therefore indicates that the falstatin model is reliable for use in the docking procedure (Eisenberg et. al., 1992). Also, the local energy profile of the amino acids (Fig 14)

showed that all residues across the sequence have negative values implying favourable energy profile and high reliability of the model.

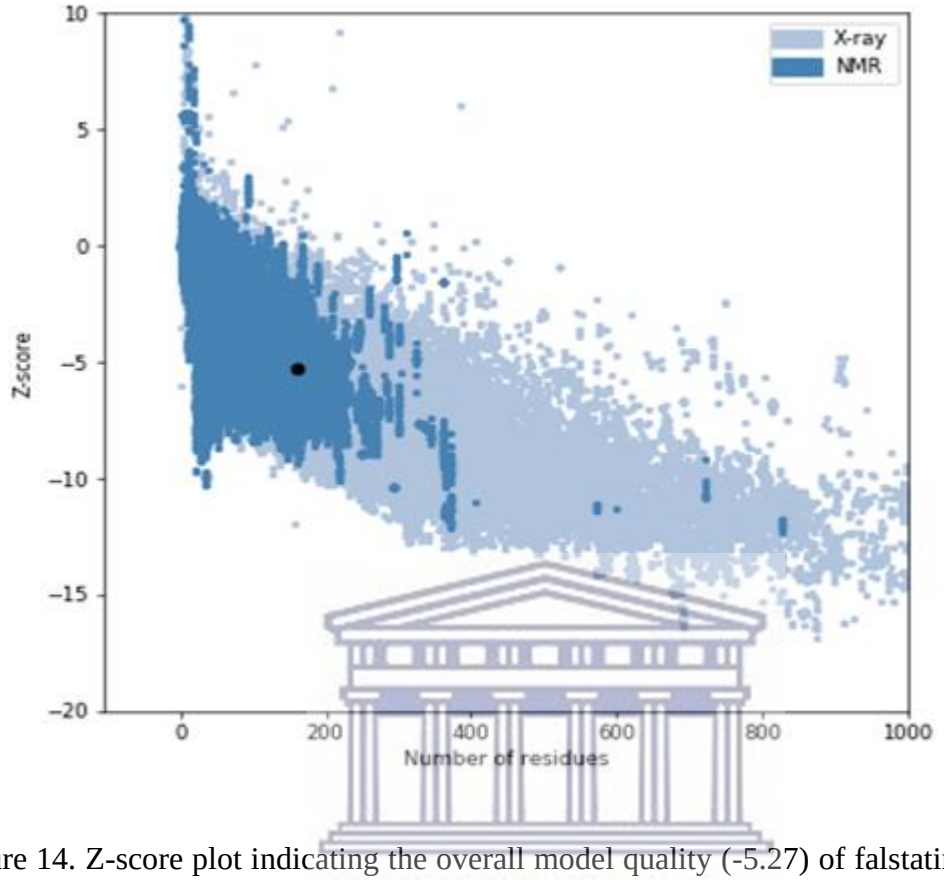

Figure 14. Z-score plot indicating the overall model quality (-5.27) of falstatin obtained from PROSA.

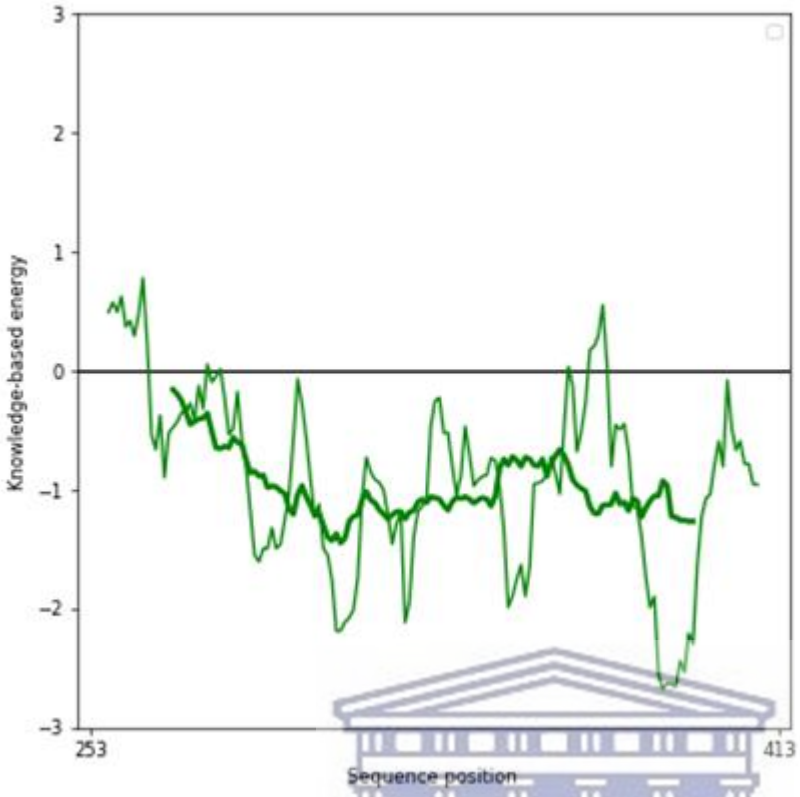

Figure 15. Amino acid local energy profile of falstatin model generated from PROSA

4.2.4 Global Quality Score

The qualitative model energy analysis (QMEAN) is an estimate of the degree of nativeness of a model, thus it was used for evaluating the structure quality of the falstatin model. Scores of 0 and not lower than -4 indicate good model quality while scores of -4 and below indicate low quality (Benkart et. al., 2011). Using SwissModel, the QMEAN score was -1.27 which is higher than -4. Hence, the results obtained showed that the modelled protein has a high level of confidence and is reliable for the molecular docking studies.

The ERRAT plot, Ramachandran plot, Z-score plot, QMEAN and local energy profile indicated that the built falstatin model is suitable for molecular docking. Consequently, the structure quality assessment of the predicted falstatin structure affirms that the falstatin model is reliable for the docking studies.

4.3 Active Site Identification of the Predicted Falstatin Model

The active site of the modelled falstatin structure was predicted using the MOE software. The active site of the predicted falstatin structure comprised of Pro-332, Lys-335, Asn-288, Asp-342, Val-293, Phe-292, Ile-333, Ile-345, Leu- 375, Tyr-393 and Trp-294.

4.4 Molecular Docking

Molecular docking was carried out to predict the compounds that have high affinity for the falstatin active site. The docking step achieved this by estimating the minimum binding energies of the ligands to the predicted falstatin structure. Based on the induced-fit model (Koshland, 1963), the molecular docking results (Appendix 1) showed that the docked compounds had their binding energies (S score) within the range of -9.798 KJ/mol and -4.033 KJ/mol. A binding score cutoff, defined as -6.10KJ/mol, was used to filter the compound library. The cut-off was determined as 60% of the highest binding energy and ligands that did not fulfil this constraint were automatically excluded from the screening. Lower binding energies predict higher affinity between the ligands and the falstatin model (Wang et. al., 2020; Chen et. al., 2006). The results (Appendix 1) suggests that all the compounds above the cutoff had negative binding energies, and a potential to bind strongly to the falstatin active site.

We can conclude that the molecular docking was able to predict compounds that could inhibit the target protein falstatin in *Plasmodium falciparum*. Also, the molecular docking excluded 9630 compounds that have low affinity for falstatin from the virtual screening corroborating the premise that structure-based virtual screening filters out low-affinity compounds from a compound library (Maia et. al., 2020).

4.5 Interaction Analysis

The interaction analysis was done to investigate the binding of the hits at the falstatin active site. This step facilitates lead optimization which is used for enhancing the affinity, activity and selectivity of a compound for the binding target which ultimately reduces the risk of adverse effects. Also, the hydrogen bonds and hydrophobic bonds of the hits can be manipulated to improve properties such as solubility while still maintaining their affinity for falstatin (Baxter and Lockey, 2001; Halogen, 2007). The binding energies and the interactions of top falstatin inhibitors are represented in Table 1.

Table 1. Table showing hydrogen bonds, hydrophobic interactions and docking scores of top binders to falstatin

Number	Compounds	Docking score (KJ)	Hydrophobic bonds	Hydrogen bonds
1	TCMDC 137201	-9.80	PRO^{332}, VAL^{331}, PRO^{396}, PHE^{292}, VAL^{293}	PRO^{332}, ASP^{342}, GLY^{289}

2	TCMDC 138644	-9.71	PRO^{332}, VAL^{293}, PHE^{361}, TYR^{393} VAL^{287}, ILE^{345}, ILE^{333}, PHE^{292}, PHE^{393}, LEU^{375}	LYS^{335}, ASP^{342} ASN^{288},
3	TCMDC 141516	-9.66	PRO^{332}, VAL^{331}, PHE^{292}, VAL^{316}, ILE^{345}, ILE^{333}, PHE^{292}	ARG^{395}, GLY^{291}, ASP^{342}
4	TCMDC 139411	-9.61	PRO^{332}, PHE^{292}, PRO^{396}, VAL^{293}, TYR^{393}, VAL^{331}, ILE^{345}, ILE^{333}, PHE^{397}, LEU^{375}	ASN^{336}, LYS^{335}, ASP^{342}
5	TCMDC 137241	-9.61	PRO^{332}, VAL^{293}, PRO^{396}, VAL^{331}, ILE^{345}, ILE^{333}, PHE^{292}, PHE^{397}, VAL^{316}, PRO^{312}	LYS^{335}, ASN^{288}
6	TCMDC 124274	-6.36	PRO^{332}, PHE^{292}, ILE^{345}, ILE^{333}, VAL^{293}, LEU^{375}	LYS^{335}, ILE^{345}, GLY^{291}, ASN^{336} ASN^{288}, SER^{344}
7	TCMDC 131646	-6.15	PRO^{332}, PHE^{292}, VAL^{293}, LEU^{375}, TYR^{393}, VAL^{287}	LYS^{335}, ILE^{345}, ASN^{228}, ASN^{336}
8	TCMDC 138266	-6.25	PRO^{332}, VAL^{293}, TYR^{393}, TRP^{294}, VAL^{287}, ILE^{345}, ILE^{333}, PHE^{292}, LEU^{375}	LYS^{335}, ASN^{288}, GLY^{289}
9	TCMDC 123844	-6.28	PRO^{332}, PHE^{292}, ILE^{345}, VAL^{293}	LYS^{335}, ASN^{288}, ASN^{336}
10	TCMDC 131234	-6.10	PRO^{332}, VAL^{293}, PHE^{292}, PRO^{396}, ILE^{345}, PHE^{397}	ASN^{336}, ASN^{288}

From the results (Table 1), it is evident that Pro-332, Val-293, Asp-342 and Lys-335 are amino-acid residues that are essential for stabilizing the ligands at the active site of falstatin. The analysis further suggests that the high number of hydrophic interactions and hydrogen bonds play a vital role in stabilizing the compounds at the active sites. Lys-335, Asp-342 and Asn-336 were involved in the formation of hydrogen bonds while Pro-332, Val-293 and Phe-292 were involved in most of the hydrophobic interactions. We also observed that 9 out of 10 of the ligands formed one or more hydrophobic bonds with PRO residues and 8 formed hydrogen bonds with LYS residues. This corroborates the report that proline is often found in the active

site of proteins and plays a dominant role in the binding of proteins to inhibitors (Williamson, 1994).

4.6 Druglikeness / ADMET Analysis

Druglikeness analysis was used for filtering the docked compounds in order to identify compounds with favourable absorption, distribution, metabolism, excretion and toxicity (ADMET) properties. Compounds with favourable ADMET properties might have greater chances of success during in-vivo experimental bioassays (Moreira et. al., 2021; Umar et. al., 2021). The analysis employed Stardrop (Earnshaw, 2010) to predict the physicochemical properties and ADME parameters of the ligands.

The druglikeness analysis (Appendix 2) revealed that the molecular descriptors of compounds with top ADME scores were all within acceptable limits. These include molecular weight ≤ 500g/mol, hydrogen bond donors ≤ 5, hydrogen bond acceptors ≤ 10, log P ≤ 5, molar refractivity between 40 and 130, the number of rotatable bonds ≤ 10, and the topological polar surface area (TPSA) ≤ 140. All the compounds with high ADME scores also conformed to Lipinski, Veber, Egan, Brenk and Muegge's rules. Similarly, the results (Appendix 2) showed that some compounds have good ADME scores but have low affinity for falstatin during the docking process while some compounds that have low ADME scores had high affinity for the falstatin active site. This necessitated the need for a ligand scoring that considers the ADME score, binding energy and toxicity profile.

We can conclude that compounds with good ADME scores are likely to have good oral bioavailability and are not likely to fail due to poor oral bioavailability. Following the ADME analysis, all the top-ranking compounds were further subjected to toxicity analysis using Datawarrior.

4.6.1 Toxicity Analysis

Toxicity analysis was conducted to predict the safety of the compounds, the toxicity analysis predicted toxicity by identifying pharmacophores that could cause hepatic, hematologic, reproductive and cardiovascular toxicity, the technique also estimated the tumorigenic, mutagenic, reproductive and irritant effects of compounds. Consequently, the toxicity analysis could lower the risk of attrition during clinical trials by filtering and eliminating compounds with low safety profiles (Kramer et. al., 2007; Dearden et. al., 2003; Tonholo et. al., 2020). OSIRIS DataWarrior software was used to predict the carcinogenic, mutagenic, irritant and

reproductive properties of the compounds (Sander et. al., 2015). The analysis categorized the toxicity potential of the compounds as none, low, or high and ligands with lower risks of adverse effects were identified as shown in Table 2.

Furthermore, the binding energy, ADME and toxicity of the compounds were computed to generate a ligand score, the ligand scores were ranked, and the top 5 compounds were selected as presented in Table 2.

Table 2. Binding energy, ligand scores and ADMET scores of prioritized compounds

CHEMBL ID	Molecular Formula	Molecular weight	Mutagenic Effect	Tumorigenic Effect	Reproductive Effect	Irritant Effect	Binding Energy	ADME Score	Toxicity Score	Ligand Score
TCMDC-131234	$C_{15}H_{15}N_2O_5S$	336.367	None	None	None	None	-6.36	0.6891	0.25	75.4
TCMDC-123844	$C_{15}H_{21}N_3O_2$	275.351	None	None	None	Low	-6.28	0.7598	0.19	73.1
TCMDC-131646	$C_{15}H_{20}N_2O_3$	272.303	None	None	None	None	-6.15	0.6922	0.25	77.1
TCMDC-124274	$C_{15}H_{15}N_2O_5S$	336.367	None	None	None	None	-6.36	0.6891	0.25	75.4
TCMDC-138266	$C_{15}H_{15}N_3O_3S$	317.368	None	None	None	None	-6.25	0.6751	0.25	75.4

The results (Table 2) suggested that the top-compounds have good safety profile, the analysis predicted that TCMDC 131234, TCMDC 138266, TCMDC 131646, TCMDC 124274 have toxicity scores of 0.25 each and showed no potential to have reproductive, mutagenic, and tumorigenic effects. On the other hand, TCMDC 123844 which was predicted to have a low irritant effect showed a toxicity score of 0.19. Nevertheless, the irritant effect can be eliminated by improving the solubility or pKa of the compound in solution.

The results suggest that all the top compounds are unlikely to suffer attrition due to toxicity. Thus, the analysis corroborates the assertion that toxicity analysis eliminates compounds with low safety profile which could in turn prevent late-stage attrition (de Sousa et. al., 2020; Rudrapal and Chetia, 2020).

4.7 Generation of Ligand Score

The ligand score is a delicate balance of the desirable parameters such as binding energy, low toxicity and good absorption, distribution, metabolism, excretion and toxicity profile (ADME) of the screened compounds. The ligand score takes into consideration the efficacy and safety of a potential antimalarial candidate. The binding energy of the hits to falstatin represents efficacy while the ADMET properties indicate the safety of the compounds. The ligand score was computed based on a total weighting of 50% efficacy, 20% on ADME properties and 30% on toxicity. The 30% weighting on toxicity is based on the premise that toxicity is a major consideration when developing antimalarial drugs. This is because malaria occurs mostly in children under 5years and pregnant women who undergo rapid growth as well as development and are therefore prone to drug toxicity (WHO, 2020).

The ligand score is computed in the equation below,

Ligand score = (50% x Binding score %) + (20% x ADME score) + (30% x Toxicity score)

Where Binding score (%) = Binding energy of ligand/Maximum Binding Energy × 100

And Toxicity = 0.25 (Tumorigenic + Mutagenic + Reproductive + Irritant) effects.

Where *Toxicity* was scored as: None = 100%

High = 80%

Low = 40%

The results obtained are shown in Table 2 above,

From the results obtained, TCMDC 131646 had the highest ligand score of 77.1 with a binding energy of -6.15 KJ/mol while TCMDC 123844, TCMDC 138266, TCMDC 124274 TCMDC 131234 had ligand scores of 73.1, 75.4, 75.4 and 75.4 respectively. The top compounds showed

a minimum and maximum ligand score of 73.1 and 77.1 respectively on a total scale of 100. TCMDC 123844 showed a markedly lower ligand score due to its predicted potential to cause irritant effects. All the top compounds are expected to have good in vitro/in vivo ADMET properties as well as high affinity for falstatin. In all, TCMDC 131646 having the highest ligand score was predicted to be the most favourable compound in terms of affinity for falstatin and satisfactory pharmacokinetic parameters.

A closer look at TCMDC 131646 showed molecular weight -272.3, hydrogen bond donor -2, hydrogen bond acceptor -3, total polar surface area -67.43, rotatable bonds -7, and log P -1.58 (conformed to Lipinski's rule). The compound also conformed to Veber's rule (molar refractivity between 40 and 130, the number of rotatable bonds ≤ 10, and the topological polar surface area (TPSA) ≤ 140). From the predicted properties, it can be concluded that TCMDC 131646 is expected to show good oral bioavailability and strong binding interaction with falstatin.

Overall, the docking studies predicted that TCMDC 131646 could be a potent inhibitor of falstatin, a multi-staged target in *Plasmodium falciparum*, while the druglikeness analysis predicted that TCMDC 131646 is expected to have favourable ADMET properties. The results suggest a potential for strong interaction between TCMDC 131646 and falstatin. Thus, TCMDC 131646 may be a promising antimalarial candidate that can be further explored as a potential inhibitor of falstatin.

4.8 Protein-Ligand Interactions Profiling (PLIP)

The protein-ligand interaction profiling was conducted to gain insight into the interaction of the prioritized hit TCMDC 131646 at the falstatin active site. The profiling of the protein-ligand complex (Fig 16) identified hydrophobic, hydrophilic, hydrogen bond donors, hydrogen bond acceptors and aromatic interactions. Hydrogen bonds, hydrophobic bonds and salt bridges are said to increase the stability of the protein-ligand complex.

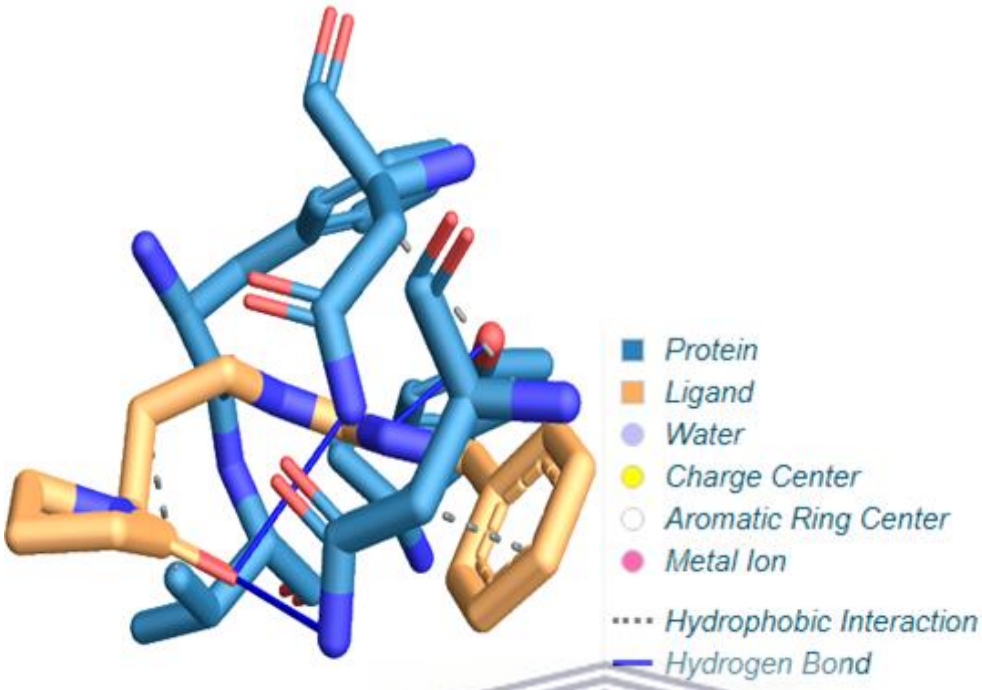

Figure 16. Protein-ligand interaction of TCMDC 131646 and the protein model falstatin showing the ligand (brown), hydrogen bonds (blue lines) and hydrophobic (broken lines) interactions

Table 3. Predicted Interactions of falstatin-ligand complex

Index	Residue	Amino Acid	Distance	Ligand Atom	Protein Atom
1	288B	Asparagine	3.85	2573	552
2	293B	Valine	3.62	2562	615
3	346B	Asparagine	3.50	2575	1457

Table 4. Hydrogen bond analysis of falstatin-ligand complex

Index	Residue	Amino Acid Type	Distance H-A	Distance D-A	Donor Angle
1	288B	Asparagine	2.00	2.94	153.99
2	292B	Phenylalanine	1.74	2.77	172.85
3	346B	Asparagine	2.66	3.47	137.41
4	393B	Tyrosine	1.94	2.82	149.71

The falstatin-ligand (TCMDC 131646) complex (Fig 16) showed three hydrophobic interactions but no salt bridge. The hydrophobic interactions were seen in asparagine at residues 288 and 346 as well as valine at residue 293 (Table 3) suggesting that asparagine and valine amino-acid residues were essential for hydrophobic interactions. The hydrophobic interactions can be attributed to the presence of the aromatic ring and aliphatic ring present in TCMDC 131646 and non-polar residues such as valine within the protein, falstatin. Hydrogen bonding interactions (Table 4) were observed at ASP-288, PHE-292, ASP-346, TYR-393 suggesting that asparagine, phenylalanine and tyrosine were crucial for hydrogen-bonding interactions. The hydrogen bonding interaction between C=O and C-O in TCMDC 131646 and falstatin could be attributed to the presence of asparagine and tyrosine which are polar amino acids. Likewise, the result (Table 4) revealed four intermolecular hydrogen bonds with bonds that fall between 1.7-3.47 Å. This implies that all the intermolecular hydrogen bonds are moderate and fall within the acceptable distance of below 3.5 Å (Fu et. al., 2018).

4.9 Molecular Dynamics

Molecular dynamics simulation was performed to evaluate the interaction between the protein target, falstatin and the prioritized hit compound TCMDC 131646 (Rastelli and Pinzi, 2019). The trajectories obtained from the simulations were used to analyze and compare the stability of the falstatin and falstatin-TCMDC 131646 complex using the following,

4.9.1 Root Mean Square Deviation (RMSD)

The root mean square deviation was used to measure changes in the conformation of the protein and protein-ligand complex over time (Elfiky, 2021). Analysis of trajectories from the molecular simulation (Fig 17) showed that the falstatin and falstatin-TCMDC 131646 complex maintained similar stability up to about 250 frames. The unbound falstatin (red) showed minimum, average and maximum RMSD at 0.450, 1.820 and 3.256 while the falstatin-TCMDC131646 complex (blue) showed a minimum, average and maximum RMSD at 0.348, 2.228 and 2.737 respectively. The RMSD of the unbound falstatin peaked at residue 381 while the RMSD of the falstatin-TCMDC complex was highest at residue 618. The RMSD plot revealed that the falstatin-ligand complex (blue) had lower RMSD values than the protein alone (red), depicting that the falstatin-ligand complex is more stable compared to the unbound falstatin.

RMSD plot for falstatin and falstatin-TCMDC 131646 complex

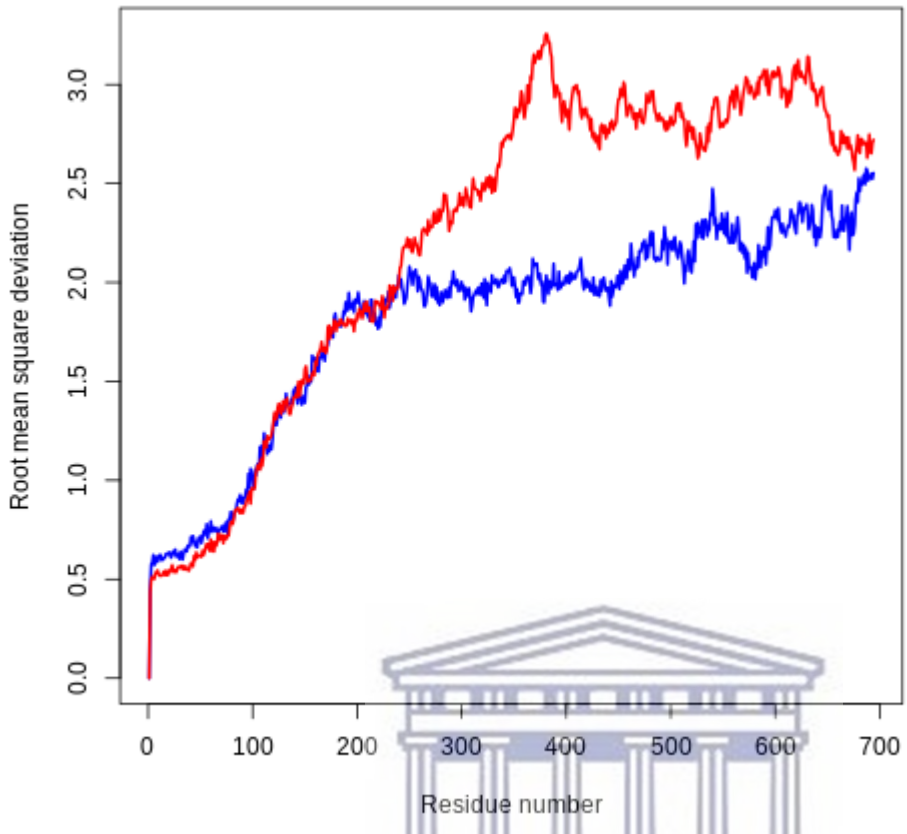

Figure 17. Root mean square deviation plot showing higher deviations for the unbound falstatin (red) and lower RMSD for the falstatin-TCMDC 131646 (blue) complex.

The result suggests that there is a strong interaction between TCMDC 131646 and falstatin. Nonetheless, a longer MD run might give better insight into the dynamics of the system.

4.9.2 Root Mean Square Fluctuation

The Root Mean Square Fluctuation (RMSF) measured the average fluctuation of residues over the simulation period (Muralidharan, 2021). Hence, the fluctuations obtained from the trajectories were plotted to compare the flexibility of the falstatin and falstatin-ligand complex. The results (Fig 18) obtained showed a minimum, average and maximum RMSF for the falstatin-ligand complex (blue) at 0.372, 1.180 and 4.710 respectively while the unbound falstatin (red) showed minimum, average and maximum fluctuation at 0.419, 1.247 and 5.345. The results showed lower fluctuations for the protein-ligand complex compared to the protein alone. Also, the flexible regions of the protein had higher fluctuations while the constrained regions bound to the ligand had lower RMSF values. The loop regions being the most flexible part of the protein had the greatest fluctuations at residue 586.

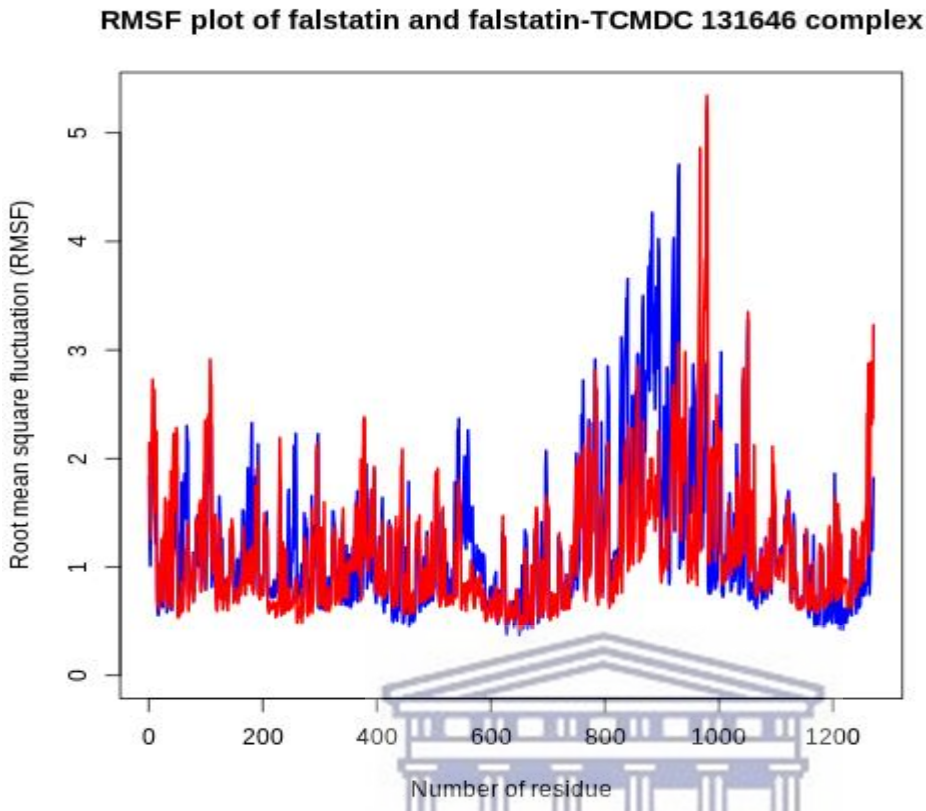

Figure 18. Root mean square fluctuation plot showing lower values for the falstatin- TCMDC 131646 complex (blue) and higher fluctuations for the unbound falstatin (red).

From the result, it appears that the falstatin-ligand complex is more stable compared to the unbound protein. Thus, we can conclude that TCMDC 131646 may strongly inhibit falstatin. The result is consistent with recent submissions that lower RMSF depicts higher stability while higher RMSF indicates lower stability (Debnath et. al., 2021; Thaillainagayam et. al., 2020).

4.9.3 Hydrogen Bonding Analysis

Hydrogen bonding plays a significant role in the absorption, metabolism, specificity and direction of binding of ligands to proteins (Joshi et. al., 2017). Hydrogen bonding analysis of the trajectories from the molecular dynamics was done to assess the structural conformation and integrity of the protein and protein-ligand complex (Ndagi et. al., 2017). Hydrogen bond analysis calculated the number and occupancy of the hydrogen bonds during the simulation period.

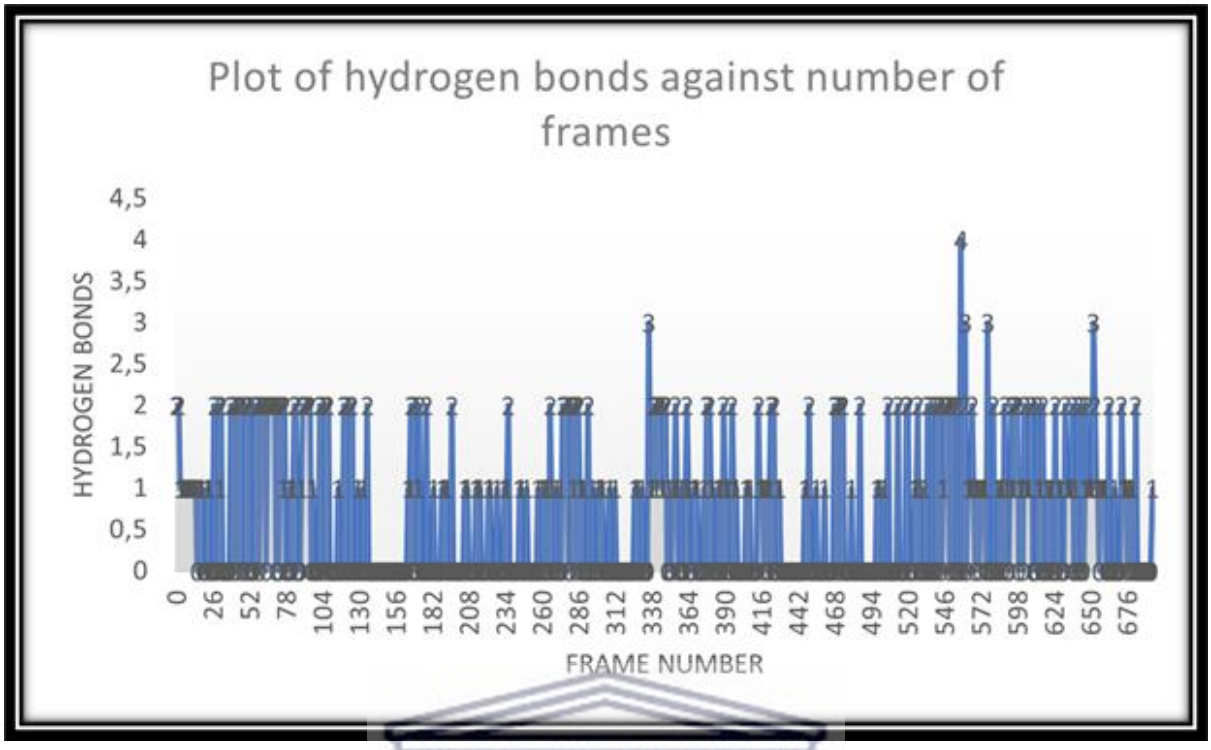

Figure 19. Hydrogen bond analysis of falstatin- TCMDC 131646 complex

Over the 700 frames of simulation, the falstatin-ligand complex showed a fluctuation of the number of hydrogen bond interactions in the complex between 1 and 4 (Figure 19). The frequency of occurrence of the one and two hydrogen bonds were more than the three and four hydrogen bonds during the simulations. The maximum number of hydrogen bonds was four with an occupancy of 52.37%, 3.17%, 5.61%, 1.73% and 0.29% for phenylalanine, asparagine, tyrosine and serine respectively. The result revealed that phenylalanine had a significantly high H-bond (52.3%) at residue 292, signifying its relevance in maintaining the structural integrity of the protein. Within the same system, H-bond occupancy of 5.61% was observed between tyrosine at residue 288.

This result seems to suggest that the presence of the ligand TCMDC 131646 increased the stability of the protein, falstatin. The stability of the complex can be explained by the higher number of hydrogen bonds seen in the fastatin-TCMDC 131646 complex. This result agrees with findings by Anuar et. al., (2021) and Sharma (2020) that hydrogen bonding increases the stability of a molecular system. The analysis therefore suggests that hydrogen bonding plays a significant role in stabilizing TCMDC 131646 at the falstatin binding site at residue 572.

4.9.4 Principal Component Analysis

The Principal Component (PC) analysis was used for evaluating the dynamics and stability of the falstatin and falstatin-TCMDC 131646 complex (Sharma et. al., 2020; Singh & Singh, 2020). Using the two-dimensional projection of PCA (PC1 and PC2), PC1 is considered the most important because it predicts the maximum variability of protein motion while PC2 accounts for the remaining variability (Pandey et al., 2019). In the 2D projection, a stable complex is usually denoted by a cluster occupying less phase space while an unstable cluster occupying more space indicates an unstable system (Sharma et. al., 2020).

From the result obtained (Fig 20 & 21), the falstatin-TCMDC 131646 complex occupied small phase spaces, while the unbound falstatin occupied more space and had a wider cluster. This implies that the falstatin-ligand complex is more stable than the unbound protein, this further indicates that the ligand conferred increased stability to the unbound protein. In addition, PC analysis as represented by the eigenvectors can also be used to assess the stability of a protein-ligand system. In general, the first few eigenvectors influence the overall motion of the protein. Lower motions of eigenvectors indicate higher stability while higher motions imply lower stability (Sharma et. al., 2020). From the PCA plot (Fig 22), it was observed that the protein-ligand complex (black) induced lower motions and higher stability while the unbound protein showed higher motions and lower stability. The results suggest that the falstatin-TCMDC 131646 complex has higher stability compared to the unbound falstatin (red).

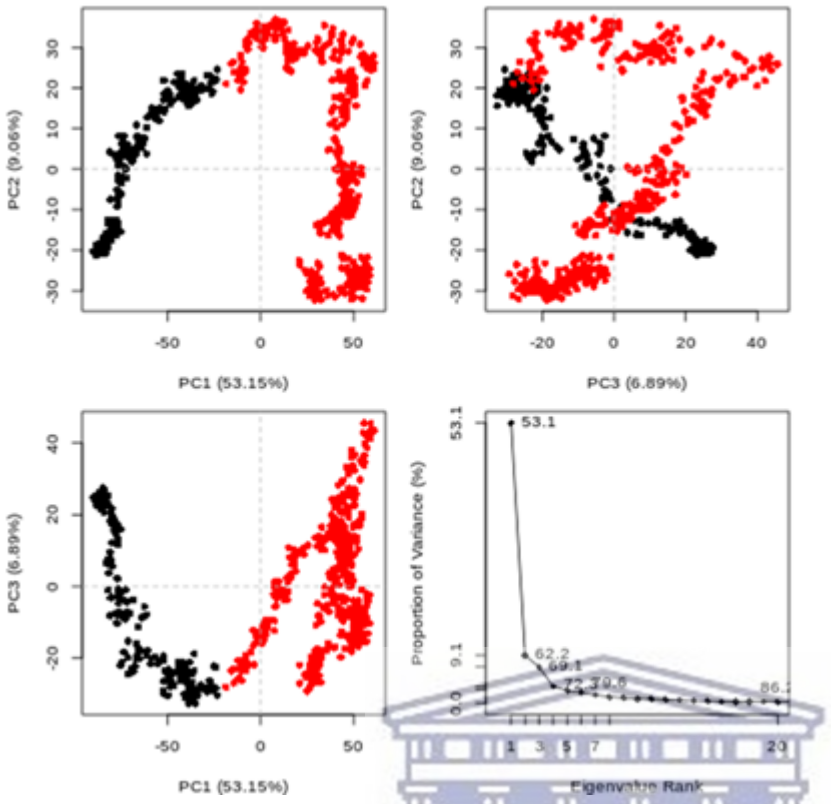

Figure 20. Principal component plot of the falstatin-ligand complex occupying smaller space

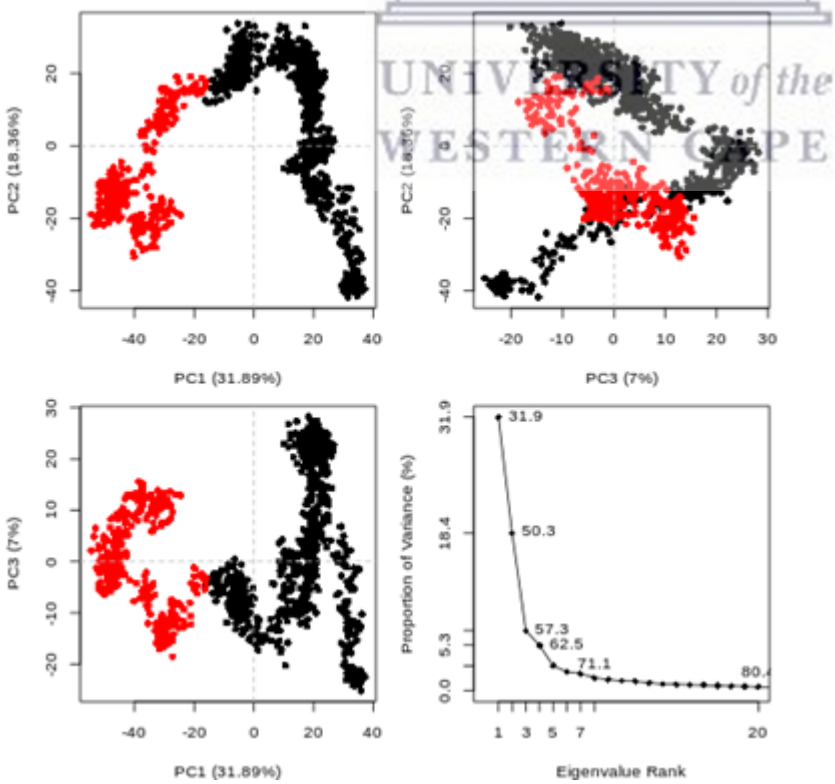

Figure 21. Principal component analysis (PCA) of unbound falstatin occupying a larger space

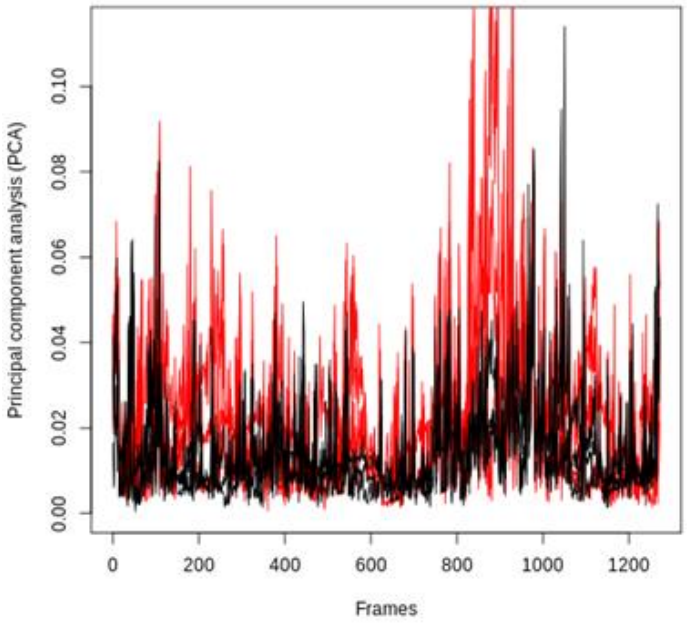

Figure 22. Principal component analysis plot showing lower motions for falstatin-ligand complex (black) and unbound protein (red).

The results were consistent with recent submission that a more stable cluster and lower motions result in higher stability (Sharma et al., 2020). The results of the PC analysis further suggest that TCMDC 131646 interracted strongly with falstatin and may potentially inhibit falstatin.

4.9.5 Dynamic Cross-Correlation Matrix

The dynamic cross-correlation matrix (DCCM) analysis was conducted to explore the correlated motion between residues of the unbound falstatin and falstatin-TCMDC131646 complex. The DCCM is a three-dimensional matrix representation that analyzes time-correlated information between the residues of the proteins in a molecular system (Ndagi et. al., 2017). Highly positive regions coloured in blue represent strongly correlated motions while negative regions coloured in pink are associated with strong anti-correlating movements (Zhang et. al., 2018; Abseher and Nilges, 1998).

Inspecting the bound and unbound protein systems (Fig 23 & 24), it was observed that there was stronger interaction in the falstatin-hit complex than the unbound falstatin system. The results showed that there were stronger cross-correlation motions (blue) than anticorrelation movements (pink) in the falstatin-hit complex compared to the unbound falstatin which showed more anticorrelation movements (pink) and fewer cross-correlation motion (blue). The result suggests intense interaction and higher stability of the falstatin-TCMDC131646 complex compared to the unbound falstatin.

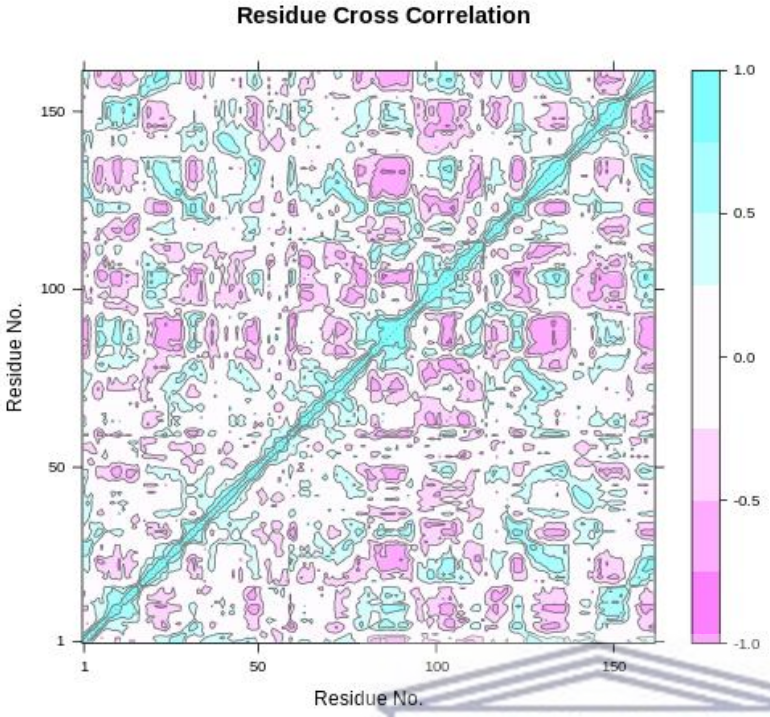

Figure 23. Dynamic cross-correlation matrix of protein showing stronger cross-correlation motions (blue) than anticorrelation movements (pink) of TCMDC 131646-falstatin complex.

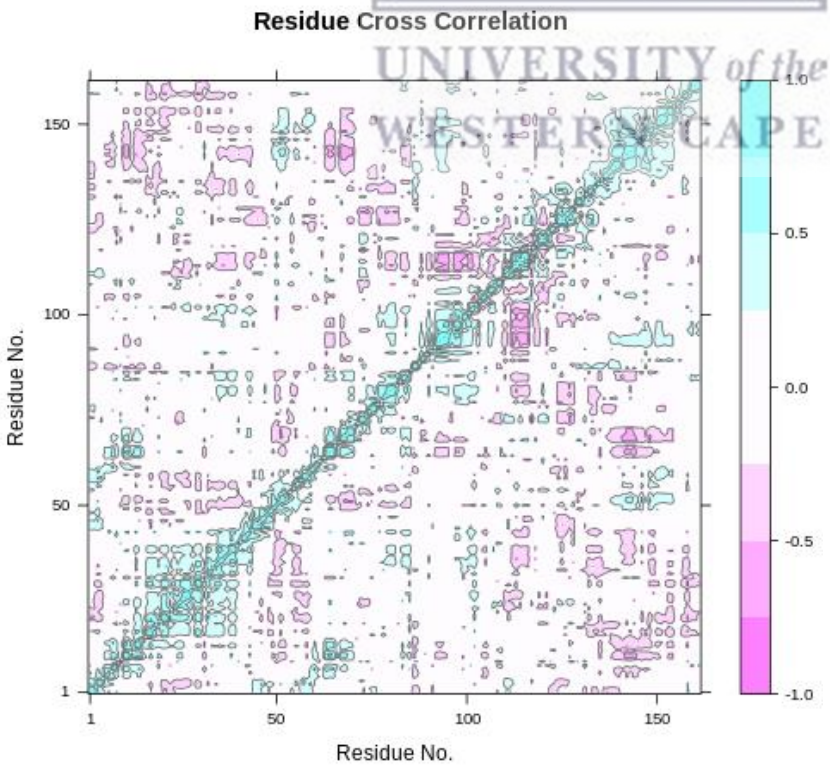

Figure 24. Dynamic cross-correlation matrix showing fewer cross-correlation movements (blue) of the unbound falstatin

The result is consistent with findings by Wu et. al., (2020) and Ndagi et. al., (2017) that inhibitory compounds have the ability to cause significant changes in the dynamic pattern of a protein target. Therefore, the observed changes in the dynamic pattern of falstatin following binding with TCMDC 131646, suggests that it could inhibit falstatin and may serve as a potent antimalarial candidate.

4.9.6 Summary of Molecular Dynamics Simulation and Analysis

MD was conducted to gain an insight into the conformational changes of the falstatin and the falstatin-ligand complex. The MD simulation verified the stability of the falstatin-TCMDC 131646 complex. From the results above, the root mean square deviation (RMSD), root mean square fluctuation (RMSF), principal component analysis (PCA) and Hydrogen bond analyses demonstrated that there was strong interaction between the target protein, falstatin and the prioritized hit, TCMDC 131646. The MD analysis revealed that the ligand TCMDC 131646 conferred higher stability on the falstatin model. The MD analysis strongly suggests that TCMDC 131646 could be a potential inhibitor of falstatin and can aid in the design of novel antimalarial agents. Following the molecular simulation step, TCMDC 131646 may be compared to chloroquine, artemisinin, artemether and lumefantrine in chemical diversity analysis.

4.10 Comparison of TCMDC 131646 to Chloroquine, Artemisinin, Artemether and Lumefantrine

Since the prioritized hit compound has been identified as a potential antimalarial lead compound, it is important to compare its physicochemical properties to chloroquine, artemisinin and artemether (currently existing antimalarial drugs). This is because chloroquine, artemisinin and artemether are existing antimalarials with good pharmacokinetic and safety profiles.

Table 5. Physicochemical properties of the hit compound (TCMDC 131646), chloroquine, artemisinin and artemether

Molecule	MW	Rotatable bonds	H-bond acceptors	Hbond donors	TPSA	Log P	Intestinal absorption	Bioavailability Score
TCMDC 131646	272.30	7	3	2	67.43	1.58	High	0.55
Chloroquine	319.87	8	2	1	28.16	4.15	High	0.55
Artemisinin	298.37	1	5	0	46.15	2.78	High	0.55
Artemether	282.33	0	5	0	53.99	2.50	High	0.55
Lumefantrine	528.94	10	2	1	23.47	7.91	Low	0.17

Table 6. Comparison of TCMDC 131646 with other antimalarials

Compounds	TCMDC 131646	Chloroquine	Artemisinin	Artemether	Lumefantrine
CYP2D6	No	Yes	No	No	Yes
CYP3A4	No	Yes	No	No	No
Lipinski	Yes	Yes	Yes	Yes	No
Ghose	Yes	Yes	Yes	Yes	No
Veber	Yes	Yes	Yes	Yes	Yes
Brenk's alert	0	0	0	0	0
PAINS alert	0	0	1	1	1
BBB permeant	No	Yes	Yes	Yes	No

Using SwissADME, the results (Table 5 & 6) showed that the pharmacokinetics of TCMDC 131646 is different from lumefantrine but comparable to that of chloroquine, artemisinin and artemether. Although TCMDC 131646 showed a similar bioavailability score of 0.55 with chloroquine, artemisinin and artemether, lumefantrine showed a lower bioavailability of 0.16. In addition, the prioritized hit, TCMDC 131646 conformed to Lipinski, Veber as well as Ghose rules of druglikeness and was predicted to have high intestinal absorption like chloroquine, artemisinin and artemether (Lipinski, 2004; Veber et. al., 2002; Ghose et. al., 2002). Likewise, the prioritized hit, chloroquine, artemisinin and artemether showed no tendency to be a

substrate of p- glycoprotein indicating that the hit compound is likely to have a desirable metabolic profile.

Even though TCMDC 131646, artemisinin and artemether showed no tendency to inhibit CYP3A4 and CYP2D6, chloroquine was predicted to inhibit CYP3A4 and CYP2D6 while lumefantrine was likely to inhibit CYP2D6 but not CYP3A4. Also, the prioritized hit and chloroquine showed no PAINS and Brenk's alert while artemisinin, artemether and lumefantrine showed Brenks alert but not PAINS alert (Brenk et. al., 2007). In addition, chloroquine, artemisinin and artemether showed good permeation for the blood-brain barrier while lumefantrine and TCMDC 131646 showed no permeability for the blood-brain barrier.

However, TCMDC 131646 can be optimized to improve its penetration into the brain. This can be achieved by increasing the lipophilicity of the compound through the addition of chemical moieties such as methyl, ethyl, thymidine, guanidine or tyrosine (Arnot and Planey, 2012; Tajes et. al., 2014). Overall, the analysis above revealed that TCMDC 131646 is expected to be a druglike and leadlike drug with an excellent efficacy and safety profile comparable to the pharmacokinetic properties of chloroquine, artemisinin and artemether.

4.11 Molecular Similarity/Chemical Diversity Analysis of TCMDC 131646 with Selected Antimalarial Drugs

The goal of chemical diversity analysis was to investigate the structural diversity between the hit TCMDC 131646, chloroquine, artemisinin, artemether and lumefantrine. The molecular diversity analysis is based on the premise that chemically diverse compounds tend to bind to different targets and have distinct mechanisms of action while compounds with structural similarity are likely to have the same mechanism of action (Medina-Franco and Maggiora, 2013; Majiora et. al., 2014,). A unique mechanism of action is particularly useful in tackling antimalarial resistance. Using DataWarrior, the chemical diversity analysis of TCMDC 131646 from chloroquine, artemisinin, artemether and lumefantrine was generated from the first principal components based on structural descriptors.

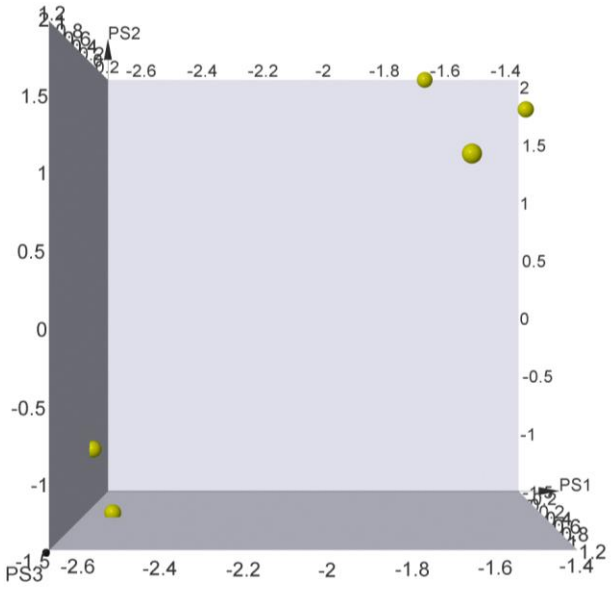

Figure 25. Chemical diversity analysis of TCMDC 131646, chloroquine, artemisinin, artemether and lumefantrine. The plot was obtained from the first three principal components based on structural descriptors.

Figure 25 depicts the result of the chemical diversity assessment. The results showed that TCMDC131646, chloroquine, artemisinin, artemether and lumefantrine were widely dispersed within the 3-D plot. This seems to suggest that the prioritized hit TCMDC 131646 is structurally diverse from existing antimalarials. The chemical diversity showed by TCMDC 131646 further indicates that the prioritized hit is likely to have a unique mechanism of action that is different from those of existing antimalarials. A novel mechanism of action of TCMDC 131646 is a desirable property in tackling antimalarial resistance.

Inspecting the chemical structure of the compounds (Fig 26), all the compounds are structurally different from each other, except for artemisinin which was chemically modified at the C10 position to produce artemether. We can conclude that TCMDC 131646 is likely to have a novel mechanism of action.

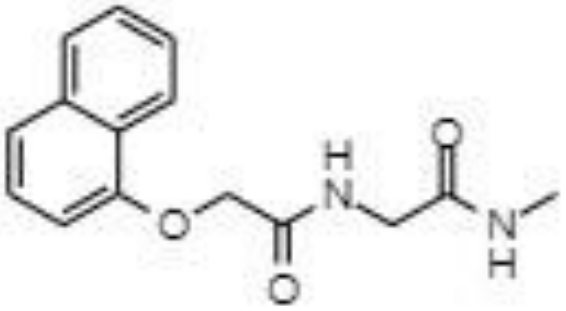

a) Chloroquine

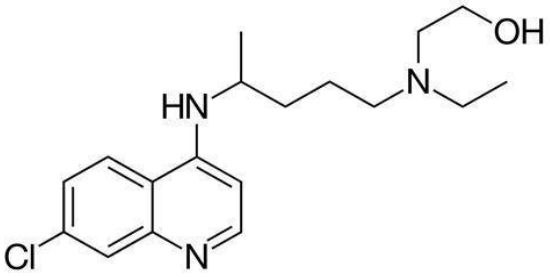

b) TCMDC 131646

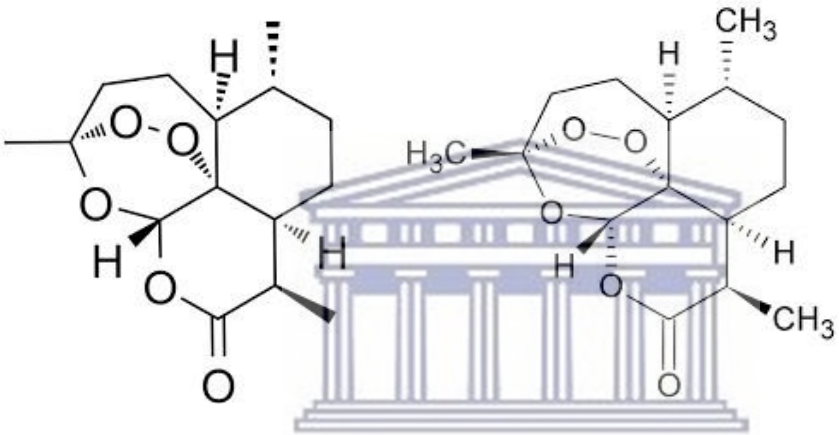

c) Artemisinin

d) Artemether

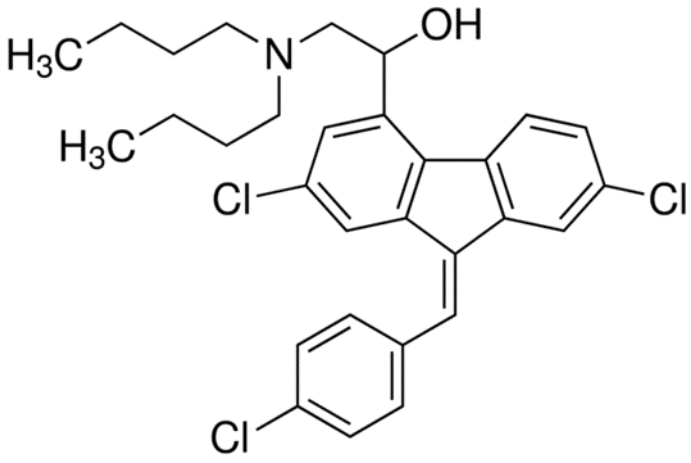

Figure 26. Chemical structures of TCMDC 131646, chloroquine, artemisinin, artemether and lumefantrine

From the analysis, it can be concluded that the prioritized hit is likely to have a novel mechanism of action. The results further support the premise that TCMDC 131646 is expected to have a novel mechanism of action. Hence, TCMDC 131646 could be targeted at inhibiting falstatin in Plasmodium falciparum and can serve as potent antimalarial candidates with a novel mechanism of action.

4.12 Rescoring of Top-ranked Compounds Using MM-GBSA

Using Schrodinger, the top-scoring compounds were rescored with the Molecular Mechanics-Generalized Born Surface Area (MM-GBSA) scoring function. The rescoring also estimated the free energy of binding of the top-scoring compounds and helped to gain insight into the component binding energies (Chinnasammy et. al., 2020). Negative binding energies indicate the feasibility of the binding while positive binding energies indicate that the binding is not plausible. The MM-GBSA analysis calculated the binding energies of the top-scoring compounds, and the component energies are shown in Table 7.

Table 7. Docking scores and component energies of the top-scoring compounds using MM-GBSA scoring function

Components	TCMDC 124274	TCMDC 131646	TCMDC 138266	TCMDC 123844	TCMDC 131234
Docking score (KJ)	-4.662	-4.538	-3.195	-3.145	-2.479
Glide energy (KJ)	-36.126	-41.636	-33.904	-36.577	-35.662
$\Delta E_{electrostatic}$ (KJ)	-10.648	-11.564	-8.219	-10.946	-9.924
ΔE_{vdw} (KJ)	-25.477	-30.071	-25.685	-25.630	-25.738
$\Delta E_{internal}$ (KJ)	4.153	4.821	4.842	7.502	6.100
$\Delta E_{lipophilic}$ (KJ)	-2.239	-2.073	-2.143	-1.611	-1.718
$\Delta G_{hydrophobic}$ (KJ)	-1.600	-1.625	-1.345	-2.074	-1.170

In the rescoring analysis, TCMDC-124274, TCMDC-131646, TCMDC-138266, TCMDC 123844 and TCMDC 131234 were predicted to have binding energies of -4.662, -4.538, -3.195, -3.145 and -2.479 KJ respectively. The negative binding energies indicate that all the docked ligands are likely to interact strongly with falstatin at the active site. Hence, the result suggests the prioritized hit, TCMDC 131646 could inhibit falstatin. The negative docking scores are also consistent with the results obtained from molecular docking on MOE. Based on the results

obtained, we can conclude that the MM-GBSA analysis provides a basis for further investigation into TCMDC 131646 as an inhibitor of falstatin.

Further investigation revealed that Van der Waals forces, electrostatic energy as well as hydrogen bonds contributed to the total free energy of binding and play an essential role in the protein-ligand binding. From Table 7, it was observed that TCMDC 131646 had the highest binding energy of - 41.636kJ/mol and all the compounds showed negative energies. Similarly, all the compounds showed negative electrostatic energy suggesting an attraction between the compounds and the falstatin active site. Observation of the Van der Waals free energy revealed that TCMDC 131646 had a negative value of -30.071KJ/mol similar to the other compounds that showed negative Van der Waals energy. The table also highlights the hydrogen binding and lipophilic binding. Overall, the energy components from the MM-GBSA analysis strongly suggested that TCMDC 131646 could potentially bind to falstatin and might be an inhibitor of falstatin.

4.13 Development of Pharmacophore Hypothesis Based on Top-scoring Compounds

Hypothesis generation was performed to obtain a pharmacophore model from the top-scoring compounds, the model obtained can be used to screen other chemical libraries in order to identify new compounds that might bind to falstatin. Employing the Phase module on Schrödinger, the pharmacophore hypothesis was developed by extracting pharmacophore features such as HBA − Hydrogen Bond Acceptor; HPh − Hydrophobic; HBD − Hydrogen Bond Donor; PI − Positive Ionisable; HBAl − Hydrogen Bond Acceptor Lipid; RA − Ring Aromaticity from 3D structures of the top-scoring ligands. The phase module aligned the 5 top-ranked ligands and generated the pharmacophore model.

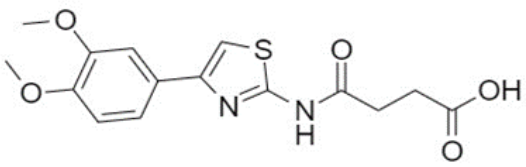

TCMDC 138266

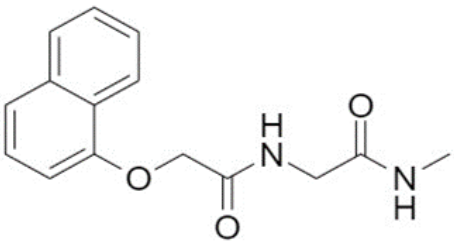

b) TCMDC 131646

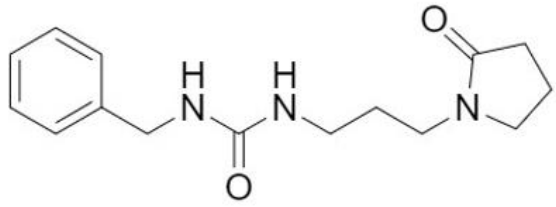

c) TCMDC 123844

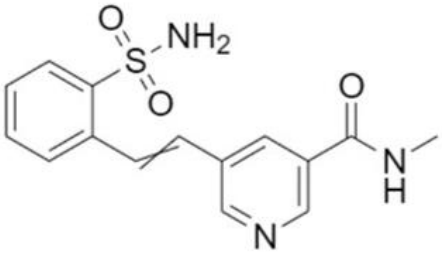

d) TCMDC 138266

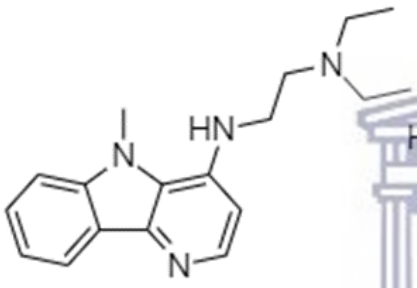

e) TCMDC 131844

Figure 27. Chemical structure of top-scoring compounds

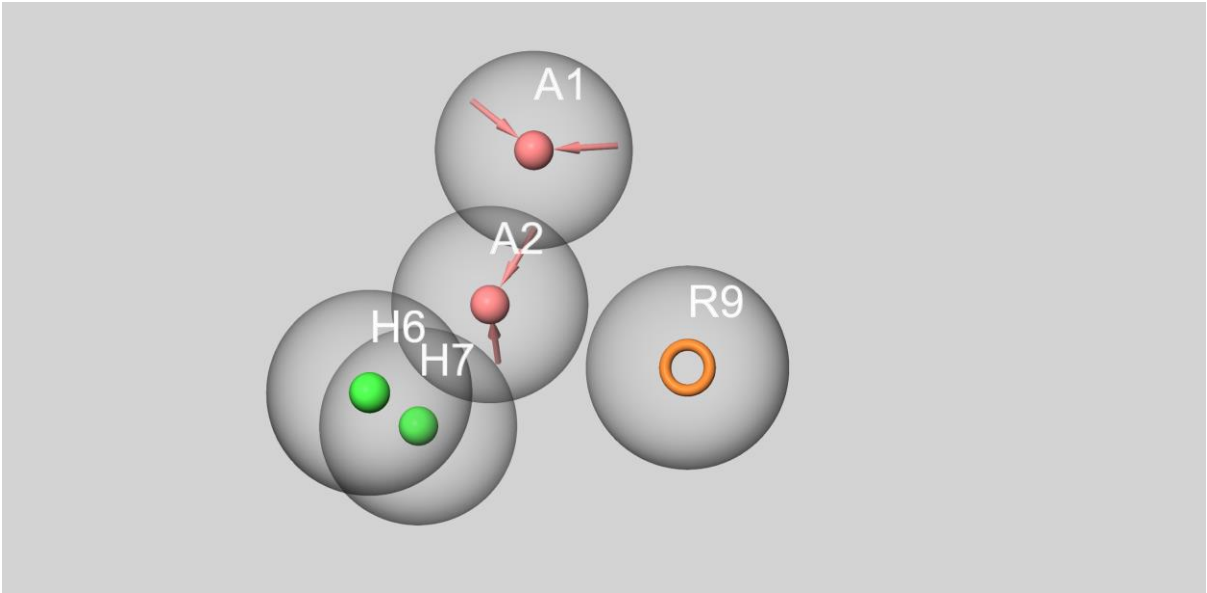

Figure 28. Pharmacophore model created based on the top-scoring compounds showing two hydrogen bond acceptors (red), two hydrophobic bonds (green) and one aromatic ring (orange)

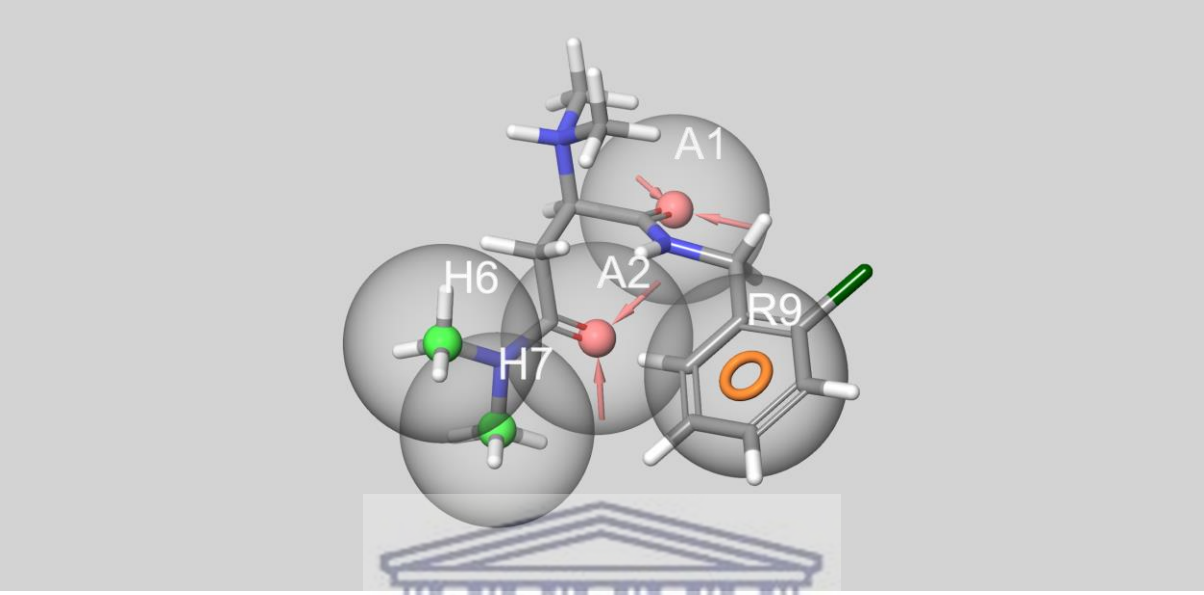

Figure 29. TCMDC 131646 aligned well with the pharmacophore model

Schrodinger generated the best pharmacophore hypothesis (Fig 28), the pharmacophore hypothesis consists of five features, two hydrogen bond acceptors (HA), two hydrophobic (HY) feature, and one ring aromatic (RA) feature. The alignment of the hypothesis over the top compounds revealed the presence of -H-N-C=O and N-H suggesting that the presence of electron-withdrawing groups could be vital for the inhibition of falstatin. From the analysis (Fig 29), we can conclude that the pharmacophore model generated fitted the compounds well and can be used to screen other virtual libraries to predict other compounds that are likely to bind to falstatin.

Summary

This chapter presented and discussed the results of homology modelling, structure evaluation and validation of the falstatin model, molecular dynamics analysis and comparison of the prioritized hit with commercially available antimalarials. The structure evaluation and validation results indicated that the protein model obtained from homology modelling had good quality and will consequently yield reliable and plausible results during the molecular docking step. The molecular docking studies predicted compounds that are likely to have good affinity for the target protein, falstatin while the ADME and toxicity screening identified compounds with desirable pharmacokinetic properties. Using a novel ligand scoring function, TCMDC

131646 was predicted to have a good affinity for falstatin and good drug-like properties. Thus, the hit compound, TCMDC 131646 could inhibit falstatin and may serve as a potential antimalarial lead.

Furthermore, the MD analysis revealed that TCMDC 131646, N-Methyl-2- [(2-naphthalen-1-yloxyacetyl) amino] acetamide conferred stability to falstatin and may be a potent inhibitor of falstatin. The molecular similarity analysis showed that TCMDC 131646 is chemically diverse from existing antimalarials predicting a novel mechanism of action. Likewise, TCMDC 131646 had comparable efficacy and safety profiles to chloroquine, artemisinin, artemether but not lumefantrine. The rescoring analysis using the MM-GBSA scoring function indicated that TCMDC could potentially bind to falstatin validating the docking results obtained from Molecular Operating Environment (MOE). Based on the top-ranking ligands obtained from the screening, a pharmacophore hypothesis representative of their molecular descriptors was developed. The pharmacophore hypothesis generated indicated that the model consists of two hydrogen bond acceptors, two hydrogen bonds and one aromatic ring, the model can be used as a reference for screening other chemical libraries in the future. Ultimately, the prioritized hit can be expanded in an approach known as hit expansion to get analogues that might have better affinity and pharmacokinetic profiles. Nonetheless, the predictions from the study require further validation through experimental testing.

Chapter Five: Conclusion and Recommendation

Antimalarial resistance places a tremendous health burden on people all over the world particularly in developing countries leading to a need for newer classes of antimalarials. The structure-based virtual screening (SBVS) approach is an invaluable tool employed in this search because it increases the chance of success during the drug development and saves the cost, time and effort required for preclinical as well as clinical drug development. Although structure-based virtual screening complements experimental assays, it does not replace experimental testing. Therefore, the structure-based approach was explored in this study. This chapter summarizes the main findings from this study. The aim, objectives, conclusion, limitations of the study and recommendation from this project are outlined below.

5.1 Aim of this Research

This study applied a structure-based virtual screening approach to identify potential antimalarial candidates with favourable physicochemical properties and high affinity for the plasmodial protein, falstatin in Plasmodium falciparum.

5.2 Objectives of the Study

The results from each of the objectives are outlined below,

I. *To carry out homology modelling and quality evaluation of the falstatin model using the online servers, Swiss model and Procheck.*

The plasmodial protease, falstatin, was successfully modelled using falcipain-2 with a sequence identity of 41.98% as the template. The protein model was structurally evaluated using Ramachandran plot, ERRAT plot, local energy profile, Z-score and global quality score. The results showed that the model has a good quality and can be used in the docking step.

II. *To perform molecular docking studies on selected antiplasmodial compounds and the protein target falstatin to obtain the minimum binding energy using Molecular Operating Environment.*

Molecular docking was conducted with 18,000 compounds retrieved from Malaria Box, a library of antiplasmodial compounds, on falstatin. Based on the induced fit model, the docking step estimated the minimum binding energies of the compounds to falstatin. The docking scores were ranked and used in computing a ligand score for the top-scoring compounds. The docking result suggests that compounds with very low binding energies could inhibit falstatin and may serve as potent antimalarial candidates.

III. *To triage and prioritize hit compounds based on favourable absorption, distribution, metabolism and toxicity (ADMET) properties using Stardrop, Optibrium and Datawarrior softwares.*

After computing the binding energy, ADME and toxicity of the compounds to obtain a ligand score, TCMDC 131646 had the highest ligand score and was selected for further analysis. The ADME analysis was based on Lipinski, Veber and Egan's rules of druglikeness while toxicity profiling of the hits was based on the search for toxicophores. The outcomes revealed that TCMDC 131646 is a druglike, leadlike and safe compound that contains no toxic moiety. Hence, TCMDC 131646 is predicted to have desirable pharmacokinetic properties and is not likely to fail during clinical trials due to poor ADME and safety profile.

IV. *To conduct molecular dynamics (MD) and compare the stability of the protein as well as protein-ligand complex using hydrogen bond, principal component analysis (PCA), Root Mean Square Fluctuation (RMSF), Root Mean Square (RMSD) and dynamic cross-correlation matrix (DCCM) analyses.*

Analysis of the trajectories obtained from the MD simulation revealed that the prioritized hit compound TCMDC conferred greater stability on the protein model. The hydrogen bond analysis, PCA, RMSD, RMSF and DCCM analyses of the trajectories showed that the presence of the hit TCMDC 131646 increased the stability of the unbound falstatin. The analysis determined the effect of the TCMDC 131646 on the modelled falstatin and further validated the docking process. Based on the molecular dynamics simulation, the results suggest a potential for strong interaction between TCMDC 131646 and falstatin. Hence, TCMDC 131646 could serve as a compound that can be further explored as a promising antimalarial candidate.

V. *To perform chemical diversity analysis and compare the prioritized hit compound with chloroquine, artemisinin and artemether which are existing antimalarials with good pharmacokinetic and safety profiles.*

The similarity analysis indicated that TCMDC 131646 is structurally diverse from chloroquine, artemisinin, artemether and lumefantrine, suggesting that the prioritized candidate is likely to have a novel mechanism of action that is different from those of currently available antimalarials. The novel mechanism of action is important for tackling the problem of antimalarial resistance. TCMDC 131646 also showed comparable physicochemical properties with chloroquine, artemisinin, artemether and lumefantrine. Therefore, the prioritized hit is expected to have a satisfactory pharmacokinetic and safety profile similar to that of chloroquine, artemisinin and artemether.

VI. *To rescore the top-ranked compounds using the Molecular Mechanics-Generalized Born Solvation Area (MM-GBSA) scoring function.*

The redocking analysis revealed that TCMDC 131646 has a negative binding energy of -4.538 KJ/mol indicating the spontaneity of the interaction between falstatin and the hit compound. The redocking step also showed that all the top-scoring compounds are capable of binding to falstatin. The result corroborates the assertion that TCMDC could be a potential inhibitor of the protein target falstatin in *Plasmodium falciparum.* Hence, TCMDC 131646 may be further investigated for use as an antimalarial agent.

VII. *To develop a pharmacophore hypothesis based on the top-ranked compounds.*

The pharmacophore hypothesis was generated based on ligands with the top ligand scores. Hypothesis generation was done to develop a pharmacophore model which is an ensemble of all the molecular descriptors in the top-scoring ligands. The model can therefore be used as a reference to screen other chemical databases. Thus, the pharmacophore model can be used to identify other compounds that are similar to the top-ranked compounds, the newly identified compounds could serve as starting points for the design and optimisation of novel compounds targeted at inhibiting falstatin.

5.3 Limitation of the Study

Although this study identified TCMDC 131646 as a potential inhibitor drug in *Plasmodium falciparum,* this study did not validate these predictions by experimental testing which is beyond the scope of this study. Therefore, in-vitro and in-vivo investigations are required to further assess the antimalarial activity of this compound. In this study, the results of the molecular docking, druglikeness analysis, molecular dynamics and MM-GBSA analysis are not confirmatory. Hence, the predictions from this study should be further substantiated by experimental testing.

5.4 Conclusion

The current study answered the research questions and demonstrated that the 3-D structure of the uncrystallized protein target falstatin can be computationally modelled and evaluated using appropriate tools and webservers. The study further revealed that the molecular docking process could predict compounds that may potentially inhibit falstatin.

The research aimed at identifying innovative antimalarial agents with novel mechanisms of action. Based on the molecular docking results, chemical diversity analysis and analysis of the

trajectories obtained from the molecular dynamics simulation, this study strongly indicates that TCMDC 131646 is a highly promising antimalarial candidate with a novel and unique mechanism of action. The findings showed that TCMDC 131646 has a high affinity for falstatin, a plasmodial protease in Plasmodium falciparum. The study also revealed that the prioritized hit is a safe, druglike and leadlike compound that has a potential to stabilize falstatin.

Ultimately, TCMDC 131646 could serve as a potent antimalarial agent that can be explored to resolve the problem of antimalarial resistance to current chemotherapeutics. This research has also contributed to the body of knowledge by providing information on potential compounds that could inhibit the protein target, falstatin in *Plasmodium falciparum*. Overall, further exploration of the hit compounds will therefore reduce the cost, time and effort involved in the antimalarial drug development pipeline.

5.5 Recommendations

This study recommends that TCMDC 131646 may be a potential antimalarial candidate that can be further explored for use in antimalarial therapy. The current study proposes that TCMDC 131646 is likely to act by inhibiting falstatin in schizonts and merozoites of *Plasmodium falciparum*. Hence, TCMDC 131646 may be further developed through hit transformation and lead optimization.

Furthermore, it is recommended that the hits obtained from this study should be further tested through in-vivo and in-vitro studies to gain more insights into its efficacy and safety in animal models. If the compounds are found useful, they could serve as leads that could be optimized for clinical trials. The lead optimization could be achieved by analog expansion involving chemical modification at the carbonyl, amide and aromatic rings of the prioritized hit, TCMDC 131646 in an approach known as hit expansion. Ultimately, the expansion of the analogues could improve the blood-brain permeation, therapeutic efficacy and safety of these hit compound.

References

Abseher, R. and Nilges, M., 1998. Are there non-trivial dynamic cross-correlations in proteins? *Journal of molecular biology*, *279*(4), pp.911-920.

Acharya, C., Coop, A., E Polli, J. and D MacKerell, A., 2011. Recent advances in ligand-based drug design: relevance and utility of the conformationally sampled pharmacophore approach. *Current computer-aided drug design*, *7*(1), pp.10-22.

Adebayo, J.O., Tijjani, H., Adegunloye, A.P., Ishola, A.A., Balogun, E.A. and Malomo, S.O., 2020. Enhancing the antimalarial activity of artesunate. *Parasitology Research*, pp.1-16.

Afgan E et al. 2016 The Galaxy platform for accessible, reproducible and collaborative biomedical analyses:2016 update. Nucleic Acids Res. 44, W3–W10.

Afgan, E., Baker, D., Van den Beek, M., Blankenberg, D., Bouvier, D., Čech, M., Chilton, J., Clements, D., Coraor, N., Eberhard, C. and Grüning, B., 2016. The Galaxy platform for accessible, reproducible and collaborative biomedical analyses: 2016 update. *Nucleic acids research*, *44*(W1), pp.W3-W10.

Agarwal, S. and Mehrotra, R., 2016. An overview of molecular docking. *JSM Chem*, *4*(2), pp.1024-1028.

Aguiar, A.C.C., da Rocha, E.M., de Souza, N.B., França, T.C. and Krettli, A.U., 2012. New approaches in antimalarial drug discovery and development: a review. *Memorias do Instituto Oswaldo Cruz*, *107*, pp.831-845.

Anuar, N.F.S.K., Wahab, R.A., Huyop, F., Amran, S.I., Hamid, A.A.A., Halim, K.B.A. and Hood, M.H.M., 2021. Molecular docking and molecular dynamics simulations of a mutant Acinetobacter haemolyticus alkaline-stable lipase against tributyrin. *Journal of Biomolecular Structure and Dynamics*, *39*(6), pp.2079-2091.

Arnott, J.A. and Planey, S.L., 2012. The influence of lipophilicity in drug discovery and design. *Expert opinion on drug discovery*, *7*(10), pp.863-875.

Baell, J.B., Ferrins, L., Falk, H. and Nikolakopoulos, G., 2013. PAINS: Relevance to tool compound discovery and fragment-based screening. *Australian Journal of Chemistry*, *66*(12), pp.1483-1494.

Bagozzi, B.E. and Koren, O., 2020. The Diplomatic Burden of Pandemics: The Case of Malaria. *SocArXiv. March*, *18*.

Banks, W.A. and Greig, N.H., 2019. Small molecules as central nervous system therapeutics: old challenges, new directions, and a philosophic divide.

Bathurst, I. and Hentschel, C., 2006. Medicines for Malaria Venture: sustaining antimalarial drug development. *Trends in parasitology*, *22*(7), pp.301-307.

Batool, M., Ahmad, B. and Choi, S., 2019. A structure-based drug discovery paradigm. *International journal of molecular sciences*, *20*(11), p.2783.

Baxter, A.D. and Lockey, P.M., 2001. 'Hit'to 'lead'and 'lead'to 'candidate'optimization using multi-parametric principles. *Drug Discov. World*, *2*, pp.9-15.

Belete, T.M., 2020. Recent progress in the development of new antimalarial drugs with novel targets. *Drug design, development and therapy*, *14*, p.3875.

Benkert, P., Biasini, M. and Schwede, T., 2011. Toward the estimation of the absolute quality of individual protein structure models. *Bioinformatics*, *27*(3), pp.343-350.

Berdigaliyev, N. and Aljofan, M., 2020. An overview of drug discovery and development. *Future medicinal chemistry*, *12*(10), pp.939-947.

Bhal, S.K., 2007. LogP—Making sense of the value. *Advanced chemistry development, Toronto, ON, Canada*, pp.1-4.

Bhal, S.K., Kassam, K., Peirson, I.G. and Pearl, G.M., 2007. The rule of five revisited: applying log D in place of log P in drug-likeness filters. *Molecular pharmaceutics*, *4*(4), pp.556-560.

Bhatnager, R., Bhasin, M., Arora, J. and Dang, A.S., 2020. Epitope based peptide vaccine against SARS-COV2: an immune-informatics approach. *Journal of Biomolecular Structure and Dynamics*, pp.1-16.

Brenk, R., Schipani, A., James, D., Krasowski, A., Gilbert, I.H., Frearson, J. and Wyatt, P.G., 2008. Lessons learnt from assembling screening libraries for drug discovery for neglected diseases. *ChemMedChem*, *3*(3), p.435.

Bull, S.C. and Doig, A.J., 2015. Properties of protein drug target classes. *PloS one*, *10*(3), p.e0117955.

Burnell, E.S., 2020. Drugs targeting mitochondrial functions. *Antimalarial Agents*, pp.375-402.

Camacho, C., Coulouris, G., Avagyan, V., Ma, N., Papadopoulos, J., Bealer, K. and Madden, T.L., 2009. BLAST+: architecture and applications. *BMC bioinformatics*, *10*(1), pp.1-9.

Çapcı, A., Lorion, M.M., Wang, H., Simon, N., Leidenberger, M., Borges Silva, M.C., Moreira, D.R., Zhu, Y., Meng, Y., Chen, J.Y. and Lee, Y.M., 2019. Artemisinin–(Iso) quinoline Hybrids by C− H Activation and Click Chemistry: Combating Multidrug-Resistant Malaria. *Angewandte Chemie International Edition*, *58*(37), pp.13066-13079.

Cavasotto, C.N. and Phatak, S.S., 2009. Homology modeling in drug discovery: current trends and applications. *Drug discovery today*, *14*(13-14), pp.676-683.

Chandrasekaran, B., Abed, S.N., Al-Attraqchi, O., Kuche, K. and Tekade, R.K., 2018. Computer-aided prediction of pharmacokinetic (ADMET) properties. In *Dosage form design parameters* (pp. 731-755). Academic Press.

Chen, G., Huang, K., Miao, M., Feng, B. and Campanella, O.H., 2019. Molecular dynamics simulation for mechanism elucidation of food processing and safety: State of the art. *Comprehensive reviews in food science and food safety*, *18*(1), pp.243-263.

Chen, H., Lyne, P.D., Giordanetto, F., Lovell, T. and Li, J., 2006. On evaluating molecular-docking methods for pose prediction and enrichment factors. *Journal of chemical information and modeling*, *46*(1), pp.401-415.

Chen, J., Wang, Y.K., Gao, Y., Hu, L.S., Yang, J.W., Wang, J.R., Sun, W.J., Liang, Z.Q., Cao, Y.M. and Cao, Y.B., 2020. Protection against COVID-19 injury by qingfei paidu decoction via anti-viral, anti-inflammatory activity and metabolic programming. *Biomedicine & Pharmacotherapy*, *129*, p.110281.

Chinnasamy, S., Selvaraj, G., Kaushik, A.C., Kaliamurthi, S., Chandrabose, S., Singh, S.K., Thirugnanasambandam, R., Gu, K. and Wei, D.Q., 2020. Molecular docking and molecular dynamics simulation studies to identify potent AURKA inhibitors: assessing the performance of density functional theory, MM-GBSA and mass action kinetics calculations. *Journal of Biomolecular Structure and Dynamics*, *38*(14), pp.4325-4335.

Chmiel, T., Mieszkowska, A., Kempińska-Kupczyk, D., Kot-Wasik, A., Namieśnik, J. and Mazerska, Z., 2019. The impact of lipophilicity on environmental processes, drug delivery and bioavailability of food components. *Microchemical Journal*, *146*, pp.393-406.

Clark, D.E., 2011. What has polar surface area ever done for drug discovery?. *Future medicinal chemistry*, *3*(4), pp.469-484.

Coatney, G.R., 1963. Pitfalls in a discovery: the chronicle of chloroquine. *The American journal of tropical medicine and hygiene*, *12*(2), pp.121-128.

Coban, C., 2020. The host targeting effect of chloroquine in malaria. *Current opinion in immunology*, *66*, pp.98-107.

Colovos, C. and Yeates, T.O., 1993. Verification of protein structures: patterns of nonbonded atomic interactions. *Protein science*, *2*(9), pp.1511-1519.

Corbeil, C.R., Williams, C.I. and Labute, P., 2012. Variability in docking success rates due to dataset preparation. *Journal of computer-aided molecular design*, *26*(6), pp.775-786.

Croston, G.E., 2017. The utility of target-based discovery. *Expert opinion on drug discovery*, *12*(5), pp.427-429.

Cui, L. and Su, X.Z., 2009. Discovery, mechanisms of action and combination therapy of artemisinin. *Expert review of anti-infective therapy*, *7*(8), pp.999-1013.

Cygan, R.T. and Kubicki, J.D. eds., 2018. *Molecular modeling theory: Applications in the geosciences* (Vol. 42). Walter de Gruyter GmbH & Co KG.

Dahlgren, D. and Lennernäs, H., 2019. Intestinal permeability and drug absorption: predictive experimental, computational and in vivo approaches. *Pharmaceutics*, *11*(8), p.411.

Daina, A., Michielin, O. and Zoete, V., 2017. SwissADME: a free web tool to evaluate pharmacokinetics, drug-likeness and medicinal chemistry friendliness of small molecules. *Scientific reports*, *7*(1), pp.1-13.

Damm, W., Frontera, A., Tirado–Rives, J. and Jorgensen, W.L., 1997. OPLS all-atom force field for carbohydrates. *Journal of computational chemistry*, *18*(16), pp.1955-1970.

Dar, A.M. and Mir, S., 2017. Molecular docking: approaches, types, applications and basic challenges. *J Anal Bioanal Tech*, *8*(2), pp.1-3.

De Beer, T.A.P., Wells, G.A., Burger, P.B., Joubert, F., Marechal, E., Birkholtz, L. and Louw, A.I., 2009. Antimalarial drug discovery: in silico structural biology and rational drug design. *Infectious Disorders-Drug Targets (Formerly Current Drug Targets-Infectious Disorders)*, *9*(3), pp.304-318.

de Bruyn Kops, C., Stork, C., Šícho, M., Kochev, N., Svozil, D., Jeliazkova, N. and Kirchmair, J., 2019. GLORY: generator of the structures of likely cytochrome P450 metabolites based on predicted sites of metabolism. *Frontiers in chemistry*, *7*, p.402.

de Lima, D.A., Andreotti, C.E.L., Antiquera Ferreira, F., Pauli, K.B., da Silva, G.R., Ribeiro, R.D.C.L., Dalsenter, P.R., Boechat, N., Gasparotto Junior, A., Lourenço, E.L.B. and Lívero, F.A.D.R., 2021. Safety assessment of MEFAS: an innovative hybrid salt of mefloquine and artesunate for malaria treatment. *Drug and chemical toxicology*, *44*(4), pp.380-385.

de Sousa, A.C.C., Combrinck, J.M., Maepa, K. and Egan, T.J., 2020. Virtual screening as a tool to discover new β-haematin inhibitors with activity against malaria parasites. *Scientific reports*, *10*(1), pp.1-10.

de Sousa, A.C.C., Combrinck, J.M., Maepa, K. and Egan, T.J., 2020. Virtual screening as a tool to discover new β-haematin inhibitors with activity against malaria parasites. *Scientific reports*, *10*(1), pp.1-10.

de Souza Pereira, C., Costa Quadros, H., Magalhaes Moreira, D.R., Castro, W., Santos De Deus Da Silva, R.I., Botelho Pereira Soares, M., Fontinha, D., Prudencio, M., Schmitz, V., Dos Santos, H.F. and Gendrot, M., 2021. A Novel Hybrid of Chloroquine and Primaquine Linked

by Gold (I): Multitarget and Multiphase Antiplasmodial Agent. *ChemMedChem*, *16*(4), pp.662-678.

Dearden, J.C., 2003. In silico prediction of drug toxicity. *Journal of computer-aided molecular design*, *17*(2), pp.119-127.

Debnath, P., Bhaumik, S., Sen, D., Muttineni, R.K. and Debnath, S., 2021. Identification of SARS-CoV-2 Main Protease Inhibitors Using Structure Based Virtual Screening and Molecular Dynamics Simulation of DrugBank Database. *Chemistry Select*, *6*(20), pp.4991-5013.

Desiraju, G.R. and Steiner, T., 2001. *The weak hydrogen bond: in structural chemistry and biology* (Vol. 9). International Union of Crystal.

Deu, E., 2017. Proteases as antimalarial targets: strategies for genetic, chemical, and therapeutic validation. *The FEBS journal*, *284*(16), pp.2604-2628.

Devi, R.V., Sathya, S.S. and Coumar, M.S., 2015. Evolutionary algorithms for de novo drug design–A survey. *Applied Soft Computing*, *27*, pp.543-552.

Dias, R., de Azevedo, J. and Walter, F., 2008. Molecular docking algorithms. *Current drug targets*, *9*(12), pp.1040-1047.

Du, J., Sun, H., Xi, L., Li, J., Yang, Y., Liu, H. and Yao, X., 2011. Molecular modeling study of checkpoint kinase 1 inhibitors by multiple docking strategies and prime/MM–GBSA calculation. *Journal of computational chemistry*, *32*(13), pp.2800-2809.

Duffy, P.E. and Gorres, J.P., 2020. Malaria vaccines since 2000: progress, priorities, products. *npj Vaccines*, *5*(1), pp.1-9.

Durrant, J.D. and McCammon, J.A., 2011. Molecular dynamics simulations and drug discovery. *BMC biology*, *9*(1), pp.1-9.

Earnshaw, C., 2010. StarDrop. *Chemistry world*, *7*(10), pp.55-55.

Egan, W.J., Merz, K.M. and Baldwin, J.J., 2000. Prediction of drug absorption using multivariate statistics. *Journal of medicinal chemistry*, *43*(21), pp.3867-3877.

Elfiky, A.A., 2021. SARS-CoV-2 RNA dependent RNA polymerase (RdRp) targeting: An in silico perspective. *Journal of Biomolecular Structure and Dynamics*, *39*(9), pp.3204-3212.

Elkwafi, G., Mohamed, N., Elabbar, F. and Alnajjar, R., 2021. Flavonoid content of the Libyan Onosma Cyrenaicum: isolation, identification, electronic chemical reactivity, drug likeness, docking, and MD study. *Journal of Biomolecular Structure and Dynamics*, pp.1-16.

Ersmark, K., Nervall, M., Hamelink, E., Janka, L.K., Clemente, J.C., Dunn, B.M., Blackman, M.J., Samuelsson, B., Åqvist, J. and Hallberg, A., 2005. Synthesis of malarial plasmepsin

inhibitors and prediction of binding modes by molecular dynamics simulations. *Journal of medicinal chemistry*, *48*(19), pp.6090-6106.

Ertl, P., Rohde, B. and Selzer, P., 2000. Fast calculation of molecular polar surface area as a sum of fragment-based contributions and its application to the prediction of drug transport properties. *Journal of medicinal chemistry*, *43*(20), pp.3714-3717.

Favuzza, P., de Lera Ruiz, M., Thompson, J.K., Triglia, T., Ngo, A., Steel, R.W., Vavrek, M., Christensen, J., Healer, J., Boyce, C. and Guo, Z., 2020. Dual plasmepsin-targeting antimalarial agents disrupt multiple stages of the malaria parasite life cycle. *Cell host & microbe*, *27*(4), pp.642-658.

Fernandez-Alvaro, E., Hong, W.D., Nixon, G.L., O'Neill, P.M. and Calderon, F., 2016. Antimalarial Chemotherapy: Natural Product Inspired Development of Preclinical and Clinical Candidates with Diverse Mechanisms of Action: Miniperspective. *Journal of medicinal chemistry*, *59*(12), pp.5587-5603.

Ferreira, L.G., Dos Santos, R.N., Oliva, G. and Andricopulo, A.D., 2015. Molecular docking and structure-based drug design strategies. *Molecules*, *20*(7), pp.13384-13421.

Flannery, E.L., Chatterjee, A.K. and Winzeler, E.A., 2013. Antimalarial drug discovery—approaches and progress towards new medicines. *Nature Reviews Microbiology*, *11*(12), pp.849-862.

Fu, Y., Zhao, J. and Chen, Z., 2018. Insights into the molecular mechanisms of protein-ligand interactions by molecular docking and molecular dynamics simulation: A case of oligopeptide binding protein. *Computational and mathematical methods in medicine*, *2018*.

Fuglebakk, E., Echave, J. and Reuter, N., 2012. Measuring and comparing structural fluctuation patterns in large protein datasets. *Bioinformatics*, *28*(19), pp.2431-2440.

Gallup, JL and Sachs, JD (2001) The economic burden of malaria. *The American Journal of Tropical Medicine Hygiene* 64, 85–96.

Garg, V.K., Avashthi, H., Tiwari, A., Jain, P.A., Ramkete, P.W., Kayastha, A.M. and Singh, V.K., 2016. MFPPI–multi FASTA ProtParam interface. *Bioinformation*, *12*(2), p.74.

Genheden, S. and Ryde, U., 2015. The MM/PBSA and MM/GBSA methods to estimate ligand-binding affinities. *Expert opinion on drug discovery*, *10*(5), pp.449-461.Wang, E., Sun, H., Wang, J., Wang, Z., Liu, H., Zhang, J.Z. and Hou, T., 2019. End-point binding free energy calculation with MM/PBSA and MM/GBSA: strategies and applications in drug design. *Chemical reviews*, *119*(16), pp.9478-9508.Keserű, G.M. and Makara, G.M., 2006. Hit discovery and hit-to-lead approaches. *Drug discovery today*, *11*(15-16), pp.741-748.

Geourjon, C. and Deleage, G., 1995. SOPMA: significant improvements in protein secondary structure prediction by consensus prediction from multiple alignments. *Bioinformatics*, *11*(6), pp.681-684.

Gimeno, A., Ojeda-Montes, M.J., Tomás-Hernández, S., Cereto-Massagué, A., Beltrán-Debón, R., Mulero, M., Pujadas, G. and Garcia-Vallvé, S., 2019. The light and dark sides of virtual screening: what is there to know?. *International journal of molecular sciences*, *20*(6), p.1375.

Good, M.F. and Stanisic, D.I., 2021. Biological strategies and political hurdles in developing malaria vaccines. *Expert Review of Vaccines*, *20*(2), pp.93-95.

Greenwood B.M., Bojang K., Whitty C.J., Targett G.A. (2005). Lancet. 365 (9469), pp 1487-98.

Guan, L., Yang, H., Cai, Y., Sun, L., Di, P., Li, W., Liu, G., & Tang, Y. (2018). ADMET-score - a comprehensive scoring function for evaluation of chemical drug-likeness. MedChemComm, 10(1), pp 148–157.

Guedes, I.A., Pereira, F.S. and Dardenne, L.E., 2018. Empirical scoring functions for structure-based virtual screening: applications, critical aspects, and challenges. *Frontiers in pharmacology*, *9*, p.1089.

Gunsaru, B., Burgess, S.J., Morrill, W., Kelly, J.X., Shomloo, S., Smilkstein, M.J., Liebman, K. and Peyton, D.H., 2017. Simplified reversed chloroquines to overcome malaria resistance to quinoline-based drugs. *Antimicrobial agents and chemotherapy*, *61*(5), pp.e01913-16.

Halgren, T., 2007. New method for fast and accurate binding-site identification and analysis. *Chemical biology & drug design*, *69*(2), pp.146-148.

Halgren, T.A., 1992. The representation of van der Waals (vdW) interactions in molecular mechanics force fields: potential form, combination rules, and vdW parameters. *Journal of the American Chemical Society*, *114*(20), pp.7827-7843.

Hamidović, A., Hasković, E., Muhić, S., Planinić, M., Omerović, N. and Škrbo, S., 2021, April. Application of In Silico Methods in Pharmacokinetic Studies During Drug Development. In *International Conference on Medical and Biological Engineering* (pp. 499-510). Springer, Cham.

Hang, J.W., Tukijan, F., Lee, E.Q.H., Abdeen, S.R., Aniweh, Y. and Malleret, B., 2021. Zoonotic Malaria: Non-Laverania Plasmodium Biology and Invasion Mechanisms. *Pathogens*, *10*(7), p.889.

Hann, M.M. and Oprea, T.I., 2004. Pursuing the leadlikeness concept in pharmaceutical research. *Current opinion in chemical biology*, *8*(3), pp.255-263.

Hasani, H.J. and Barakat, K., 2017. Homology modeling: an overview of fundamentals and tools. *Int. Rev. Model. Simul.*, *10*(2), pp.1-14.

Hillisch, A., Pineda, L.F. and Hilgenfeld, R., 2004. Utility of homology models in the drug discovery process. *Drug discovery today*, *9*(15), pp.659-669.

Hollingsworth, S.A. and Dror, R.O., 2018. Molecular dynamics simulation for all. *Neuron*, *99*(6), pp.1129-1143.

Hou, T., Wang, J., Li, Y. and Wang, W., 2011. Assessing the performance of the MM/PBSA and MM/GBSA methods. 1. The accuracy of binding free energy calculations based on molecular dynamics simulations. *Journal of chemical information and modeling*, *51*(1), pp.69-82.

Huang, F., Jacob, C.G., Takala-Harrison, S., Adams, M., Yang, H.L., Liu, H., Xia, Z.G., Zhou, S.S., Tang, L.H. and Plowe, C.V., 2021. Genomic epidemiology of antimalarial drug resistance in Plasmodium falciparum in Southern China. *Frontiers in cellular and infection microbiology*, *10*, p.809

Huang, S.Y., 2018. Comprehensive assessment of flexible-ligand docking algorithms: current effectiveness and challenges. *Briefings in bioinformatics*, *19*(5), pp.982-994.

Huimin Luo, Min Li, Mengyun Yang, Fang-Xiang Wu, Yaohang Li, Jianxin Wang, Biomedical data and computational models for drug repositioning: a comprehensive review, Briefings in Bioinformatics, 2020, p.176.

Humphrey, W., Dalke, A. and Schulten, K., 1996. VMD: visual molecular dynamics. *Journal of molecular graphics*, *14*(1), pp.33-38.

Idris, M.O., Yekeen, A.A., Alakanse, O.S. and Durojaye, O.A., 2021. Computer-aided screening for potential TMPRSS2 inhibitors: a combination of pharmacophore modeling, molecular docking and molecular dynamics simulation approaches. *Journal of Biomolecular Structure and Dynamics*, *39*(15), pp.5638-5656.

Ikeda, T., Behera, S.K., Morioka, Y., Minakawa, N., Hashizume, M., Tsuzuki, A., Maharaj, R. and Kruger, P., 2017. Seasonally lagged effects of climatic factors on malaria incidence in South Africa. *Scientific reports*, *7*(1), pp.1-9.

Imam, S.S. and Gilani, S.J., 2017. Computer aided drug design: a novel loom to drug discovery. *Organic & Medicinal Chemistry International Journal*, *1*(3), pp.113-118.

Imam, S.S. and Gilani, S.J., 2017. Computer aided drug design: a novel loom to drug discovery. *Organic & Medicinal Chemistry International Journal*, *1*(3), pp.113-118.

Ishengoma, D.S., Saidi, Q., Sibley, C.H., Roper, C. and Alifrangis, M., 2019. Deployment and utilization of next-generation sequencing of Plasmodium falciparum to guide anti-malarial

drug policy decisions in sub-Saharan Africa: opportunities and challenges. *Malaria journal*, *18*(1), pp.1-10.

Işık, M., Levorse, D., Mobley, D.L., Rhodes, T. and Chodera, J.D., 2019. Octanol–water partition coefficient measurements for the SAMPL6 blind prediction challenge. *Journal of computer-aided molecular design*, pp.1-16.

Islam, R., Parves, M.R., Paul, A.S., Uddin, N., Rahman, M.S., Mamun, A.A., Hossain, M.N., Ali, M.A. and Halim, M.A., 2021. A molecular modeling approach to identify effective antiviral phytochemicals against the main protease of SARS-CoV-2. *Journal of Biomolecular Structure and Dynamics*, *39*(9), pp.3213-3224.

Jorgensen, W.L. and Tirado-Rives, J., 1988. The OPLS [optimized potentials for liquid simulations] potential functions for proteins, energy minimizations for crystals of cyclic peptides and crambin. *Journal of the American Chemical Society*, *110*(6), pp.1657-1666.

Jorgensen, W.L. and Tirado-Rives, J., 1988. The OPLS [optimized potentials for liquid simulations] potential functions for proteins, energy minimizations for crystals of cyclic peptides and crambin. *Journal of the American Chemical Society*, *110*(6), pp.1657-1666.

Jorgensen, W.L., 1986. Optimized intermolecular potential functions for liquid alcohols. *The Journal of Physical Chemistry*, *90*(7), pp.1276-1284.

Joshi, T., Joshi, T., Sharma, P., Chandra, S. and Pande, V., 2021. Molecular docking and molecular dynamics simulation approach to screen natural compounds for inhibition of Xanthomonas oryzae pv. Oryzae by targeting peptide deformylase. *Journal of Biomolecular Structure and Dynamics*, *39*(3), pp.823-840.

Kaminski, G.A., Friesner, R.A., Tirado-Rives, J. and Jorgensen, W.L., 2001. Evaluation and reparametrization of the OPLS-AA force field for proteins via comparison with accurate quantum chemical calculations on peptides. *The Journal of Physical Chemistry B*, *105*(28), pp.6474-6487.

Kanoi, B., Nagaoka, H., Morita, M., Tsuboi, T. and Takashima, E., 2020. Leveraging the wheat germ cell-free protein synthesis system to accelerate malaria vaccine development. *Parasitology International*, p.102224.

Karri, S., Sharma, S. and Kaur, G., 2019. Pharmacological and analytical aspects of artemisinin for malaria: Advances and challenges. *Asian Pacific Journal of Tropical Medicine*, *12*(8), p.339.

Kazmi, S.R., Jun, R., Yu, M.S., Jung, C. and Na, D., 2019. In silico approaches and tools for the prediction of drug metabolism and fate: A review. *Computers in biology and medicine*, *106*, pp.54-64.

Kinirons, M.T. and O'Mahony, M.S., 2004. Drug metabolism and ageing. *British journal of clinical pharmacology*, *57*(5), pp.540-544.

Koshland, D.E., 1963. Correlation of structure and function in enzyme action. *Science*, *142*(3599), pp.1533-1541.

Kramer, J.A., Sagartz, J.E. and Morris, D.L., 2007. The application of discovery toxicology and pathology towards the design of safer pharmaceutical lead candidates. *Nature Reviews Drug Discovery*, *6*(8), pp.636-649.

Kumar, S. and Kumar, S., 2019. Molecular docking: a structure-based approach for drug repurposing. *In Silico Drug Design* (pp. 161-189). Academic Press.

Kutlushina, A., Khakimova, A., Madzhidov, T. and Polishchuk, P., 2018. Ligand-based pharmacophore modeling using novel 3D pharmacophore signatures. *Molecules*, *23*(12), p.3094.

Labarga, A., Valentin, F., Anderson, M. and Lopez, R., 2007. Web services at the European bioinformatics institute. *Nucleic acids research*, *35*(suppl_2), pp.W6-W11.

L'abbate, F.P., Müller, R., Openshaw, R., Combrinck, J.M., de Villiers, K.A., Hunter, R. and Egan, T.J., 2018. Hemozoin inhibiting 2-phenylbenzimidazoles active against malaria parasites. *European journal of medicinal chemistry*, *159*, pp.243-254.

Lagorce, D., Bouslama, L., Becot, J., Miteva, M.A. and Villoutreix, B.O., 2017. FAF-Drugs4: free ADME-tox filtering computations for chemical biology and early stages drug discovery. *Bioinformatics*, *33*(22), pp.3658-3660.

Lagorce, D., Douguet, D., Miteva, M.A. and Villoutreix, B.O., 2017. Computational analysis of calculated physicochemical and ADMET properties of protein-protein interaction inhibitors. *Scientific reports*, *7*(1), pp.1-15.

Laskowski, R.A., MacArthur, M.W., Moss, D.S. and Thornton, J.M., 1993. PROCHECK: a program to check the stereochemical quality of protein structures. *Journal of applied crystallography*, *26*(2), pp.283-291.

Lewis, D.F., 2003. Human cytochromes P450 associated with the phase 1 metabolism of drugs and other xenobiotics: a compilation of substrates and inhibitors of the CYP1, CYP2 and CYP3 families. *Current medicinal chemistry*, *10*(19), pp.1955-1972.

Li, J., Fu, A. and Zhang, L., 2019. An overview of scoring functions used for protein–ligand interactions in molecular docking. *Interdisciplinary Sciences: Computational Life Sciences*, *11*(2), pp.320-328.

Li, Q. and Shah, S., 2017. Structure-based virtual screening. In *Protein Bioinformatics*, pp. 111-124. Humana Press, New York, NY.

Li, Y., Zhang, X. and Cao, D., 2013. The role of shape complementarity in the protein-protein interactions. *Scientific reports*, *3*(1), pp.1-7.

Lipinski, C.A., 2004. Lead-and drug-like compounds: the rule-of-five revolution. *Drug discovery today: Technologies*, *1*(4), pp.337-341.

Lipinski, C.A., 2012. *Phenotypic and in vivo screening: Lead discovery and drug repurposing* (pp. 86-93). Royal Society of Chemistry.

Lipinski, C.A., Lombardo, F., Dominy, B.W. and Feeney, P.J., 1997. Experimental and computational approaches to estimate solubility and permeability in drug discovery and development settings. *Advanced drug delivery reviews*, *23*(1-3), pp.3-25.

Lipinski, C.A.L.F., 2002. Poor aqueous solubility—an industry wide problem in drug discovery. *Am Pharm Rev*, *5*(3), pp.82-85.

Liu, Y., Tikunov, Y., Schouten, R.E., Marcelis, L.F., Visser, R.G. and Bovy, A., 2018. Anthocyanin biosynthesis and degradation mechanisms in Solanaceous vegetables: a review. *Frontiers in Chemistry*, *6*, p.52.

Lozano, J.M., Rodríguez Parra, Z., Hernández-Martínez, S., Yasnot-Acosta, M.F., Rojas, A.P., Marín-Waldo, L.S. and Rincón, J.E., 2021. The Search of a Malaria Vaccine: The Time for Modified Immuno-Potentiating Probes. *Vaccines*, *9*(2), p.115.

Luo, H., Li, M., Yang, M., Wu, F.X., Li, Y. and Wang, J., 2021. Biomedical data and computational models for drug repositioning: a comprehensive review. *Briefings in bioinformatics*, *22*(2), pp.1604-1619.

Lyke, K.E., 2017. Steady progress toward a malaria vaccine. *Current opinion in infectious diseases*, *30*(5), pp.463-470.

Macalino, S.J.Y., Gosu, V., Hong, S. and Choi, S., 2015. Role of computer-aided drug design in modern drug discovery. *Archives of pharmacal research*, *38*(9), pp.1686-1701.

Maia, E.H.B., Assis, L.C., de Oliveira, T.A., da Silva, A.M. and Taranto, A.G., 2020. Structure-based virtual screening: from classical to artificial intelligence. *Frontiers in chemistry*, *8*, p.343.

Makenga, G., Menon, S., Baraka, V., Minja, D.T., Nakato, S., Delgado-Ratto, C., Francis, F., Lusingu, J.P. and Van Geertruyden, J.P., 2020. Prevalence of malaria parasitaemia in school-aged children and pregnant women in endemic settings of sub-Saharan Africa: A systematic review and meta-analysis. *Parasite Epidemiology and Control*, p.e00188.

Manana, P.N., Kuonza, L., Musekiwa, A., Mpangane, H.D. and Koekemoer, L.L., 2018. Knowledge, attitudes and practices on malaria transmission in Mamfene, KwaZulu-Natal Province, South Africa 2015. *BMC Public Health*, *18*(1), pp.1-7.

Mbohou Nchetnkou, C., Kojom Foko, L.P. and Lehman, L.G., 2020. Knowledge, Attitude, and Practices towards Malaria among Employees from Enterprises in the Town of Douala, Cameroon. *BioMed research international, 2020. medicine and hygiene, 103*(5), p.1871.

Medina-Franco, J.L., Giulianotti, M.A., Welmaker, G.S. and Houghten, R.A., 2013. Shifting from the single to the multitarget paradigm in drug discovery. *Drug discovery today*, *18*(9-10), pp.495-501.

Meng, X.Y., Zhang, H.X., Mezei, M. and Cui, M., 2011. Molecular docking: a powerful approach for structure-based drug discovery. *Current computer-aided drug design*, *7*(2), pp.146-157.

Miguel-Blanco, C., Murithi, J.M., Benavente, E.D., Angrisano, F., Sala, K.A., van Schalkwyk, D.A., Vanaerschot, M., Schwach, F., Fuchter, M.J., Billker, O. and Sutherland, C.J., 2021. The antimalarial efficacy and mechanism of resistance of the novel chemotype DDD01034957. *Scientific reports*, *11*(1), pp.1-9.

Mishra, D., Maurya, R.R., Kumar, K., Munjal, N.S., Bahadur, V., Sharma, S., Singh, P. and Bahadur, I., 2021. Structurally modified compounds of hydroxychloroquine, remdesivir and tetrahydrocannabinol against main protease of SARS-CoV-2, a possible hope for COVID-19: Docking and molecular dynamics simulation studies. *Journal of Molecular Liquids*, *335*, p.116185.

Mishra, M., Mishra, V.K., Kashaw, V., Iyer, A.K. and Kashaw, S.K., 2017. Comprehensive review on various strategies for antimalarial drug discovery. *European journal of medicinal chemistry*, *125*, pp.1300-1320.

Momen, R., Azizi, A., Wang, L., Yang, P., Xu, T., Kirk, S.R., Li, W., Manzhos, S. and Jenkins, S., 2018. The role of weak interactions in characterizing peptide folding preferences using a QTAIM interpretation of the Ramachandran plot (ϕ-ψ). *International Journal of Quantum Chemistry*, *118*(2), p.e25456.

Muegge, I., 2002. Pharmacophore features of potential drugs. *Chemistry–A European Journal*, *8*(9), pp.1976-1981.

Muegge, I., 2003. Selection criteria for drug-like compounds. *Medicinal research reviews*, *23*(3), pp.302-321.

Muegge, I., Heald, S.L. and Brittelli, D., 2001. Simple selection criteria for drug-like chemical matter. *Journal of medicinal chemistry*, *44*(12), pp.1841-1846.

Muhammed, M.T. and Aki-Yalcin, E., 2019. Homology modeling in drug discovery: Overview, current applications, and future perspectives. *Chemical biology & drug design*, *93*(1), pp.12-20.

Muralidharan, N., Sakthivel, R., Velmurugan, D. and Gromiha, M.M., 2021. Computational studies of drug repurposing and synergism of lopinavir, oseltamivir and ritonavir binding with SARS-CoV-2 protease against COVID-19. *Journal of Biomolecular Structure and Dynamics*, *39*(7), pp.2673-2678.

Muratov, E.N., Bajorath, J., Sheridan, R.P., Tetko, I.V., Filimonov, D., Poroikov, V., Oprea, T.I., Baskin, I.I., Varnek, A., Roitberg, A. and Isayev, O., 2020. QSAR without borders. *Chemical Society Reviews*, *49*(11), pp.3525-3564.

Muregi, F.W. and Ishih, A., 2010. Next-generation antimalarial drugs: hybrid molecules as a new strategy in drug design. *Drug development research*, *71*(1), pp.20-32.

Naqvi, A.A., Mohammad, T., Hasan, G.M. and Hassan, M., 2018. Advancements in docking and molecular dynamics simulations towards ligand-receptor interactions and structure-function relationships. *Current topics in medicinal chemistry*, *18*(20), pp.1755-1768.

Ndagi, U., Mhlongo, N.N. and Soliman, M.E., 2017. The impact of Thr91 mutation on c-Src resistance to UM-164: molecular dynamics study revealed a new opportunity for drug design. *Molecular Biosystems*, *13*(6), pp.1157-1171.

Nduka, C.C., Chineke, H.N., Adogu, P.O. and Chizoba, A.F., 2020. Socioeconomic Determinants of Malaria in Selected Urban and Rural Areas in Anambra State, Nigeria. *International Journal of TROPICAL DISEASE & Health*, pp.53-64.

Neves, B.J., Braga, R.C., Melo-Filho, C.C., Moreira-Filho, J.T., Muratov, E.N. and Andrade, C.H., 2018. QSAR-based virtual screening: advances and applications in drug discovery. *Frontiers in pharmacology*, *9*, p.1275.

Nunes, R.R., Fonseca, A.L.D., Pinto, A.C.D.S., Maia, E.H.B., Silva, A.M.D., Varotti, F.D.P. and Taranto, A.G., 2019. Brazilian malaria molecular targets (BraMMT): selected receptors for virtual high-throughput screening experiments. *Memórias do Instituto Oswaldo Cruz*, *114*.

Nureye, D. and Assefa, S., 2020. Old and recent advances in life cycle, pathogenesis, diagnosis, prevention, and treatment of malaria including perspectives in Ethiopia. *The Scientific World Journal*, *2020*.

O Achieng, A., Rawat, M., Ogutu, B., Guyah, B., Michael Ong'echa, J., J Perkins, D. and Kempaiah, P., 2017. Antimalarials: molecular drug targets and mechanism of action. *Current topics in medicinal chemistry*, *17*(19), pp.2114-2128.

Okombo, J., Brunschwig, C., Singh, K., Dziwornu, G.A., Barnard, L., Njoroge, M., Wittlin, S. and Chibale, K., 2019. Antimalarial pyrido [1, 2-a] benzimidazole derivatives with Mannich base side chains: synthesis, pharmacological evaluation, and reactive metabolite trapping studies. *ACS infectious diseases*, *5*(3), pp.372-384.

Oliveira, R., Miranda, D., Magalhães, J., Capela, R., Perry, M.J., O'Neill, P.M., Moreira, R. and Lopes, F., 2015. From hybrid compounds to targeted drug delivery in antimalarial therapy. *Bioorganic & medicinal chemistry*, *23*(16), pp.5120-5130.

Ouji, M., Augereau, J.M., Paloque, L. and Benoit-Vical, F., 2018. Plasmodium falciparum resistance to artemisinin-based combination therapies: A sword of Damocles in the path toward malaria elimination. *Parasite*, *25*.

Oyinloye, B.E., Iwaloye, O. and Ajiboye, B.O., 2021. Polypharmacology of Gongronema latifolium leaf secondary metabolites against protein kinases implicated in Parkinson's disease and Alzheimer's disease. *Scientific African*, p.e00826.

Pandey, K.C. and Dixit, R., 2012. Structure-function of falcipains: malarial cysteine proteases. *Journal of Tropical Medicine*, pp212-214.

Pandey, K.C., Singh, N., Arastu-Kapur, S., Bogyo, M. and Rosenthal, P.J., 2006. Falstatin, a cysteine protease inhibitor of Plasmodium falciparum, facilitates erythrocyte invasion. *PLoS pathogens*, *2*(11), p.e117.

Paramashivam, S. and Dhiraviam, K.N., 2021. Computational insights into the identification of a potent matrix metalloproteinase inhibitor from Indigofera aspalathoides to control cancer metastasis. *3 Biotech*, *11*(5), pp.1-19.

Pazhayam, N.M., Chhibber-Goel, J. and Sharma, A., 2019. New leads for drug repurposing against malaria. *Drug Discovery Today*, *24*(1), pp.263-271.

Phillips, J.C., Braun, R., Wang, W., Gumbart, J., Tajkhorshid, E., Villa, E., Chipot, C., Skeel, R.D., Kale, L. and Schulten, K., 2005. Scalable molecular dynamics with NAMD. *Journal of computational chemistry*, *26*(16), pp.1781-1802.

Pinzi, L. and Rastelli, G., 2019. Molecular docking: shifting paradigms in drug discovery. *International journal of molecular sciences*, *20*(18), p.4331.

Pollastri, M.P., 2010. Overview on the Rule of Five. *Current protocols in pharmacology*, *49*(1), pp.9-12

Poongavanam, V., Doak, B.C. and Kihlberg, J., 2018. Opportunities and guidelines for discovery of orally absorbed drugs in beyond rule of 5 space. *Current opinion in chemical biology*, *44*, pp.23-29.

Prada-Gracia, D., Huerta-Yépez, S. and Moreno-Vargas, L.M., 2016. Application of computational methods for anticancer drug discovery, design, and optimization. *Boletín Médico Del Hospital Infantil de México (English Edition)*, *73*(6), pp.411-423.

Prasanna, S. and Doerksen, R.J., 2009. Topological polar surface area: a useful descriptor in 2D-QSAR. *Current medicinal chemistry*, *16*(1), pp.21-41.

Prieto-Martínez, F.D., Arciniega, M. and Medina-Franco, J.L., 2018. Molecular docking: current advances and challenges. *TIP. Revista especializada en ciencias químico-biológicas*, *21*.
Prieto-Martínez, F.D., Arciniega, M. and Medina-Franco, J.L., 2018. Molecular docking: current advances and challenges. *TIP. Revista especializada en ciencias químico-biológicas*, *21*.
Pushpakom, S., Iorio, F., Eyers, P.A., Escott, K.J., Hopper, S., Wells, A., Doig, A., Guilliams, T., Latimer, J., McNamee, C. and Norris, A., 2019. Drug repurposing: progress, challenges and recommendations. *Nature reviews Drug discovery*, *18*(1), pp.41-58.

Räder, A.F., Weinmüller, M., Reichart, F., Schumacher-Klinger, A., Merzbach, S., Gilon, C., Hoffman, A. and Kessler, H., 2018. Orally active peptides: is there a magic bullet?. *Angewandte Chemie International Edition*, *57*(44), pp.14414-14438.

Ramsay, R.R., Popovic-Nikolic, M.R., Nikolic, K., Uliassi, E. and Bolognesi, M.L., 2018. A perspective on multi-target drug discovery and design for complex diseases. *Clinical and translational medicine*, *7*(1), pp.1-14.

Rennenberg, A., Lehmann, C., Heitmann, A., Witt, T., Hansen, G., Nagarajan, K., Deschermeier, C., Turk, V., Hilgenfeld, R. and Heussler, V.T., 2010. Exoerythrocytic Plasmodium parasites secrete a cysteine protease inhibitor involved in sporozoite invasion and capable of blocking cell death of host hepatocytes. *PLoS pathogens*, *6*(3), p.e1000825.

Riggle, B.A., Miller, L.H. and Pierce, S.K., 2020. Desperately seeking therapies for cerebral malaria. *The Journal of Immunology*, *204*(2), pp.327-334.

Rim, K.T., 2020. In silico prediction of toxicity and its applications for chemicals at work. *Toxicology and Environmental Health Sciences*, p.1.
Rim, K.T., 2020. In silico prediction of toxicity and its applications for chemicals at work. *Toxicology and Environmental Health Sciences*, p.1.
Roccatano, D., 2020. The Molecular Dynamics Simulation of Peptides on Gold Nanosurfaces. In *Nanoparticles in Biology and Medicine* (pp. 177-197). Humana, New York, NY.

Rose, S., Ali, M.F., Bakhsh, K., Ashfaq, M. and Hassan, S., 2020. Linking environment, malaria, and agricultural returns: a labor time use analysis at different stages of production using 3SLS. *Environmental Science and Pollution Research*, *27*(16), pp.19714-19723.

Rosenthal, P., Sundararaj, S., Saxena, A.K., Sharma, R., Vashisht, K., Sharma, S., Anvikar, A., Dixit, R., Rosenthal, P.J. and Pandey, K.C., 2014. Cross-talk between malarial cysteine proteases and falstatin: The BC loop as a hot-spot target.

Rosenthal, P.J., 2003. Antimalarial drug discovery: old and new approaches. *Journal of Experimental Biology*, *206*(21), pp.3735-3744.

Rosenthal, P.J., 2011. Falcipains and other cysteine proteases of malaria parasites. *Cysteine proteases of pathogenic organisms*, pp.30-48.

Rosenthal, P.J., John, C.C. and Rabinovich, N.R., 2019. Malaria: how are we doing and how can we do better? *The American journal of tropical medicine and hygiene*, *100*(2), p.239.

Rout, S. and Mahapatra, R.K., 2019. Plasmodium falciparum: Multidrug resistance. *Chemical biology & drug design*, *93*(5), pp.737-759.

Rowaiye, A.B., Tecamendes, Y.J., Olofinsae, S.A., Oche, J.B., Oladipo, O.H., Okpalefe, O.A. and Ogidigo, J.O., 2021. Camptothecin shows better promise than Curcumin in the inhibition of the Human Telomerase: A computational study. *Heliyon*, p.e07742.

Rudrapal, M. and Chetia, D., 2020. Virtual screening, molecular docking and QSAR studies in drug discovery and development programme. *Journal of Drug Delivery and Therapeutics*, *10*(4), pp.225-233.

Ruswanto, R., Miftah, A.M. and Tjahjono, D.H., 2021. In silico study of 1-benzoyl-3-methylthiourea derivatives activity as epidermal growth factor receptor (EGFR) tyrosine kinase inhibitor candidates. *Chemical Data Collections*, p.100741.

Saikia, S. and Bordoloi, M., 2019. Molecular docking: challenges, advances and its use in drug discovery perspective. *Current drug targets*, *20*(5), pp.501-521.

Salentin, S., Schreiber, S., Haupt, V.J., Adasme, M.F. and Schroeder, M., 2015. PLIP: fully automated protein–ligand interaction profiler. *Nucleic acids research*, *43*(W1), pp.W443-W447.

Salentin, S., Schreiber, S., Haupt, V.J., Adasme, M.F. and Schroeder, M., 2015. PLIP: fully automated protein–ligand interaction profiler. *Nucleic acids research*, *43*(W1), pp.W443-W447.

Salman, M.M., Al-Obaidi, Z., Kitchen, P., Loreto, A., Bill, R.M. and Wade-Martins, R., 2021. Advances in applying computer-aided drug design for neurodegenerative diseases. *International Journal of Molecular Sciences*, *22*(9), p.4688.

Salman, M.M., Al-Obaidi, Z., Kitchen, P., Loreto, A., Bill, R.M. and Wade-Martins, R., 2021. Advances in applying computer-aided drug design for neurodegenerative diseases. *International Journal of Molecular Sciences*, *22*(9), p.4688.

Salmaso, V. and Moro, S., 2018. Bridging molecular docking to molecular dynamics in exploring ligand-protein recognition process: an overview. *Frontiers in pharmacology*, *9*, p.923.

Salmaso, V. and Moro, S., 2018. Bridging molecular docking to molecular dynamics in exploring ligand-protein recognition process: an overview. *Frontiers in pharmacology*, *9*, p.923.

Sander, T., Freyss, J., von Korff, M. and Rufener, C., 2015. DataWarrior: an open-source program for chemistry aware data visualization and analysis. *Journal of chemical information and modeling*, *55*(2), pp.460-473.

Sato, S., 2021. Plasmodium—a brief introduction to the parasites causing human malaria and their basic biology. *Journal of physiological anthropology*, *40*(1), pp.1-13.

Sayed, A.M., Khattab, A.R., AboulMagd, A.M., Hassan, H.M., Rateb, M.E., Zaid, H. and Abdelmohsen, U.R., 2020. Nature as a treasure trove of potential anti-SARS-CoV drug leads: a structural/mechanistic rationale. *RSC Advances*, *10*(34), pp.19790-19802.

Seeliger, D. and de Groot, B.L., 2010. Ligand docking and binding site analysis with PyMOL and Autodock/Vina. *Journal of computer-aided molecular design*, *24*(5), pp.417-422.

Segall, M., 2014. Advances in multiparameter optimization methods for de novo drug design. *Expert opinion on drug discovery*, *9*(7), pp.803-817.

Selvaraj, C., Dinesh, D.C., Panwar, U., Abhirami, R., Boura, E. and Singh, S.K., 2021. Structure-based virtual screening and molecular dynamics simulation of SARS-CoV-2 Guanine-N7 methyltransferase (nsp14) for identifying antiviral inhibitors against COVID-19. *Journal of Biomolecular Structure and Dynamics*, *39*(13), pp.4582-4593.

Sethi, A., Sanam, S., Munagalasetty, S., Jayanthi, S. and Alvala, M., 2020. Understanding the role of galectin inhibitors as potential candidates for SARS-CoV-2 spike protein: in silico studies. *RSC Advances*, *10*(50), pp.29873-29884.Du, J., Sun, H., Xi, L., Li, J., Yang, Y., Liu, H. and Yao, X., 2011. Molecular modeling study of checkpoint kinase 1 inhibitors by multiple docking strategies and prime/MM–GBSA calculation. *Journal of computational chemistry*, *32*(13), pp.2800-2809.

Sharma, C. and Awasthi, S.K., 2015. Recent Advances in Antimalarial Drug Discovery—Challenges and Opportunities. *An Overview of Tropical Diseases*, p.39.

Sharma, P., Joshi, T., Mathpal, S., Joshi, T., Pundir, H., Chandra, S. and Tamta, S., 2020. Identification of natural inhibitors against Mpro of SARS-CoV-2 by molecular docking, molecular dynamics simulation, and MM/PBSA methods. *Journal of Biomolecular Structure and Dynamics*, pp.1-12.

Shibeshi, M.A., Kifle, Z.D. and Atnafie, S.A., 2020. Antimalarial drug resistance and novel targets for antimalarial drug discovery. *Infection and Drug Resistance*, *13*, p.4047.

Shretta, R., Silal, S.P., Malm, K., Mohammed, W., Narh, J., Piccinini, D., Bertram, K., Rockwood, J. and Lynch, M., 2020. Estimating the risk of declining funding for malaria in Ghana: the case for continued investment in the malaria response. *Malaria journal*, *19*, pp.1-15.

Sinden, R.E. and Gilles, H.M., 2017. The malaria parasites. In *Essential malariology* (pp. 8-34). CRC Press.

Singh, S. and Singh, V.K., 2020. Molecular Dynamics Simulation: Methods and Application. In *Frontiers in Protein Structure, Function, and Dynamics* (pp. 213-238). Springer, Singapore.

Singh, S. and Singh, V.K., 2020. Molecular Dynamics Simulation: Methods and Application. In *Frontiers in Protein Structure, Function, and Dynamics* (pp. 213-238). Springer, Singapore.

Sivaramakrishnan, M., Kandaswamy, K., Natesan, S., Devarajan, R.D., Ramakrishnan, S.G. and Kothandan, R., 2020. Molecular docking and dynamics studies on plasmepsin v of malarial parasite Plasmodium vivax. *Informatics in Medicine Unlocked*, *19*, p.100331.

Smeralda, W., Since, M., Corvaisier, S., Legay, R., Voisin-Chiret, A.S. and Malzert-Freon, A., 2019. Microplate assay for lipophilicity determination using intrinsic fluorescence of drugs: Application to a promising anticancer lead, pyridoclax. *European Journal of Pharmaceutical Sciences*, *131*, pp.75-83.

Smith, R.D., Keogh-Brown, M.R., Chico, R.M., Bretscher, M.T., Drakeley, C. and Jensen, H.T., 2020. Will More of the Same Achieve Malaria Elimination? Results from an Integrated Macroeconomic Epidemiological Demographic Model. *The American journal of tropical medicine and hygiene*, *103*(5), p.1871.

Stefaniu, A., 2019. Introductory chapter: molecular docking and molecular dynamics techniques to achieve rational drug design. In *Molecular Docking and Molecular Dynamics*. IntechOpen.

Stefaniu, A., 2019. Introductory chapter: molecular docking and molecular dynamics techniques to achieve rational drug design. In *Molecular Docking and Molecular Dynamics*. IntechOpen.

Structure-based methods in drug discovery: An overview of combined virtual screening approaches. *Molecules*, *25*(20), p.4723.

Studio, D., 2008. Discovery Studio. *Accelrys [2.1]*.

Studio, D., 2008. Discovery Studio. *Accelrys [2.1]*.

Sturgeon, J.B. and Laird, B.B., 2000. Symplectic algorithm for constant-pressure molecular dynamics using a Nosé–Poincaré thermostat. *The Journal of Chemical Physics*, *112*(8), pp.3474-3482.

Sturgeon, J.B. and Laird, B.B., 2000. Symplectic algorithm for constant-pressure molecular dynamics using a Nosé–Poincaré thermostat. *The Journal of Chemical Physics*, *112*(8), pp.3474-3482.

Sun, H., Li, Y., Tian, S., Xu, L. and Hou, T., 2014. Assessing the performance of MM/PBSA and MM/GBSA methods. 4. Accuracies of MM/PBSA and MM/GBSA methodologies evaluated by various simulation protocols using PDBbind data set. *Physical Chemistry Chemical Physics*, *16*(31), pp.16719-16729.

Sundararaj, S., Saxena, A.K., Sharma, R., Vashisht, K., Sharma, S., Anvikar, A., Dixit, R., Rosenthal, P.J. and Pandey, K.C., 2014. Cross-talk between malarial cysteine proteases and falstatin: the BC loop as a hot-spot target. *PLoS One*, *9*(4), p.93008.

Sundararaj, S., Saxena, A.K., Sharma, R., Vashisht, K., Sharma, S., Anvikar, A., Dixit, R., Rosenthal, P.J. and Pandey, K.C., 2014. Cross-talk between malarial cysteine proteases and falstatin: the BC loop as a hot-spot target. *PLoS One*, *9*(4), p.93008.

Surabhi, S. and Singh, B.K., 2018. Computer aided drug design: an overview. *Journal of Drug delivery and Therapeutics*, *8*(5), pp.504-509.

Surabhi, S. and Singh, B.K., 2018. Computer aided drug design: an overview. *Journal of Drug delivery and Therapeutics*, *8*(5), pp.504-509.

Suzek, B.E., Huang, H., McGarvey, P., Mazumder, R. and Wu, C.H., 2007. UniRef: comprehensive and non-redundant UniProt reference clusters. *Bioinformatics*, *23*(10), pp.1282-1288.

Syahri, J., Yuanita, E., Nurohmah, B.A., Armunanto, R. and Purwono, B., 2017. Chalcone analogue as potent anti-malarial compounds against Plasmodium falciparum: Synthesis, biological evaluation, and docking simulation study. *Asian Pacific Journal of Tropical Biomedicine*, *7*(8), pp.675-679.

Tajes, M., Ramos-Fernández, E., Weng-Jiang, X., Bosch-Morato, M., Guivernau, B., Eraso-Pichot, A., Salvador, B., Fernandez-Busquets, X., Roquer, J. and Munoz, F.J., 2014. The blood-brain barrier: structure, function and therapeutic approaches to cross it. *Molecular membrane biology*, *31*(5), pp.152-167.

Talapko, J., Škrlec, I., Alebić, T., Jukić, M. and Včev, A., 2019. Malaria: the past and the present. *Microorganisms*, *7*(6), p.179.

Talevi, A., 2018. Computer-aided drug design: An overview. *Computational drug discovery and design*, pp.1-19.

Tao, X., Huang, Y., Wang, C., Chen, F., Yang, L., Ling, L., Che, Z. and Chen, X., 2020. Recent developments in molecular docking technology applied in food science: a review. *International Journal of Food Science & Technology*, *55*(1), pp.33-45.

Tastan Bishop, A.O., De Beer, T.A. and Joubert, F., 2008. Protein homology modelling and its use in South Africa: research in action. *South African Journal of Science*, *104*(1), pp.2-6.

Tebben, K., Bradwell, K. and Serre, D., 2021. Variation in selective constraints along the Plasmodium life cycle. *Infection, Genetics and Evolution*, *92*, p.104908.

Tembe-Fokunang, E.A., Charles, F., Kaba, N., Donatien, G., Michael, A. and Bonaventure, N., 2019. The potential pharmacological and medicinal properties of neem (Azadirachta indica A. Juss) in the drug development of phytomedicine. *Journal of Complementary and Alternative Medical Research*, pp.1-18.

Thillainayagam, M., Ramaiah, S. and Anbarasu, A., 2020. Molecular docking and dynamics studies on novel benzene sulfonamide substituted pyrazole-pyrazoline analogues as potent inhibitors of Plasmodium falciparum Histo aspartic protease. *Journal of Biomolecular Structure and Dynamics*, *38*(11), pp.3235-3245.

Tibon, N.S., Ng, C.H. and Cheong, S.L., 2020. Current progress in antimalarial pharmacotherapy and multi-target drug discovery. *European journal of medicinal chemistry*, *188*, p.111983.

Tonholo, D.R., Maltarollo, V.G., Kronenberger, T., Silva, I.R., Azevedo, P.O., Oliveira, R.B., Souza, L.C.R. and Tagliati, G.A., 2020. Preclinical toxicity of innovative molecules: In vitro, in vivo and metabolism prediction. *Chemico-biological interactions*, *315*, p.108896.

Torres, P.H., Sodero, A.C., Jofily, P. and Silva-Jr, F.P., 2019. Key topics in molecular docking for drug design. *International journal of molecular sciences*, *20*(18), p.4574.

Tripathi, A. and Misra, K., 2017. Molecular docking: A structure-based drug designing approach. *JSM Chem*, *5*(2), pp.1042-1047.

Trott, O. and Olson, A.J., 2010. AutoDock Vina: improving the speed and accuracy of docking with a new scoring function, efficient optimization, and multithreading. *Journal of computational chemistry*, *31*(2), pp.455-461.

Trott, O. and Olson, A.J., 2010. AutoDock Vina: improving the speed and accuracy of docking with a new scoring function, efficient optimization, and multithreading. *Journal of computational chemistry*, *31*(2), pp.455-461.

Tsui, V. and Case, D.A., 2000. Theory and applications of the generalized Born solvation model in macromolecular simulations. *Biopolymers: Original Research on Biomolecules*, *56*(4), pp.275-291.

Tušar, L., Usenik, A., Turk, B. and Turk, D., 2021. Mechanisms Applied by Protein Inhibitors to Inhibit Cysteine Proteases. *International Journal of Molecular Sciences*, *22*(3), p.997.

Tyzack, J.D. and Kirchmair, J., 2019. Computational methods and tools to predict cytochrome P450 metabolism for drug discovery. *Chemical biology & drug design*, *93*(4), pp.377-386.

Umar, A.B., Uzairu, A., Shallangwa, G.A. and Uba, S., 2021. Molecular Docking Strategy to Design Novel V600E-BRAF Kinase Inhibitors with Prediction of Their Drug-Likeness and Pharmacokinetics ADMET Properties. *Chemistry Africa*, *4*(1), pp.189-205.

Uzor, P.F., 2020. Alkaloids from plants with antimalarial activity: a review of recent studies. *Evidence-Based Complementary and Alternative Medicine*, *2020*.

Uzunova, K., Filipova, E., Pavlova, V. and Vekov, T., 2020. Insights into antiviral mechanisms of remdesivir, lopinavir/ritonavir and chloroquine/hydroxychloroquine affecting the new SARS-CoV-2. *Biomedicine & Pharmacotherapy*, p.110668.

Van Der Spoel, D., Lindahl, E., Hess, B., Groenhof, G., Mark, A.E. and Berendsen, H.J., 2005. GROMACS: fast, flexible, and free. *Journal of computational chemistry*, *26*(16), pp.1701-1718.

Varela-Rial, A., Majewski, M. and De Fabritiis, G., 2021. Structure based virtual screening: Fast and slow. *Wiley Interdisciplinary Reviews: Computational Molecular Science*, p.e1544.

Vázquez, J., López, M., Gibert, E., Herrero, E. and Luque, F.J., 2020. Merging ligand-based and structure-based methods in drug discovery: An overview of combined virtual screening approaches. *Molecules*, *25*(20), p.4723.

Veber, D., Johnson, S., Cheng, H., Smith, B., Ward, K. and Kopple, K., 2002. Differential Uptake and Selective Permeability of Fusarochromanone (FC101), a Novel Membrane Permeable Anticancer Naturally Fluorescent Compound in Tumor and Normal Cells. *J. Med. Chem*, *45*, pp.2615-2623.

Veber, D.F., Johnson, S.R., Cheng, H.Y., Smith, B.R., Ward, K.W. and Kopple, K.D., 2002. Molecular properties that influence the oral bioavailability of drug candidates. *Journal of medicinal chemistry*, *45*(12), pp.2615-2623.

Venugopal, K., Hentzschel, F., Valkiūnas, G. and Marti, M., 2020. Plasmodium asexual growth and sexual development in the haematopoietic niche of the host. *Nature Reviews Microbiology*, *18*(3), pp.177-189.

Verma, P., Tiwari, M. and Tiwari, V., 2018. In silico high-throughput virtual screening and molecular dynamics simulation study to identify inhibitor for AdeABC efflux pump of Acinetobacter baumannii. *Journal of Biomolecular Structure and Dynamics*, *36*(5), pp.1182-1194.

Vilar, S., Cozza, G. and Moro, S., 2008. Medicinal chemistry and the molecular operating environment (MOE): application of QSAR and molecular docking to drug discovery. *Current topics in medicinal chemistry*, *8*(18), pp.1555-1572.
Vilar, S., Cozza, G. and Moro, S., 2008. Medicinal chemistry and the molecular operating environment (MOE): application of QSAR and molecular docking to drug discovery. *Current topics in medicinal chemistry*, *8*(18), pp.1555-1572.
Vlachakis, D. ed., 2018. *Molecular Docking* - Overview, Background, Application and What the Future Holds, Molecular Docking, BoD–Books on Demand.

Vyas, V.K., Ukawala, R.D., Ghate, M. and Chintha, C., 2012. Homology modeling a fast tool for drug discovery: current perspectives. *Indian journal of pharmaceutical sciences*, *74*(1), p.1.

Walters, W.P., Stahl, M.T. and Murcko, M.A., 1998. Virtual screening—an overview. *Drug discovery today*, *3*(4), pp.160-178.

Wang, J., Wolf, R.M., Caldwell, J.W., Kollman, P.A. and Case, D.A., 2004. Development and testing of a general amber force field. *Journal of computational chemistry*, *25*(9), pp.1157-1174.

Wang, Z., Sun, H., Shen, C., Hu, X., Gao, J., Li, D., Cao, D. and Hou, T., 2020. Combined strategies in structure-based virtual screening. *Physical Chemistry Chemical Physics*, *22*(6), pp.3149-3159.

Warrandyte Road Clinic, 2021. Accessed March 14, 2021. https://wrclinic.com.au/img/malaria/southafrica_3.14.16.jpg.webp

Waterhouse, A., Bertoni, M., Bienert, S., Studer, G., Tauriello, G., Gumienny, R., Heer, F.T., de Beer, T.A.P., Rempfer, C., Bordoli, L. and Lepore, R., 2018. SWISS-MODEL: homology modelling of protein structures and complexes. *Nucleic acids research*, *46*(W1), pp W296-W303.

Wiederstein, M. and Sippl, M.J., 2007. ProSA-web: interactive web service for the recognition of errors in three-dimensional structures of proteins. *Nucleic acids research*, *35*(suppl_2), pp.W407-W410.

Williamson, M.P., 1994. The structure and function of proline-rich regions in proteins. *Biochemical journal*, *297*(Pt 2), p.249.

Wolber, G. and Langer, T., 2005. LigandScout: 3-D pharmacophores derived from protein-bound ligands and their use as virtual screening filters. *Journal of chemical information and modeling*, *45*(1), pp.160-169.

World Health Organization (WHO) 2011, "Global Malaria Action Plan", *World Health*

World Health Organization, 2016. *World malaria report 2015*. World Health Organization. http:www.who.int malaria publications world_malaria_report_2015.

World Health Organization, 2020. World malaria report 2020: 20 years of global progress and challenges. In *World malaria report 2020: 20 years of global progress and challenges*.

Wu, S.L., Wang, L.F., Sun, H.B., Wang, W. and Yu, Y.X., 2020. Probing molecular mechanism of inhibitor bindings to bromodomain-containing protein 4 based on molecular dynamics simulations and principal component analysis. *SAR and QSAR in Environmental Research*, *31*(7),pp.547-570.

Selvaraj, C., Dinesh, D.C., Panwar, U., Abhirami, R., Boura, E. and Singh, S.K., 2021. Structure-based virtual screening and molecular dynamics simulation of SARS-CoV-2 Guanine-N7 methyltransferase (nsp14) for identifying antiviral inhibitors against COVID-19. *Journal of Biomolecular Structure and Dynamics*, *39*(13), pp.4582-4593.

Xiao, Z., Morris-Natschke, S.L. and Lee, K.H., 2016. Strategies for the optimization of natural leads to anticancer drugs or drug candidates. *Medicinal research reviews*, *36*(1), pp.32-91.

Yang, S.Q., Ye, Q., Ding, J.J., Lu, A.P., Chen, X., Hou, T.J. and Cao, D.S., 2021. Current advances in ligand-based target prediction. *Wiley Interdisciplinary Reviews: Computational Molecular Science*, *11*(3), pp.1504.

Zhang, L., Lin, D., Sun, X., Curth, U., Drosten, C., Sauerhering, L., Becker, S., Rox, K. and Hilgenfeld, R., 2020. Crystal structure of SARS-CoV-2 main protease provides a basis for design of improved α-ketoamide inhibitors. *Science*, *368*(6489), pp.409-412.

Zhao, X., Thanapongtharm, W., Lawawirojwong, S., Wei, C., Tang, Y., Zhou, Y., Sun, X., Sattabongkot, J. and Kaewkungwal, J., 2020. Spatiotemporal Trends of Malaria in Relation to Economic Development and Cross-Border Movement along the China–Myanmar Border in Yunnan Province. *The Korean Journal of Parasitology*, *58*(3), p.267.

Zheng, J., Pan, H., Gu, Y., Zuo, X., Ran, N., Yuan, Y., Zhang, C. and Wang, F., 2019. Prospects for malaria vaccines: pre-erythrocytic stages, blood stages, and transmission-blocking stages. *BioMed research international*, *2019*. 34(1), pp 88-90.

Zheng, W., Sun, W. and Simeonov, A., 2018. Drug repurposing screens and synergistic drug-combinations for infectious diseases. *British journal of pharmacology*, *175*(2), pp.181-191.

Appendix 1- Binding Scores of docked compounds

CHEMICAL ID	S	CHEMICAL ID	S	CHEMICAL ID	S
TCMDC-136148	-7.4254093	TCMDC-139870	-7.2151766	TCMDC-141414	-7.0160637
TCMDC-137781	-7.4251118	TCMDC-131948	-7.2151361	TCMDC-136037	-7.01543
TCMDC-141731	-7.4247398	TCMDC-139786	-7.2148542	TCMDC-131648	-7.0151496
TCMDC-141713	-7.4246197	TCMDC-124115	-7.2148046	TCMDC-125157	-7.0150318
TCMDC-135741	-7.4244752	TCMDC-132430	-7.2147064	TCMDC-124093	-7.0149503
TCMDC-141475	-7.424336	TCMDC-133666	-7.2144527	TCMDC-132839	-7.0148392
TCMDC-137324	-7.4239864	TCMDC-138393	-7.2143745	TCMDC-133032	-7.0147734
TCMDC-137763	-7.4239192	TCMDC-139174	-7.2138929	TCMDC-134425	-7.0146809
TCMDC-140102	-7.4237413	TCMDC-139603	-7.2138805	TCMDC-138745	-7.0145488
TCMDC-134940	-7.4236603	TCMDC-134173	-7.2136512	TCMDC-133128	-7.0143852
TCMDC-132285	-7.4234405	TCMDC-137482	-7.2135491	TCMDC-142342	-7.0143566
TCMDC-140490	-7.4230394	TCMDC-131272	-7.2135234	TCMDC-133231	-7.014287
TCMDC-139550	-7.4225688	TCMDC-136979	-7.2134051	TCMDC-141183	-7.0141239
TCMDC-138056	-7.4219975	TCMDC-136130	-7.2133684	TCMDC-136854	-7.0140829
TCMDC-132949	-7.4218044	TCMDC-133949	-7.2133031	TCMDC-141006	-7.0140786
TCMDC-141766	-7.4214501	TCMDC-139127	-7.2132983	TCMDC-133157	-7.0138965
TCMDC-137054	-7.4212103	TCMDC-136489	-7.213037	TCMDC-132978	-7.0131941
TCMDC-134443	-7.4212055	TCMDC-133222	-7.212945	TCMDC-124389	-7.0129285
TCMDC-139113	-7.420825	TCMDC-141186	-7.2125363	TCMDC-141203	-7.0125537
TCMDC-132962	-7.4207048	TCMDC-139134	-7.2124987	TCMDC-140078	-7.0124431
TCMDC-141717	-7.4206314	TCMDC-138577	-7.2119246	TCMDC-134837	-7.012064
TCMDC-124369	-7.4206038	TCMDC-132445	-7.2118344	TCMDC-136734	-7.0119734
TCMDC-135970	-7.4205794	TCMDC-134057	-7.2113647	TCMDC-135322	-7.0118909
TCMDC-135965	-7.4205718	TCMDC-134963	-7.211237	TCMDC-134422	-7.0116706
TCMDC-134236	-7.4199977	TCMDC-134099	-7.2107911	TCMDC-141373	-7.0114274
TCMDC-132192	-7.4197869	TCMDC-125240	-7.2107029	TCMDC-134407	-7.0114141
TCMDC-134017	-7.4197598	TCMDC-125030	-7.2102094	TCMDC-141409	-7.0112085
TCMDC-138424	-7.4193931	TCMDC-139261	-7.2099881	TCMDC-140576	-7.0111804
TCMDC-132816	-7.4193048	TCMDC-132044	-7.2099595	TCMDC-124121	-7.0111117
TCMDC-138479	-7.4186063	TCMDC-138430	-7.2089777	TCMDC-139430	-7.0110683
TCMDC-141708	-7.4185219	TCMDC-134961	-7.2088556	TCMDC-134115	-7.0110135
TCMDC-135723	-7.4183154	TCMDC-133752	-7.2087426	TCMDC-124667	-7.0109329
TCMDC-138211	-7.4182887	TCMDC-132894	-7.2084799	TCMDC-133536	-7.0109
TCMDC-139621	-7.4182739	TCMDC-140245	-7.2081723	TCMDC-125686	-7.0104613
TCMDC-133260	-7.4181371	TCMDC-137012	-7.2079482	TCMDC-125252	-7.0103631
TCMDC-141550	-7.4179935	TCMDC-135864	-7.2078896	TCMDC-133558	-7.0102358
TCMDC-141533	-7.4178133	TCMDC-132462	-7.20783	TCMDC-139366	-7.0098171
TCMDC-140841	-7.4177594	TCMDC-124708	-7.2076583	TCMDC-133865	-7.0095124
TCMDC-137019	-7.4176636	TCMDC-142338	-7.2073998	TCMDC-125459	-7.0093703
TCMDC-132273	-7.4171109	TCMDC-142247	-7.2072501	TCMDC-141386	-7.0091276
TCMDC-138161	-7.4170785	TCMDC-134875	-7.2072196	TCMDC-134901	-7.0090985

TCMDC-136139	-7.4167237	TCMDC-141215	-7.2070947	TCMDC-140575	-7.0090661
TCMDC-132298	-7.4166098	TCMDC-139299	-7.2068911	TCMDC-124329	-7.008945
TCMDC-141568	-7.4163189	TCMDC-139850	-7.2067704	TCMDC-136357	-7.008934
TCMDC-124277	-7.4162545	TCMDC-136978	-7.2066669	TCMDC-139204	-7.0087557
TCMDC-134509	-7.4158978	TCMDC-132888	-7.2066426	TCMDC-141178	-7.008532
TCMDC-138911	-7.4158053	TCMDC-142008	-7.2066231	TCMDC-140254	-7.0084558
TCMDC-132152	-7.4156728	TCMDC-134882	-7.2062321	TCMDC-134323	-7.007905
TCMDC-125117	-7.4154429	TCMDC-139537	-7.2061396	TCMDC-135638	-7.00773
TCMDC-125530	-7.415432	TCMDC-131501	-7.2059894	TCMDC-135364	-7.007617
TCMDC-133636	-7.4154115	TCMDC-141140	-7.2056165	TCMDC-132953	-7.007545
TCMDC-139256	-7.4151244	TCMDC-141182	-7.2055593	TCMDC-132821	-7.007298
TCMDC-125781	-7.4150543	TCMDC-135086	-7.2053332	TCMDC-138636	-7.0070868
TCMDC-137089	-7.4147053	TCMDC-124940	-7.2051616	TCMDC-132190	-7.0070429
TCMDC-124230	-7.414227	TCMDC-132601	-7.2047057	TCMDC-124095	-7.0069189
TCMDC-132448	-7.4139104	TCMDC-139976	-7.2044621	TCMDC-137207	-7.006793
TCMDC-135267	-7.4136581	TCMDC-139346	-7.2041984	TCMDC-133968	-7.0063505
TCMDC-140316	-7.4134617	TCMDC-136024	-7.2039227	TCMDC-139667	-7.0063453
TCMDC-137215	-7.4134555	TCMDC-134742	-7.2038527	TCMDC-125152	-7.0059948
TCMDC-132909	-7.4124703	TCMDC-140097	-7.2036419	TCMDC-136874	-7.0059881
TCMDC-133002	-7.4123964	TCMDC-125676	-7.203548	TCMDC-125529	-7.0058036
TCMDC-135173	-7.4122448	TCMDC-139655	-7.2032514	TCMDC-134203	-7.0054841
TCMDC-140669	-7.4120936	TCMDC-139410	-7.2031579	TCMDC-124868	-7.0054016
TCMDC-133606	-7.4120922	TCMDC-132097	-7.2031255	TCMDC-131418	-7.0052695
TCMDC-134876	-7.4120865	TCMDC-135694	-7.2030921	TCMDC-140430	-7.0052204
TCMDC-141382	-7.4119148	TCMDC-124864	-7.2029991	TCMDC-135388	-7.0050831
TCMDC-139825	-7.4116268	TCMDC-133601	-7.202826	TCMDC-134528	-7.004703
TCMDC-132792	-7.411593	TCMDC-139811	-7.2024403	TCMDC-142248	-7.0045128
TCMDC-134400	-7.4114985	TCMDC-132850	-7.2023416	TCMDC-139263	-7.0043411
TCMDC-136815	-7.4113221	TCMDC-141106	-7.2023125	TCMDC-138638	-7.0036697
TCMDC-138416	-7.4112573	TCMDC-141123	-7.202075	TCMDC-139431	-7.0033255
TCMDC-136922	-7.411139	TCMDC-134332	-7.202044	TCMDC-138695	-7.0032463
TCMDC-139986	-7.4111204	TCMDC-140038	-7.2018623	TCMDC-139181	-7.0032387
TCMDC-132785	-7.4109774	TCMDC-136696	-7.2016878	TCMDC-124975	-7.0030642
TCMDC-132901	-7.4107375	TCMDC-141152	-7.2015357	TCMDC-139978	-7.0029421
TCMDC-135714	-7.4106665	TCMDC-136910	-7.2014842	TCMDC-125201	-7.0028229
TCMDC-139939	-7.4105806	TCMDC-137782	-7.2012215	TCMDC-134016	-7.0027304
TCMDC-140926	-7.4103875	TCMDC-124784	-7.2010164	TCMDC-137231	-7.0022035
TCMDC-124318	-7.4102759	TCMDC-140355	-7.2009621	TCMDC-132745	-7.0021591
TCMDC-140763	-7.4102268	TCMDC-134159	-7.2008696	TCMDC-138795	-7.0012097
TCMDC-139606	-7.4101725	TCMDC-133642	-7.2007127	TCMDC-125381	-7.001071
TCMDC-132808	-7.4101391	TCMDC-133034	-7.2003984	TCMDC-132649	-7.0006971
TCMDC-124969	-7.4101143	TCMDC-133973	-7.200264	TCMDC-124593	-7.0005836
TCMDC-132677	-7.4097109	TCMDC-136523	-7.2001386	TCMDC-135134	-6.9999747
TCMDC-136707	-7.4094534	TCMDC-125496	-7.1996112	TCMDC-139541	-6.9998221

TCMDC-137028	-7.4092646	TCMDC-139938	-7.1990395	TCMDC-139361	-6.999424
TCMDC-133808	-7.4090524	TCMDC-123582	-7.1982937	TCMDC-141299	-6.9993453
TCMDC-140114	-7.4087481	TCMDC-138371	-7.1982503	TCMDC-125089	-6.9993443
TCMDC-132374	-7.4086313	TCMDC-125279	-7.1981831	TCMDC-134428	-6.9993176
TCMDC-135031	-7.4082918	TCMDC-132151	-7.198082	TCMDC-123822	-6.999239
TCMDC-141763	-7.4076772	TCMDC-135003	-7.197928	TCMDC-141193	-6.9991074
TCMDC-139668	-7.4074659	TCMDC-133696	-7.1973424	TCMDC-138767	-6.9990005
TCMDC-125588	-7.4074197	TCMDC-132146	-7.197269	TCMDC-133978	-6.9987602
TCMDC-132970	-7.4072418	TCMDC-136189	-7.1972098	TCMDC-135997	-6.9986038
TCMDC-133931	-7.4068413	TCMDC-134618	-7.1971974	TCMDC-137083	-6.9985695
TCMDC-136616	-7.4065399	TCMDC-125681	-7.1969004	TCMDC-140263	-6.9981203
TCMDC-132848	-7.4063396	TCMDC-139658	-7.1968708	TCMDC-124039	-6.9980803
TCMDC-135868	-7.4060211	TCMDC-132424	-7.1968083	TCMDC-137023	-6.9979372
TCMDC-132278	-7.4058862	TCMDC-136203	-7.1966014	TCMDC-124364	-6.9977746
TCMDC-133394	-7.4058633	TCMDC-124103	-7.196384	TCMDC-124330	-6.9977064
TCMDC-133805	-7.4056058	TCMDC-134240	-7.1960497	TCMDC-135822	-6.9974756
TCMDC-140416	-7.4055614	TCMDC-140703	-7.1959109	TCMDC-137059	-6.9974504
TCMDC-131582	-7.4055543	TCMDC-136518	-7.1954923	TCMDC-138549	-6.997354
TCMDC-133080	-7.4054565	TCMDC-135947	-7.1954913	TCMDC-124728	-6.9973249
TCMDC-138661	-7.405376	TCMDC-140832	-7.1953936	TCMDC-125146	-6.9970369
TCMDC-141009	-7.4050622	TCMDC-136782	-7.1952806	TCMDC-123603	-6.9968624
TCMDC-133370	-7.4047823	TCMDC-141308	-7.1952801	TCMDC-125766	-6.99684
TCMDC-134092	-7.4045982	TCMDC-135139	-7.1952043	TCMDC-134103	-6.9967718
TCMDC-141003	-7.4045677	TCMDC-125294	-7.1952033	TCMDC-141385	-6.9966111
TCMDC-135428	-7.404284	TCMDC-140788	-7.1949167	TCMDC-134475	-6.9964657
TCMDC-139103	-7.4039474	TCMDC-136474	-7.1947923	TCMDC-133281	-6.9962163
TCMDC-132191	-7.4037685	TCMDC-139073	-7.1947522	TCMDC-136923	-6.9961548
TCMDC-124089	-7.403451	TCMDC-141062	-7.1937728	TCMDC-124244	-6.9960766
TCMDC-141715	-7.4034362	TCMDC-136411	-7.1936727	TCMDC-135096	-6.9959083
TCMDC-136285	-7.4020877	TCMDC-136886	-7.1933174	TCMDC-139199	-6.9956708
TCMDC-139140	-7.4014845	TCMDC-134485	-7.1933064	TCMDC-125626	-6.9954643
TCMDC-138990	-7.4013348	TCMDC-125261	-7.1932487	TCMDC-136544	-6.9950352
TCMDC-123539	-7.4012513	TCMDC-140658	-7.1931891	TCMDC-140438	-6.9949303
TCMDC-140670	-7.400723	TCMDC-133228	-7.1931262	TCMDC-140296	-6.9945078
TCMDC-136397	-7.4007125	TCMDC-140844	-7.1929822	TCMDC-138876	-6.9942803
TCMDC-141876	-7.4006729	TCMDC-132406	-7.192862	TCMDC-125882	-6.9941368
TCMDC-135738	-7.3999863	TCMDC-136713	-7.1927733	TCMDC-132825	-6.9939809
TCMDC-132348	-7.3999476	TCMDC-134465	-7.1926079	TCMDC-140463	-6.9938879
TCMDC-131350	-7.3999295	TCMDC-139716	-7.1922331	TCMDC-133930	-6.9938393
TCMDC-132718	-7.3998079	TCMDC-139276	-7.1920171	TCMDC-135082	-6.99369
TCMDC-137342	-7.3995061	TCMDC-140356	-7.1919632	TCMDC-139937	-6.9933286
TCMDC-132801	-7.3991742	TCMDC-135083	-7.1919084	TCMDC-134227	-6.9932594
TCMDC-138079	-7.3991551	TCMDC-134019	-7.1918592	TCMDC-135815	-6.9932022
TCMDC-132219	-7.3988342	TCMDC-139872	-7.1916389	TCMDC-138300	-6.9931107

TCMDC-137344	-7.3987565	TCMDC-137055	-7.1915722	TCMDC-135232	-6.9923739
TCMDC-133624	-7.3983998	TCMDC-140672	-7.1915212	TCMDC-142278	-6.9922161
TCMDC-136719	-7.3980894	TCMDC-132090	-7.1914229	TCMDC-125777	-6.9916463
TCMDC-139192	-7.3980136	TCMDC-133286	-7.1913781	TCMDC-124948	-6.9910283
TCMDC-133208	-7.3970671	TCMDC-134204	-7.191267	TCMDC-133910	-6.9909911
TCMDC-132308	-7.3969979	TCMDC-141390	-7.1910172	TCMDC-133572	-6.9907227
TCMDC-138809	-7.3967762	TCMDC-124036	-7.1908035	TCMDC-141351	-6.9905791
TCMDC-132943	-7.3967609	TCMDC-133746	-7.1904454	TCMDC-124673	-6.9903603
TCMDC-136633	-7.3965888	TCMDC-136898	-7.1904449	TCMDC-133774	-6.9900908
TCMDC-132959	-7.3965569	TCMDC-132180	-7.1903934	TCMDC-132195	-6.9899607
TCMDC-136400	-7.395545	TCMDC-138396	-7.1903172	TCMDC-136215	-6.9899178
TCMDC-138156	-7.395421	TCMDC-125095	-7.1901479	TCMDC-140697	-6.9889827
TCMDC-136122	-7.3953395	TCMDC-134743	-7.1899872	TCMDC-133235	-6.9889083
TCMDC-134925	-7.3953385	TCMDC-136829	-7.1899662	TCMDC-132513	-6.9885478
TCMDC-134360	-7.3953223	TCMDC-134617	-7.1899085	TCMDC-138395	-6.9884148
TCMDC-140933	-7.3948679	TCMDC-132215	-7.1898427	TCMDC-125761	-6.9880538
TCMDC-139304	-7.3948646	TCMDC-132845	-7.18964	TCMDC-135438	-6.9879222
TCMDC-137684	-7.3947697	TCMDC-132443	-7.1895595	TCMDC-133593	-6.9879179
TCMDC-136848	-7.3947043	TCMDC-131499	-7.1894083	TCMDC-136926	-6.9879079
TCMDC-132974	-7.394659	TCMDC-139184	-7.1893554	TCMDC-136540	-6.9877248
TCMDC-133695	-7.3942814	TCMDC-132444	-7.1893177	TCMDC-137278	-6.9877152
TCMDC-139761	-7.3938174	TCMDC-140084	-7.188592	TCMDC-136610	-6.9874349
TCMDC-140140	-7.3937836	TCMDC-133084	-7.1885133	TCMDC-141015	-6.9873791
TCMDC-139902	-7.3934817	TCMDC-140198	-7.1884346	TCMDC-133456	-6.9872408
TCMDC-136647	-7.3932471	TCMDC-134764	-7.1881213	TCMDC-134854	-6.9870009
TCMDC-132999	-7.3927188	TCMDC-134022	-7.187633	TCMDC-132720	-6.986918
TCMDC-134947	-7.3920355	TCMDC-136832	-7.1876259	TCMDC-132428	-6.9863114
TCMDC-134686	-7.39188	TCMDC-139210	-7.1876049	TCMDC-132366	-6.9859099
TCMDC-136708	-7.3917389	TCMDC-135146	-7.1872911	TCMDC-125651	-6.9858155
TCMDC-138721	-7.3916984	TCMDC-136278	-7.1865053	TCMDC-140300	-6.9856458
TCMDC-139746	-7.3911839	TCMDC-135851	-7.1863117	TCMDC-133248	-6.9847093
TCMDC-141408	-7.3908849	TCMDC-133367	-7.1860723	TCMDC-141066	-6.9843802
TCMDC-139622	-7.3907189	TCMDC-134650	-7.1859341	TCMDC-131694	-6.9840469
TCMDC-141174	-7.3903337	TCMDC-137699	-7.185925	TCMDC-125578	-6.9839773
TCMDC-124339	-7.389533	TCMDC-134190	-7.1858201	TCMDC-134462	-6.9839673
TCMDC-140807	-7.3895144	TCMDC-139842	-7.1857405	TCMDC-141134	-6.9837437
TCMDC-134794	-7.3894496	TCMDC-140469	-7.1846004	TCMDC-132474	-6.9834557
TCMDC-137473	-7.3891129	TCMDC-133743	-7.1843328	TCMDC-139483	-6.9833603
TCMDC-136386	-7.3886137	TCMDC-133957	-7.1843162	TCMDC-125467	-6.9832349
TCMDC-123679	-7.3884854	TCMDC-132263	-7.1841965	TCMDC-124750	-6.9831891
TCMDC-139349	-7.3883858	TCMDC-141113	-7.1840901	TCMDC-124184	-6.9826641
TCMDC-134928	-7.3881421	TCMDC-135852	-7.1839318	TCMDC-135133	-6.9825511
TCMDC-136666	-7.3879375	TCMDC-136087	-7.1837821	TCMDC-125352	-6.9823728
TCMDC-133615	-7.3878469	TCMDC-140143	-7.1837797	TCMDC-142306	-6.9822559

TCMDC-124800	-7.387629	TCMDC-140850	-7.1836691	TCMDC-136509	-6.9815831
TCMDC-141254	-7.3874345	TCMDC-139600	-7.1833129	TCMDC-124839	-6.9811354
TCMDC-139182	-7.3873749	TCMDC-135350	-7.1832557	TCMDC-135020	-6.9809408
TCMDC-141873	-7.3870478	TCMDC-140775	-7.183074	TCMDC-135599	-6.9807353
TCMDC-132045	-7.3869872	TCMDC-139482	-7.1824174	TCMDC-138671	-6.9801116
TCMDC-138922	-7.3869748	TCMDC-139910	-7.1824017	TCMDC-131894	-6.9799995
TCMDC-138589	-7.3868265	TCMDC-136658	-7.1822801	TCMDC-141185	-6.9799676
TCMDC-132520	-7.3868084	TCMDC-123644	-7.1822281	TCMDC-140726	-6.9799252
TCMDC-131236	-7.3867264	TCMDC-138432	-7.1821518	TCMDC-141734	-6.9797139
TCMDC-138033	-7.3859687	TCMDC-137119	-7.1820912	TCMDC-139433	-6.9795518
TCMDC-125687	-7.3855772	TCMDC-141149	-7.1818542	TCMDC-133120	-6.9792638
TCMDC-140116	-7.3855057	TCMDC-139823	-7.1818414	TCMDC-124265	-6.9789157
TCMDC-125585	-7.3854523	TCMDC-131495	-7.1814203	TCMDC-140519	-6.9785242
TCMDC-140515	-7.3854408	TCMDC-136975	-7.1807895	TCMDC-124370	-6.9775538
TCMDC-136946	-7.3844118	TCMDC-140688	-7.1807346	TCMDC-124027	-6.9771771
TCMDC-141883	-7.3840594	TCMDC-135958	-7.1806006	TCMDC-136450	-6.9771523
TCMDC-136855	-7.3839517	TCMDC-140673	-7.1805682	TCMDC-139452	-6.9770107
TCMDC-136328	-7.3836374	TCMDC-137888	-7.1805215	TCMDC-133880	-6.9766822
TCMDC-138397	-7.3835659	TCMDC-141208	-7.1805182	TCMDC-140837	-6.9766712
TCMDC-124195	-7.3829484	TCMDC-124711	-7.1804056	TCMDC-140783	-6.9766083
TCMDC-133898	-7.3829117	TCMDC-124388	-7.1801019	TCMDC-131312	-6.9765329
TCMDC-135849	-7.3828568	TCMDC-140698	-7.1799297	TCMDC-133490	-6.9763455
TCMDC-140027	-7.3828225	TCMDC-136642	-7.1797638	TCMDC-136565	-6.9762869
TCMDC-138918	-7.3822861	TCMDC-139453	-7.1795769	TCMDC-133965	-6.976058
TCMDC-133600	-7.3817811	TCMDC-123500	-7.179368	TCMDC-140857	-6.9760013
TCMDC-136407	-7.3802352	TCMDC-134562	-7.1793423	TCMDC-133969	-6.9759974
TCMDC-138412	-7.3800316	TCMDC-137155	-7.1793342	TCMDC-136916	-6.975821
TCMDC-134873	-7.3796949	TCMDC-134724	-7.1788244	TCMDC-134809	-6.9755874
TCMDC-139355	-7.3795433	TCMDC-132172	-7.1787767	TCMDC-138448	-6.9755511
TCMDC-132984	-7.3793392	TCMDC-136488	-7.1787519	TCMDC-132527	-6.9752436
TCMDC-138437	-7.3792901	TCMDC-132106	-7.1786542	TCMDC-132699	-6.9752331
TCMDC-135526	-7.3792415	TCMDC-132713	-7.1772356	TCMDC-133970	-6.9747615
TCMDC-132398	-7.3790326	TCMDC-131953	-7.1772103	TCMDC-134247	-6.9746885
TCMDC-141222	-7.3787208	TCMDC-132698	-7.1772084	TCMDC-135379	-6.9745183
TCMDC-136625	-7.3783302	TCMDC-132757	-7.1767607	TCMDC-135611	-6.9738007
TCMDC-124565	-7.378283	TCMDC-124087	-7.1766872	TCMDC-136560	-6.9734616
TCMDC-135648	-7.3782601	TCMDC-131997	-7.1760979	TCMDC-133127	-6.9734449
TCMDC-136953	-7.377975	TCMDC-132989	-7.1760473	TCMDC-136484	-6.9733405
TCMDC-123716	-7.3774095	TCMDC-141663	-7.1756244	TCMDC-132837	-6.9731932
TCMDC-139170	-7.3770251	TCMDC-140716	-7.1754737	TCMDC-136307	-6.9731698
TCMDC-125173	-7.376821	TCMDC-131268	-7.1750817	TCMDC-132507	-6.9731517
TCMDC-137629	-7.3765674	TCMDC-136827	-7.175015	TCMDC-124960	-6.9730701
TCMDC-134781	-7.3764224	TCMDC-134479	-7.1745749	TCMDC-132822	-6.9730453
TCMDC-134775	-7.3762031	TCMDC-140063	-7.1738033	TCMDC-140192	-6.9726973

TCMDC-136174	-7.3761387	TCMDC-137290	-7.1733274	TCMDC-139753	-6.9726672
TCMDC-141052	-7.3760805	TCMDC-135435	-7.1730747	TCMDC-141477	-6.9725852
TCMDC-137291	-7.3759918	TCMDC-132759	-7.1729436	TCMDC-136081	-6.9723864
TCMDC-141494	-7.3759089	TCMDC-138187	-7.1729174	TCMDC-132504	-6.9722772
TCMDC-124766	-7.3758674	TCMDC-137088	-7.1725121	TCMDC-138433	-6.9720035
TCMDC-138418	-7.3757701	TCMDC-124008	-7.172009	TCMDC-132522	-6.9718137
TCMDC-136574	-7.3756328	TCMDC-137744	-7.1715746	TCMDC-135446	-6.9717431
TCMDC-125866	-7.3754649	TCMDC-137026	-7.1713409	TCMDC-124450	-6.971283
TCMDC-134369	-7.3745408	TCMDC-140687	-7.1713266	TCMDC-136187	-6.9705634
TCMDC-140037	-7.3744721	TCMDC-138838	-7.171309	TCMDC-124679	-6.9703479
TCMDC-136237	-7.3743129	TCMDC-131526	-7.1710935	TCMDC-142339	-6.9700327
TCMDC-137102	-7.3740463	TCMDC-140135	-7.171082	TCMDC-139664	-6.9699879
TCMDC-138153	-7.3737645	TCMDC-141133	-7.1701632	TCMDC-137293	-6.9699669
TCMDC-134287	-7.3737602	TCMDC-136067	-7.1700644	TCMDC-141311	-6.9695964
TCMDC-125423	-7.3732314	TCMDC-139320	-7.1694822	TCMDC-137681	-6.968924
TCMDC-132022	-7.3731031	TCMDC-133549	-7.1689525	TCMDC-131885	-6.9686971
TCMDC-124994	-7.3730264	TCMDC-134255	-7.1689482	TCMDC-141732	-6.9686751
TCMDC-139686	-7.3730245	TCMDC-135331	-7.1685333	TCMDC-141371	-6.9678044
TCMDC-134313	-7.3729534	TCMDC-138730	-7.1685328	TCMDC-124499	-6.9674468
TCMDC-140058	-7.3725424	TCMDC-141485	-7.1685033	TCMDC-137126	-6.9670281
TCMDC-124689	-7.3725271	TCMDC-136447	-7.1682339	TCMDC-124065	-6.9666352
TCMDC-132455	-7.3714552	TCMDC-125229	-7.1680717	TCMDC-136766	-6.9661674
TCMDC-141296	-7.3712392	TCMDC-132449	-7.1679988	TCMDC-132764	-6.9659424
TCMDC-139696	-7.3712354	TCMDC-141770	-7.1679168	TCMDC-141460	-6.9658656
TCMDC-135930	-7.3699131	TCMDC-136721	-7.1677589	TCMDC-133455	-6.9658637
TCMDC-137842	-7.3687367	TCMDC-125068	-7.1676307	TCMDC-137583	-6.9657726
TCMDC-133102	-7.3686972	TCMDC-132924	-7.1675248	TCMDC-135351	-6.9657021
TCMDC-133244	-7.3686943	TCMDC-136912	-7.1671391	TCMDC-136663	-6.9650354
TCMDC-124319	-7.3684111	TCMDC-123572	-7.167027	TCMDC-132402	-6.9647274
TCMDC-141464	-7.3684096	TCMDC-139924	-7.1667948	TCMDC-125050	-6.9645739
TCMDC-133792	-7.3681545	TCMDC-125703	-7.1664796	TCMDC-135857	-6.9644747
TCMDC-132950	-7.3678327	TCMDC-138197	-7.1663938	TCMDC-124084	-6.9640045
TCMDC-140914	-7.3677773	TCMDC-138968	-7.166029	TCMDC-139917	-6.9639969
TCMDC-131915	-7.3673615	TCMDC-140042	-7.1659498	TCMDC-138764	-6.9639363
TCMDC-133436	-7.3673062	TCMDC-139196	-7.1657963	TCMDC-123567	-6.9639354
TCMDC-141197	-7.3671203	TCMDC-140661	-7.1655416	TCMDC-138710	-6.9636245
TCMDC-124368	-7.367095	TCMDC-140660	-7.1654744	TCMDC-125469	-6.9635715
TCMDC-141911	-7.3668995	TCMDC-140164	-7.1653709	TCMDC-125059	-6.9635515
TCMDC-137384	-7.366776	TCMDC-124352	-7.1646075	TCMDC-139470	-6.9627833
TCMDC-136093	-7.3664217	TCMDC-135104	-7.1645947	TCMDC-139265	-6.9626508
TCMDC-141258	-7.366251	TCMDC-134750	-7.1645379	TCMDC-133714	-6.9625401
TCMDC-140910	-7.3660097	TCMDC-140905	-7.1645298	TCMDC-124491	-6.9624372
TCMDC-124670	-7.3659372	TCMDC-138213	-7.1644945	TCMDC-125576	-6.9623165
TCMDC-137733	-7.3653088	TCMDC-125343	-7.1644683	TCMDC-137724	-6.9617662

TCMDC-134145	-7.3648343	TCMDC-135645	-7.1640511	TCMDC-140392	-6.9616785
TCMDC-132620	-7.3647709	TCMDC-123719	-7.163672	TCMDC-132663	-6.9614935
TCMDC-135249	-7.3645926	TCMDC-133540	-7.1635504	TCMDC-140041	-6.9614687
TCMDC-136441	-7.3644476	TCMDC-136571	-7.1634831	TCMDC-137523	-6.9610209
TCMDC-140151	-7.3641896	TCMDC-135378	-7.1633153	TCMDC-132709	-6.9609303
TCMDC-136331	-7.3640141	TCMDC-125764	-7.1632309	TCMDC-142208	-6.9609189
TCMDC-132541	-7.3637657	TCMDC-133834	-7.1631846	TCMDC-133522	-6.9605584
TCMDC-136394	-7.3637385	TCMDC-133136	-7.162899	TCMDC-134283	-6.9605074
TCMDC-132703	-7.3636918	TCMDC-138486	-7.1625199	TCMDC-132798	-6.9604955
TCMDC-140870	-7.3635573	TCMDC-131924	-7.1625013	TCMDC-140823	-6.9604249
TCMDC-132313	-7.3629942	TCMDC-134230	-7.1623483	TCMDC-132767	-6.9603715
TCMDC-135639	-7.3627925	TCMDC-132439	-7.1621661	TCMDC-141589	-6.959795
TCMDC-134697	-7.3621788	TCMDC-134486	-7.1620903	TCMDC-139143	-6.9596243
TCMDC-139824	-7.3620806	TCMDC-141383	-7.1604619	TCMDC-132939	-6.9595041
TCMDC-133310	-7.3620462	TCMDC-123860	-7.1603608	TCMDC-139768	-6.9590602
TCMDC-139079	-7.3620067	TCMDC-133138	-7.1597414	TCMDC-132747	-6.9589534
TCMDC-133617	-7.3619971	TCMDC-134474	-7.1596189	TCMDC-133955	-6.9586225
TCMDC-132483	-7.3614902	TCMDC-134020	-7.1595979	TCMDC-124132	-6.9584775
TCMDC-136236	-7.361445	TCMDC-135474	-7.1593699	TCMDC-124979	-6.9582462
TCMDC-132695	-7.361114	TCMDC-132178	-7.1588731	TCMDC-141144	-6.9580288
TCMDC-125690	-7.3605723	TCMDC-131493	-7.1583552	TCMDC-136522	-6.9578419
TCMDC-139963	-7.3605194	TCMDC-123554	-7.1577964	TCMDC-133813	-6.9577265
TCMDC-132945	-7.3603377	TCMDC-132671	-7.1576786	TCMDC-133716	-6.957509
TCMDC-140048	-7.3599091	TCMDC-138678	-7.1576614	TCMDC-137899	-6.957509
TCMDC-133932	-7.3596272	TCMDC-139191	-7.1569738	TCMDC-136755	-6.9574795
TCMDC-141179	-7.3595824	TCMDC-123837	-7.1568508	TCMDC-133641	-6.9572258
TCMDC-137685	-7.3595314	TCMDC-141447	-7.1567035	TCMDC-137157	-6.9571886
TCMDC-139068	-7.3594327	TCMDC-133676	-7.1565008	TCMDC-132574	-6.9566379
TCMDC-139040	-7.359159	TCMDC-136311	-7.1564069	TCMDC-131276	-6.9564695
TCMDC-134932	-7.3591218	TCMDC-125136	-7.1563849	TCMDC-135155	-6.9564171
TCMDC-135589	-7.3586841	TCMDC-135074	-7.1563597	TCMDC-124859	-6.9561968
TCMDC-133262	-7.358387	TCMDC-137592	-7.1562629	TCMDC-136930	-6.9559884
TCMDC-133964	-7.3583822	TCMDC-133155	-7.1558704	TCMDC-136392	-6.9552822
TCMDC-136943	-7.3581038	TCMDC-133189	-7.1558514	TCMDC-141097	-6.9550204
TCMDC-124659	-7.3580942	TCMDC-124102	-7.1557088	TCMDC-133103	-6.9549484
TCMDC-136556	-7.3580761	TCMDC-125706	-7.1556015	TCMDC-141972	-6.9549098
TCMDC-136989	-7.357945	TCMDC-125241	-7.1555681	TCMDC-124169	-6.9546943
TCMDC-135895	-7.3578053	TCMDC-132048	-7.1555276	TCMDC-139539	-6.9545093
TCMDC-139266	-7.3576922	TCMDC-137790	-7.1555247	TCMDC-133255	-6.9544587
TCMDC-136429	-7.3575182	TCMDC-140371	-7.1554623	TCMDC-132980	-6.9542789
TCMDC-140923	-7.3574381	TCMDC-132653	-7.1553645	TCMDC-141218	-6.9540763
TCMDC-141664	-7.3573661	TCMDC-135407	-7.155169	TCMDC-136612	-6.9540715
TCMDC-134235	-7.3572869	TCMDC-139358	-7.155138	TCMDC-140477	-6.9540606
TCMDC-141230	-7.3570919	TCMDC-139630	-7.1548815	TCMDC-139010	-6.9539394

TCMDC-138425	-7.3567185	TCMDC-135085	-7.15485	TCMDC-124710	-6.9529715
TCMDC-136769	-7.3566074	TCMDC-136232	-7.1546607	TCMDC-135157	-6.9529338
TCMDC-132680	-7.3564134	TCMDC-140453	-7.154521	TCMDC-137045	-6.952363
TCMDC-134109	-7.3561444	TCMDC-137206	-7.1543612	TCMDC-134244	-6.9520383
TCMDC-132686	-7.3561401	TCMDC-140932	-7.1542249	TCMDC-132638	-6.9515047
TCMDC-132386	-7.3558931	TCMDC-132456	-7.1537466	TCMDC-137098	-6.9513235
TCMDC-133075	-7.3558393	TCMDC-141163	-7.1535301	TCMDC-134278	-6.9511414
TCMDC-124157	-7.3558154	TCMDC-131542	-7.1534071	TCMDC-132906	-6.950892
TCMDC-138007	-7.3555636	TCMDC-133158	-7.1533279	TCMDC-139045	-6.9507971
TCMDC-133020	-7.3555346	TCMDC-142335	-7.1529493	TCMDC-138105	-6.9506879
TCMDC-139254	-7.3555279	TCMDC-131271	-7.152885	TCMDC-140064	-6.9506011
TCMDC-137519	-7.3547668	TCMDC-124715	-7.1525025	TCMDC-139965	-6.9505796
TCMDC-140701	-7.3543773	TCMDC-134141	-7.1524115	TCMDC-141217	-6.950429
TCMDC-141836	-7.3541098	TCMDC-134310	-7.1522045	TCMDC-136651	-6.9503841
TCMDC-136127	-7.3540215	TCMDC-141718	-7.1519103	TCMDC-125348	-6.9497333
TCMDC-134612	-7.3536806	TCMDC-132863	-7.1517901	TCMDC-134926	-6.9495201
TCMDC-133960	-7.353334	TCMDC-124251	-7.1509237	TCMDC-125216	-6.9493699
TCMDC-133086	-7.3530755	TCMDC-124755	-7.1509047	TCMDC-140507	-6.9491291
TCMDC-140880	-7.3530364	TCMDC-132067	-7.1507277	TCMDC-135067	-6.9490042
TCMDC-140666	-7.352962	TCMDC-140183	-7.1507225	TCMDC-133137	-6.9489775
TCMDC-132257	-7.3525414	TCMDC-124070	-7.1502771	TCMDC-137448	-6.9489489
TCMDC-124001	-7.3524294	TCMDC-139543	-7.1501946	TCMDC-142263	-6.9488916
TCMDC-132233	-7.3510113	TCMDC-138807	-7.1501021	TCMDC-134639	-6.9488187
TCMDC-139053	-7.3508968	TCMDC-139031	-7.1497655	TCMDC-124615	-6.9487929
TCMDC-124552	-7.3506942	TCMDC-140748	-7.1495419	TCMDC-133026	-6.9487901
TCMDC-136132	-7.3505473	TCMDC-133498	-7.1493597	TCMDC-125698	-6.9487762
TCMDC-131546	-7.3504281	TCMDC-124907	-7.1492219	TCMDC-139983	-6.9487076
TCMDC-137540	-7.3503489	TCMDC-135385	-7.1491842	TCMDC-139205	-6.9482536
TCMDC-132603	-7.3502836	TCMDC-141656	-7.1491084	TCMDC-132797	-6.9480386
TCMDC-135570	-7.3501945	TCMDC-124931	-7.1490002	TCMDC-140159	-6.9470806
TCMDC-133239	-7.350131	TCMDC-133240	-7.148716	TCMDC-136039	-6.9470453
TCMDC-134497	-7.3501	TCMDC-133123	-7.1480913	TCMDC-141038	-6.9470191
TCMDC-136047	-7.3496323	TCMDC-141436	-7.1477122	TCMDC-140777	-6.9464998
TCMDC-135867	-7.3492055	TCMDC-139321	-7.1474929	TCMDC-133405	-6.9461012
TCMDC-131828	-7.3490767	TCMDC-136931	-7.1473842	TCMDC-124743	-6.9459863
TCMDC-136054	-7.3490424	TCMDC-132427	-7.1471491	TCMDC-124709	-6.9457898
TCMDC-132182	-7.348877	TCMDC-132851	-7.1466784	TCMDC-132392	-6.9451084
TCMDC-141255	-7.3488193	TCMDC-133721	-7.1464071	TCMDC-136346	-6.9448581
TCMDC-137752	-7.3486433	TCMDC-139707	-7.1462235	TCMDC-135070	-6.9448457
TCMDC-124030	-7.3480606	TCMDC-135295	-7.1461058	TCMDC-136947	-6.9447956
TCMDC-125260	-7.3478312	TCMDC-137849	-7.1459703	TCMDC-132692	-6.9447842
TCMDC-132014	-7.3472619	TCMDC-123735	-7.1454701	TCMDC-139792	-6.9445853
TCMDC-133135	-7.3471689	TCMDC-131796	-7.1454058	TCMDC-140465	-6.9445105
TCMDC-124706	-7.3470283	TCMDC-133182	-7.1453519	TCMDC-140069	-6.9443865

TCMDC-138142	-7.3470106	TCMDC-140248	-7.1452975	TCMDC-131741	-6.9443426
TCMDC-133214	-7.3463602	TCMDC-124933	-7.1449165	TCMDC-124638	-6.9441266
TCMDC-139563	-7.3463244	TCMDC-134024	-7.1448703	TCMDC-138936	-6.9441085
TCMDC-135840	-7.3462172	TCMDC-138718	-7.1448045	TCMDC-134125	-6.9439754
TCMDC-141987	-7.3458004	TCMDC-136356	-7.1442213	TCMDC-137788	-6.9438496
TCMDC-132004	-7.3456993	TCMDC-134257	-7.144208	TCMDC-139085	-6.943471
TCMDC-133091	-7.3456707	TCMDC-124727	-7.1441817	TCMDC-131802	-6.9433832
TCMDC-139252	-7.3455133	TCMDC-139327	-7.1441045	TCMDC-123476	-6.9427052
TCMDC-132388	-7.3454285	TCMDC-133110	-7.1440516	TCMDC-132202	-6.9424715
TCMDC-133179	-7.3452182	TCMDC-135827	-7.1439934	TCMDC-140884	-6.9423804
TCMDC-136581	-7.3447208	TCMDC-125176	-7.1437745	TCMDC-125334	-6.9419694
TCMDC-138696	-7.3445749	TCMDC-140074	-7.1437273	TCMDC-125005	-6.9415016
TCMDC-133433	-7.3445268	TCMDC-134401	-7.1435242	TCMDC-132018	-6.9414558
TCMDC-133115	-7.3445163	TCMDC-140412	-7.1435065	TCMDC-136413	-6.9413395
TCMDC-139954	-7.34446	TCMDC-140867	-7.1433768	TCMDC-139837	-6.9409728
TCMDC-133967	-7.3443961	TCMDC-135354	-7.1430073	TCMDC-135502	-6.940928
TCMDC-137292	-7.3440018	TCMDC-134270	-7.1428986	TCMDC-134252	-6.9407592
TCMDC-140951	-7.3436937	TCMDC-124999	-7.1428609	TCMDC-139047	-6.9404597
TCMDC-136405	-7.3436198	TCMDC-136808	-7.1426382	TCMDC-140122	-6.9394422
TCMDC-135260	-7.3434834	TCMDC-133988	-7.1425781	TCMDC-141808	-6.9392085
TCMDC-140653	-7.343379	TCMDC-136567	-7.1423554	TCMDC-139432	-6.9391623
TCMDC-136231	-7.3431764	TCMDC-135284	-7.1417732	TCMDC-135621	-6.9388485
TCMDC-135081	-7.3429527	TCMDC-133162	-7.141717	TCMDC-140364	-6.9387155
TCMDC-123854	-7.3428335	TCMDC-133799	-7.1416383	TCMDC-124005	-6.9386687
TCMDC-134564	-7.3428159	TCMDC-141967	-7.1413779	TCMDC-132336	-6.9380717
TCMDC-135737	-7.3425641	TCMDC-133737	-7.1410689	TCMDC-141041	-6.9379807
TCMDC-137793	-7.3425183	TCMDC-142223	-7.1410036	TCMDC-134329	-6.937952
TCMDC-136554	-7.3424959	TCMDC-139907	-7.1409197	TCMDC-135504	-6.9372478
TCMDC-133090	-7.3424625	TCMDC-133563	-7.1408339	TCMDC-134018	-6.9367499
TCMDC-139974	-7.341939	TCMDC-125508	-7.1406608	TCMDC-125267	-6.9362555
TCMDC-124053	-7.3408923	TCMDC-132038	-7.140584	TCMDC-132281	-6.9361115
TCMDC-135700	-7.3404474	TCMDC-140727	-7.139595	TCMDC-136528	-6.9359756
TCMDC-124443	-7.3403335	TCMDC-132291	-7.1394053	TCMDC-133599	-6.9358711
TCMDC-136823	-7.3402362	TCMDC-132537	-7.1393404	TCMDC-141573	-6.9357967
TCMDC-135617	-7.339951	TCMDC-140237	-7.1392961	TCMDC-132876	-6.9355288
TCMDC-133122	-7.3397856	TCMDC-133297	-7.139267	TCMDC-133652	-6.935226
TCMDC-124420	-7.3396983	TCMDC-140117	-7.1392403	TCMDC-137062	-6.9351125
TCMDC-132544	-7.3396811	TCMDC-132724	-7.1391673	TCMDC-141036	-6.9349742
TCMDC-133242	-7.3392634	TCMDC-140714	-7.1390862	TCMDC-137210	-6.9339843
TCMDC-139169	-7.3392396	TCMDC-137586	-7.1389461	TCMDC-134061	-6.9338722
TCMDC-133547	-7.3392129	TCMDC-136443	-7.1388345	TCMDC-133355	-6.9338522
TCMDC-134155	-7.3391714	TCMDC-134304	-7.1385732	TCMDC-140966	-6.9337306
TCMDC-125432	-7.3390431	TCMDC-142283	-7.1384754	TCMDC-125607	-6.9334798
TCMDC-139248	-7.3389587	TCMDC-125463	-7.1383414	TCMDC-138495	-6.9334536

TCMDC-135476	-7.3387375	TCMDC-133093	-7.1382289	TCMDC-136355	-6.9334083
TCMDC-134648	-7.3386111	TCMDC-131308	-7.137732	TCMDC-133184	-6.9331222
TCMDC-132969	-7.3379774	TCMDC-141472	-7.1377273	TCMDC-136542	-6.9330378
TCMDC-135066	-7.3377185	TCMDC-139454	-7.1375594	TCMDC-136069	-6.9329534
TCMDC-135069	-7.3376098	TCMDC-132502	-7.1360435	TCMDC-131974	-6.9329367
TCMDC-140919	-7.3366265	TCMDC-131579	-7.1358852	TCMDC-125418	-6.9328251
TCMDC-141546	-7.3365097	TCMDC-131829	-7.1357388	TCMDC-125108	-6.9328198
TCMDC-135790	-7.33638	TCMDC-132774	-7.135509	TCMDC-135326	-6.93262
TCMDC-141399	-7.3362827	TCMDC-133908	-7.1355004	TCMDC-132982	-6.932477
TCMDC-134222	-7.3361058	TCMDC-133637	-7.1354837	TCMDC-137082	-6.9324007
TCMDC-138931	-7.335844	TCMDC-139268	-7.1352525	TCMDC-132990	-6.9319615
TCMDC-132714	-7.3357821	TCMDC-123903	-7.1350031	TCMDC-136410	-6.9317122
TCMDC-140652	-7.3357306	TCMDC-141871	-7.1348238	TCMDC-125139	-6.931232
TCMDC-139223	-7.33567	TCMDC-135266	-7.1347136	TCMDC-138427	-6.9308014
TCMDC-140247	-7.3355622	TCMDC-124126	-7.1346679	TCMDC-132459	-6.9307671
TCMDC-139711	-7.3354816	TCMDC-137548	-7.1345997	TCMDC-125245	-6.9305158
TCMDC-132503	-7.3353686	TCMDC-133866	-7.1344624	TCMDC-140772	-6.9301391
TCMDC-138165	-7.3353043	TCMDC-132772	-7.1343675	TCMDC-131624	-6.9300408
TCMDC-137020	-7.3348122	TCMDC-134649	-7.1341443	TCMDC-141176	-6.9292817
TCMDC-139851	-7.3340845	TCMDC-135071	-7.1341329	TCMDC-137474	-6.9291201
TCMDC-132361	-7.3335066	TCMDC-125680	-7.1341166	TCMDC-134399	-6.9285393
TCMDC-134791	-7.3334742	TCMDC-136515	-7.1339498	TCMDC-131902	-6.9281149
TCMDC-132127	-7.3333473	TCMDC-133556	-7.1338954	TCMDC-136483	-6.9278498
TCMDC-133682	-7.3333101	TCMDC-138594	-7.1336532	TCMDC-136627	-6.9278221
TCMDC-139117	-7.3332601	TCMDC-133234	-7.1335325	TCMDC-133633	-6.9275508
TCMDC-139005	-7.3330998	TCMDC-124739	-7.1333313	TCMDC-135612	-6.9272895
TCMDC-140049	-7.3327718	TCMDC-136291	-7.1331344	TCMDC-134267	-6.9271464
TCMDC-136856	-7.3327355	TCMDC-132794	-7.1329207	TCMDC-137123	-6.9269524
TCMDC-134391	-7.3324947	TCMDC-132681	-7.1325989	TCMDC-133022	-6.9265127
TCMDC-135491	-7.3324881	TCMDC-142300	-7.1321712	TCMDC-137383	-6.9264736
TCMDC-140451	-7.332458	TCMDC-140916	-7.1321473	TCMDC-139886	-6.9264116
TCMDC-132605	-7.3322368	TCMDC-134566	-7.1313386	TCMDC-125295	-6.9262094
TCMDC-134631	-7.3319974	TCMDC-133875	-7.1309023	TCMDC-132442	-6.9260464
TCMDC-131992	-7.3318009	TCMDC-138900	-7.1307774	TCMDC-125492	-6.9260349
TCMDC-136913	-7.3315144	TCMDC-138524	-7.1306291	TCMDC-125338	-6.925858
TCMDC-136225	-7.3311429	TCMDC-125883	-7.1303678	TCMDC-125198	-6.925838
TCMDC-124508	-7.3310938	TCMDC-132942	-7.1303515	TCMDC-140522	-6.9257221
TCMDC-133271	-7.3309193	TCMDC-137768	-7.129611	TCMDC-124308	-6.925385
TCMDC-141828	-7.330884	TCMDC-124937	-7.1293287	TCMDC-125056	-6.925272
TCMDC-133274	-7.3307576	TCMDC-136882	-7.1288218	TCMDC-123652	-6.9252286
TCMDC-141488	-7.330616	TCMDC-125159	-7.1283689	TCMDC-139331	-6.9251585
TCMDC-125177	-7.330451	TCMDC-140249	-7.1281509	TCMDC-133873	-6.9250622
TCMDC-140808	-7.3303542	TCMDC-139929	-7.1280661	TCMDC-140196	-6.9248605
TCMDC-139106	-7.3297796	TCMDC-124854	-7.1279464	TCMDC-136985	-6.9245887

TCMDC-142332	-7.3296108	TCMDC-125715	-7.1278863	TCMDC-124233	-6.924314
TCMDC-134453	-7.3292012	TCMDC-140904	-7.1277661	TCMDC-134153	-6.9242783
TCMDC-136968	-7.3290987	TCMDC-137052	-7.1277575	TCMDC-137087	-6.924026
TCMDC-124028	-7.3286257	TCMDC-136329	-7.1275434	TCMDC-136415	-6.9239755
TCMDC-141025	-7.3284998	TCMDC-133174	-7.1274519	TCMDC-132951	-6.9235806
TCMDC-139672	-7.3284431	TCMDC-141172	-7.1274319	TCMDC-138173	-6.9233847
TCMDC-132523	-7.3283372	TCMDC-133750	-7.1272979	TCMDC-139151	-6.9232645
TCMDC-138716	-7.3282275	TCMDC-136871	-7.1270189	TCMDC-139623	-6.9227099
TCMDC-132923	-7.3279929	TCMDC-137362	-7.1269751	TCMDC-125053	-6.9223814
TCMDC-132578	-7.3277936	TCMDC-136864	-7.1269436	TCMDC-131390	-6.9222875
TCMDC-125555	-7.3274469	TCMDC-132450	-7.1268697	TCMDC-136917	-6.9219618
TCMDC-140350	-7.3273487	TCMDC-134966	-7.1268597	TCMDC-125670	-6.9219193
TCMDC-140016	-7.3269296	TCMDC-125712	-7.1268477	TCMDC-136746	-6.9218583
TCMDC-135300	-7.3266087	TCMDC-137174	-7.1265426	TCMDC-131335	-6.921834
TCMDC-141471	-7.3264871	TCMDC-138372	-7.1262851	TCMDC-136631	-6.9217572
TCMDC-124257	-7.3261013	TCMDC-141462	-7.1262803	TCMDC-131439	-6.9214387
TCMDC-135826	-7.3258719	TCMDC-138750	-7.1261797	TCMDC-137128	-6.9213319
TCMDC-138413	-7.3254776	TCMDC-134164	-7.1260042	TCMDC-132243	-6.9211535
TCMDC-134392	-7.3252559	TCMDC-133021	-7.1258531	TCMDC-133543	-6.9208298
TCMDC-141349	-7.3251157	TCMDC-139141	-7.1255364	TCMDC-123505	-6.9207664
TCMDC-136952	-7.3243227	TCMDC-141198	-7.1254153	TCMDC-138452	-6.9204378
TCMDC-136753	-7.323916	TCMDC-134335	-7.125175	TCMDC-136700	-6.9204268
TCMDC-134466	-7.3237801	TCMDC-123561	-7.1251607	TCMDC-133876	-6.9202414
TCMDC-140473	-7.3237629	TCMDC-136622	-7.1249709	TCMDC-135239	-6.9201298
TCMDC-137070	-7.3233638	TCMDC-132623	-7.1247802	TCMDC-140132	-6.9200783
TCMDC-140030	-7.3233438	TCMDC-132371	-7.1247554	TCMDC-125298	-6.9200597
TCMDC-131238	-7.3231196	TCMDC-140191	-7.1246562	TCMDC-123856	-6.9199986
TCMDC-132893	-7.3228235	TCMDC-132551	-7.1245227	TCMDC-133376	-6.9197698
TCMDC-132755	-7.3222284	TCMDC-133331	-7.1243534	TCMDC-135565	-6.9193678
TCMDC-138772	-7.3217006	TCMDC-132733	-7.12431	TCMDC-133730	-6.9190845
TCMDC-135842	-7.3216429	TCMDC-134390	-7.1242628	TCMDC-125798	-6.9189062
TCMDC-132488	-7.3215737	TCMDC-124323	-7.1241646	TCMDC-139645	-6.9186082
TCMDC-134334	-7.3215671	TCMDC-136478	-7.1238837	TCMDC-123516	-6.9180174
TCMDC-133980	-7.3214049	TCMDC-133369	-7.1232281	TCMDC-140202	-6.9179835
TCMDC-124726	-7.321384	TCMDC-135660	-7.1231546	TCMDC-139918	-6.9178915
TCMDC-132957	-7.3210921	TCMDC-132391	-7.1228437	TCMDC-133893	-6.9178209
TCMDC-140187	-7.3210244	TCMDC-139285	-7.1228318	TCMDC-134054	-6.9176702
TCMDC-131261	-7.3209076	TCMDC-139345	-7.1227665	TCMDC-125135	-6.9174762
TCMDC-135862	-7.3207726	TCMDC-134214	-7.1225276	TCMDC-134297	-6.9168863
TCMDC-125693	-7.3204918	TCMDC-132919	-7.1216335	TCMDC-131860	-6.9163871
TCMDC-124442	-7.319859	TCMDC-141490	-7.1215549	TCMDC-123908	-6.9163775
TCMDC-131270	-7.3192468	TCMDC-136448	-7.119997	TCMDC-133740	-6.9160509
TCMDC-125768	-7.3186512	TCMDC-137444	-7.1195102	TCMDC-140256	-6.9158034
TCMDC-132063	-7.3185706	TCMDC-139357	-7.1191678	TCMDC-141290	-6.9151559

TCMDC-125470	-7.3181434	TCMDC-134856	-7.1190543	TCMDC-135594	-6.915031
TCMDC-134336	-7.3179355	TCMDC-141800	-7.1190171	TCMDC-138163	-6.914968
TCMDC-132900	-7.3178415	TCMDC-124714	-7.11833	TCMDC-124869	-6.9148736
TCMDC-136577	-7.3172598	TCMDC-132453	-7.1182246	TCMDC-131878	-6.9147964
TCMDC-140302	-7.3170266	TCMDC-141367	-7.1179461	TCMDC-136845	-6.9143801
TCMDC-125719	-7.316967	TCMDC-124407	-7.1175146	TCMDC-125153	-6.9142842
TCMDC-134671	-7.3169127	TCMDC-139934	-7.1175084	TCMDC-137113	-6.9141226
TCMDC-135306	-7.3164988	TCMDC-132687	-7.1174707	TCMDC-140090	-6.9140716
TCMDC-141261	-7.3164401	TCMDC-141716	-7.1174474	TCMDC-131715	-6.9134793
TCMDC-135740	-7.3162875	TCMDC-134261	-7.1174355	TCMDC-135377	-6.9131641
TCMDC-139135	-7.3159647	TCMDC-137934	-7.1173234	TCMDC-125667	-6.9130578
TCMDC-138862	-7.315908	TCMDC-137041	-7.1172113	TCMDC-135119	-6.9121614
TCMDC-132734	-7.3158398	TCMDC-136289	-7.1171608	TCMDC-125577	-6.912066
TCMDC-131782	-7.3157535	TCMDC-134429	-7.1170835	TCMDC-138698	-6.9116597
TCMDC-134921	-7.3151956	TCMDC-124887	-7.1168532	TCMDC-139540	-6.9114742
TCMDC-132789	-7.3151937	TCMDC-139953	-7.1166449	TCMDC-133763	-6.911459
TCMDC-140785	-7.314991	TCMDC-125393	-7.1166077	TCMDC-132185	-6.9112253
TCMDC-138162	-7.3148003	TCMDC-138391	-7.1163635	TCMDC-123817	-6.9108338
TCMDC-133217	-7.314785	TCMDC-134035	-7.1163182	TCMDC-137528	-6.9105549
TCMDC-136819	-7.3145008	TCMDC-140712	-7.1162286	TCMDC-138009	-6.9104323
TCMDC-141952	-7.314096	TCMDC-140693	-7.1161509	TCMDC-140702	-6.9098797
TCMDC-133220	-7.3140082	TCMDC-124378	-7.1160288	TCMDC-124858	-6.9097137
TCMDC-141564	-7.3138313	TCMDC-123729	-7.11589	TCMDC-134265	-6.9090261
TCMDC-132205	-7.3137341	TCMDC-132331	-7.1158528	TCMDC-140927	-6.9085908
TCMDC-131724	-7.3135476	TCMDC-141616	-7.1158285	TCMDC-125685	-6.9083095
TCMDC-139876	-7.3134861	TCMDC-125101	-7.1152911	TCMDC-142045	-6.9082627
TCMDC-140756	-7.3134613	TCMDC-132997	-7.1150913	TCMDC-135487	-6.9081669
TCMDC-132621	-7.3133926	TCMDC-132131	-7.1149569	TCMDC-132635	-6.9080787
TCMDC-137129	-7.313128	TCMDC-125302	-7.1148448	TCMDC-141406	-6.9079738
TCMDC-125065	-7.3130078	TCMDC-140708	-7.1144657	TCMDC-140089	-6.9078956
TCMDC-134246	-7.3129663	TCMDC-134445	-7.1143317	TCMDC-138445	-6.9076929
TCMDC-133591	-7.3127384	TCMDC-131474	-7.1143308	TCMDC-136780	-6.9075017
TCMDC-137579	-7.3126345	TCMDC-141807	-7.114315	TCMDC-124945	-6.907187
TCMDC-139803	-7.3122849	TCMDC-132912	-7.1141496	TCMDC-137018	-6.9069691
TCMDC-131886	-7.3121748	TCMDC-134864	-7.1140738	TCMDC-136324	-6.9069438
TCMDC-134243	-7.3119564	TCMDC-138302	-7.1134744	TCMDC-139535	-6.906734
TCMDC-137769	-7.3119154	TCMDC-137108	-7.1134467	TCMDC-132756	-6.9067035
TCMDC-135768	-7.31183	TCMDC-131863	-7.1133676	TCMDC-140260	-6.9066629
TCMDC-137716	-7.3117476	TCMDC-134228	-7.113286	TCMDC-141189	-6.9061255
TCMDC-133437	-7.3117218	TCMDC-135347	-7.113245	TCMDC-132409	-6.9059114
TCMDC-131865	-7.3116522	TCMDC-124825	-7.1132154	TCMDC-123680	-6.9058604
TCMDC-135093	-7.3116117	TCMDC-142304	-7.1132035	TCMDC-123894	-6.9058399
TCMDC-133027	-7.3115449	TCMDC-142268	-7.1131353	TCMDC-125022	-6.9053788
TCMDC-135825	-7.3113618	TCMDC-132878	-7.1130714	TCMDC-140694	-6.9053144

TCMDC-139259	-7.3112845	TCMDC-140651	-7.1128254	TCMDC-134353	-6.9050875
TCMDC-125271	-7.3112617	TCMDC-140548	-7.1124487	TCMDC-141912	-6.9046874
TCMDC-137799	-7.3112202	TCMDC-135440	-7.112318	TCMDC-137461	-6.9044299
TCMDC-131803	-7.3111658	TCMDC-141000	-7.1121855	TCMDC-137443	-6.904161
TCMDC-136822	-7.3108788	TCMDC-137146	-7.1115456	TCMDC-138643	-6.9041176
TCMDC-139951	-7.3108435	TCMDC-138877	-7.1115012	TCMDC-123711	-6.9039407
TCMDC-139881	-7.31071	TCMDC-140454	-7.111371	TCMDC-132927	-6.9036703
TCMDC-132377	-7.3106542	TCMDC-141216	-7.1112294	TCMDC-124113	-6.9035907
TCMDC-141291	-7.3103018	TCMDC-133164	-7.1109223	TCMDC-141646	-6.9034739
TCMDC-139871	-7.3101463	TCMDC-132827	-7.1108394	TCMDC-138679	-6.9034247
TCMDC-132570	-7.3099899	TCMDC-133749	-7.1105366	TCMDC-133151	-6.9033332
TCMDC-137575	-7.309907	TCMDC-135275	-7.110323	TCMDC-125436	-6.9032125
TCMDC-137176	-7.3097434	TCMDC-125070	-7.1102805	TCMDC-136742	-6.902689
TCMDC-140739	-7.3095145	TCMDC-138558	-7.1100726	TCMDC-132302	-6.9023042
TCMDC-125663	-7.3087564	TCMDC-132727	-7.1100302	TCMDC-124762	-6.9018455
TCMDC-131743	-7.3084679	TCMDC-132512	-7.109899	TCMDC-125350	-6.9018159
TCMDC-140798	-7.3084259	TCMDC-141079	-7.1097207	TCMDC-132204	-6.9011574
TCMDC-141531	-7.3084025	TCMDC-135019	-7.1092386	TCMDC-133567	-6.9009686
TCMDC-140199	-7.3083849	TCMDC-133245	-7.1089783	TCMDC-139436	-6.9008164
TCMDC-137256	-7.3083339	TCMDC-140759	-7.1085567	TCMDC-140624	-6.9007173
TCMDC-138867	-7.3082213	TCMDC-136629	-7.1085377	TCMDC-133711	-6.9004478
TCMDC-141536	-7.3081121	TCMDC-139869	-7.1083026	TCMDC-136716	-6.9002819
TCMDC-132627	-7.3076563	TCMDC-134836	-7.1080494	TCMDC-138179	-6.8993735
TCMDC-125127	-7.3076134	TCMDC-136223	-7.1074481	TCMDC-135087	-6.8992329
TCMDC-131729	-7.3072124	TCMDC-137450	-7.1074424	TCMDC-125063	-6.8991084
TCMDC-140357	-7.3066387	TCMDC-136322	-7.1074138	TCMDC-131429	-6.8990812
TCMDC-140229	-7.3066292	TCMDC-141872	-7.1072178	TCMDC-133417	-6.898952
TCMDC-139333	-7.3066092	TCMDC-134033	-7.106483	TCMDC-141146	-6.8989487
TCMDC-123611	-7.3065829	TCMDC-139158	-7.106308	TCMDC-124725	-6.8988123
TCMDC-140864	-7.3065438	TCMDC-134064	-7.106277	TCMDC-138508	-6.8987899
TCMDC-141043	-7.3062558	TCMDC-124134	-7.106019	TCMDC-139429	-6.8983645
TCMDC-124353	-7.3062143	TCMDC-136390	-7.1058536	TCMDC-140103	-6.8980856
TCMDC-139663	-7.3060966	TCMDC-136875	-7.1058369	TCMDC-139177	-6.8977709
TCMDC-138719	-7.3058753	TCMDC-134120	-7.1057582	TCMDC-134413	-6.8974528
TCMDC-141841	-7.3055148	TCMDC-125228	-7.1054554	TCMDC-133757	-6.8972502
TCMDC-131699	-7.3055148	TCMDC-141825	-7.1052575	TCMDC-135011	-6.8972306
TCMDC-132128	-7.3048959	TCMDC-134616	-7.1050367	TCMDC-124817	-6.897038
TCMDC-136551	-7.3041377	TCMDC-125795	-7.1047101	TCMDC-136703	-6.8969469
TCMDC-140819	-7.3041263	TCMDC-134142	-7.1046586	TCMDC-137204	-6.8968449
TCMDC-141681	-7.3039422	TCMDC-134950	-7.1046562	TCMDC-141917	-6.8968282
TCMDC-132160	-7.3038945	TCMDC-139545	-7.1045179	TCMDC-135908	-6.8964348
TCMDC-141845	-7.3036666	TCMDC-135182	-7.1041465	TCMDC-136729	-6.8961639
TCMDC-131657	-7.3036408	TCMDC-140354	-7.104125	TCMDC-139301	-6.8960857
TCMDC-139544	-7.303586	TCMDC-132854	-7.1037335	TCMDC-132075	-6.8959708

TCMDC-132153	-7.3028817	TCMDC-140358	-7.1035142	TCMDC-124213	-6.8957715
TCMDC-133700	-7.3028641	TCMDC-124212	-7.1034627	TCMDC-134038	-6.8954611
TCMDC-139962	-7.3027549	TCMDC-132569	-7.1034393	TCMDC-140093	-6.8954287
TCMDC-125803	-7.3023491	TCMDC-124705	-7.1030898	TCMDC-141566	-6.8953571
TCMDC-139409	-7.302176	TCMDC-132625	-7.1029005	TCMDC-141869	-6.8951874
TCMDC-139179	-7.3017378	TCMDC-136079	-7.1026859	TCMDC-131618	-6.894217
TCMDC-124677	-7.3016696	TCMDC-140692	-7.102674	TCMDC-138455	-6.8938022
TCMDC-136928	-7.3016014	TCMDC-140242	-7.1025829	TCMDC-125333	-6.8937297
TCMDC-140415	-7.3013897	TCMDC-136770	-7.1025457	TCMDC-134437	-6.8936067
TCMDC-139873	-7.3013492	TCMDC-131940	-7.102489	TCMDC-134042	-6.893405
TCMDC-140339	-7.3012748	TCMDC-134821	-7.1024475	TCMDC-124686	-6.8932681
TCMDC-140258	-7.3011694	TCMDC-141298	-7.1022487	TCMDC-138675	-6.8930807
TCMDC-139163	-7.3010821	TCMDC-142308	-7.1021509	TCMDC-139657	-6.8930616
TCMDC-125304	-7.3007898	TCMDC-137955	-7.1019516	TCMDC-137552	-6.8929787
TCMDC-133152	-7.3003731	TCMDC-124238	-7.1017818	TCMDC-140120	-6.8926597
TCMDC-139973	-7.2999992	TCMDC-124778	-7.1015086	TCMDC-140683	-6.8925109
TCMDC-125462	-7.2997775	TCMDC-136635	-7.1012917	TCMDC-125275	-6.8921981
TCMDC-132869	-7.2996869	TCMDC-139187	-7.1011662	TCMDC-132824	-6.89184
TCMDC-139461	-7.2995353	TCMDC-134489	-7.1008935	TCMDC-133531	-6.8913326
TCMDC-133141	-7.2995124	TCMDC-138447	-7.1008115	TCMDC-133148	-6.8912597
TCMDC-132691	-7.2995124	TCMDC-136088	-7.1006927	TCMDC-136773	-6.8911643
TCMDC-132501	-7.2993188	TCMDC-131269	-7.100575	TCMDC-137299	-6.8904939
TCMDC-136290	-7.298903	TCMDC-138113	-7.100389	TCMDC-125184	-6.8900561
TCMDC-132898	-7.2986193	TCMDC-123795	-7.1002331	TCMDC-132883	-6.8900237
TCMDC-132944	-7.2985492	TCMDC-135188	-7.1001391	TCMDC-125180	-6.8899446
TCMDC-125503	-7.2984366	TCMDC-132470	-7.10007	TCMDC-137002	-6.8892031
TCMDC-132416	-7.2983785	TCMDC-139948	-7.0999193	TCMDC-138540	-6.8882985
TCMDC-132367	-7.2981043	TCMDC-135459	-7.0995722	TCMDC-137547	-6.887938
TCMDC-132736	-7.2978539	TCMDC-124216	-7.0995011	TCMDC-135591	-6.8879261
TCMDC-134651	-7.2977018	TCMDC-133385	-7.0994787	TCMDC-140781	-6.887722
TCMDC-136706	-7.29738	TCMDC-132885	-7.0994263	TCMDC-125122	-6.8874345
TCMDC-138392	-7.2973094	TCMDC-135079	-7.0993338	TCMDC-140510	-6.8874249
TCMDC-133384	-7.2971797	TCMDC-136034	-7.0993338	TCMDC-133823	-6.8872919
TCMDC-133553	-7.2966876	TCMDC-135088	-7.0991673	TCMDC-139618	-6.8871059
TCMDC-132188	-7.2963567	TCMDC-135327	-7.0989304	TCMDC-124211	-6.8869009
TCMDC-136333	-7.2960296	TCMDC-134062	-7.0984402	TCMDC-134597	-6.8868952
TCMDC-134553	-7.2960119	TCMDC-141283	-7.0983219	TCMDC-123609	-6.8863072
TCMDC-139681	-7.2956982	TCMDC-138954	-7.0977464	TCMDC-132086	-6.8860321
TCMDC-141755	-7.295681	TCMDC-137477	-7.097486	TCMDC-142330	-6.8859625
TCMDC-141619	-7.2952199	TCMDC-141192	-7.0974727	TCMDC-125346	-6.8853183
TCMDC-131611	-7.2949538	TCMDC-125802	-7.0973148	TCMDC-125400	-6.8841405
TCMDC-134889	-7.2949452	TCMDC-132139	-7.097209	TCMDC-134872	-6.8840613
TCMDC-137134	-7.2944336	TCMDC-138150	-7.0970345	TCMDC-132813	-6.8838401
TCMDC-132716	-7.2943563	TCMDC-132669	-7.0970101	TCMDC-141793	-6.88375

TCMDC-141372	-7.2940583	TCMDC-124697	-7.0969419	TCMDC-131456	-6.8835783
TCMDC-142311	-7.2939715	TCMDC-137514	-7.0962534	TCMDC-138557	-6.8834004
TCMDC-141849	-7.2937431	TCMDC-138032	-7.0962234	TCMDC-133241	-6.883214
TCMDC-132678	-7.2936983	TCMDC-133745	-7.0960875	TCMDC-133886	-6.88311
TCMDC-137140	-7.2935271	TCMDC-140843	-7.0960703	TCMDC-138364	-6.8825326
TCMDC-132376	-7.2933855	TCMDC-132849	-7.0958662	TCMDC-135111	-6.8820605
TCMDC-141381	-7.2927256	TCMDC-133976	-7.0957899	TCMDC-132594	-6.8819356
TCMDC-132811	-7.2925982	TCMDC-135114	-7.0955706	TCMDC-123659	-6.8817649
TCMDC-133884	-7.2919922	TCMDC-132981	-7.0953727	TCMDC-131944	-6.8804727
TCMDC-134496	-7.2919612	TCMDC-134811	-7.0952229	TCMDC-132359	-6.8802209
TCMDC-137310	-7.2919536	TCMDC-141831	-7.0950041	TCMDC-136090	-6.8802099
TCMDC-136352	-7.2919145	TCMDC-135442	-7.0949783	TCMDC-133073	-6.8800387
TCMDC-132401	-7.2917361	TCMDC-131273	-7.0948057	TCMDC-134312	-6.8797827
TCMDC-133605	-7.2911997	TCMDC-141457	-7.0947871	TCMDC-132156	-6.8795562
TCMDC-133861	-7.2911911	TCMDC-138082	-7.0944996	TCMDC-141691	-6.8794627
TCMDC-137823	-7.290452	TCMDC-125430	-7.0943136	TCMDC-132497	-6.8791361
TCMDC-134438	-7.2903414	TCMDC-131921	-7.0940237	TCMDC-138208	-6.8788996
TCMDC-134896	-7.290247	TCMDC-141170	-7.0936384	TCMDC-134767	-6.8788657
TCMDC-131245	-7.2902002	TCMDC-133160	-7.0935817	TCMDC-139352	-6.8786893
TCMDC-132451	-7.2901659	TCMDC-139791	-7.0935049	TCMDC-140647	-6.8782234
TCMDC-132719	-7.2896476	TCMDC-124083	-7.0933657	TCMDC-141277	-6.8782072
TCMDC-136201	-7.2896366	TCMDC-123815	-7.0932436	TCMDC-135179	-6.878118
TCMDC-131914	-7.2896304	TCMDC-133144	-7.0931468	TCMDC-124463	-6.8770666
TCMDC-141394	-7.2894483	TCMDC-123678	-7.0925317	TCMDC-137017	-6.8768005
TCMDC-134679	-7.2892265	TCMDC-133340	-7.0924859	TCMDC-124045	-6.8767214
TCMDC-141711	-7.2891803	TCMDC-141033	-7.0923543	TCMDC-125130	-6.8764329
TCMDC-141169	-7.2889147	TCMDC-139329	-7.0923057	TCMDC-140337	-6.8762236
TCMDC-141950	-7.2883716	TCMDC-140211	-7.0918779	TCMDC-125671	-6.8760362
TCMDC-135184	-7.2883224	TCMDC-132357	-7.0916462	TCMDC-125507	-6.8753605
TCMDC-125332	-7.2882009	TCMDC-133106	-7.0912867	TCMDC-134844	-6.8752389
TCMDC-124925	-7.2878876	TCMDC-136956	-7.0908971	TCMDC-124685	-6.8750401
TCMDC-125659	-7.2878156	TCMDC-140208	-7.0905657	TCMDC-139558	-6.8748069
TCMDC-139245	-7.2876263	TCMDC-132654	-7.0905223	TCMDC-140747	-6.8742824
TCMDC-137791	-7.2875342	TCMDC-141588	-7.0902739	TCMDC-131482	-6.874259
TCMDC-133981	-7.2875161	TCMDC-136776	-7.0902014	TCMDC-133638	-6.8739944
TCMDC-135453	-7.287291	TCMDC-124822	-7.0898638	TCMDC-137203	-6.8739314
TCMDC-132189	-7.2869124	TCMDC-133202	-7.0896907	TCMDC-140903	-6.8735843
TCMDC-134333	-7.2868462	TCMDC-125488	-7.0895867	TCMDC-125248	-6.8732409
TCMDC-134967	-7.286551	TCMDC-136797	-7.0894427	TCMDC-139319	-6.8732185
TCMDC-136221	-7.286377	TCMDC-136463	-7.0893636	TCMDC-139150	-6.8722134
TCMDC-137152	-7.2862844	TCMDC-135551	-7.0893569	TCMDC-133761	-6.8718209
TCMDC-139947	-7.2859592	TCMDC-133816	-7.0893168	TCMDC-137364	-6.871634
TCMDC-135180	-7.2856932	TCMDC-139239	-7.0890107	TCMDC-136207	-6.8715568
TCMDC-134980	-7.285563	TCMDC-141816	-7.0889974	TCMDC-131241	-6.8714838

TCMDC-139283	-7.284821	TCMDC-133639	-7.0888362	TCMDC-132085	-6.8712125
TCMDC-133176	-7.2845483	TCMDC-139324	-7.0888109	TCMDC-135878	-6.8710289
TCMDC-139272	-7.2844934	TCMDC-133602	-7.0884151	TCMDC-139725	-6.8705549
TCMDC-125407	-7.2844801	TCMDC-136935	-7.0881968	TCMDC-131659	-6.8703499
TCMDC-139180	-7.2843676	TCMDC-124444	-7.0879064	TCMDC-136750	-6.8701286
TCMDC-132203	-7.2842832	TCMDC-124163	-7.0878887	TCMDC-133971	-6.8701062
TCMDC-136424	-7.2840838	TCMDC-137122	-7.0878086	TCMDC-141214	-6.8698726
TCMDC-141947	-7.2839503	TCMDC-136040	-7.0877957	TCMDC-131973	-6.869525
TCMDC-125293	-7.2839479	TCMDC-139322	-7.087235	TCMDC-132519	-6.8692837
TCMDC-136406	-7.283854	TCMDC-132830	-7.0870509	TCMDC-133517	-6.8690553
TCMDC-132778	-7.2837434	TCMDC-133283	-7.0870032	TCMDC-134753	-6.8690324
TCMDC-139508	-7.2835717	TCMDC-132404	-7.0868649	TCMDC-141081	-6.8688455
TCMDC-137456	-7.283567	TCMDC-140446	-7.086103	TCMDC-138352	-6.8688302
TCMDC-141925	-7.2833853	TCMDC-125683	-7.086103	TCMDC-131786	-6.8685756
TCMDC-132697	-7.2833843	TCMDC-123706	-7.0860114	TCMDC-135766	-6.8683105
TCMDC-134640	-7.283123	TCMDC-139682	-7.0859194	TCMDC-136778	-6.8682523
TCMDC-134245	-7.2826266	TCMDC-136620	-7.0853758	TCMDC-139812	-6.868238
TCMDC-124139	-7.2824483	TCMDC-141833	-7.0851998	TCMDC-133950	-6.8676643
TCMDC-132403	-7.282371	TCMDC-140240	-7.0851741	TCMDC-135128	-6.8666186
TCMDC-140423	-7.2819571	TCMDC-141058	-7.0849028	TCMDC-135469	-6.8665061
TCMDC-141023	-7.281702	TCMDC-139875	-7.084548	TCMDC-140839	-6.8663836
TCMDC-134936	-7.2813902	TCMDC-141881	-7.0844965	TCMDC-137156	-6.8660598
TCMDC-133104	-7.2811732	TCMDC-134987	-7.084074	TCMDC-132023	-6.8660355
TCMDC-132841	-7.2811193	TCMDC-134471	-7.0837913	TCMDC-133190	-6.8658218
TCMDC-141051	-7.2807803	TCMDC-140678	-7.0833917	TCMDC-125191	-6.8657088
TCMDC-131910	-7.2806625	TCMDC-125208	-7.0831709	TCMDC-124496	-6.8655128
TCMDC-140577	-7.2805552	TCMDC-141105	-7.0828724	TCMDC-132644	-6.8652525
TCMDC-137460	-7.2804937	TCMDC-140761	-7.0827928	TCMDC-137572	-6.8649492
TCMDC-132369	-7.2799067	TCMDC-133475	-7.0822964	TCMDC-123588	-6.8647013
TCMDC-138429	-7.279501	TCMDC-123579	-7.0821624	TCMDC-123534	-6.8646512
TCMDC-132068	-7.2792397	TCMDC-140349	-7.0815248	TCMDC-134581	-6.8645244
TCMDC-133280	-7.2791457	TCMDC-140705	-7.0810347	TCMDC-123909	-6.8640485
TCMDC-134613	-7.2783837	TCMDC-134508	-7.0807824	TCMDC-131285	-6.8639174
TCMDC-140472	-7.2783446	TCMDC-124493	-7.0807538	TCMDC-139966	-6.8637767
TCMDC-138205	-7.2782512	TCMDC-125181	-7.0806251	TCMDC-136837	-6.8637204
TCMDC-137016	-7.2781363	TCMDC-132810	-7.080524	TCMDC-132666	-6.8634806
TCMDC-140574	-7.2779408	TCMDC-133237	-7.0804992	TCMDC-125207	-6.8631563
TCMDC-132941	-7.2778749	TCMDC-137543	-7.0804124	TCMDC-133650	-6.8628559
TCMDC-132891	-7.2772651	TCMDC-135058	-7.0802231	TCMDC-134284	-6.8627248
TCMDC-135384	-7.2769499	TCMDC-142334	-7.0796309	TCMDC-124804	-6.8624239
TCMDC-139646	-7.2761784	TCMDC-139444	-7.0793915	TCMDC-135628	-6.8622303
TCMDC-138189	-7.2758384	TCMDC-135691	-7.0792694	TCMDC-124704	-6.8621249
TCMDC-136252	-7.2754531	TCMDC-137569	-7.0792279	TCMDC-133765	-6.8617344
TCMDC-125331	-7.2752509	TCMDC-141001	-7.0789933	TCMDC-141196	-6.8615141

TCMDC-135073	-7.2751093	TCMDC-136471	-7.0781894	TCMDC-139019	-6.8607688
TCMDC-132340	-7.2749681	TCMDC-141031	-7.0778704	TCMDC-141540	-6.8606701
TCMDC-134507	-7.2744093	TCMDC-140295	-7.0778461	TCMDC-135363	-6.8603354
TCMDC-134218	-7.2743964	TCMDC-134418	-7.0778046	TCMDC-134051	-6.860333
TCMDC-135373	-7.2742319	TCMDC-134716	-7.0773964	TCMDC-132738	-6.8593903
TCMDC-133835	-7.2738247	TCMDC-135646	-7.077322	TCMDC-124626	-6.8592958
TCMDC-124081	-7.2738118	TCMDC-140965	-7.0771527	TCMDC-135489	-6.8592529
TCMDC-140668	-7.2737641	TCMDC-141418	-7.0755792	TCMDC-133153	-6.8590403
TCMDC-139766	-7.2736716	TCMDC-125737	-7.0752201	TCMDC-141984	-6.8587213
TCMDC-124955	-7.2735906	TCMDC-135990	-7.075213	TCMDC-136685	-6.8582969
TCMDC-142333	-7.2734804	TCMDC-125269	-7.0751891	TCMDC-131949	-6.8582282
TCMDC-139289	-7.2733216	TCMDC-132254	-7.0750432	TCMDC-124040	-6.8580861
TCMDC-132396	-7.2733192	TCMDC-124510	-7.0749402	TCMDC-125635	-6.8575544
TCMDC-138480	-7.2729068	TCMDC-136168	-7.0749164	TCMDC-131506	-6.8575416
TCMDC-136323	-7.2718544	TCMDC-140696	-7.0748839	TCMDC-125143	-6.8569813
TCMDC-136841	-7.2717991	TCMDC-139303	-7.0747018	TCMDC-124906	-6.8566132
TCMDC-132200	-7.2716813	TCMDC-136969	-7.0745964	TCMDC-123672	-6.8565388
TCMDC-140207	-7.2714934	TCMDC-137787	-7.0745707	TCMDC-135156	-6.8563762
TCMDC-133451	-7.2714696	TCMDC-124957	-7.0739574	TCMDC-133833	-6.8562918
TCMDC-138459	-7.2714353	TCMDC-139435	-7.0739193	TCMDC-133548	-6.8561735
TCMDC-124373	-7.2713475	TCMDC-125699	-7.0737619	TCMDC-132196	-6.8559904
TCMDC-139195	-7.2712455	TCMDC-138574	-7.0737395	TCMDC-124591	-6.8558731
TCMDC-132194	-7.2701201	TCMDC-134504	-7.0736732	TCMDC-134638	-6.8558722
TCMDC-141024	-7.2700443	TCMDC-133012	-7.0736666	TCMDC-125448	-6.8558273
TCMDC-134971	-7.2699594	TCMDC-138688	-7.0728164	TCMDC-140324	-6.8553705
TCMDC-132920	-7.2698994	TCMDC-133453	-7.0725813	TCMDC-134300	-6.8553262
TCMDC-136604	-7.2694263	TCMDC-132853	-7.0721192	TCMDC-141419	-6.854948
TCMDC-134238	-7.2693701	TCMDC-136787	-7.0720181	TCMDC-132937	-6.8545232
TCMDC-132563	-7.2691288	TCMDC-141395	-7.0719061	TCMDC-133879	-6.8544164
TCMDC-124273	-7.2690253	TCMDC-125032	-7.0718436	TCMDC-134242	-6.854135
TCMDC-132788	-7.2687044	TCMDC-133760	-7.0717072	TCMDC-135454	-6.8538818
TCMDC-141440	-7.2684808	TCMDC-133198	-7.0715313	TCMDC-136563	-6.8538308
TCMDC-134393	-7.2684708	TCMDC-133509	-7.0711193	TCMDC-133698	-6.8534479
TCMDC-136857	-7.268404	TCMDC-132890	-7.070004	TCMDC-140509	-6.8529625
TCMDC-132567	-7.2682967	TCMDC-125636	-7.0699396	TCMDC-135871	-6.8529286
TCMDC-141526	-7.2676334	TCMDC-141020	-7.0698729	TCMDC-131952	-6.8528647
TCMDC-134898	-7.267283	TCMDC-134884	-7.0692844	TCMDC-124454	-6.8525109
TCMDC-136112	-7.2671957	TCMDC-133972	-7.0689731	TCMDC-124700	-6.8524823
TCMDC-136949	-7.2669673	TCMDC-125044	-7.0688992	TCMDC-125288	-6.852026
TCMDC-132337	-7.2666669	TCMDC-132557	-7.0688343	TCMDC-140455	-6.8514862
TCMDC-125276	-7.2666306	TCMDC-125264	-7.0687013	TCMDC-131354	-6.8513427
TCMDC-133706	-7.2665701	TCMDC-141361	-7.0685048	TCMDC-124745	-6.8513365
TCMDC-137068	-7.2663941	TCMDC-139779	-7.0682654	TCMDC-125611	-6.8512526
TCMDC-133998	-7.2662778	TCMDC-124101	-7.0679183	TCMDC-124954	-6.8507175

TCMDC-133614	-7.2661123	TCMDC-140389	-7.0679135	TCMDC-136728	-6.849875
TCMDC-139542	-7.2659373	TCMDC-136955	-7.0677595	TCMDC-139373	-6.8497815
TCMDC-123576	-7.2654305	TCMDC-139878	-7.0676112	TCMDC-125045	-6.8497577
TCMDC-132815	-7.2650719	TCMDC-138390	-7.0674562	TCMDC-140838	-6.8495269
TCMDC-135838	-7.2650251	TCMDC-141525	-7.0673389	TCMDC-139360	-6.849206
TCMDC-133305	-7.2646961	TCMDC-124721	-7.0670309	TCMDC-124141	-6.8489819
TCMDC-141121	-7.2642207	TCMDC-139683	-7.0669508	TCMDC-125550	-6.8488946
TCMDC-141819	-7.2642026	TCMDC-142013	-7.0665984	TCMDC-133529	-6.8485584
TCMDC-136792	-7.2641301	TCMDC-140521	-7.0663109	TCMDC-125700	-6.8485556
TCMDC-135240	-7.2638021	TCMDC-132799	-7.0661688	TCMDC-124926	-6.8484654
TCMDC-140664	-7.2637653	TCMDC-139171	-7.0657983	TCMDC-139855	-6.8481727
TCMDC-132928	-7.2632227	TCMDC-124785	-7.0653496	TCMDC-135622	-6.8481069
TCMDC-140803	-7.2624726	TCMDC-132322	-7.0650525	TCMDC-124390	-6.8476639
TCMDC-136171	-7.2623787	TCMDC-138510	-7.0645208	TCMDC-134426	-6.8474984
TCMDC-132842	-7.2623038	TCMDC-139194	-7.0644946	TCMDC-131580	-6.8474221
TCMDC-136876	-7.2617059	TCMDC-131875	-7.0644231	TCMDC-139699	-6.8471022
TCMDC-133571	-7.2616057	TCMDC-137105	-7.0641289	TCMDC-131515	-6.8470244
TCMDC-136826	-7.2612534	TCMDC-137347	-7.0639782	TCMDC-139785	-6.8469267
TCMDC-139549	-7.2608695	TCMDC-138683	-7.0639606	TCMDC-135023	-6.8464842
TCMDC-132446	-7.260848	TCMDC-136632	-7.0639091	TCMDC-131705	-6.846107
TCMDC-137044	-7.2608185	TCMDC-134342	-7.0638332	TCMDC-133541	-6.8458543
TCMDC-136275	-7.2606502	TCMDC-136084	-7.0636163	TCMDC-133206	-6.8456712
TCMDC-139980	-7.2604518	TCMDC-140645	-7.0635724	TCMDC-136209	-6.8456526
TCMDC-136809	-7.2604494	TCMDC-140445	-7.063426	TCMDC-134041	-6.8454032
TCMDC-134096	-7.2604299	TCMDC-140243	-7.0633931	TCMDC-138406	-6.8448296
TCMDC-132777	-7.2601776	TCMDC-137240	-7.0633774	TCMDC-124840	-6.8446999
TCMDC-133143	-7.2600832	TCMDC-136468	-7.0631561	TCMDC-140230	-6.8442898
TCMDC-131862	-7.2599745	TCMDC-139914	-7.0628939	TCMDC-136541	-6.8442745
TCMDC-135521	-7.2598467	TCMDC-139710	-7.0627141	TCMDC-134113	-6.8439054
TCMDC-139884	-7.2595367	TCMDC-137060	-7.0626898	TCMDC-140461	-6.8438497
TCMDC-138989	-7.2593999	TCMDC-124476	-7.0625386	TCMDC-125227	-6.843648
TCMDC-134433	-7.2592864	TCMDC-137380	-7.0624957	TCMDC-136675	-6.8436365
TCMDC-132274	-7.2592154	TCMDC-125311	-7.06248	TCMDC-133654	-6.8434472
TCMDC-132140	-7.2589488	TCMDC-137120	-7.0617661	TCMDC-124179	-6.8426447
TCMDC-134219	-7.2589116	TCMDC-136993	-7.0615158	TCMDC-138381	-6.8424983
TCMDC-141570	-7.2588544	TCMDC-138104	-7.0607929	TCMDC-136347	-6.8424788
TCMDC-139860	-7.2587199	TCMDC-136041	-7.0607634	TCMDC-133966	-6.8424721
TCMDC-134225	-7.2586713	TCMDC-136909	-7.0603733	TCMDC-139491	-6.8421993
TCMDC-134454	-7.2584167	TCMDC-131742	-7.0603733	TCMDC-132554	-6.8421493
TCMDC-132622	-7.2580943	TCMDC-131512	-7.0602875	TCMDC-138578	-6.8413548
TCMDC-132722	-7.2579474	TCMDC-133851	-7.0600634	TCMDC-132823	-6.8407712
TCMDC-137678	-7.257762	TCMDC-139278	-7.0596194	TCMDC-134478	-6.8407478
TCMDC-141184	-7.2576065	TCMDC-138590	-7.0595298	TCMDC-133025	-6.8397765
TCMDC-136326	-7.2575827	TCMDC-135340	-7.0594912	TCMDC-139687	-6.8396592

TCMDC-133121	-7.2566061	TCMDC-133334	-7.0593309	TCMDC-142120	-6.8395786
TCMDC-131246	-7.2564464	TCMDC-133900	-7.0593028	TCMDC-132552	-6.8392897
TCMDC-140137	-7.2563734	TCMDC-125788	-7.0590863	TCMDC-132914	-6.8387642
TCMDC-131584	-7.256176	TCMDC-133781	-7.0588789	TCMDC-135010	-6.8386903
TCMDC-124469	-7.2561226	TCMDC-125263	-7.0586061	TCMDC-135814	-6.8385711
TCMDC-125116	-7.2560415	TCMDC-135839	-7.0584388	TCMDC-141747	-6.838109
TCMDC-124481	-7.2559032	TCMDC-131701	-7.0584273	TCMDC-136476	-6.8380828
TCMDC-125701	-7.2555337	TCMDC-124720	-7.0582237	TCMDC-135620	-6.837976
TCMDC-133859	-7.2551308	TCMDC-124959	-7.0579262	TCMDC-132433	-6.8376942
TCMDC-134220	-7.2550769	TCMDC-134824	-7.0575485	TCMDC-134772	-6.8369946
TCMDC-133083	-7.2548389	TCMDC-141817	-7.0574627	TCMDC-140793	-6.836936
TCMDC-135230	-7.2547803	TCMDC-132435	-7.0574474	TCMDC-137576	-6.8366137
TCMDC-133938	-7.2543926	TCMDC-139166	-7.0574384	TCMDC-139968	-6.8361216
TCMDC-132074	-7.2543468	TCMDC-136145	-7.0573502	TCMDC-137974	-6.8360667
TCMDC-123874	-7.2542596	TCMDC-140425	-7.0567627	TCMDC-131401	-6.8357506
TCMDC-135207	-7.2538342	TCMDC-134430	-7.0564699	TCMDC-136594	-6.8346581
TCMDC-136470	-7.2533436	TCMDC-137022	-7.0563607	TCMDC-133236	-6.834619
TCMDC-132487	-7.2532616	TCMDC-133867	-7.0563374	TCMDC-134254	-6.8345828
TCMDC-132318	-7.2531495	TCMDC-132731	-7.0559626	TCMDC-133826	-6.8344321
TCMDC-139721	-7.2526846	TCMDC-123927	-7.0558867	TCMDC-138075	-6.8343749
TCMDC-125019	-7.2526584	TCMDC-138119	-7.0557318	TCMDC-137252	-6.8343534
TCMDC-141360	-7.2523284	TCMDC-136589	-7.0554519	TCMDC-138998	-6.8343482
TCMDC-132400	-7.252142	TCMDC-141429	-7.0553889	TCMDC-138439	-6.8342986
TCMDC-133101	-7.2519293	TCMDC-124676	-7.0552392	TCMDC-140428	-6.8342385
TCMDC-138212	-7.2513857	TCMDC-142310	-7.0551796	TCMDC-140405	-6.8341794
TCMDC-134780	-7.2513814	TCMDC-139553	-7.0551596	TCMDC-125412	-6.8341455
TCMDC-133701	-7.2511978	TCMDC-138613	-7.0550876	TCMDC-125021	-6.8341184
TCMDC-136549	-7.2511687	TCMDC-135829	-7.0550752	TCMDC-131991	-6.8339086
TCMDC-125174	-7.2510638	TCMDC-139024	-7.0550728	TCMDC-135334	-6.833467
TCMDC-133147	-7.2510109	TCMDC-134962	-7.0548782	TCMDC-142252	-6.8332353
TCMDC-123627	-7.2508516	TCMDC-141278	-7.0548601	TCMDC-133821	-6.8331985
TCMDC-125460	-7.2508316	TCMDC-124515	-7.0548158	TCMDC-132704	-6.8331819
TCMDC-140276	-7.2505431	TCMDC-140185	-7.0546827	TCMDC-133768	-6.8331451
TCMDC-139685	-7.2503982	TCMDC-140379	-7.0545697	TCMDC-133380	-6.8329382
TCMDC-134814	-7.2503085	TCMDC-132325	-7.0536532	TCMDC-138349	-6.8328433
TCMDC-134575	-7.2501554	TCMDC-140342	-7.0536361	TCMDC-134715	-6.8326812
TCMDC-134337	-7.2500978	TCMDC-139066	-7.0535359	TCMDC-140118	-6.8324847
TCMDC-133257	-7.2500668	TCMDC-140138	-7.05336	TCMDC-132743	-6.8320074
TCMDC-141757	-7.2498894	TCMDC-125468	-7.0530696	TCMDC-134610	-6.8317542
TCMDC-136942	-7.2496395	TCMDC-136044	-7.052949	TCMDC-134915	-6.831656
TCMDC-133099	-7.2493958	TCMDC-137630	-7.0528164	TCMDC-132746	-6.8315191
TCMDC-133401	-7.2492166	TCMDC-141968	-7.0522866	TCMDC-140397	-6.8312497
TCMDC-140938	-7.2491331	TCMDC-133999	-7.0519099	TCMDC-125724	-6.8308949
TCMDC-134250	-7.2491288	TCMDC-132977	-7.0518818	TCMDC-133033	-6.8308859

TCMDC-140045	-7.2489252	TCMDC-134158	-7.0511951	TCMDC-124482	-6.8308287
TCMDC-123591	-7.2487707	TCMDC-139014	-7.0506997	TCMDC-142000	-6.8307691
TCMDC-135944	-7.2486777	TCMDC-138303	-7.0504904	TCMDC-133646	-6.8303375
TCMDC-137915	-7.2484293	TCMDC-136624	-7.0502892	TCMDC-140110	-6.8292031
TCMDC-139136	-7.2484231	TCMDC-123646	-7.0502195	TCMDC-142249	-6.829124
TCMDC-125637	-7.2483377	TCMDC-134406	-7.0496221	TCMDC-124657	-6.8287563
TCMDC-136423	-7.248023	TCMDC-139160	-7.0493617	TCMDC-124154	-6.8284116
TCMDC-135978	-7.2476931	TCMDC-136601	-7.0491905	TCMDC-134000	-6.8283763
TCMDC-139203	-7.2474985	TCMDC-124372	-7.0490155	TCMDC-138214	-6.828125
TCMDC-136166	-7.2474971	TCMDC-124718	-7.0489101	TCMDC-125349	-6.8279324
TCMDC-134415	-7.2474294	TCMDC-133024	-7.0488172	TCMDC-124355	-6.8277459
TCMDC-134912	-7.2473564	TCMDC-132610	-7.0485277	TCMDC-142200	-6.8275585
TCMDC-135552	-7.246736	TCMDC-139674	-7.0484776	TCMDC-139046	-6.8274775
TCMDC-136008	-7.2466512	TCMDC-137541	-7.0477133	TCMDC-124730	-6.8274574
TCMDC-136904	-7.2464805	TCMDC-138394	-7.0476832	TCMDC-136271	-6.8271661
TCMDC-131266	-7.2464161	TCMDC-136033	-7.0476022	TCMDC-124961	-6.8271031
TCMDC-140749	-7.2463298	TCMDC-136767	-7.047564	TCMDC-133649	-6.8268967
TCMDC-132334	-7.2462945	TCMDC-124630	-7.0473695	TCMDC-125243	-6.8268819
TCMDC-139111	-7.2456822	TCMDC-131858	-7.0473123	TCMDC-135604	-6.8266993
TCMDC-132985	-7.2455955	TCMDC-141582	-7.0472918	TCMDC-137432	-6.8263106
TCMDC-132525	-7.2448936	TCMDC-133911	-7.0469089	TCMDC-134299	-6.8262801
TCMDC-135992	-7.2444386	TCMDC-132516	-7.0460792	TCMDC-134039	-6.8259554
TCMDC-142010	-7.2444372	TCMDC-125341	-7.0460072	TCMDC-124237	-6.8258529
TCMDC-139089	-7.2443857	TCMDC-136234	-7.0459623	TCMDC-131889	-6.8256264
TCMDC-134469	-7.2441363	TCMDC-140374	-7.0456514	TCMDC-136312	-6.8253846
TCMDC-139669	-7.2439599	TCMDC-135367	-7.0455809	TCMDC-136553	-6.8253121
TCMDC-132855	-7.243845	TCMDC-132437	-7.0454893	TCMDC-133139	-6.824903
TCMDC-136173	-7.2438116	TCMDC-140733	-7.045372	TCMDC-132664	-6.8245807
TCMDC-137555	-7.2437983	TCMDC-125722	-7.0449615	TCMDC-136597	-6.8244343
TCMDC-133166	-7.2437868	TCMDC-140331	-7.0449071	TCMDC-135000	-6.8244019
TCMDC-133036	-7.24366	TCMDC-132027	-7.0448012	TCMDC-123715	-6.8241711
TCMDC-123628	-7.243597	TCMDC-137079	-7.0447078	TCMDC-124376	-6.8235221
TCMDC-141190	-7.243504	TCMDC-133001	-7.0446572	TCMDC-133447	-6.8232942
TCMDC-136899	-7.2434702	TCMDC-134714	-7.0445647	TCMDC-140570	-6.8232436
TCMDC-132904	-7.2433772	TCMDC-132852	-7.0445471	TCMDC-135276	-6.82269
TCMDC-135395	-7.2433529	TCMDC-141761	-7.0442762	TCMDC-136932	-6.8225484
TCMDC-134913	-7.2432008	TCMDC-132689	-7.0442595	TCMDC-139083	-6.8224645
TCMDC-136621	-7.2427368	TCMDC-139404	-7.0440674	TCMDC-132547	-6.822444
TCMDC-133738	-7.2427297	TCMDC-142182	-7.043767	TCMDC-133156	-6.8212218
TCMDC-136664	-7.2426729	TCMDC-132992	-7.0437565	TCMDC-138345	-6.8207579
TCMDC-133266	-7.2425113	TCMDC-125746	-7.043385	TCMDC-132500	-6.8207417
TCMDC-134751	-7.2424736	TCMDC-137180	-7.0432096	TCMDC-138022	-6.8205066
TCMDC-138112	-7.2423387	TCMDC-125682	-7.0432029	TCMDC-133524	-6.8204803
TCMDC-125713	-7.2422447	TCMDC-132466	-7.04284	TCMDC-140410	-6.8202481

TCMDC-136131	-7.2418861	TCMDC-140827	-7.0426202	TCMDC-141771	-6.8200603
TCMDC-137830	-7.2418213	TCMDC-137182	-7.0425458	TCMDC-124140	-6.8200426
TCMDC-135692	-7.2417197	TCMDC-139212	-7.0416808	TCMDC-135281	-6.8198962
TCMDC-133154	-7.2415724	TCMDC-136042	-7.0412407	TCMDC-140679	-6.8197131
TCMDC-133065	-7.2413611	TCMDC-140931	-7.0412369	TCMDC-135436	-6.8196478
TCMDC-132394	-7.2408676	TCMDC-133896	-7.0411553	TCMDC-136226	-6.8195324
TCMDC-136840	-7.2407174	TCMDC-138329	-7.0411439	TCMDC-132829	-6.819509
TCMDC-133832	-7.2399411	TCMDC-125848	-7.040761	TCMDC-139708	-6.8195
TCMDC-134652	-7.2394061	TCMDC-141068	-7.0403328	TCMDC-137385	-6.8194137
TCMDC-125692	-7.2390652	TCMDC-138417	-7.040297	TCMDC-134069	-6.8193879
TCMDC-133537	-7.2387371	TCMDC-137212	-7.0400753	TCMDC-136513	-6.8190346
TCMDC-125105	-7.2385998	TCMDC-142257	-7.0397749	TCMDC-133550	-6.8190308
TCMDC-139642	-7.2383718	TCMDC-140141	-7.0397387	TCMDC-141297	-6.8186884
TCMDC-136428	-7.2382751	TCMDC-141107	-7.0395865	TCMDC-141322	-6.8183465
TCMDC-139767	-7.2380199	TCMDC-136757	-7.0394955	TCMDC-139437	-6.8182831
TCMDC-140707	-7.2377348	TCMDC-135443	-7.0392828	TCMDC-124879	-6.8181386
TCMDC-139892	-7.2377172	TCMDC-140365	-7.0391436	TCMDC-139964	-6.81777
TCMDC-139735	-7.2373071	TCMDC-140704	-7.039114	TCMDC-136204	-6.8174505
TCMDC-139213	-7.2369566	TCMDC-125257	-7.0390434	TCMDC-133901	-6.8172865
TCMDC-139115	-7.2367644	TCMDC-124525	-7.0388756	TCMDC-124150	-6.817173
TCMDC-131538	-7.2364497	TCMDC-139246	-7.038785	TCMDC-136976	-6.8167272
TCMDC-134163	-7.2363443	TCMDC-136385	-7.038692	TCMDC-138191	-6.8165674
TCMDC-140197	-7.2361851	TCMDC-132766	-7.0386891	TCMDC-139222	-6.81637
TCMDC-140493	-7.2360702	TCMDC-131887	-7.0383825	TCMDC-125695	-6.8163538
TCMDC-136055	-7.2359734	TCMDC-139533	-7.0379062	TCMDC-132645	-6.8163157
TCMDC-132447	-7.2352624	TCMDC-133480	-7.037641	TCMDC-140959	-6.8160353
TCMDC-135904	-7.2348099	TCMDC-139439	-7.0372672	TCMDC-133072	-6.8157916
TCMDC-140231	-7.2345281	TCMDC-141181	-7.0368886	TCMDC-131492	-6.8144054
TCMDC-125684	-7.2344146	TCMDC-139380	-7.0368686	TCMDC-140109	-6.8143473
TCMDC-133449	-7.2339468	TCMDC-136177	-7.0368609	TCMDC-132721	-6.8142982
TCMDC-125262	-7.2339244	TCMDC-133346	-7.0366583	TCMDC-125197	-6.8142543
TCMDC-140778	-7.2338996	TCMDC-123839	-7.0365624	TCMDC-139059	-6.813725
TCMDC-124678	-7.2336249	TCMDC-133210	-7.0365443	TCMDC-133831	-6.8135328
TCMDC-131424	-7.2334752	TCMDC-125770	-7.0360546	TCMDC-124487	-6.812377
TCMDC-136239	-7.2331619	TCMDC-138384	-7.0352874	TCMDC-137484	-6.8122811
TCMDC-123615	-7.2325816	TCMDC-136045	-7.0352864	TCMDC-136038	-6.8117132
TCMDC-134569	-7.2322812	TCMDC-139718	-7.0350642	TCMDC-131655	-6.8115354
TCMDC-131979	-7.2320471	TCMDC-138338	-7.0345101	TCMDC-139499	-6.8111262
TCMDC-125296	-7.2318001	TCMDC-138298	-7.0342965	TCMDC-141594	-6.8107519
TCMDC-138659	-7.2317452	TCMDC-134348	-7.0335517	TCMDC-132711	-6.8105006
TCMDC-124707	-7.2314577	TCMDC-123545	-7.0335069	TCMDC-125189	-6.8103509
TCMDC-132790	-7.2314372	TCMDC-138122	-7.0334945	TCMDC-125329	-6.8103447
TCMDC-134975	-7.2314329	TCMDC-132840	-7.0328526	TCMDC-133825	-6.8100867
TCMDC-140790	-7.2312455	TCMDC-137751	-7.0325465	TCMDC-133683	-6.8100772

TCMDC-139697	-7.2311969	TCMDC-125674	-7.0319905	TCMDC-125575	-6.8099174
TCMDC-140101	-7.2302022	TCMDC-134107	-7.0319586	TCMDC-133804	-6.8098187
TCMDC-141541	-7.2299023	TCMDC-125828	-7.0318065	TCMDC-141530	-6.8096933
TCMDC-125451	-7.2298112	TCMDC-140431	-7.0317292	TCMDC-133862	-6.8095088
TCMDC-140146	-7.2296515	TCMDC-125443	-7.0313835	TCMDC-132814	-6.8094959
TCMDC-134389	-7.2295842	TCMDC-136330	-7.0309315	TCMDC-131917	-6.8091173
TCMDC-132460	-7.2294188	TCMDC-140195	-7.030334	TCMDC-134347	-6.8083057
TCMDC-134431	-7.2291064	TCMDC-138938	-7.0292115	TCMDC-141782	-6.8080659
TCMDC-125046	-7.2289586	TCMDC-132925	-7.0292096	TCMDC-141914	-6.8077393
TCMDC-134383	-7.2286458	TCMDC-123540	-7.0290713	TCMDC-138348	-6.8076773
TCMDC-134253	-7.2282472	TCMDC-139916	-7.028583	TCMDC-140513	-6.8075643
TCMDC-139323	-7.2280493	TCMDC-132926	-7.0285678	TCMDC-138831	-6.8072166
TCMDC-140735	-7.2279568	TCMDC-136138	-7.0284152	TCMDC-124574	-6.8064365
TCMDC-133188	-7.2278323	TCMDC-142279	-7.0282879	TCMDC-123625	-6.8063226
TCMDC-124807	-7.227716	TCMDC-139383	-7.0282397	TCMDC-125161	-6.8062329
TCMDC-140119	-7.227386	TCMDC-138588	-7.0281911	TCMDC-123818	-6.8059883
TCMDC-136617	-7.2272024	TCMDC-137085	-7.0281835	TCMDC-124870	-6.8057323
TCMDC-124221	-7.2270317	TCMDC-133890	-7.027535	TCMDC-139126	-6.8056993
TCMDC-125449	-7.2268281	TCMDC-141069	-7.0272927	TCMDC-140713	-6.8050098
TCMDC-124416	-7.2267556	TCMDC-135215	-7.0269737	TCMDC-124332	-6.8042192
TCMDC-125431	-7.2266459	TCMDC-133096	-7.0268974	TCMDC-138389	-6.8040442
TCMDC-141878	-7.2265897	TCMDC-139443	-7.026547	TCMDC-125744	-6.8036189
TCMDC-136083	-7.2262053	TCMDC-138709	-7.0264254	TCMDC-124892	-6.8035941
TCMDC-135473	-7.226089	TCMDC-139673	-7.0260515	TCMDC-141483	-6.8034434
TCMDC-133753	-7.225718	TCMDC-132828	-7.0255351	TCMDC-137188	-6.8031034
TCMDC-132616	-7.2256823	TCMDC-135441	-7.0254645	TCMDC-131524	-6.8029218
TCMDC-131988	-7.2256651	TCMDC-125805	-7.0254254	TCMDC-136372	-6.8026056
TCMDC-139496	-7.2256007	TCMDC-139221	-7.0251002	TCMDC-125129	-6.8023653
TCMDC-137908	-7.2251797	TCMDC-139198	-7.0249887	TCMDC-133905	-6.801753
TCMDC-138263	-7.2251353	TCMDC-136072	-7.024931	TCMDC-132457	-6.8013563
TCMDC-123804	-7.2249312	TCMDC-133030	-7.024878	TCMDC-124622	-6.8012218
TCMDC-133596	-7.2248273	TCMDC-124086	-7.0248756	TCMDC-140220	-6.8011227
TCMDC-137515	-7.2248268	TCMDC-139677	-7.0246644	TCMDC-134271	-6.8005271
TCMDC-136023	-7.2246013	TCMDC-125440	-7.0245814	TCMDC-133230	-6.8005009
TCMDC-133767	-7.2240505	TCMDC-124748	-7.0242944	TCMDC-124509	-6.800458
TCMDC-133199	-7.2232337	TCMDC-135321	-7.0242472	TCMDC-133422	-6.8004527
TCMDC-134178	-7.2230163	TCMDC-141364	-7.0239921	TCMDC-140459	-6.8002396
TCMDC-134397	-7.2229786	TCMDC-124538	-7.0238352	TCMDC-133713	-6.8002009
TCMDC-133590	-7.2227907	TCMDC-138835	-7.0229826	TCMDC-135695	-6.800137
TCMDC-136958	-7.2227044	TCMDC-125172	-7.0229006	TCMDC-136361	-6.8001142
TCMDC-132360	-7.2226038	TCMDC-141356	-7.0228162	TCMDC-134319	-6.7998457
TCMDC-132581	-7.222548	TCMDC-132806	-7.0227356	TCMDC-140684	-6.7994394
TCMDC-141441	-7.2224712	TCMDC-136172	-7.0225573	TCMDC-133756	-6.7994366
TCMDC-134388	-7.2223859	TCMDC-134121	-7.0221171	TCMDC-132227	-6.7994313

TCMDC-136235	-7.2222738	TCMDC-138484	-7.0220737	TCMDC-141271	-6.7993746
TCMDC-124473	-7.222178	TCMDC-132042	-7.0220065	TCMDC-123599	-6.7992282
TCMDC-123712	-7.2219892	TCMDC-139556	-7.0218496	TCMDC-136749	-6.7985458
TCMDC-134398	-7.2217083	TCMDC-139893	-7.0217924	TCMDC-133583	-6.7984862
TCMDC-140325	-7.2216835	TCMDC-133697	-7.0208969	TCMDC-137209	-6.7979484
TCMDC-140537	-7.2215257	TCMDC-124209	-7.0206804	TCMDC-142329	-6.7978044
TCMDC-133877	-7.2210512	TCMDC-138916	-7.0206761	TCMDC-124965	-6.7976656
TCMDC-124967	-7.2210293	TCMDC-125745	-7.0204177	TCMDC-123552	-6.7975354
TCMDC-139342	-7.220757	TCMDC-136929	-7.0201654	TCMDC-136046	-6.7974882
TCMDC-132818	-7.2206182	TCMDC-140083	-7.0200872	TCMDC-124068	-6.7974038
TCMDC-132702	-7.2204585	TCMDC-139275	-7.0198779	TCMDC-136751	-6.797267
TCMDC-134855	-7.2203941	TCMDC-131972	-7.0197353	TCMDC-139931	-6.7970147
TCMDC-136996	-7.2200994	TCMDC-124048	-7.0196209	TCMDC-136873	-6.7969747
TCMDC-133173	-7.2200894	TCMDC-137232	-7.0193868	TCMDC-141103	-6.7968168
TCMDC-123734	-7.2197161	TCMDC-134224	-7.0192962	TCMDC-136035	-6.7961664
TCMDC-132468	-7.219676	TCMDC-125425	-7.0192609	TCMDC-138699	-6.7954559
TCMDC-124629	-7.2196097	TCMDC-135320	-7.0191617	TCMDC-138568	-6.7953353
TCMDC-140784	-7.2193809	TCMDC-133670	-7.0190315	TCMDC-139359	-6.7953186
TCMDC-132579	-7.2191982	TCMDC-132481	-7.0187521	TCMDC-134322	-6.7952914
TCMDC-135332	-7.2187338	TCMDC-134853	-7.0187068	TCMDC-124985	-6.7952337
TCMDC-133974	-7.2185946	TCMDC-138137	-7.0186949	TCMDC-123655	-6.7951727
TCMDC-135664	-7.218441	TCMDC-137109	-7.0185966	TCMDC-123900	-6.7951064
TCMDC-141946	-7.2178316	TCMDC-125202	-7.0184331	TCMDC-139760	-6.7949467
TCMDC-133249	-7.2174368	TCMDC-133754	-7.0184278	TCMDC-140433	-6.7944617
TCMDC-132875	-7.2172589	TCMDC-138279	-7.0179019	TCMDC-138434	-6.7943497
TCMDC-132573	-7.2168388	TCMDC-132245	-7.0178285	TCMDC-125014	-6.7943206
TCMDC-124935	-7.2168369	TCMDC-141910	-7.0168681	TCMDC-123630	-6.7942839
TCMDC-141227	-7.2166228	TCMDC-133640	-7.0167298	TCMDC-133000	-6.7942448
TCMDC-134206	-7.2166047	TCMDC-139406	-7.0167255	TCMDC-133994	-6.7941051
TCMDC-133037	-7.2163887	TCMDC-123541	-7.0167112	TCMDC-141005	-6.7937512
TCMDC-140971	-7.216311	TCMDC-138126	-7.016675	TCMDC-139056	-6.7936168
TCMDC-137631	-7.2162523	TCMDC-123917	-7.0166116	TCMDC-133830	-6.7934389
TCMDC-141528	-7.2158375	TCMDC-132862	-7.0162759	TCMDC-140413	-6.793355
TCMDC-125434	-7.2157583	TCMDC-132333	-7.0162592	TCMDC-133715	-6.7927504
TCMDC-132421	-7.2156472	TCMDC-138446	-7.0161033	TCMDC-140562	-6.7920198
TCMDC-137201	-9.7981062	TCMDC-140021	-8.035924	TCMDC-141545	-7.6761408
TCMDC-138644	-9.7082491	TCMDC-138221	-8.0358639	TCMDC-141072	-7.6760526
TCMDC-141516	-9.6638422	TCMDC-135107	-8.0355396	TCMDC-141199	-7.6759186
TCMDC-139411	-9.6058197	TCMDC-139817	-8.0347748	TCMDC-137778	-7.6756606
TCMDC-137241	-9.59799	TCMDC-133442	-8.0345488	TCMDC-132335	-7.6754069
TCMDC-135039	-9.5238552	TCMDC-132946	-8.0343637	TCMDC-133694	-7.6749439
TCMDC-131821	-9.5185537	TCMDC-135189	-8.0338564	TCMDC-133195	-7.6745367
TCMDC-137187	-9.5103445	TCMDC-140620	-8.033205	TCMDC-133044	-7.6744876

TCMDC-135913	-9.4539337	TCMDC-141576	-8.0321674	TCMDC-133326	-7.6744118
TCMDC-135362	-9.4145079	TCMDC-139520	-8.0314159	TCMDC-131893	-7.6741066
TCMDC-139456	-9.4038839	TCMDC-141690	-8.0307074	TCMDC-136121	-7.6740351
TCMDC-131871	-9.3596945	TCMDC-132968	-8.0304728	TCMDC-139270	-7.6736665
TCMDC-139970	-9.3475571	TCMDC-141014	-8.0301495	TCMDC-132580	-7.6735578
TCMDC-139016	-9.3385801	TCMDC-131567	-8.0299482	TCMDC-140860	-7.6731143
TCMDC-137200	-9.3342552	TCMDC-139569	-8.0298357	TCMDC-133919	-7.673069
TCMDC-139020	-9.2973871	TCMDC-141548	-8.0296621	TCMDC-135494	-7.6729083
TCMDC-140555	-9.2298012	TCMDC-134402	-8.0296364	TCMDC-134490	-7.6716967
TCMDC-137487	-9.207593	TCMDC-138487	-8.0295601	TCMDC-141886	-7.6698284
TCMDC-138883	-9.207406	TCMDC-138866	-8.0293093	TCMDC-133497	-7.669796
TCMDC-138789	-9.206315	TCMDC-125169	-8.028883	TCMDC-140209	-7.669642
TCMDC-131550	-9.2050161	TCMDC-124810	-8.0284853	TCMDC-141728	-7.6695042
TCMDC-140947	-9.2042274	TCMDC-139509	-8.0283451	TCMDC-136292	-7.668767
TCMDC-131810	-9.1895227	TCMDC-138892	-8.0281096	TCMDC-132343	-7.668725
TCMDC-131870	-9.1879435	TCMDC-132966	-8.0278502	TCMDC-140659	-7.6684761
TCMDC-140588	-9.1736269	TCMDC-139813	-8.0265894	TCMDC-133015	-7.6683192
TCMDC-134522	-9.1703568	TCMDC-136602	-8.0261087	TCMDC-135532	-7.6682091
TCMDC-139041	-9.1606226	TCMDC-132477	-8.025877	TCMDC-141047	-7.6676178
TCMDC-135319	-9.1575613	TCMDC-131815	-8.0258265	TCMDC-137075	-7.6672096
TCMDC-141524	-9.1573935	TCMDC-141609	-8.0254984	TCMDC-124874	-7.6672072
TCMDC-134525	-9.1476021	TCMDC-135060	-8.0252371	TCMDC-134756	-7.6664057
TCMDC-137288	-9.1444674	TCMDC-136052	-8.0243378	TCMDC-125800	-7.6662545
TCMDC-131571	-9.1427717	TCMDC-134938	-8.0239134	TCMDC-132052	-7.6648331
TCMDC-132059	-9.1364517	TCMDC-141892	-8.0236969	TCMDC-138491	-7.6644502
TCMDC-135999	-9.1330404	TCMDC-138369	-8.0234337	TCMDC-138062	-7.6642156
TCMDC-138564	-9.0866795	TCMDC-135238	-8.02178	TCMDC-138441	-7.6640029
TCMDC-138315	-9.070509	TCMDC-133040	-8.0217304	TCMDC-134179	-7.6639123
TCMDC-141520	-9.0686016	TCMDC-139517	-8.0213757	TCMDC-132093	-7.663579
TCMDC-139613	-9.0588808	TCMDC-135034	-8.0203724	TCMDC-141167	-7.6635523
TCMDC-138318	-9.0452156	TCMDC-137773	-8.0202932	TCMDC-140682	-7.6634841
TCMDC-141627	-9.0402164	TCMDC-135781	-8.0202389	TCMDC-132304	-7.6634426
TCMDC-135307	-9.020134	TCMDC-138256	-8.0193367	TCMDC-140475	-7.6627216
TCMDC-132020	-9.0128994	TCMDC-137618	-8.0190191	TCMDC-135542	-7.6626291
TCMDC-134674	-9.0063944	TCMDC-136370	-8.0185766	TCMDC-132267	-7.6621799
TCMDC-138085	-9.0059319	TCMDC-134761	-8.0179434	TCMDC-135875	-7.6618266
TCMDC-132584	-8.9969549	TCMDC-141756	-8.0178099	TCMDC-135806	-7.6616087
TCMDC-131565	-8.9906731	TCMDC-135051	-8.0176392	TCMDC-141384	-7.6613679
TCMDC-124174	-8.9821119	TCMDC-135313	-8.0174751	TCMDC-140968	-7.6613355
TCMDC-131564	-8.9820652	TCMDC-140852	-8.0170507	TCMDC-135888	-7.6612091
TCMDC-141496	-8.9771919	TCMDC-134888	-8.0165777	TCMDC-140909	-7.6605091
TCMDC-137827	-8.9741116	TCMDC-136018	-8.0156546	TCMDC-132817	-7.6600838
TCMDC-136028	-8.973032	TCMDC-141644	-8.0145931	TCMDC-141077	-7.6597924
TCMDC-139659	-8.9726791	TCMDC-138870	-8.0143719	TCMDC-141422	-7.659596

TCMDC-131544	-8.9705133	TCMDC-141463	-8.0129194	TCMDC-139531	-7.6595616
TCMDC-139744	-8.9701118	TCMDC-139178	-8.0128984	TCMDC-133679	-7.6595354
TCMDC-138316	-8.9686708	TCMDC-133389	-8.0123405	TCMDC-141809	-7.6590314
TCMDC-138893	-8.9680977	TCMDC-135291	-8.0120716	TCMDC-141257	-7.6586213
TCMDC-136511	-8.9627514	TCMDC-136558	-8.0111589	TCMDC-134982	-7.6585736
TCMDC-141337	-8.9540844	TCMDC-137833	-8.0107431	TCMDC-123577	-7.6584396
TCMDC-138967	-8.9512482	TCMDC-139678	-8.0097809	TCMDC-133204	-7.6582384
TCMDC-137674	-8.9510336	TCMDC-137761	-8.0088692	TCMDC-139280	-7.6577706
TCMDC-136208	-8.9460602	TCMDC-138151	-8.0084085	TCMDC-135928	-7.6576557
TCMDC-135529	-8.945714	TCMDC-139866	-8.0083847	TCMDC-132948	-7.657568
TCMDC-135361	-8.9396763	TCMDC-135507	-8.0079231	TCMDC-141138	-7.6573215
TCMDC-131817	-8.9387093	TCMDC-135288	-8.0061274	TCMDC-140970	-7.6571198
TCMDC-138760	-8.9386625	TCMDC-140346	-8.005496	TCMDC-132482	-7.656034
TCMDC-140558	-8.9375782	TCMDC-137892	-8.0054216	TCMDC-124208	-7.655931
TCMDC-131809	-8.9369049	TCMDC-141387	-8.0053339	TCMDC-135900	-7.655231
TCMDC-134991	-8.934907	TCMDC-141583	-8.0052481	TCMDC-139992	-7.6549749
TCMDC-140987	-8.9333858	TCMDC-131852	-8.0050306	TCMDC-135748	-7.6547837
TCMDC-134557	-8.9290848	TCMDC-135264	-8.0046539	TCMDC-132134	-7.654696
TCMDC-134378	-8.9261484	TCMDC-136253	-8.003315	TCMDC-139574	-7.6543446
TCMDC-131812	-8.9155445	TCMDC-133841	-8.0024061	TCMDC-138546	-7.6542912
TCMDC-137275	-8.912941	TCMDC-139392	-8.0023394	TCMDC-137999	-7.6540475
TCMDC-140554	-8.9115486	TCMDC-124808	-8.0021915	TCMDC-135563	-7.6537051
TCMDC-131906	-8.8987217	TCMDC-134696	-8.0014763	TCMDC-139077	-7.6526551
TCMDC-139636	-8.8880453	TCMDC-131850	-8.0006685	TCMDC-140278	-7.65169
TCMDC-137819	-8.888031	TCMDC-135652	-8.0002213	TCMDC-132105	-7.6511703
TCMDC-140758	-8.8865347	TCMDC-140779	-7.9997473	TCMDC-139819	-7.6505375
TCMDC-141513	-8.8846684	TCMDC-135866	-7.9990802	TCMDC-140530	-7.6502895
TCMDC-141053	-8.8810987	TCMDC-141794	-7.9984827	TCMDC-141388	-7.6502066
TCMDC-135311	-8.8799086	TCMDC-135533	-7.9984641	TCMDC-132218	-7.6501179
TCMDC-131818	-8.8764095	TCMDC-140560	-7.9982581	TCMDC-132028	-7.6495605
TCMDC-136227	-8.8756113	TCMDC-140047	-7.997983	TCMDC-138099	-7.6492205
TCMDC-141292	-8.8718357	TCMDC-134563	-7.9978786	TCMDC-141949	-7.6491446
TCMDC-136154	-8.8669806	TCMDC-140361	-7.9978499	TCMDC-140934	-7.6489348
TCMDC-131873	-8.8663311	TCMDC-125442	-7.997499	TCMDC-125277	-7.64889
TCMDC-136564	-8.8606892	TCMDC-139306	-7.9970675	TCMDC-140792	-7.6487546
TCMDC-139835	-8.8604183	TCMDC-135032	-7.9968853	TCMDC-140752	-7.6483989
TCMDC-138260	-8.8602209	TCMDC-136192	-7.9967232	TCMDC-133888	-7.648263
TCMDC-136198	-8.8600845	TCMDC-138753	-7.9966655	TCMDC-137132	-7.6469989
TCMDC-134675	-8.8586569	TCMDC-135422	-7.9963908	TCMDC-138735	-7.6468406
TCMDC-141593	-8.8542194	TCMDC-138188	-7.996316	TCMDC-135811	-7.6467776
TCMDC-138579	-8.8538456	TCMDC-140025	-7.9962702	TCMDC-138506	-7.6466246
TCMDC-140595	-8.8505659	TCMDC-140952	-7.996007	TCMDC-141035	-7.6464653
TCMDC-138086	-8.8496618	TCMDC-133010	-7.9957576	TCMDC-135896	-7.6462603
TCMDC-136502	-8.8483	TCMDC-135755	-7.9956245	TCMDC-141856	-7.646245

TCMDC-138357	-8.8445778	TCMDC-133622	-7.9953737	TCMDC-133935	-7.6461673
TCMDC-134279	-8.8383369	TCMDC-132207	-7.9951606	TCMDC-139911	-7.6457195
TCMDC-140617	-8.8359079	TCMDC-141013	-7.9949846	TCMDC-137738	-7.6456475
TCMDC-134559	-8.835885	TCMDC-141250	-7.9947829	TCMDC-135974	-7.6454978
TCMDC-140591	-8.8343153	TCMDC-136258	-7.9947271	TCMDC-139988	-7.6454468
TCMDC-141687	-8.8310175	TCMDC-134116	-7.9939065	TCMDC-140711	-7.6451192
TCMDC-134684	-8.8274775	TCMDC-132791	-7.9923568	TCMDC-135824	-7.6445951
TCMDC-135360	-8.827301	TCMDC-140546	-7.9918818	TCMDC-123849	-7.6444187
TCMDC-139476	-8.8230171	TCMDC-140505	-7.991642	TCMDC-141922	-7.6440916
TCMDC-139334	-8.8223524	TCMDC-141305	-7.9911895	TCMDC-132047	-7.6440735
TCMDC-137792	-8.819087	TCMDC-137236	-7.9909468	TCMDC-140854	-7.64396
TCMDC-134371	-8.8066988	TCMDC-136152	-7.9906459	TCMDC-135401	-7.6439338
TCMDC-141795	-8.8035345	TCMDC-135482	-7.990622	TCMDC-140814	-7.6437759
TCMDC-141567	-8.8011189	TCMDC-134687	-7.9904923	TCMDC-137024	-7.6434836
TCMDC-134558	-8.7965603	TCMDC-131854	-7.9889517	TCMDC-140136	-7.6433167
TCMDC-139822	-8.7952166	TCMDC-133059	-7.9888635	TCMDC-135984	-7.6429291
TCMDC-139653	-8.7949667	TCMDC-138694	-7.988831	TCMDC-135703	-7.6418853
TCMDC-135392	-8.7893591	TCMDC-141088	-7.9886899	TCMDC-141499	-7.6413159
TCMDC-138306	-8.7883492	TCMDC-141098	-7.9885693	TCMDC-140946	-7.6412363
TCMDC-141156	-8.7793531	TCMDC-124021	-7.9884896	TCMDC-139481	-7.6412287
TCMDC-131814	-8.7782078	TCMDC-140869	-7.9879255	TCMDC-132225	-7.640718
TCMDC-131806	-8.7755919	TCMDC-132963	-7.9879208	TCMDC-132896	-7.6404681
TCMDC-132117	-8.7752132	TCMDC-139511	-7.9878211	TCMDC-133098	-7.6401901
TCMDC-141726	-8.7745762	TCMDC-138596	-7.9876833	TCMDC-136097	-7.6398845
TCMDC-138720	-8.770689	TCMDC-135797	-7.9874163	TCMDC-141879	-7.6398673
TCMDC-131563	-8.7663889	TCMDC-132102	-7.9870782	TCMDC-133165	-7.6397791
TCMDC-141083	-8.764123	TCMDC-135892	-7.9863825	TCMDC-137196	-7.6396399
TCMDC-138868	-8.7602339	TCMDC-140922	-7.9862685	TCMDC-141700	-7.6394634
TCMDC-135406	-8.7598934	TCMDC-139770	-7.9860907	TCMDC-135479	-7.6389933
TCMDC-139774	-8.759223	TCMDC-141778	-7.9859796	TCMDC-141117	-7.638587
TCMDC-136170	-8.7571068	TCMDC-136508	-7.9850779	TCMDC-138184	-7.6382842
TCMDC-139413	-8.7520008	TCMDC-132282	-7.9829726	TCMDC-136465	-7.6381283
TCMDC-134372	-8.7486992	TCMDC-138088	-7.9825583	TCMDC-138431	-7.637929
TCMDC-135510	-8.7480602	TCMDC-136458	-7.9825315	TCMDC-134849	-7.6378641
TCMDC-135817	-8.7473602	TCMDC-134796	-7.9824977	TCMDC-139987	-7.6373439
TCMDC-131905	-8.7459068	TCMDC-133005	-7.9816012	TCMDC-132320	-7.636518
TCMDC-132001	-8.7454815	TCMDC-140543	-7.9813328	TCMDC-139502	-7.636467
TCMDC-134990	-8.7450275	TCMDC-125665	-7.9807854	TCMDC-140340	-7.6364527
TCMDC-138541	-8.7398357	TCMDC-139900	-7.9805984	TCMDC-124861	-7.6363935
TCMDC-135196	-8.7363005	TCMDC-134574	-7.9803843	TCMDC-140032	-7.6363921
TCMDC-131847	-8.7318535	TCMDC-139514	-7.9793167	TCMDC-133538	-7.6356549
TCMDC-138005	-8.730505	TCMDC-135277	-7.9792171	TCMDC-138114	-7.6354594
TCMDC-135920	-8.7303095	TCMDC-138242	-7.9791651	TCMDC-138958	-7.635406
TCMDC-136026	-8.7232428	TCMDC-140949	-7.9783835	TCMDC-123589	-7.6354032

TCMDC-140529	-8.7223797	TCMDC-141100	-7.9777942	TCMDC-135865	-7.6344795
TCMDC-141515	-8.7222986	TCMDC-139834	-7.9774718	TCMDC-140836	-7.6344032
TCMDC-136007	-8.7221889	TCMDC-132807	-7.975399	TCMDC-136074	-7.6343226
TCMDC-135225	-8.7218571	TCMDC-141392	-7.9751229	TCMDC-135804	-7.6341944
TCMDC-137832	-8.7217131	TCMDC-135940	-7.9744291	TCMDC-138339	-7.6341295
TCMDC-138258	-8.7190552	TCMDC-138499	-7.9743371	TCMDC-132050	-7.6336365
TCMDC-135204	-8.7138767	TCMDC-135194	-7.9736304	TCMDC-136986	-7.6334553
TCMDC-141966	-8.7134552	TCMDC-134688	-7.9735436	TCMDC-133609	-7.6333127
TCMDC-137777	-8.7128315	TCMDC-135728	-7.9730248	TCMDC-135177	-7.6330795
TCMDC-138849	-8.7116671	TCMDC-133315	-7.9724503	TCMDC-139548	-7.6320438
TCMDC-141377	-8.7115107	TCMDC-141682	-7.9719143	TCMDC-141772	-7.6318903
TCMDC-136163	-8.7103319	TCMDC-124441	-7.9717908	TCMDC-138250	-7.6309953
TCMDC-140925	-8.6995754	TCMDC-138347	-7.97158	TCMDC-135959	-7.630271
TCMDC-135421	-8.6970024	TCMDC-140228	-7.9711256	TCMDC-141560	-7.6301031
TCMDC-135380	-8.6908627	TCMDC-137316	-7.9688196	TCMDC-141796	-7.629869
TCMDC-135506	-8.6900673	TCMDC-134656	-7.9678459	TCMDC-132422	-7.6298571
TCMDC-140753	-8.6875648	TCMDC-136464	-7.9664707	TCMDC-135721	-7.6294155
TCMDC-140929	-8.6875458	TCMDC-141924	-7.9649472	TCMDC-134992	-7.62887
TCMDC-140601	-8.68573	TCMDC-140079	-7.9648829	TCMDC-136743	-7.6288166
TCMDC-138267	-8.681386	TCMDC-138535	-7.9645696	TCMDC-135221	-7.6286731
TCMDC-137355	-8.6801147	TCMDC-135650	-7.964355	TCMDC-133357	-7.628355
TCMDC-137529	-8.6795464	TCMDC-141102	-7.9641948	TCMDC-136974	-7.6278963
TCMDC-140646	-8.6789045	TCMDC-135672	-7.9640427	TCMDC-141478	-7.6277242
TCMDC-135538	-8.6783257	TCMDC-135782	-7.9635463	TCMDC-135932	-7.6272807
TCMDC-131816	-8.6767502	TCMDC-135670	-7.9634337	TCMDC-137071	-7.6270633
TCMDC-132003	-8.6752014	TCMDC-141727	-7.9633298	TCMDC-132696	-7.6268702
TCMDC-131807	-8.6686773	TCMDC-135171	-7.962429	TCMDC-141389	-7.6267848
TCMDC-141605	-8.664258	TCMDC-133393	-7.96211	TCMDC-134117	-7.6265941
TCMDC-139972	-8.6623564	TCMDC-139670	-7.9620667	TCMDC-138168	-7.6265588
TCMDC-140008	-8.6619968	TCMDC-138419	-7.9620266	TCMDC-141410	-7.6263566
TCMDC-140282	-8.6556883	TCMDC-140818	-7.9619184	TCMDC-135800	-7.6261101
TCMDC-131960	-8.6545296	TCMDC-124223	-7.9610038	TCMDC-135898	-7.626092
TCMDC-139637	-8.6521635	TCMDC-139562	-7.9609494	TCMDC-136118	-7.6260371
TCMDC-140690	-8.6517353	TCMDC-133330	-7.9608006	TCMDC-133060	-7.6257524
TCMDC-137844	-8.6513252	TCMDC-140000	-7.9604735	TCMDC-133041	-7.625309
TCMDC-141598	-8.6499338	TCMDC-139369	-7.9601631	TCMDC-141866	-7.6242476
TCMDC-134276	-8.6493387	TCMDC-133909	-7.959651	TCMDC-140341	-7.6242423
TCMDC-136559	-8.6479959	TCMDC-140875	-7.9596272	TCMDC-135049	-7.6242228
TCMDC-134573	-8.6473703	TCMDC-135412	-7.9592748	TCMDC-138089	-7.6239214
TCMDC-131452	-8.6471891	TCMDC-141054	-7.9590969	TCMDC-135837	-7.6238747
TCMDC-138606	-8.6458302	TCMDC-136262	-7.9588223	TCMDC-137956	-7.6238008
TCMDC-140736	-8.6458206	TCMDC-138143	-7.9584503	TCMDC-140523	-7.6235595
TCMDC-135447	-8.6354942	TCMDC-140060	-7.9584446	TCMDC-133564	-7.6232204
TCMDC-131808	-8.6354532	TCMDC-136270	-7.9584193	TCMDC-133225	-7.6229849

TCMDC-140612	-8.6353483	TCMDC-133048	-7.9584112	TCMDC-135794	-7.6228218
TCMDC-136645	-8.6304817	TCMDC-134893	-7.9582253	TCMDC-140896	-7.6226034
TCMDC-135955	-8.6301661	TCMDC-134801	-7.9577951	TCMDC-135765	-7.6218362
TCMDC-141253	-8.6282501	TCMDC-135024	-7.9575191	TCMDC-133058	-7.6214991
TCMDC-132297	-8.6256685	TCMDC-139991	-7.9572611	TCMDC-124207	-7.6208997
TCMDC-140616	-8.6255465	TCMDC-124664	-7.9566135	TCMDC-125351	-7.6200094
TCMDC-138532	-8.6253872	TCMDC-135216	-7.9563866	TCMDC-141774	-7.6196246
TCMDC-135921	-8.6221781	TCMDC-134567	-7.9563532	TCMDC-136615	-7.6193886
TCMDC-140604	-8.6218729	TCMDC-141649	-7.9562163	TCMDC-132708	-7.6193333
TCMDC-139927	-8.618845	TCMDC-138620	-7.9561729	TCMDC-140721	-7.6190362
TCMDC-134523	-8.6186333	TCMDC-139798	-7.9550667	TCMDC-135090	-7.6189437
TCMDC-138869	-8.6161661	TCMDC-133054	-7.9547334	TCMDC-135667	-7.6189041
TCMDC-124284	-8.6161337	TCMDC-131822	-7.9546738	TCMDC-140813	-7.6188812
TCMDC-141466	-8.61549	TCMDC-140082	-7.9545383	TCMDC-137057	-7.6185164
TCMDC-138744	-8.614912	TCMDC-135561	-7.9542913	TCMDC-132955	-7.6183701
TCMDC-138850	-8.6142578	TCMDC-132911	-7.9540462	TCMDC-135149	-7.6176095
TCMDC-138004	-8.6129885	TCMDC-135742	-7.9532237	TCMDC-138864	-7.6174064
TCMDC-135357	-8.6102047	TCMDC-140125	-7.9529853	TCMDC-140344	-7.6173368
TCMDC-135425	-8.608387	TCMDC-139743	-7.9524302	TCMDC-141584	-7.6169662
TCMDC-141812	-8.6070528	TCMDC-141575	-7.9524083	TCMDC-135431	-7.6168709
TCMDC-139475	-8.606802	TCMDC-138626	-7.9519544	TCMDC-124206	-7.6168242
TCMDC-139273	-8.6052303	TCMDC-138330	-7.9509926	TCMDC-132931	-7.6163855
TCMDC-140584	-8.6046991	TCMDC-135771	-7.950942	TCMDC-140862	-7.6158004
TCMDC-140600	-8.6041756	TCMDC-140367	-7.9499884	TCMDC-135707	-7.6157017
TCMDC-141608	-8.6003466	TCMDC-139258	-7.9498544	TCMDC-132735	-7.6155853
TCMDC-141552	-8.5985317	TCMDC-137150	-7.9490261	TCMDC-134500	-7.6155152
TCMDC-135408	-8.596447	TCMDC-125616	-7.9482832	TCMDC-134681	-7.6149321
TCMDC-141519	-8.5944967	TCMDC-140115	-7.9480166	TCMDC-125408	-7.6148314
TCMDC-138865	-8.593545	TCMDC-140359	-7.947679	TCMDC-135730	-7.6144605
TCMDC-136011	-8.5926762	TCMDC-139557	-7.9476762	TCMDC-135147	-7.6142693
TCMDC-138610	-8.5868549	TCMDC-138824	-7.9472957	TCMDC-132100	-7.614007
TCMDC-138467	-8.5867701	TCMDC-137982	-7.9468851	TCMDC-139887	-7.6137328
TCMDC-131907	-8.5849123	TCMDC-141704	-7.9466901	TCMDC-136951	-7.6135526
TCMDC-135451	-8.5816965	TCMDC-138160	-7.9461303	TCMDC-137516	-7.6134887
TCMDC-135854	-8.5797396	TCMDC-141139	-7.9450607	TCMDC-141468	-7.6133237
TCMDC-140999	-8.5794487	TCMDC-132350	-7.944315	TCMDC-137377	-7.6133156
TCMDC-131959	-8.5786228	TCMDC-135417	-7.9432793	TCMDC-132429	-7.6131053
TCMDC-137248	-8.5779734	TCMDC-137654	-7.9430537	TCMDC-134212	-7.613101
TCMDC-138770	-8.5709553	TCMDC-140007	-7.9425144	TCMDC-132161	-7.6124444
TCMDC-124809	-8.5690136	TCMDC-132144	-7.9413271	TCMDC-140945	-7.6124439
TCMDC-142256	-8.568737	TCMDC-139281	-7.9411569	TCMDC-131340	-7.6124239
TCMDC-141603	-8.5668964	TCMDC-135702	-7.9410901	TCMDC-132685	-7.6121216
TCMDC-141453	-8.5653582	TCMDC-138827	-7.9406786	TCMDC-136063	-7.6118808
TCMDC-137550	-8.5650616	TCMDC-138733	-7.9404001	TCMDC-133277	-7.6118059

TCMDC-131677	-8.5622511	TCMDC-136000	-7.9391146	TCMDC-137885	-7.6117654
TCMDC-136049	-8.5590582	TCMDC-141702	-7.9390712	TCMDC-141835	-7.611721
TCMDC-138664	-8.558713	TCMDC-135915	-7.9390283	TCMDC-132175	-7.6112432
TCMDC-141945	-8.5577898	TCMDC-132975	-7.938271	TCMDC-131922	-7.6103783
TCMDC-131819	-8.5568743	TCMDC-133311	-7.9380999	TCMDC-141758	-7.6103387
TCMDC-134098	-8.5549154	TCMDC-135856	-7.9380999	TCMDC-131561	-7.6099472
TCMDC-139638	-8.5539036	TCMDC-141592	-7.937181	TCMDC-139492	-7.6099215
TCMDC-135398	-8.5535126	TCMDC-140267	-7.9364543	TCMDC-135553	-7.6094513
TCMDC-138084	-8.5527678	TCMDC-134806	-7.9362173	TCMDC-137183	-7.609448
TCMDC-138607	-8.5525331	TCMDC-138889	-7.9358163	TCMDC-139391	-7.6092782
TCMDC-135397	-8.552165	TCMDC-135698	-7.9354162	TCMDC-141791	-7.6091204
TCMDC-135404	-8.5500374	TCMDC-132770	-7.9348803	TCMDC-138458	-7.6088376
TCMDC-137305	-8.5487003	TCMDC-138282	-7.9346628	TCMDC-132752	-7.6087632
TCMDC-138662	-8.5486031	TCMDC-137162	-7.9346576	TCMDC-138186	-7.6073594
TCMDC-135205	-8.5425444	TCMDC-132812	-7.9342432	TCMDC-124249	-7.6072755
TCMDC-135405	-8.5369959	TCMDC-135508	-7.9338646	TCMDC-134916	-7.6071978
TCMDC-139581	-8.5357847	TCMDC-138690	-7.9337201	TCMDC-131575	-7.6071334
TCMDC-135455	-8.5352573	TCMDC-131904	-7.9331441	TCMDC-132465	-7.6066089
TCMDC-131569	-8.5328894	TCMDC-140474	-7.9323735	TCMDC-124460	-7.6065784
TCMDC-134127	-8.5327206	TCMDC-141124	-7.9319687	TCMDC-141788	-7.6062946
TCMDC-141506	-8.53265	TCMDC-135198	-7.9319386	TCMDC-138779	-7.6059599
TCMDC-141022	-8.531908	TCMDC-136105	-7.9318089	TCMDC-140848	-7.6057777
TCMDC-137455	-8.5313101	TCMDC-140390	-7.9316487	TCMDC-140939	-7.6056433
TCMDC-141101	-8.5304375	TCMDC-135945	-7.931644	TCMDC-140982	-7.6056318
TCMDC-136092	-8.5288496	TCMDC-135346	-7.930191	TCMDC-140026	-7.6046572
TCMDC-140596	-8.5287704	TCMDC-135876	-7.9300771	TCMDC-140206	-7.6043944
TCMDC-140799	-8.5246325	TCMDC-135567	-7.9296255	TCMDC-132252	-7.604353
TCMDC-136155	-8.5211897	TCMDC-134907	-7.9290977	TCMDC-135882	-7.603961
TCMDC-140288	-8.5194931	TCMDC-139530	-7.9285326	TCMDC-124152	-7.6039047
TCMDC-133388	-8.519228	TCMDC-137039	-7.9283485	TCMDC-138663	-7.6037245
TCMDC-135464	-8.517828	TCMDC-138798	-7.9276719	TCMDC-136110	-7.6035872
TCMDC-140611	-8.5165396	TCMDC-139284	-7.9276152	TCMDC-132226	-7.6030526
TCMDC-136205	-8.516448	TCMDC-138740	-7.9275746	TCMDC-141868	-7.6028457
TCMDC-135381	-8.5152645	TCMDC-134521	-7.9274778	TCMDC-139940	-7.6025763
TCMDC-135910	-8.5141182	TCMDC-140962	-7.9273176	TCMDC-124860	-7.6024804
TCMDC-141707	-8.5133858	TCMDC-141938	-7.9261699	TCMDC-139155	-7.6012807
TCMDC-138324	-8.5129414	TCMDC-135720	-7.9260068	TCMDC-133616	-7.6009927
TCMDC-140565	-8.5123005	TCMDC-137137	-7.9258819	TCMDC-132934	-7.6005397
TCMDC-131813	-8.5109797	TCMDC-140167	-7.9256716	TCMDC-124871	-7.6004539
TCMDC-140609	-8.5087414	TCMDC-135535	-7.9251504	TCMDC-140372	-7.5998988
TCMDC-135669	-8.5054197	TCMDC-140511	-7.9250669	TCMDC-134746	-7.5998812
TCMDC-135403	-8.5050526	TCMDC-140950	-7.9245224	TCMDC-124294	-7.599534
TCMDC-135886	-8.5019102	TCMDC-137616	-7.92449	TCMDC-141934	-7.5992413
TCMDC-135778	-8.5018768	TCMDC-138402	-7.9222426	TCMDC-136796	-7.5991354

TCMDC-139607	-8.501771	TCMDC-133008	-7.9220853	TCMDC-133881	-7.599061
TCMDC-141510	-8.5013609	TCMDC-135671	-7.9212766	TCMDC-140040	-7.5987926
TCMDC-141581	-8.5005808	TCMDC-140821	-7.9212761	TCMDC-136919	-7.5985956
TCMDC-140590	-8.5001984	TCMDC-141937	-7.9210443	TCMDC-132726	-7.5982804
TCMDC-134678	-8.4980154	TCMDC-140930	-7.920609	TCMDC-132307	-7.5981531
TCMDC-135668	-8.4976587	TCMDC-135649	-7.9198875	TCMDC-138817	-7.5979924
TCMDC-140420	-8.4974651	TCMDC-135528	-7.9197955	TCMDC-134149	-7.5978279
TCMDC-140292	-8.4945993	TCMDC-134282	-7.9193869	TCMDC-135165	-7.5978122
TCMDC-138851	-8.4945059	TCMDC-135539	-7.9193444	TCMDC-137452	-7.597085
TCMDC-139588	-8.4934196	TCMDC-124592	-7.9189329	TCMDC-141147	-7.5966282
TCMDC-140561	-8.49335	TCMDC-131897	-7.9188437	TCMDC-139110	-7.5962758
TCMDC-138132	-8.4908209	TCMDC-132395	-7.9187098	TCMDC-133793	-7.5962601
TCMDC-138645	-8.4902115	TCMDC-136053	-7.91856	TCMDC-136835	-7.5959568
TCMDC-138852	-8.4899454	TCMDC-138229	-7.9183316	TCMDC-140186	-7.595572
TCMDC-138755	-8.4891338	TCMDC-131523	-7.9182978	TCMDC-139832	-7.5954576
TCMDC-141889	-8.4875898	TCMDC-139523	-7.9181142	TCMDC-132387	-7.5952682
TCMDC-138935	-8.48701	TCMDC-138726	-7.9180384	TCMDC-141784	-7.5946226
TCMDC-138227	-8.486412	TCMDC-136256	-7.9176741	TCMDC-141544	-7.5944376
TCMDC-139573	-8.4826937	TCMDC-125669	-7.9175982	TCMDC-141034	-7.5944276
TCMDC-140630	-8.4821701	TCMDC-140817	-7.9172444	TCMDC-133018	-7.5940681
TCMDC-138882	-8.4798946	TCMDC-141607	-7.9172392	TCMDC-135767	-7.5938487
TCMDC-138625	-8.4789848	TCMDC-134986	-7.9168777	TCMDC-131534	-7.593657
TCMDC-140667	-8.4782267	TCMDC-139998	-7.9168315	TCMDC-141549	-7.5934467
TCMDC-138714	-8.4770002	TCMDC-132033	-7.9166765	TCMDC-141842	-7.5933957
TCMDC-135821	-8.4762373	TCMDC-136638	-7.9165821	TCMDC-135931	-7.5930781
TCMDC-135195	-8.4759836	TCMDC-138561	-7.9164801	TCMDC-139271	-7.5930448
TCMDC-135684	-8.473834	TCMDC-141302	-7.9164701	TCMDC-125557	-7.5930357
TCMDC-140989	-8.4735518	TCMDC-140044	-7.9152689	TCMDC-132922	-7.5929332
TCMDC-138605	-8.4733601	TCMDC-135427	-7.9149685	TCMDC-136695	-7.5921931
TCMDC-140980	-8.4727631	TCMDC-132171	-7.914865	TCMDC-135986	-7.5921011
TCMDC-134699	-8.4722176	TCMDC-140898	-7.9143167	TCMDC-125246	-7.5920272
TCMDC-141585	-8.4691105	TCMDC-135089	-7.9137311	TCMDC-137271	-7.5912747
TCMDC-135791	-8.4671688	TCMDC-136062	-7.9133105	TCMDC-138547	-7.5912523
TCMDC-135478	-8.4667778	TCMDC-136765	-7.9129038	TCMDC-140343	-7.5911107
TCMDC-135268	-8.4665298	TCMDC-141725	-7.9126472	TCMDC-138758	-7.590486
TCMDC-139648	-8.4659195	TCMDC-133899	-7.912631	TCMDC-139507	-7.5903797
TCMDC-135199	-8.4649076	TCMDC-137036	-7.9124923	TCMDC-135828	-7.5899324
TCMDC-137189	-8.4637442	TCMDC-142269	-7.9122047	TCMDC-135493	-7.589498
TCMDC-134690	-8.4629574	TCMDC-135674	-7.9120922	TCMDC-140677	-7.5892944
TCMDC-139804	-8.4627266	TCMDC-134377	-7.9112263	TCMDC-133332	-7.5889306
TCMDC-138612	-8.4617357	TCMDC-138036	-7.9100041	TCMDC-133187	-7.588654
TCMDC-138829	-8.4614115	TCMDC-125171	-7.9099956	TCMDC-135287	-7.5885782
TCMDC-140085	-8.4600277	TCMDC-135046	-7.9099221	TCMDC-132979	-7.5879941
TCMDC-131811	-8.4598227	TCMDC-132508	-7.9094577	TCMDC-132007	-7.5871592

TCMDC-139568	-8.4594088	TCMDC-138653	-7.9091396	TCMDC-132142	-7.586163
TCMDC-141624	-8.4590464	TCMDC-136294	-7.9075055	TCMDC-139582	-7.5856452
TCMDC-137261	-8.4587097	TCMDC-137944	-7.9072471	TCMDC-135274	-7.585556
TCMDC-138311	-8.4585838	TCMDC-138825	-7.9071536	TCMDC-123918	-7.5853968
TCMDC-139232	-8.4537706	TCMDC-136140	-7.9061551	TCMDC-139641	-7.5841265
TCMDC-135229	-8.4533548	TCMDC-135745	-7.906127	TCMDC-137869	-7.5840707
TCMDC-141625	-8.4528675	TCMDC-136107	-7.9060493	TCMDC-136248	-7.5833297
TCMDC-138536	-8.4527617	TCMDC-124286	-7.9059453	TCMDC-141487	-7.5832424
TCMDC-134571	-8.4512291	TCMDC-138217	-7.905879	TCMDC-135729	-7.5829911
TCMDC-134668	-8.4509487	TCMDC-133925	-7.9058361	TCMDC-136997	-7.5828605
TCMDC-135262	-8.4507723	TCMDC-140804	-7.905303	TCMDC-125137	-7.5825253
TCMDC-132119	-8.4501743	TCMDC-139990	-7.9050522	TCMDC-140598	-7.582325
TCMDC-141629	-8.4498892	TCMDC-136375	-7.9048228	TCMDC-134765	-7.5821285
TCMDC-138572	-8.4496708	TCMDC-140250	-7.9046388	TCMDC-133003	-7.5817957
TCMDC-135681	-8.4475298	TCMDC-140502	-7.904614	TCMDC-139790	-7.58114
TCMDC-135569	-8.4457874	TCMDC-132261	-7.9044275	TCMDC-139738	-7.5808768
TCMDC-141604	-8.4455738	TCMDC-141957	-7.904326	TCMDC-136146	-7.5807161
TCMDC-140587	-8.4447765	TCMDC-138177	-7.9041777	TCMDC-125562	-7.5805202
TCMDC-136247	-8.4433002	TCMDC-141683	-7.9031491	TCMDC-141790	-7.5801768
TCMDC-125615	-8.4423771	TCMDC-139733	-7.9027958	TCMDC-132972	-7.5800524
TCMDC-131866	-8.4419203	TCMDC-124187	-7.9021096	TCMDC-140981	-7.579916
TCMDC-133546	-8.4415388	TCMDC-137047	-7.9020543	TCMDC-132858	-7.5798945
TCMDC-138308	-8.4408922	TCMDC-135393	-7.901885	TCMDC-132907	-7.5798907
TCMDC-140501	-8.440032	TCMDC-139036	-7.901691	TCMDC-135325	-7.5796595
TCMDC-137794	-8.4388933	TCMDC-135223	-7.9014039	TCMDC-141010	-7.579555
TCMDC-141089	-8.4377956	TCMDC-140984	-7.9005818	TCMDC-137136	-7.5791426
TCMDC-135317	-8.4367523	TCMDC-141775	-7.9003034	TCMDC-123803	-7.5791125
TCMDC-141512	-8.4358253	TCMDC-141765	-7.9002366	TCMDC-136867	-7.5787745
TCMDC-138237	-8.4336519	TCMDC-135511	-7.8998032	TCMDC-132345	-7.5786858
TCMDC-135818	-8.4333792	TCMDC-138225	-7.8991842	TCMDC-132393	-7.5785823
TCMDC-138264	-8.4329348	TCMDC-133043	-7.898881	TCMDC-135336	-7.5783949
TCMDC-138732	-8.4312019	TCMDC-134807	-7.8981194	TCMDC-141012	-7.5779428
TCMDC-138081	-8.4303303	TCMDC-137679	-7.8980317	TCMDC-136114	-7.577559
TCMDC-140552	-8.429925	TCMDC-138823	-7.8979259	TCMDC-132609	-7.5774188
TCMDC-139844	-8.4245863	TCMDC-139003	-7.8975511	TCMDC-135976	-7.5773625
TCMDC-137323	-8.4237871	TCMDC-125087	-7.8971658	TCMDC-136634	-7.5766544
TCMDC-135391	-8.4235315	TCMDC-134778	-7.8968153	TCMDC-139497	-7.575633
TCMDC-140406	-8.4233894	TCMDC-131964	-7.8961706	TCMDC-125266	-7.5752954
TCMDC-134561	-8.422492	TCMDC-135736	-7.8942161	TCMDC-140029	-7.5752869
TCMDC-134672	-8.4203844	TCMDC-135273	-7.8940878	TCMDC-132342	-7.5750618
TCMDC-139616	-8.4185486	TCMDC-138794	-7.8939629	TCMDC-135343	-7.575006
TCMDC-138771	-8.4173231	TCMDC-141895	-7.8938599	TCMDC-140170	-7.5747056
TCMDC-134725	-8.4172602	TCMDC-138757	-7.8938079	TCMDC-140992	-7.5743837
TCMDC-138616	-8.4171791	TCMDC-139237	-7.8937154	TCMDC-140273	-7.5741315

TCMDC-138921	-8.4171724	TCMDC-140710	-7.8935909	TCMDC-138742	-7.5740123
TCMDC-138245	-8.4147415	TCMDC-135697	-7.8924022	TCMDC-140825	-7.5738268
TCMDC-135359	-8.4133787	TCMDC-124880	-7.8922358	TCMDC-124495	-7.5734682
TCMDC-134311	-8.4122734	TCMDC-141558	-7.891892	TCMDC-136078	-7.5729375
TCMDC-141055	-8.4112616	TCMDC-132016	-7.8918858	TCMDC-132217	-7.5725012
TCMDC-138649	-8.4111414	TCMDC-134861	-7.8917475	TCMDC-138723	-7.5721464
TCMDC-138855	-8.411109	TCMDC-138460	-7.8905392	TCMDC-137158	-7.5721364
TCMDC-140636	-8.4111061	TCMDC-135477	-7.89009	TCMDC-140284	-7.5720811
TCMDC-138365	-8.4106083	TCMDC-135492	-7.8892817	TCMDC-125405	-7.5719762
TCMDC-138747	-8.4100628	TCMDC-141789	-7.8887372	TCMDC-139388	-7.5719357
TCMDC-136050	-8.4096937	TCMDC-134841	-7.888371	TCMDC-138890	-7.5713091
TCMDC-134136	-8.4090033	TCMDC-135774	-7.8876982	TCMDC-139796	-7.5711508
TCMDC-138286	-8.4082718	TCMDC-131399	-7.8875079	TCMDC-135231	-7.571126
TCMDC-138350	-8.4058437	TCMDC-135226	-7.8861971	TCMDC-136066	-7.5710564
TCMDC-140920	-8.4032545	TCMDC-139012	-7.8860707	TCMDC-135760	-7.5708785
TCMDC-135309	-8.402317	TCMDC-134128	-7.8859773	TCMDC-132426	-7.570776
TCMDC-140998	-8.4020081	TCMDC-141108	-7.8857532	TCMDC-134852	-7.5707664
TCMDC-141600	-8.4006777	TCMDC-138239	-7.8856773	TCMDC-140077	-7.5697651
TCMDC-139139	-8.3984156	TCMDC-132905	-7.8846159	TCMDC-141473	-7.5696344
TCMDC-139805	-8.3977032	TCMDC-140802	-7.8843803	TCMDC-125096	-7.5694523
TCMDC-141339	-8.3975868	TCMDC-134703	-7.8838706	TCMDC-138241	-7.569221
TCMDC-135059	-8.3972864	TCMDC-134909	-7.8835073	TCMDC-133360	-7.5691371
TCMDC-137568	-8.3969936	TCMDC-138895	-7.8834453	TCMDC-139317	-7.5690889
TCMDC-135210	-8.3968267	TCMDC-140957	-7.8830557	TCMDC-138415	-7.568903
TCMDC-131845	-8.3963566	TCMDC-135549	-7.8820057	TCMDC-131631	-7.5688839
TCMDC-135717	-8.3926382	TCMDC-139257	-7.8809438	TCMDC-135793	-7.5688505
TCMDC-138403	-8.3926125	TCMDC-125657	-7.8801932	TCMDC-140380	-7.5685296
TCMDC-138226	-8.3919249	TCMDC-138553	-7.8797178	TCMDC-141434	-7.5684428
TCMDC-138736	-8.3914785	TCMDC-139372	-7.8793397	TCMDC-132683	-7.5682178
TCMDC-131528	-8.3909826	TCMDC-124007	-7.8778138	TCMDC-136101	-7.5680552
TCMDC-138483	-8.3905611	TCMDC-135505	-7.8777766	TCMDC-135387	-7.5679832
TCMDC-141096	-8.3904152	TCMDC-135834	-7.8776345	TCMDC-138614	-7.5676351
TCMDC-139244	-8.39013	TCMDC-138183	-7.8776102	TCMDC-140312	-7.5665565
TCMDC-141340	-8.390111	TCMDC-138881	-7.8766966	TCMDC-139440	-7.5665197
TCMDC-140289	-8.3863411	TCMDC-132751	-7.8766236	TCMDC-136073	-7.5662913
TCMDC-141452	-8.3863039	TCMDC-141454	-7.8765206	TCMDC-138801	-7.5651584
TCMDC-140607	-8.3856344	TCMDC-141173	-7.8764448	TCMDC-140885	-7.5647531
TCMDC-136519	-8.3847885	TCMDC-136098	-7.8759336	TCMDC-134114	-7.564517
TCMDC-138738	-8.3841829	TCMDC-133267	-7.8750186	TCMDC-124799	-7.5645018
TCMDC-141643	-8.383769	TCMDC-133912	-7.8743973	TCMDC-140744	-7.5643678
TCMDC-135355	-8.3817387	TCMDC-139512	-7.874136	TCMDC-133185	-7.5640635
TCMDC-138657	-8.3814697	TCMDC-133941	-7.8736525	TCMDC-138804	-7.5635905
TCMDC-138533	-8.3806429	TCMDC-131823	-7.8736339	TCMDC-134874	-7.5632834
TCMDC-140935	-8.3800936	TCMDC-139921	-7.8735104	TCMDC-138337	-7.5632291

TCMDC-137074	-8.3788528	TCMDC-138746	-7.8732033	TCMDC-141759	-7.5631218
TCMDC-134934	-8.3781652	TCMDC-134802	-7.8724442	TCMDC-141160	-7.5630794
TCMDC-138285	-8.3768473	TCMDC-132264	-7.8722663	TCMDC-141902	-7.5630679
TCMDC-133050	-8.3763008	TCMDC-135841	-7.8722544	TCMDC-133837	-7.5627775
TCMDC-140991	-8.3758068	TCMDC-136206	-7.8720555	TCMDC-140051	-7.562696
TCMDC-131966	-8.3753004	TCMDC-135259	-7.8719101	TCMDC-137116	-7.5625825
TCMDC-131396	-8.373147	TCMDC-133317	-7.8717484	TCMDC-140695	-7.5623174
TCMDC-141469	-8.3728762	TCMDC-141455	-7.8711257	TCMDC-133702	-7.5619316
TCMDC-134527	-8.3699408	TCMDC-141370	-7.8700085	TCMDC-139090	-7.56177
TCMDC-138309	-8.3697605	TCMDC-135061	-7.8696823	TCMDC-132266	-7.5615807
TCMDC-139591	-8.3690081	TCMDC-141437	-7.8695107	TCMDC-133213	-7.5611777
TCMDC-135972	-8.3688307	TCMDC-132165	-7.8694892	TCMDC-132136	-7.5611763
TCMDC-131849	-8.3680172	TCMDC-140699	-7.8691173	TCMDC-137816	-7.5610504
TCMDC-138648	-8.3680162	TCMDC-140080	-7.8688211	TCMDC-141709	-7.5608726
TCMDC-131957	-8.3670311	TCMDC-139325	-7.8686423	TCMDC-133077	-7.5605187
TCMDC-138912	-8.3663559	TCMDC-135936	-7.8672328	TCMDC-140954	-7.5604157
TCMDC-131986	-8.3658714	TCMDC-140210	-7.8672037	TCMDC-132776	-7.5602317
TCMDC-135037	-8.3634415	TCMDC-138488	-7.8670998	TCMDC-140835	-7.5601125
TCMDC-139619	-8.3625546	TCMDC-140791	-7.8663812	TCMDC-124043	-7.5600009
TCMDC-135203	-8.3611298	TCMDC-135396	-7.8663087	TCMDC-136838	-7.5596681
TCMDC-141503	-8.3611155	TCMDC-136783	-7.8657861	TCMDC-134669	-7.559577
TCMDC-139993	-8.3602142	TCMDC-137076	-7.8655858	TCMDC-137169	-7.5595098
TCMDC-139049	-8.3597527	TCMDC-133630	-7.8654718	TCMDC-133592	-7.559463
TCMDC-138609	-8.3597364	TCMDC-138512	-7.8654089	TCMDC-134416	-7.5591888
TCMDC-141894	-8.3593082	TCMDC-136089	-7.8645716	TCMDC-132749	-7.5591807
TCMDC-138802	-8.3592634	TCMDC-138410	-7.8644767	TCMDC-141286	-7.5590534
TCMDC-141132	-8.359231	TCMDC-137131	-7.8637738	TCMDC-141693	-7.5590339
TCMDC-134989	-8.3580084	TCMDC-140812	-7.863255	TCMDC-132540	-7.5584702
TCMDC-138219	-8.3577566	TCMDC-140941	-7.863215	TCMDC-131351	-7.5584559
TCMDC-141318	-8.3574562	TCMDC-141155	-7.8630819	TCMDC-140271	-7.5583906
TCMDC-131874	-8.3559647	TCMDC-135624	-7.8627234	TCMDC-139402	-7.5579643
TCMDC-134654	-8.3548117	TCMDC-141357	-7.8625956	TCMDC-134911	-7.5577459
TCMDC-140534	-8.3531885	TCMDC-134132	-7.8625221	TCMDC-137110	-7.5577116
TCMDC-140988	-8.3512907	TCMDC-133443	-7.8622484	TCMDC-139693	-7.5569553
TCMDC-135206	-8.3494425	TCMDC-139374	-7.8608856	TCMDC-138562	-7.556952
TCMDC-140497	-8.349268	TCMDC-131530	-7.8606396	TCMDC-132441	-7.5569305
TCMDC-141639	-8.3491497	TCMDC-136273	-7.8597207	TCMDC-139632	-7.5569048
TCMDC-133011	-8.3486395	TCMDC-138361	-7.859715	TCMDC-135941	-7.5561681
TCMDC-141611	-8.3485651	TCMDC-141907	-7.8587394	TCMDC-124022	-7.5560904
TCMDC-135850	-8.3484669	TCMDC-134905	-7.8583722	TCMDC-123794	-7.5560327
TCMDC-140470	-8.3483572	TCMDC-139506	-7.8569164	TCMDC-135699	-7.5555263
TCMDC-135353	-8.3475866	TCMDC-131529	-7.8568621	TCMDC-132454	-7.5549836
TCMDC-136085	-8.3472891	TCMDC-124471	-7.8563709	TCMDC-133857	-7.5549664
TCMDC-137178	-8.3471394	TCMDC-135751	-7.8560619	TCMDC-140190	-7.5540862

TCMDC-132413	-8.3470984	TCMDC-138530	-7.8560138	TCMDC-135562	-7.5532432
TCMDC-141517	-8.346036	TCMDC-131411	-7.8559232	TCMDC-137030	-7.552887
TCMDC-138252	-8.3460102	TCMDC-139583	-7.8556561	TCMDC-133809	-7.5528493
TCMDC-138843	-8.3435326	TCMDC-134248	-7.8541207	TCMDC-123583	-7.5528207
TCMDC-138519	-8.343276	TCMDC-135843	-7.8538418	TCMDC-138451	-7.5527596
TCMDC-137258	-8.3431797	TCMDC-135241	-7.8534737	TCMDC-139338	-7.5526719
TCMDC-139521	-8.3424397	TCMDC-135724	-7.8532825	TCMDC-135912	-7.5526285
TCMDC-131566	-8.3419333	TCMDC-139815	-7.8529696	TCMDC-137138	-7.5519276
TCMDC-137274	-8.3409777	TCMDC-139519	-7.8528533	TCMDC-136451	-7.5518742
TCMDC-132283	-8.339673	TCMDC-140265	-7.8524671	TCMDC-132548	-7.5514622
TCMDC-141980	-8.3392372	TCMDC-135718	-7.8523936	TCMDC-141004	-7.5514426
TCMDC-138853	-8.3390055	TCMDC-134822	-7.8522882	TCMDC-140370	-7.5513382
TCMDC-138240	-8.3384638	TCMDC-135498	-7.8516626	TCMDC-140514	-7.5506473
TCMDC-134156	-8.3374224	TCMDC-133386	-7.8509989	TCMDC-132954	-7.5502839
TCMDC-133811	-8.3339071	TCMDC-135939	-7.849802	TCMDC-131371	-7.5500379
TCMDC-138841	-8.3338356	TCMDC-138383	-7.8497548	TCMDC-140388	-7.5499473
TCMDC-138327	-8.3323708	TCMDC-139527	-7.8490114	TCMDC-136521	-7.5497584
TCMDC-138891	-8.3317451	TCMDC-138727	-7.8490028	TCMDC-133038	-7.5494895
TCMDC-134134	-8.3317232	TCMDC-138514	-7.8486719	TCMDC-138382	-7.5485578
TCMDC-135772	-8.3301764	TCMDC-139525	-7.848423	TCMDC-132897	-7.5484142
TCMDC-139577	-8.3292274	TCMDC-139510	-7.8479357	TCMDC-136467	-7.5480285
TCMDC-137972	-8.3272009	TCMDC-132177	-7.8470411	TCMDC-132247	-7.5478888
TCMDC-135176	-8.3266869	TCMDC-139794	-7.8452935	TCMDC-137027	-7.5478401
TCMDC-141786	-8.3261003	TCMDC-138408	-7.8449769	TCMDC-140654	-7.547749
TCMDC-139575	-8.3257284	TCMDC-133013	-7.8449454	TCMDC-136890	-7.5475364
TCMDC-140937	-8.3253126	TCMDC-141614	-7.8448873	TCMDC-135756	-7.5473557
TCMDC-136003	-8.3247862	TCMDC-134826	-7.8448763	TCMDC-124020	-7.5471878
TCMDC-139564	-8.3227119	TCMDC-136689	-7.8447433	TCMDC-132280	-7.5470662
TCMDC-125170	-8.3200531	TCMDC-140856	-7.8445253	TCMDC-133254	-7.5461388
TCMDC-138175	-8.3188581	TCMDC-137961	-7.8444538	TCMDC-133051	-7.5458937
TCMDC-135197	-8.3187647	TCMDC-132224	-7.8439374	TCMDC-133467	-7.5451078
TCMDC-137199	-8.3184547	TCMDC-138135	-7.8437214	TCMDC-139161	-7.5449328
TCMDC-138846	-8.3163633	TCMDC-135465	-7.8436542	TCMDC-136896	-7.5449219
TCMDC-138269	-8.315731	TCMDC-134404	-7.8426781	TCMDC-138834	-7.5438552
TCMDC-138734	-8.3155317	TCMDC-133842	-7.842104	TCMDC-136839	-7.5438333
TCMDC-135968	-8.3150806	TCMDC-133882	-7.8420591	TCMDC-132210	-7.5434632
TCMDC-133412	-8.3148251	TCMDC-133055	-7.8416033	TCMDC-140019	-7.5432596
TCMDC-141439	-8.3138695	TCMDC-132760	-7.8414855	TCMDC-133269	-7.5431714
TCMDC-135302	-8.312295	TCMDC-132899	-7.8411956	TCMDC-136366	-7.5430193
TCMDC-140217	-8.3119898	TCMDC-138520	-7.8405924	TCMDC-141294	-7.5428162
TCMDC-136849	-8.3111734	TCMDC-135323	-7.8400164	TCMDC-140872	-7.5425653
TCMDC-139608	-8.3111076	TCMDC-135758	-7.8392878	TCMDC-133913	-7.5424924
TCMDC-135743	-8.3109856	TCMDC-132055	-7.8390317	TCMDC-132275	-7.5419211
TCMDC-135812	-8.3103065	TCMDC-138490	-7.8390207	TCMDC-139218	-7.541914

TCMDC-135540	-8.3086414	TCMDC-139572	-7.8382444	TCMDC-137796	-7.5418448
TCMDC-138861	-8.3086329	TCMDC-141776	-7.8377776	TCMDC-132017	-7.5417867
TCMDC-132295	-8.3077765	TCMDC-132505	-7.8370714	TCMDC-134944	-7.5417681
TCMDC-138368	-8.3062515	TCMDC-138860	-7.8365536	TCMDC-132434	-7.5413857
TCMDC-135933	-8.3031273	TCMDC-136257	-7.8364935	TCMDC-138993	-7.5411491
TCMDC-125591	-8.3030348	TCMDC-135625	-7.836359	TCMDC-133775	-7.5410876
TCMDC-140542	-8.3023376	TCMDC-135394	-7.8359814	TCMDC-138401	-7.541007
TCMDC-139843	-8.3021412	TCMDC-141086	-7.8354321	TCMDC-133920	-7.5409942
TCMDC-141119	-8.301754	TCMDC-135252	-7.8352399	TCMDC-132802	-7.540916
TCMDC-131912	-8.3015728	TCMDC-136200	-7.8350296	TCMDC-137591	-7.5408607
TCMDC-140985	-8.3013134	TCMDC-140993	-7.8346148	TCMDC-138421	-7.5408359
TCMDC-135568	-8.300724	TCMDC-140096	-7.8341379	TCMDC-133705	-7.5406418
TCMDC-133318	-8.3002453	TCMDC-140662	-7.833889	TCMDC-135527	-7.5405841
TCMDC-135265	-8.2996454	TCMDC-135174	-7.8334074	TCMDC-124958	-7.5405269
TCMDC-139522	-8.2987843	TCMDC-139985	-7.833178	TCMDC-141213	-7.5403347
TCMDC-134524	-8.2975187	TCMDC-135719	-7.8330526	TCMDC-135635	-7.540062
TCMDC-137848	-8.2973614	TCMDC-137259	-7.8330131	TCMDC-140671	-7.5396166
TCMDC-140978	-8.2944117	TCMDC-138582	-7.8328156	TCMDC-133699	-7.539588
TCMDC-134943	-8.2910147	TCMDC-141358	-7.832561	TCMDC-132965	-7.5395732
TCMDC-140566	-8.2905302	TCMDC-132145	-7.83255	TCMDC-136754	-7.5394335
TCMDC-141319	-8.2902651	TCMDC-138899	-7.8325324	TCMDC-139808	-7.5394173
TCMDC-138216	-8.2900152	TCMDC-141555	-7.8321562	TCMDC-141391	-7.5393791
TCMDC-135356	-8.2894678	TCMDC-136276	-7.8319616	TCMDC-138840	-7.539279
TCMDC-138529	-8.289443	TCMDC-132903	-7.830225	TCMDC-132041	-7.5392637
TCMDC-137315	-8.2888165	TCMDC-140997	-7.8298702	TCMDC-133111	-7.5391889
TCMDC-135374	-8.2886734	TCMDC-140888	-7.8295393	TCMDC-139292	-7.5387588
TCMDC-139955	-8.2878036	TCMDC-140268	-7.8295383	TCMDC-134745	-7.5384274
TCMDC-140541	-8.2876959	TCMDC-133889	-7.8289576	TCMDC-125709	-7.5383601
TCMDC-138321	-8.287055	TCMDC-135285	-7.8280725	TCMDC-137698	-7.5380821
TCMDC-136374	-8.2861738	TCMDC-133064	-7.8274183	TCMDC-135005	-7.5378537
TCMDC-138897	-8.2859793	TCMDC-137238	-7.8268471	TCMDC-132493	-7.5373931
TCMDC-139793	-8.2855501	TCMDC-132762	-7.8263597	TCMDC-132288	-7.5365424
TCMDC-133413	-8.2855186	TCMDC-135747	-7.8262439	TCMDC-135673	-7.5364509
TCMDC-138110	-8.2846994	TCMDC-141233	-7.8259826	TCMDC-131901	-7.5358014
TCMDC-138523	-8.2823477	TCMDC-123865	-7.8255248	TCMDC-136810	-7.5356479
TCMDC-136194	-8.2821579	TCMDC-139891	-7.8254075	TCMDC-133049	-7.5356083
TCMDC-137734	-8.280283	TCMDC-138423	-7.8246584	TCMDC-141820	-7.5355802
TCMDC-134151	-8.2802315	TCMDC-140583	-7.8243966	TCMDC-139838	-7.5355101
TCMDC-138737	-8.2798786	TCMDC-136990	-7.8243484	TCMDC-139661	-7.5354075
TCMDC-141018	-8.2794418	TCMDC-135725	-7.8243003	TCMDC-142312	-7.5352564
TCMDC-135168	-8.2777777	TCMDC-141008	-7.8237262	TCMDC-139385	-7.5351152
TCMDC-135211	-8.2776136	TCMDC-135344	-7.8236241	TCMDC-139214	-7.5349569
TCMDC-141120	-8.2770796	TCMDC-132871	-7.8223891	TCMDC-138443	-7.5349059
TCMDC-134673	-8.2768803	TCMDC-139466	-7.8221741	TCMDC-141877	-7.5345597

TCMDC-140990	-8.2760334	TCMDC-124950	-7.8218689	TCMDC-137294	-7.5345144
TCMDC-137780	-8.2751808	TCMDC-138244	-7.8214254	TCMDC-135075	-7.5343943
TCMDC-135686	-8.2745991	TCMDC-139787	-7.8212528	TCMDC-132750	-7.5343404
TCMDC-137237	-8.2743387	TCMDC-124019	-7.8210983	TCMDC-140789	-7.5339403
TCMDC-135845	-8.2742767	TCMDC-135935	-7.8207207	TCMDC-134784	-7.5338469
TCMDC-134920	-8.2739944	TCMDC-138752	-7.8206353	TCMDC-132847	-7.533783
TCMDC-135769	-8.27176	TCMDC-131548	-7.8199463	TCMDC-136280	-7.5334754
TCMDC-134044	-8.27145	TCMDC-134865	-7.8197455	TCMDC-138051	-7.5333843
TCMDC-141474	-8.270278	TCMDC-135922	-7.8193259	TCMDC-138435	-7.5329242
TCMDC-140553	-8.2686167	TCMDC-132961	-7.8186812	TCMDC-135731	-7.5325537
TCMDC-135212	-8.2684002	TCMDC-137520	-7.8184848	TCMDC-125885	-7.5325141
TCMDC-138837	-8.2681208	TCMDC-141686	-7.8184071	TCMDC-133921	-7.5320067
TCMDC-137233	-8.2674103	TCMDC-131911	-7.8177533	TCMDC-125141	-7.5317736
TCMDC-138702	-8.2660227	TCMDC-133061	-7.8177509	TCMDC-123998	-7.531405
TCMDC-141580	-8.2652283	TCMDC-123836	-7.8175211	TCMDC-139644	-7.5313191
TCMDC-125666	-8.2644482	TCMDC-136242	-7.8163304	TCMDC-140858	-7.5304461
TCMDC-139750	-8.2642164	TCMDC-138583	-7.8154168	TCMDC-140385	-7.5302711
TCMDC-139651	-8.2641449	TCMDC-141697	-7.815259	TCMDC-141162	-7.5298672
TCMDC-133883	-8.2640781	TCMDC-137037	-7.8149199	TCMDC-135208	-7.5290885
TCMDC-135512	-8.2617531	TCMDC-132101	-7.8144379	TCMDC-140960	-7.5290403
TCMDC-140936	-8.261219	TCMDC-132256	-7.8142099	TCMDC-137225	-7.5290365
TCMDC-138332	-8.2608862	TCMDC-131531	-7.8135128	TCMDC-139807	-7.5288668
TCMDC-141511	-8.2608032	TCMDC-139854	-7.8132901	TCMDC-133300	-7.5281897
TCMDC-135434	-8.2603073	TCMDC-133323	-7.8130727	TCMDC-138277	-7.5278492
TCMDC-138326	-8.2599096	TCMDC-137617	-7.812407	TCMDC-140055	-7.5274463
TCMDC-133936	-8.2581081	TCMDC-134818	-7.8113122	TCMDC-137742	-7.5274105
TCMDC-136373	-8.2563477	TCMDC-135632	-7.8113012	TCMDC-124289	-7.5271201
TCMDC-138224	-8.2543993	TCMDC-137282	-7.8109365	TCMDC-135038	-7.5258269
TCMDC-137040	-8.2542963	TCMDC-135802	-7.8104434	TCMDC-139449	-7.5257654
TCMDC-124181	-8.2531433	TCMDC-136308	-7.8099518	TCMDC-139524	-7.525456
TCMDC-138474	-8.2528849	TCMDC-140004	-7.808403	TCMDC-140824	-7.5252881
TCMDC-132056	-8.2526865	TCMDC-137202	-7.8078141	TCMDC-137855	-7.5251565
TCMDC-137317	-8.2525101	TCMDC-136260	-7.8076835	TCMDC-139188	-7.525075
TCMDC-138854	-8.2515783	TCMDC-136103	-7.8072724	TCMDC-139330	-7.5247111
TCMDC-125873	-8.250329	TCMDC-138340	-7.8066053	TCMDC-136409	-7.5243921
TCMDC-137615	-8.2500229	TCMDC-136175	-7.8065448	TCMDC-133035	-7.5243344
TCMDC-135169	-8.2497091	TCMDC-132166	-7.8063502	TCMDC-136646	-7.5237875
TCMDC-133539	-8.2485619	TCMDC-138682	-7.8060327	TCMDC-135735	-7.5234885
TCMDC-131851	-8.2482595	TCMDC-132251	-7.8059697	TCMDC-137834	-7.5229211
TCMDC-138527	-8.2470617	TCMDC-134498	-7.8058286	TCMDC-140815	-7.5228286
TCMDC-136512	-8.2465134	TCMDC-133672	-7.8057203	TCMDC-137063	-7.5227499
TCMDC-138223	-8.2464581	TCMDC-139909	-7.8056321	TCMDC-138658	-7.5226226
TCMDC-141780	-8.2464056	TCMDC-139656	-7.8054123	TCMDC-136811	-7.5224619
TCMDC-138257	-8.2460938	TCMDC-141135	-7.8052335	TCMDC-133081	-7.5224261

TCMDC-139828	-8.2460175	TCMDC-123858	-7.8051996	TCMDC-133800	-7.5220165
TCMDC-141692	-8.2456636	TCMDC-131328	-7.8048429	TCMDC-136479	-7.521915
TCMDC-141326	-8.2454891	TCMDC-134593	-7.8044014	TCMDC-136812	-7.5216608
TCMDC-140633	-8.2454739	TCMDC-133608	-7.8043823	TCMDC-140895	-7.5215049
TCMDC-137824	-8.2422361	TCMDC-132230	-7.8041716	TCMDC-125335	-7.5210924
TCMDC-140291	-8.2414761	TCMDC-132607	-7.804153	TCMDC-140742	-7.5209813
TCMDC-138725	-8.241003	TCMDC-139999	-7.8038201	TCMDC-132276	-7.5206928
TCMDC-136353	-8.2408237	TCMDC-141080	-7.8037291	TCMDC-136233	-7.5201025
TCMDC-138555	-8.240716	TCMDC-140244	-7.8037138	TCMDC-140918	-7.5200276
TCMDC-134552	-8.2406492	TCMDC-133441	-7.8028722	TCMDC-140266	-7.519557
TCMDC-138377	-8.2405005	TCMDC-133314	-7.8018274	TCMDC-134427	-7.5192852
TCMDC-137962	-8.2401505	TCMDC-138476	-7.8017998	TCMDC-140689	-7.5191927
TCMDC-138006	-8.2400351	TCMDC-133962	-7.8017035	TCMDC-124973	-7.5191522
TCMDC-136002	-8.2395144	TCMDC-141688	-7.8012991	TCMDC-133844	-7.5190229
TCMDC-138629	-8.2386627	TCMDC-133904	-7.8007345	TCMDC-140375	-7.518538
TCMDC-136609	-8.2375164	TCMDC-135712	-7.8007135	TCMDC-138686	-7.5180182
TCMDC-137802	-8.2372942	TCMDC-135897	-7.8002763	TCMDC-140787	-7.5179272
TCMDC-138149	-8.2364655	TCMDC-140318	-7.7995577	TCMDC-141591	-7.5176973
TCMDC-138148	-8.2341938	TCMDC-139611	-7.7993989	TCMDC-134025	-7.5175028
TCMDC-141112	-8.2333136	TCMDC-137145	-7.7993779	TCMDC-139260	-7.5169325
TCMDC-138181	-8.23246	TCMDC-141777	-7.7985487	TCMDC-138409	-7.516809
TCMDC-140948	-8.2309723	TCMDC-133163	-7.7976022	TCMDC-138002	-7.5165706
TCMDC-137272	-8.2300711	TCMDC-133046	-7.7974195	TCMDC-132242	-7.5162716
TCMDC-141071	-8.2282934	TCMDC-131868	-7.7972403	TCMDC-138466	-7.5155005
TCMDC-138704	-8.2275467	TCMDC-132167	-7.7971797	TCMDC-135531	-7.5152488
TCMDC-138398	-8.2271032	TCMDC-135934	-7.7964664	TCMDC-135068	-7.5150776
TCMDC-135025	-8.2256327	TCMDC-141863	-7.7962689	TCMDC-136420	-7.5150051
TCMDC-135836	-8.224658	TCMDC-138930	-7.7961464	TCMDC-132135	-7.5147762
TCMDC-139797	-8.224618	TCMDC-137489	-7.7961373	TCMDC-132986	-7.5147185
TCMDC-131478	-8.2246122	TCMDC-138407	-7.7952623	TCMDC-132277	-7.5141301
TCMDC-139532	-8.2242384	TCMDC-139836	-7.7950387	TCMDC-140368	-7.5139623
TCMDC-136133	-8.2225485	TCMDC-133677	-7.7947259	TCMDC-133678	-7.513845
TCMDC-141783	-8.2223377	TCMDC-135499	-7.7946677	TCMDC-141188	-7.5136456
TCMDC-133395	-8.2218714	TCMDC-141551	-7.7945046	TCMDC-140127	-7.5135255
TCMDC-131961	-8.2212267	TCMDC-125717	-7.7936263	TCMDC-136327	-7.5129032
TCMDC-134748	-8.2197094	TCMDC-138158	-7.7934618	TCMDC-136662	-7.5125594
TCMDC-131551	-8.2194042	TCMDC-137144	-7.7932253	TCMDC-134740	-7.512464
TCMDC-138768	-8.2192917	TCMDC-136142	-7.7931657	TCMDC-132492	-7.5124445
TCMDC-140009	-8.2192488	TCMDC-133623	-7.7924986	TCMDC-140062	-7.5120034
TCMDC-141813	-8.2189827	TCMDC-132908	-7.7920556	TCMDC-140028	-7.5113616
TCMDC-135445	-8.2186337	TCMDC-139560	-7.7914648	TCMDC-140912	-7.5112181
TCMDC-140737	-8.2185726	TCMDC-139416	-7.791378	TCMDC-136337	-7.5108113
TCMDC-141521	-8.2177172	TCMDC-134286	-7.7911544	TCMDC-138554	-7.5106664
TCMDC-138020	-8.2158804	TCMDC-141602	-7.7908583	TCMDC-141857	-7.5106273

TCMDC-133045	-8.2156572	TCMDC-134072	-7.7907968	TCMDC-137797	-7.5102735
TCMDC-138602	-8.2151308	TCMDC-137611	-7.7899179	TCMDC-137582	-7.5102258
TCMDC-138159	-8.2147541	TCMDC-140806	-7.7897139	TCMDC-140351	-7.5101538
TCMDC-141696	-8.2141905	TCMDC-138845	-7.7896304	TCMDC-134143	-7.5095363
TCMDC-135456	-8.2135792	TCMDC-136193	-7.7892108	TCMDC-132411	-7.5095015
TCMDC-131971	-8.2127743	TCMDC-135744	-7.7888479	TCMDC-139340	-7.5093832
TCMDC-135537	-8.2123127	TCMDC-141724	-7.7887073	TCMDC-132604	-7.5093212
TCMDC-138385	-8.2115145	TCMDC-140882	-7.7884345	TCMDC-136184	-7.509089
TCMDC-138879	-8.2111435	TCMDC-141141	-7.7884192	TCMDC-140871	-7.5086079
TCMDC-141948	-8.2102432	TCMDC-134867	-7.7876778	TCMDC-138538	-7.5083618
TCMDC-140953	-8.2100878	TCMDC-132141	-7.7874923	TCMDC-138422	-7.5083518
TCMDC-141044	-8.2091227	TCMDC-136967	-7.7873168	TCMDC-135874	-7.5083375
TCMDC-135764	-8.208375	TCMDC-135449	-7.7868943	TCMDC-138818	-7.5082211
TCMDC-133390	-8.2074776	TCMDC-138567	-7.7866244	TCMDC-138325	-7.5078573
TCMDC-135550	-8.2071371	TCMDC-133892	-7.7860255	TCMDC-139626	-7.5077233
TCMDC-131956	-8.2068958	TCMDC-138701	-7.7859039	TCMDC-131805	-7.5075254
TCMDC-132051	-8.2068596	TCMDC-138457	-7.7858019	TCMDC-134452	-7.5074878
TCMDC-141940	-8.2064838	TCMDC-136637	-7.7853193	TCMDC-133878	-7.5071769
TCMDC-135696	-8.2061367	TCMDC-133028	-7.7853127	TCMDC-134900	-7.5071235
TCMDC-137914	-8.2061062	TCMDC-140861	-7.7852178	TCMDC-140188	-7.5068235
TCMDC-135777	-8.2057791	TCMDC-136920	-7.7850375	TCMDC-133017	-7.5066142
TCMDC-142301	-8.2055664	TCMDC-140126	-7.7846479	TCMDC-141860	-7.506424
TCMDC-140944	-8.2046356	TCMDC-135706	-7.7843566	TCMDC-139332	-7.5063553
TCMDC-138800	-8.20436	TCMDC-135863	-7.7843103	TCMDC-124034	-7.5061269
TCMDC-139571	-8.2036619	TCMDC-140317	-7.7843056	TCMDC-132560	-7.505971
TCMDC-138238	-8.2032061	TCMDC-141730	-7.7841411	TCMDC-140352	-7.5058999
TCMDC-135785	-8.2022142	TCMDC-141309	-7.7839336	TCMDC-139555	-7.5052576
TCMDC-141785	-8.2002382	TCMDC-135883	-7.783875	TCMDC-137620	-7.5052247
TCMDC-141896	-8.1999025	TCMDC-137952	-7.783814	TCMDC-125491	-7.505137
TCMDC-138765	-8.1989861	TCMDC-133391	-7.7837238	TCMDC-139552	-7.5048909
TCMDC-135661	-8.1976986	TCMDC-134825	-7.7836647	TCMDC-141498	-7.5040002
TCMDC-138796	-8.1970387	TCMDC-141590	-7.783453	TCMDC-133686	-7.5032811
TCMDC-135572	-8.196907	TCMDC-138473	-7.7834339	TCMDC-135786	-7.5030208
TCMDC-140165	-8.1966248	TCMDC-132292	-7.782403	TCMDC-137066	-7.5023584
TCMDC-139928	-8.196559	TCMDC-140643	-7.7822161	TCMDC-138934	-7.5019221
TCMDC-141059	-8.1962929	TCMDC-135746	-7.7813716	TCMDC-139399	-7.5014672
TCMDC-139176	-8.1944628	TCMDC-135662	-7.7813611	TCMDC-140111	-7.5008435
TCMDC-141126	-8.1942205	TCMDC-133047	-7.7809734	TCMDC-141397	-7.5007768
TCMDC-140479	-8.1934385	TCMDC-136983	-7.7807908	TCMDC-139690	-7.5003247
TCMDC-141806	-8.1929893	TCMDC-135483	-7.7805271	TCMDC-134735	-7.4997115
TCMDC-138522	-8.1929674	TCMDC-135566	-7.7804298	TCMDC-138465	-7.4996018
TCMDC-141612	-8.1926308	TCMDC-138999	-7.7797523	TCMDC-134076	-7.4994969
TCMDC-140750	-8.1922646	TCMDC-141413	-7.7794967	TCMDC-132138	-7.4993858
TCMDC-138611	-8.1914005	TCMDC-140770	-7.7793093	TCMDC-133016	-7.4993606

TCMDC-140293	-8.1913929	TCMDC-138581	-7.7782602	TCMDC-124032	-7.4991326
TCMDC-135411	-8.1909113	TCMDC-140194	-7.778079	TCMDC-133565	-7.4984641
TCMDC-133625	-8.1907425	TCMDC-136250	-7.7760887	TCMDC-132533	-7.4984484
TCMDC-135214	-8.1895361	TCMDC-133922	-7.7749729	TCMDC-139081	-7.4982243
TCMDC-140039	-8.1878548	TCMDC-137289	-7.7748203	TCMDC-141621	-7.4980249
TCMDC-138102	-8.1875772	TCMDC-141435	-7.7747264	TCMDC-133689	-7.4978285
TCMDC-138769	-8.1870146	TCMDC-134171	-7.7746196	TCMDC-140725	-7.4977741
TCMDC-135627	-8.1865416	TCMDC-141904	-7.773881	TCMDC-142290	-7.4975176
TCMDC-138492	-8.184124	TCMDC-138146	-7.7731094	TCMDC-133180	-7.4971771
TCMDC-133319	-8.1839266	TCMDC-131987	-7.7725191	TCMDC-132467	-7.496819
TCMDC-133062	-8.1837015	TCMDC-135754	-7.7721148	TCMDC-135437	-7.4966311
TCMDC-141908	-8.1830921	TCMDC-138426	-7.7720428	TCMDC-140810	-7.4965706
TCMDC-140994	-8.182024	TCMDC-132796	-7.7717896	TCMDC-137095	-7.4963369
TCMDC-141280	-8.1816416	TCMDC-136202	-7.7717519	TCMDC-132958	-7.4960814
TCMDC-135293	-8.180357	TCMDC-141928	-7.7716842	TCMDC-134320	-7.4958663
TCMDC-132099	-8.1800966	TCMDC-135233	-7.7705836	TCMDC-140088	-7.4956765
TCMDC-140996	-8.1794567	TCMDC-136704	-7.7697115	TCMDC-138155	-7.4954472
TCMDC-134933	-8.1790171	TCMDC-135801	-7.7696929	TCMDC-138305	-7.4954
TCMDC-139516	-8.1787519	TCMDC-132132	-7.7692437	TCMDC-132417	-7.4953079
TCMDC-131853	-8.178153	TCMDC-139959	-7.7690349	TCMDC-141897	-7.4952302
TCMDC-135468	-8.1780396	TCMDC-135749	-7.7689805	TCMDC-140113	-7.4949393
TCMDC-141137	-8.1775703	TCMDC-125088	-7.7687292	TCMDC-132399	-7.4947171
TCMDC-140921	-8.1768599	TCMDC-132960	-7.7680955	TCMDC-134621	-7.4944658
TCMDC-140024	-8.1756601	TCMDC-135902	-7.7671723	TCMDC-132380	-7.4937019
TCMDC-134046	-8.1748266	TCMDC-132956	-7.7670627	TCMDC-135704	-7.4936399
TCMDC-136520	-8.174716	TCMDC-138440	-7.7668996	TCMDC-137185	-7.4935966
TCMDC-134196	-8.1747112	TCMDC-138127	-7.7661052	TCMDC-139226	-7.4935246
TCMDC-139652	-8.1740942	TCMDC-131339	-7.7650099	TCMDC-136884	-7.4934564
TCMDC-132116	-8.1739073	TCMDC-132163	-7.7649422	TCMDC-138304	-7.4933395
TCMDC-140535	-8.1733227	TCMDC-135716	-7.7649136	TCMDC-132880	-7.493269
TCMDC-134551	-8.1732941	TCMDC-140830	-7.7646232	TCMDC-141228	-7.4928775
TCMDC-133379	-8.172821	TCMDC-133327	-7.7644672	TCMDC-139353	-7.4927468
TCMDC-137983	-8.1718912	TCMDC-136126	-7.7642145	TCMDC-132562	-7.4926443
TCMDC-125793	-8.1712685	TCMDC-138400	-7.7636042	TCMDC-132553	-7.4925504
TCMDC-138280	-8.1702452	TCMDC-133735	-7.7631612	TCMDC-136748	-7.4924054
TCMDC-135450	-8.1701632	TCMDC-139649	-7.7627125	TCMDC-125175	-7.4921684
TCMDC-132476	-8.1693621	TCMDC-140071	-7.7625709	TCMDC-138759	-7.4921508
TCMDC-135452	-8.169323	TCMDC-137965	-7.7623253	TCMDC-132231	-7.4920287
TCMDC-138518	-8.1689425	TCMDC-141256	-7.7617612	TCMDC-134994	-7.4918771
TCMDC-134676	-8.16887	TCMDC-135333	-7.7617311	TCMDC-140238	-7.4914355
TCMDC-136191	-8.1685076	TCMDC-140958	-7.7615643	TCMDC-133929	-7.4912271
TCMDC-137758	-8.168438	TCMDC-132216	-7.7614603	TCMDC-140246	-7.4909577
TCMDC-138570	-8.1683035	TCMDC-134316	-7.7611628	TCMDC-134952	-7.4907203
TCMDC-138808	-8.1681852	TCMDC-135193	-7.7609272	TCMDC-131825	-7.4904709

TCMDC-124774	-8.1674604	TCMDC-133126	-7.7608399	TCMDC-134866	-7.4904504
TCMDC-141264	-8.1669016	TCMDC-135106	-7.7607923	TCMDC-137340	-7.4897084
TCMDC-138420	-8.1665487	TCMDC-135803	-7.7596087	TCMDC-138685	-7.4893351
TCMDC-134829	-8.1665354	TCMDC-142189	-7.7592616	TCMDC-132299	-7.4892707
TCMDC-141622	-8.1663561	TCMDC-139956	-7.7589889	TCMDC-141762	-7.4890351
TCMDC-135172	-8.1657877	TCMDC-136433	-7.7582521	TCMDC-133192	-7.4885225
TCMDC-138842	-8.1657152	TCMDC-133693	-7.7582026	TCMDC-140261	-7.4884639
TCMDC-138109	-8.163723	TCMDC-138844	-7.7581735	TCMDC-141431	-7.4883432
TCMDC-136156	-8.1636086	TCMDC-139995	-7.7573819	TCMDC-132775	-7.4881763
TCMDC-133943	-8.1630135	TCMDC-140046	-7.7570601	TCMDC-137149	-7.4879651
TCMDC-138507	-8.1628075	TCMDC-133629	-7.7570548	TCMDC-137382	-7.4878197
TCMDC-140729	-8.1625004	TCMDC-132566	-7.7569227	TCMDC-133250	-7.4873734
TCMDC-138858	-8.1606226	TCMDC-134520	-7.7567763	TCMDC-141823	-7.487205
TCMDC-138859	-8.1599731	TCMDC-138603	-7.7567396	TCMDC-138754	-7.4868774
TCMDC-135263	-8.1598787	TCMDC-137726	-7.7562551	TCMDC-141259	-7.4862261
TCMDC-135855	-8.1590462	TCMDC-140873	-7.7559934	TCMDC-134785	-7.4860792
TCMDC-131788	-8.1579914	TCMDC-133200	-7.7559886	TCMDC-138910	-7.4851537
TCMDC-138254	-8.1567154	TCMDC-140251	-7.7556038	TCMDC-141168	-7.4849467
TCMDC-138261	-8.1566896	TCMDC-141632	-7.7552705	TCMDC-137942	-7.4848514
TCMDC-132408	-8.1566591	TCMDC-134931	-7.7551446	TCMDC-133914	-7.4845581
TCMDC-131848	-8.1566229	TCMDC-124661	-7.7550921	TCMDC-124069	-7.4844413
TCMDC-139565	-8.1563759	TCMDC-131275	-7.7550373	TCMDC-142221	-7.4844074
TCMDC-137939	-8.156352	TCMDC-141050	-7.7548909	TCMDC-132066	-7.4843016
TCMDC-133053	-8.1562834	TCMDC-132382	-7.7525787	TCMDC-134877	-7.4839973
TCMDC-138871	-8.155262	TCMDC-132062	-7.7523527	TCMDC-141899	-7.4838867
TCMDC-137826	-8.1547995	TCMDC-134749	-7.7516246	TCMDC-139264	-7.4838758
TCMDC-134758	-8.1547375	TCMDC-135209	-7.7508955	TCMDC-138472	-7.4835086
TCMDC-141327	-8.1545725	TCMDC-139175	-7.750277	TCMDC-141804	-7.4834456
TCMDC-138604	-8.1536694	TCMDC-132494	-7.7502737	TCMDC-141905	-7.4831676
TCMDC-140153	-8.1534834	TCMDC-132571	-7.7501283	TCMDC-133066	-7.4830112
TCMDC-135727	-8.1531649	TCMDC-141042	-7.7496533	TCMDC-132326	-7.4829555
TCMDC-140594	-8.1524792	TCMDC-132710	-7.7496476	TCMDC-132510	-7.4823561
TCMDC-138343	-8.152319	TCMDC-125661	-7.7491651	TCMDC-131479	-7.4820986
TCMDC-138323	-8.1523123	TCMDC-134789	-7.7488928	TCMDC-139604	-7.4818597
TCMDC-141554	-8.1518173	TCMDC-134556	-7.7488637	TCMDC-137195	-7.4817457
TCMDC-132327	-8.1516247	TCMDC-134793	-7.748734	TCMDC-124173	-7.481391
TCMDC-141301	-8.1510792	TCMDC-141610	-7.7485781	TCMDC-133954	-7.4810362
TCMDC-138832	-8.1510258	TCMDC-140831	-7.7485099	TCMDC-139961	-7.4809542
TCMDC-135496	-8.1508665	TCMDC-131343	-7.7482834	TCMDC-135689	-7.4809051
TCMDC-135416	-8.1506281	TCMDC-132323	-7.7479086	TCMDC-140657	-7.4806657
TCMDC-134572	-8.1504974	TCMDC-141769	-7.7471976	TCMDC-124953	-7.4800839
TCMDC-139474	-8.1496305	TCMDC-137503	-7.7468028	TCMDC-137905	-7.4797344
TCMDC-136506	-8.1494217	TCMDC-141613	-7.7463889	TCMDC-140709	-7.4795685
TCMDC-139680	-8.1493053	TCMDC-141093	-7.7461505	TCMDC-140061	-7.4794655

TCMDC-134309	-8.1489096	TCMDC-133708	-7.7457337	TCMDC-138543	-7.4793115
TCMDC-132250	-8.1468029	TCMDC-138534	-7.7457261	TCMDC-135338	-7.4791207
TCMDC-135108	-8.1462011	TCMDC-141701	-7.745698	TCMDC-135495	-7.4789619
TCMDC-141797	-8.1461525	TCMDC-139816	-7.7455382	TCMDC-141078	-7.4784622
TCMDC-132420	-8.1460066	TCMDC-136859	-7.745019	TCMDC-137303	-7.4784436
TCMDC-141148	-8.1452961	TCMDC-131841	-7.7449956	TCMDC-139679	-7.4783564
TCMDC-138232	-8.1451015	TCMDC-136960	-7.7447753	TCMDC-138878	-7.4780936
TCMDC-134828	-8.1447678	TCMDC-133129	-7.7447143	TCMDC-132397	-7.4777412
TCMDC-135820	-8.1439009	TCMDC-132321	-7.7437177	TCMDC-138573	-7.4776268
TCMDC-140650	-8.1437731	TCMDC-133618	-7.7434812	TCMDC-132809	-7.4776216
TCMDC-133258	-8.1436186	TCMDC-139448	-7.7431755	TCMDC-132763	-7.4775629
TCMDC-125618	-8.1428366	TCMDC-135981	-7.7424021	TCMDC-132220	-7.4774318
TCMDC-141508	-8.1427755	TCMDC-135122	-7.7423697	TCMDC-136348	-7.4774113
TCMDC-133444	-8.1426001	TCMDC-132091	-7.7421579	TCMDC-141402	-7.4772696
TCMDC-135708	-8.1425753	TCMDC-135458	-7.7412724	TCMDC-133975	-7.4772291
TCMDC-138667	-8.1422577	TCMDC-133042	-7.7412066	TCMDC-135269	-7.4769864
TCMDC-135884	-8.1422062	TCMDC-135183	-7.7409201	TCMDC-133771	-7.4759912
TCMDC-134660	-8.1420336	TCMDC-135371	-7.7407427	TCMDC-137750	-7.4756436
TCMDC-135312	-8.141902	TCMDC-137803	-7.7405348	TCMDC-139339	-7.4755259
TCMDC-138222	-8.1414804	TCMDC-137941	-7.7405119	TCMDC-139172	-7.4754024
TCMDC-138903	-8.1412659	TCMDC-141767	-7.7402263	TCMDC-135084	-7.4750862
TCMDC-140052	-8.140708	TCMDC-132269	-7.7394772	TCMDC-135651	-7.4749665
TCMDC-140150	-8.140336	TCMDC-133704	-7.7393885	TCMDC-132324	-7.4748926
TCMDC-137975	-8.1402292	TCMDC-136825	-7.739078	TCMDC-137805	-7.4748254
TCMDC-140586	-8.1401978	TCMDC-137577	-7.7386818	TCMDC-138786	-7.4747024
TCMDC-135201	-8.1386957	TCMDC-132158	-7.7385979	TCMDC-135316	-7.4745612
TCMDC-135064	-8.1385956	TCMDC-132967	-7.7385831	TCMDC-132844	-7.4743996
TCMDC-135784	-8.1385546	TCMDC-133961	-7.7374992	TCMDC-139200	-7.4743195
TCMDC-139810	-8.1384583	TCMDC-136128	-7.7372036	TCMDC-135301	-7.4742293
TCMDC-135548	-8.138032	TCMDC-139105	-7.7371712	TCMDC-135145	-7.4740219
TCMDC-137198	-8.137393	TCMDC-140496	-7.7369137	TCMDC-125790	-7.4737115
TCMDC-141773	-8.1365442	TCMDC-139225	-7.7366409	TCMDC-131278	-7.4735332
TCMDC-135541	-8.1364393	TCMDC-135246	-7.73634	TCMDC-134906	-7.4735031
TCMDC-141915	-8.1359453	TCMDC-136833	-7.7363286	TCMDC-131965	-7.4734778
TCMDC-136100	-8.1344986	TCMDC-138888	-7.736187	TCMDC-140901	-7.4732485
TCMDC-135314	-8.1344795	TCMDC-140482	-7.7359943	TCMDC-133940	-7.4730334
TCMDC-138494	-8.1341267	TCMDC-135471	-7.7357936	TCMDC-137475	-7.4722686
TCMDC-124185	-8.13381	TCMDC-135247	-7.7356939	TCMDC-135950	-7.472209
TCMDC-136259	-8.1316004	TCMDC-139094	-7.7355518	TCMDC-132874	-7.4720821
TCMDC-141507	-8.1315365	TCMDC-138087	-7.7348108	TCMDC-133193	-7.4716396
TCMDC-138228	-8.1310968	TCMDC-132556	-7.734314	TCMDC-133926	-7.4715466
TCMDC-141848	-8.1305609	TCMDC-140269	-7.7341728	TCMDC-136116	-7.4713378
TCMDC-137326	-8.1301746	TCMDC-133589	-7.7335906	TCMDC-139936	-7.4711823
TCMDC-135750	-8.1300058	TCMDC-132258	-7.733573	TCMDC-140213	-7.4711475

TCMDC-135481	-8.1299562	TCMDC-139853	-7.7335377	TCMDC-139343	-7.4709997
TCMDC-138743	-8.1299496	TCMDC-135389	-7.7335296	TCMDC-138414	-7.4709973
TCMDC-138358	-8.1294947	TCMDC-138489	-7.7332983	TCMDC-139387	-7.4706364
TCMDC-138497	-8.1294832	TCMDC-139742	-7.733264	TCMDC-139777	-7.4705181
TCMDC-138374	-8.1291409	TCMDC-136020	-7.7332006	TCMDC-135472	-7.4703302
TCMDC-138464	-8.1288414	TCMDC-135924	-7.733016	TCMDC-140892	-7.470263
TCMDC-135937	-8.1277084	TCMDC-135705	-7.7327776	TCMDC-132769	-7.4699554
TCMDC-136180	-8.1273928	TCMDC-141955	-7.7327509	TCMDC-124335	-7.4686527
TCMDC-141142	-8.1262197	TCMDC-134259	-7.7327414	TCMDC-134904	-7.4675732
TCMDC-138351	-8.1261339	TCMDC-132619	-7.7320905	TCMDC-137950	-7.4675374
TCMDC-137759	-8.1248064	TCMDC-132234	-7.7319679	TCMDC-138617	-7.4675317
TCMDC-140811	-8.1232557	TCMDC-125689	-7.7318177	TCMDC-135715	-7.4673929
TCMDC-138819	-8.1228294	TCMDC-139960	-7.7313576	TCMDC-139831	-7.4671774
TCMDC-138608	-8.1227026	TCMDC-138015	-7.7311559	TCMDC-132362	-7.4668694
TCMDC-135448	-8.1209335	TCMDC-141007	-7.730968	TCMDC-133168	-7.4668021
TCMDC-139771	-8.1205883	TCMDC-140676	-7.7306414	TCMDC-133923	-7.4667916
TCMDC-137205	-8.120491	TCMDC-141438	-7.7301807	TCMDC-141442	-7.4666638
TCMDC-132164	-8.1196718	TCMDC-133773	-7.7297163	TCMDC-138442	-7.4663925
TCMDC-135916	-8.1192017	TCMDC-140866	-7.7296076	TCMDC-141492	-7.466146
TCMDC-135432	-8.1191559	TCMDC-136860	-7.7293911	TCMDC-133320	-7.4660487
TCMDC-133324	-8.1186419	TCMDC-124956	-7.7293859	TCMDC-140384	-7.465353
TCMDC-138528	-8.1182899	TCMDC-132157	-7.7291164	TCMDC-134792	-7.4647694
TCMDC-134993	-8.1169109	TCMDC-123853	-7.7290993	TCMDC-140323	-7.4647341
TCMDC-141537	-8.1168804	TCMDC-132910	-7.7290349	TCMDC-139741	-7.4646211
TCMDC-138283	-8.1161118	TCMDC-133871	-7.7286563	TCMDC-133703	-7.4644766
TCMDC-138569	-8.1160116	TCMDC-139162	-7.7283053	TCMDC-133076	-7.4642792
TCMDC-138773	-8.1159668	TCMDC-132284	-7.7275534	TCMDC-133272	-7.4638748
TCMDC-136501	-8.1155367	TCMDC-140853	-7.7275043	TCMDC-138712	-7.4630299
TCMDC-131958	-8.1138916	TCMDC-139035	-7.7270279	TCMDC-141021	-7.462975
TCMDC-137184	-8.1131859	TCMDC-138399	-7.7265506	TCMDC-124190	-7.4626698
TCMDC-137853	-8.1127844	TCMDC-134929	-7.7262206	TCMDC-133435	-7.4625759
TCMDC-135400	-8.1112642	TCMDC-141084	-7.7259417	TCMDC-133956	-7.4619546
TCMDC-141246	-8.1110058	TCMDC-141951	-7.7257853	TCMDC-134144	-7.4619179
TCMDC-140568	-8.110836	TCMDC-124470	-7.7253523	TCMDC-132732	-7.4607644
TCMDC-135858	-8.1106186	TCMDC-137483	-7.7253084	TCMDC-132253	-7.4606462
TCMDC-140961	-8.1101847	TCMDC-138477	-7.7250328	TCMDC-140020	-7.4606247
TCMDC-131552	-8.1095972	TCMDC-124247	-7.7249751	TCMDC-132349	-7.4604692
TCMDC-139473	-8.1092863	TCMDC-140348	-7.7249074	TCMDC-140517	-7.4599533
TCMDC-136251	-8.1087265	TCMDC-140855	-7.7249064	TCMDC-137048	-7.4599099
TCMDC-139654	-8.1073008	TCMDC-124786	-7.7248793	TCMDC-133680	-7.4594154
TCMDC-140886	-8.1065626	TCMDC-140173	-7.7244134	TCMDC-134455	-7.4592905
TCMDC-135290	-8.1062994	TCMDC-133328	-7.7243924	TCMDC-138107	-7.4592767
TCMDC-135352	-8.1058941	TCMDC-133270	-7.7242756	TCMDC-125165	-7.4591537
TCMDC-138761	-8.1057644	TCMDC-134328	-7.7238421	TCMDC-135680	-7.4588642

TCMDC-141798	-8.105628	TCMDC-141165	-7.7236419	TCMDC-132214	-7.4587731
TCMDC-135063	-8.104991	TCMDC-134140	-7.7235589	TCMDC-134871	-7.4587584
TCMDC-132479	-8.1048613	TCMDC-135761	-7.7231088	TCMDC-132682	-7.4585128
TCMDC-140592	-8.1042871	TCMDC-139091	-7.7226257	TCMDC-140649	-7.4583874
TCMDC-140579	-8.1039858	TCMDC-132296	-7.7223649	TCMDC-139945	-7.4582858
TCMDC-134847	-8.1037607	TCMDC-138571	-7.7217989	TCMDC-140214	-7.4582572
TCMDC-140879	-8.1035023	TCMDC-124033	-7.7211208	TCMDC-134858	-7.4581628
TCMDC-133627	-8.102066	TCMDC-139763	-7.7208886	TCMDC-132082	-7.4580631
TCMDC-140527	-8.10147	TCMDC-135701	-7.7202539	TCMDC-140665	-7.4575796
TCMDC-134543	-8.1013966	TCMDC-124125	-7.7197943	TCMDC-139282	-7.4570746
TCMDC-140053	-8.1000299	TCMDC-139996	-7.7193937	TCMDC-132936	-7.4568944
TCMDC-135390	-8.1000252	TCMDC-141045	-7.7192988	TCMDC-137078	-7.4564118
TCMDC-138856	-8.099472	TCMDC-133291	-7.7192168	TCMDC-132877	-7.4557576
TCMDC-135424	-8.0993719	TCMDC-141903	-7.7189293	TCMDC-137213	-7.455534
TCMDC-135887	-8.0988235	TCMDC-138363	-7.7186947	TCMDC-133276	-7.4548588
TCMDC-138630	-8.098568	TCMDC-138545	-7.7183475	TCMDC-141944	-7.4548078
TCMDC-135282	-8.0984764	TCMDC-141427	-7.7181301	TCMDC-139484	-7.4548078
TCMDC-134176	-8.098465	TCMDC-133684	-7.7179675	TCMDC-136552	-7.4547548
TCMDC-139923	-8.0970087	TCMDC-141161	-7.7178974	TCMDC-140099	-7.4545989
TCMDC-134701	-8.0968533	TCMDC-140573	-7.717515	TCMDC-135762	-7.454565
TCMDC-138847	-8.0964546	TCMDC-137838	-7.7175145	TCMDC-134935	-7.4544339
TCMDC-138147	-8.0957527	TCMDC-135903	-7.7173533	TCMDC-140481	-7.4540682
TCMDC-131919	-8.0956402	TCMDC-136722	-7.7173233	TCMDC-140320	-7.4537745
TCMDC-135557	-8.0955973	TCMDC-135711	-7.7172914	TCMDC-139235	-7.453589
TCMDC-132506	-8.0955124	TCMDC-133205	-7.7172599	TCMDC-138674	-7.4534774
TCMDC-135544	-8.0947208	TCMDC-138438	-7.7169671	TCMDC-139293	-7.4532638
TCMDC-140476	-8.0947123	TCMDC-136915	-7.716465	TCMDC-133594	-7.4532557
TCMDC-135780	-8.0942841	TCMDC-141787	-7.715929	TCMDC-141306	-7.4532189
TCMDC-140626	-8.0929508	TCMDC-133009	-7.7157788	TCMDC-141571	-7.4531932
TCMDC-138762	-8.0927658	TCMDC-134665	-7.7150292	TCMDC-135040	-7.4524012
TCMDC-140986	-8.0916958	TCMDC-134787	-7.7147903	TCMDC-132765	-7.4520531
TCMDC-133707	-8.0913	TCMDC-135809	-7.7145705	TCMDC-132469	-7.4519157
TCMDC-136850	-8.0911045	TCMDC-131938	-7.7143135	TCMDC-140644	-7.4518924
TCMDC-134664	-8.0910378	TCMDC-133014	-7.7142124	TCMDC-132917	-7.4517488
TCMDC-134174	-8.0897112	TCMDC-141529	-7.7141542	TCMDC-137034	-7.4517159
TCMDC-134193	-8.0895777	TCMDC-141703	-7.7134924	TCMDC-136885	-7.4514771
TCMDC-141929	-8.0891905	TCMDC-132311	-7.7133684	TCMDC-133183	-7.451457
TCMDC-140602	-8.0891285	TCMDC-139242	-7.7132697	TCMDC-133610	-7.4514084
TCMDC-141125	-8.08885	TCMDC-132993	-7.7131243	TCMDC-139969	-7.4510612
TCMDC-135847	-8.0885134	TCMDC-135844	-7.7131124	TCMDC-136684	-7.4507732
TCMDC-133112	-8.0877085	TCMDC-140578	-7.7130661	TCMDC-140681	-7.4507327
TCMDC-135536	-8.0868311	TCMDC-125301	-7.7126322	TCMDC-138548	-7.4503121
TCMDC-133142	-8.0864897	TCMDC-140156	-7.7124076	TCMDC-140283	-7.4502187
TCMDC-141574	-8.0863571	TCMDC-135734	-7.712286	TCMDC-134394	-7.4499712

TCMDC-138478	-8.0862684	TCMDC-137619	-7.7120309	TCMDC-132679	-7.4499669
TCMDC-135509	-8.0860901	TCMDC-138198	-7.7118444	TCMDC-134620	-7.4498553
TCMDC-132754	-8.0858793	TCMDC-135679	-7.7115664	TCMDC-139889	-7.4494672
TCMDC-139867	-8.0849676	TCMDC-139302	-7.7114754	TCMDC-136858	-7.449234
TCMDC-139614	-8.0843906	TCMDC-134886	-7.7113142	TCMDC-140107	-7.4489646
TCMDC-134129	-8.0836725	TCMDC-134483	-7.7111225	TCMDC-140172	-7.4487295
TCMDC-132728	-8.0835676	TCMDC-136831	-7.7111015	TCMDC-140728	-7.4479785
TCMDC-131602	-8.0826807	TCMDC-141547	-7.7109418	TCMDC-125702	-7.4477983
TCMDC-137673	-8.0825853	TCMDC-141615	-7.7099643	TCMDC-132024	-7.4473934
TCMDC-135050	-8.0823603	TCMDC-133928	-7.7098918	TCMDC-137480	-7.4466085
TCMDC-132782	-8.0822439	TCMDC-136106	-7.7097921	TCMDC-134421	-7.4465542
TCMDC-131962	-8.08144	TCMDC-137817	-7.7094078	TCMDC-139082	-7.4461246
TCMDC-138453	-8.0802956	TCMDC-135170	-7.708879	TCMDC-141932	-7.4460106
TCMDC-138288	-8.0797272	TCMDC-137745	-7.7088218	TCMDC-133675	-7.4458241
TCMDC-137627	-8.0794258	TCMDC-131855	-7.7085519	TCMDC-139386	-7.4457211
TCMDC-135030	-8.0790529	TCMDC-137481	-7.7082977	TCMDC-136570	-7.4457045
TCMDC-133056	-8.0790062	TCMDC-139684	-7.7080002	TCMDC-133321	-7.4453878
TCMDC-141563	-8.0784817	TCMDC-139389	-7.7078943	TCMDC-136238	-7.4445124
TCMDC-135891	-8.0779324	TCMDC-139230	-7.7078576	TCMDC-140540	-7.4445119
TCMDC-138236	-8.0758982	TCMDC-138475	-7.7062559	TCMDC-137104	-7.4443884
TCMDC-125617	-8.075182	TCMDC-140874	-7.7056775	TCMDC-139063	-7.4438529
TCMDC-133371	-8.0746565	TCMDC-125688	-7.7052913	TCMDC-135078	-7.4437943
TCMDC-139370	-8.0735216	TCMDC-141157	-7.7049336	TCMDC-135076	-7.4433823
TCMDC-137966	-8.0733414	TCMDC-133534	-7.7047424	TCMDC-134713	-7.4433446
TCMDC-140005	-8.0733175	TCMDC-138691	-7.7045741	TCMDC-140018	-7.443141
TCMDC-141645	-8.0720043	TCMDC-140347	-7.704453	TCMDC-134738	-7.4428711
TCMDC-140500	-8.0719147	TCMDC-133057	-7.70399	TCMDC-137135	-7.4427304
TCMDC-138215	-8.0716648	TCMDC-139849	-7.7032838	TCMDC-132379	-7.4427252
TCMDC-132565	-8.0715675	TCMDC-136119	-7.7032294	TCMDC-138979	-7.4427052
TCMDC-134403	-8.0714455	TCMDC-141030	-7.7029786	TCMDC-140338	-7.4421535
TCMDC-138756	-8.071353	TCMDC-138600	-7.7029381	TCMDC-124446	-7.4418669
TCMDC-140983	-8.0708179	TCMDC-140822	-7.7027617	TCMDC-136469	-7.441298
TCMDC-133939	-8.0705605	TCMDC-134516	-7.7027349	TCMDC-138145	-7.4408422
TCMDC-132884	-8.0701818	TCMDC-140532	-7.7020206	TCMDC-137175	-7.4402461
TCMDC-138366	-8.0700693	TCMDC-135833	-7.7019219	TCMDC-132916	-7.4400516
TCMDC-139930	-8.0696325	TCMDC-135659	-7.7015805	TCMDC-139087	-7.4398084
TCMDC-132272	-8.0675192	TCMDC-140847	-7.7015386	TCMDC-133092	-7.4395938
TCMDC-138692	-8.0672226	TCMDC-132133	-7.701323	TCMDC-138388	-7.4394207
TCMDC-141122	-8.0667276	TCMDC-134776	-7.7007279	TCMDC-138880	-7.4394021
TCMDC-141026	-8.0664005	TCMDC-134435	-7.7005167	TCMDC-132860	-7.4391546
TCMDC-140277	-8.0663576	TCMDC-139695	-7.7004828	TCMDC-141900	-7.4390993
TCMDC-138700	-8.0662689	TCMDC-136821	-7.7002745	TCMDC-132262	-7.4384317
TCMDC-140006	-8.0661879	TCMDC-135571	-7.7002397	TCMDC-141303	-7.4378624
TCMDC-141638	-8.0658598	TCMDC-137171	-7.6999621	TCMDC-134444	-7.4378605

TCMDC-141484	-8.065814	TCMDC-138830	-7.6994753	TCMDC-140235	-7.4376287
TCMDC-135759	-8.0658026	TCMDC-137953	-7.6990781	TCMDC-133843	-7.4375176
TCMDC-139628	-8.0638685	TCMDC-135349	-7.6987739	TCMDC-140182	-7.4374614
TCMDC-138739	-8.0638533	TCMDC-141153	-7.6986208	TCMDC-132613	-7.4373159
TCMDC-141685	-8.0635118	TCMDC-136497	-7.6983528	TCMDC-124380	-7.4372983
TCMDC-136720	-8.0632038	TCMDC-136123	-7.6981974	TCMDC-134519	-7.4371538
TCMDC-141553	-8.062974	TCMDC-135138	-7.6980724	TCMDC-138706	-7.4371495
TCMDC-141225	-8.0625095	TCMDC-135710	-7.6972947	TCMDC-141403	-7.4370618
TCMDC-137458	-8.0622158	TCMDC-135035	-7.6972508	TCMDC-139137	-7.4366059
TCMDC-125723	-8.0619202	TCMDC-138206	-7.697228	TCMDC-140227	-7.4358969
TCMDC-141150	-8.0612135	TCMDC-136287	-7.6958289	TCMDC-137531	-7.435874
TCMDC-136255	-8.0610132	TCMDC-138595	-7.6954122	TCMDC-125849	-7.4357934
TCMDC-138444	-8.0609484	TCMDC-136712	-7.6953702	TCMDC-132935	-7.4356484
TCMDC-138235	-8.0605831	TCMDC-134548	-7.6952925	TCMDC-138124	-7.4355001
TCMDC-140286	-8.0603495	TCMDC-141430	-7.6951752	TCMDC-137815	-7.4351926
TCMDC-136195	-8.0602589	TCMDC-132458	-7.6950188	TCMDC-133339	-7.4350042
TCMDC-140551	-8.059701	TCMDC-132558	-7.6947436	TCMDC-140362	-7.4348221
TCMDC-136678	-8.0591059	TCMDC-133903	-7.6946616	TCMDC-134682	-7.4345407
TCMDC-132347	-8.0586157	TCMDC-137981	-7.6942263	TCMDC-139894	-7.4344001
TCMDC-141166	-8.05861	TCMDC-139069	-7.6940665	TCMDC-133795	-7.4342008
TCMDC-141601	-8.058547	TCMDC-138660	-7.6934304	TCMDC-136945	-7.4340463
TCMDC-141509	-8.0584707	TCMDC-133278	-7.693295	TCMDC-139121	-7.4339991
TCMDC-135376	-8.0581827	TCMDC-132478	-7.692039	TCMDC-138053	-7.4338984
TCMDC-140421	-8.0580912	TCMDC-138515	-7.6919193	TCMDC-138647	-7.4338288
TCMDC-140218	-8.0576143	TCMDC-140408	-7.6917253	TCMDC-132717	-7.4338078
TCMDC-137163	-8.0572948	TCMDC-136091	-7.691658	TCMDC-131627	-7.4337478
TCMDC-138317	-8.0555773	TCMDC-139490	-7.6914186	TCMDC-132375	-7.4336209
TCMDC-138462	-8.0546322	TCMDC-140757	-7.6911211	TCMDC-137160	-7.4332323
TCMDC-138672	-8.0538683	TCMDC-136064	-7.6907573	TCMDC-134800	-7.4331422
TCMDC-135152	-8.0531931	TCMDC-139107	-7.6907415	TCMDC-137114	-7.4331212
TCMDC-138584	-8.0525417	TCMDC-140017	-7.6905861	TCMDC-137222	-7.4331107
TCMDC-138805	-8.0525112	TCMDC-140797	-7.6900096	TCMDC-132115	-7.4330697
TCMDC-138359	-8.0521841	TCMDC-138814	-7.6899152	TCMDC-136548	-7.4329023
TCMDC-132112	-8.0521212	TCMDC-135899	-7.6898756	TCMDC-140786	-7.4328794
TCMDC-135773	-8.0519276	TCMDC-132973	-7.6887565	TCMDC-140328	-7.432179
TCMDC-138585	-8.0518951	TCMDC-136690	-7.688488	TCMDC-140400	-7.4319186
TCMDC-132211	-8.0509043	TCMDC-131560	-7.6883163	TCMDC-139781	-7.4317508
TCMDC-134677	-8.0508671	TCMDC-138925	-7.6879139	TCMDC-133681	-7.4315548
TCMDC-138806	-8.0506773	TCMDC-141011	-7.6878133	TCMDC-136718	-7.4312792
TCMDC-140330	-8.0506325	TCMDC-136115	-7.687479	TCMDC-140329	-7.4311185
TCMDC-141420	-8.0504417	TCMDC-141136	-7.6873751	TCMDC-134777	-7.4308829
TCMDC-138003	-8.0498409	TCMDC-136865	-7.6860909	TCMDC-138255	-7.4308462
TCMDC-141620	-8.0496664	TCMDC-141040	-7.6857958	TCMDC-132913	-7.4307661
TCMDC-133387	-8.049449	TCMDC-138428	-7.6849294	TCMDC-140377	-7.4306574

TCMDC-134529	-8.049367	TCMDC-136911	-7.6846428	TCMDC-135065	-7.4303489
TCMDC-136243	-8.0491972	TCMDC-135315	-7.6842203	TCMDC-136921	-7.4298854
TCMDC-141559	-8.0490141	TCMDC-135722	-7.6841521	TCMDC-133004	-7.4297824
TCMDC-141779	-8.048789	TCMDC-125055	-7.6840286	TCMDC-140168	-7.4296174
TCMDC-138218	-8.0482826	TCMDC-133963	-7.6837854	TCMDC-124691	-7.4295793
TCMDC-139691	-8.047678	TCMDC-139946	-7.68361	TCMDC-136525	-7.4294944
TCMDC-135414	-8.0467167	TCMDC-134760	-7.6835036	TCMDC-140897	-7.4294744
TCMDC-135045	-8.0463829	TCMDC-133150	-7.6832957	TCMDC-134249	-7.4291992
TCMDC-141061	-8.0461378	TCMDC-139897	-7.6821842	TCMDC-139566	-7.4289193
TCMDC-136299	-8.0460644	TCMDC-134396	-7.6820016	TCMDC-133924	-7.4287834
TCMDC-137958	-8.0458126	TCMDC-136965	-7.681232	TCMDC-141562	-7.4285655
TCMDC-138013	-8.0458097	TCMDC-135619	-7.6812015	TCMDC-139814	-7.4285603
TCMDC-134126	-8.0443478	TCMDC-138171	-7.681006	TCMDC-134812	-7.4283533
TCMDC-134706	-8.0429659	TCMDC-135633	-7.6799412	TCMDC-136980	-7.4282722
TCMDC-135348	-8.0429506	TCMDC-124182	-7.6794391	TCMDC-135757	-7.4282207
TCMDC-141891	-8.0422087	TCMDC-140121	-7.6788578	TCMDC-135080	-7.4275007
TCMDC-133535	-8.0416975	TCMDC-140675	-7.67801	TCMDC-132857	-7.4274392
TCMDC-135763	-8.0410538	TCMDC-140174	-7.6776719	TCMDC-138785	-7.4273739
TCMDC-138289	-8.0408936	TCMDC-136124	-7.6775064	TCMDC-140732	-7.4273167
TCMDC-134647	-8.040556	TCMDC-140746	-7.6773477	TCMDC-134285	-7.4270573
TCMDC-141689	-8.0379353	TCMDC-139620	-7.6772981	TCMDC-140232	-7.4266591
TCMDC-137776	-8.0375957	TCMDC-138631	-7.6770492	TCMDC-135055	-7.4260902
TCMDC-135783	-8.0359869	TCMDC-134790	-7.6768975	TCMDC-132148	-7.4259148
TCMDC-142228	-6.1689725	TCMDC-138728	-7.6762328	TCMDC-138820	-7.425581
TCMDC-136655	-6.7919173	TCMDC-135942	-6.5339069		
TCMDC-125778	-6.7917814	TCMDC-137014	-6.5336938		
TCMDC-138509	-6.7917166	TCMDC-124911	-6.5336428		
TCMDC-131737	-6.7910972	TCMDC-138128	-6.5336113		
TCMDC-138284	-6.7909322	TCMDC-140754	-6.533525		
TCMDC-133496	-6.7907186	TCMDC-125361	-6.5331616		
TCMDC-123888	-6.7900281	TCMDC-135243	-6.5331264		
TCMDC-140086	-6.7895441	TCMDC-133897	-6.5326538		
TCMDC-133927	-6.7893252	TCMDC-133566	-6.5324101		
TCMDC-132932	-6.7892504	TCMDC-132786	-6.5323625		
TCMDC-125537	-6.7891955	TCMDC-133667	-6.5320821		
TCMDC-133657	-6.7891679	TCMDC-124611	-6.5308394		
TCMDC-137485	-6.7889895	TCMDC-131832	-6.5302448		
TCMDC-138485	-6.7885895	TCMDC-136335	-6.5302367		
TCMDC-136705	-6.7884793	TCMDC-125150	-6.5300531		
TCMDC-131527	-6.7882743	TCMDC-125192	-6.5298276		
TCMDC-132739	-6.7880883	TCMDC-141336	-6.5297461		
TCMDC-135943	-6.7880735	TCMDC-131651	-6.5292115		
TCMDC-141998	-6.7880564	TCMDC-125823	-6.5292048		
TCMDC-125456	-6.7880068	TCMDC-140299	-6.5290952		

TCMDC-124616	-6.7878833	TCMDC-132833	-6.5290122		
TCMDC-138336	-6.7876191	TCMDC-137754	-6.5288167		
TCMDC-125572	-6.7871723	TCMDC-123913	-6.5288138		
TCMDC-139441	-6.787024	TCMDC-124243	-6.5286522		
TCMDC-132705	-6.7864146	TCMDC-135560	-6.5280113		
TCMDC-131511	-6.7861271	TCMDC-140506	-6.5278296		
TCMDC-142205	-6.7860465	TCMDC-125155	-6.5274906		
TCMDC-134104	-6.7856264	TCMDC-123745	-6.5274429		
TCMDC-140456	-6.7855501	TCMDC-125072	-6.5273108		
TCMDC-123892	-6.7854953	TCMDC-138008	-6.5268059		
TCMDC-140013	-6.7853951	TCMDC-131746	-6.5262146		
TCMDC-123648	-6.7850637	TCMDC-140144	-6.5257168		
TCMDC-141362	-6.7849073	TCMDC-135102	-6.5253897		
TCMDC-139478	-6.7846146	TCMDC-136377	-6.5250721		
TCMDC-124533	-6.7842255	TCMDC-123677	-6.5246511		
TCMDC-142318	-6.784059	TCMDC-134281	-6.5241256		
TCMDC-125098	-6.7839479	TCMDC-124619	-6.523931		
TCMDC-136336	-6.7835422	TCMDC-140717	-6.5237002		
TCMDC-136344	-6.7834735	TCMDC-136500	-6.5235195		
TCMDC-140014	-6.7830758	TCMDC-134162	-6.5232019		
TCMDC-133488	-6.7829881	TCMDC-131421	-6.5231366		
TCMDC-141207	-6.7829103	TCMDC-133993	-6.5229664		
TCMDC-123643	-6.782423	TCMDC-135419	-6.5228724		
TCMDC-136999	-6.7817388	TCMDC-131827	-6.5228047		
TCMDC-125203	-6.7815027	TCMDC-141740	-6.522613		
TCMDC-131978	-6.7814732	TCMDC-140495	-6.5222731		
TCMDC-133603	-6.7813759	TCMDC-142294	-6.5218954		
TCMDC-123614	-6.7811298	TCMDC-140452	-6.5212555		
TCMDC-133989	-6.7809896	TCMDC-139489	-6.5207014		
TCMDC-131253	-6.7808318	TCMDC-134492	-6.5200367		
TCMDC-133588	-6.780767	TCMDC-124201	-6.5196805		
TCMDC-132315	-6.7805619	TCMDC-141672	-6.5194564		
TCMDC-132591	-6.7804017	TCMDC-142188	-6.5193753		
TCMDC-131999	-6.7802057	TCMDC-136580	-6.5193377		
TCMDC-138346	-6.7802024	TCMDC-136747	-6.5193286		
TCMDC-131363	-6.7796655	TCMDC-125079	-6.5189972		
TCMDC-140241	-6.779531	TCMDC-125100	-6.5188589		
TCMDC-136320	-6.7793097	TCMDC-123796	-6.5185089		
TCMDC-124189	-6.7792521	TCMDC-141677	-6.5183878		
TCMDC-138411	-6.779109	TCMDC-136217	-6.5183392		
TCMDC-138375	-6.778924	TCMDC-133476	-6.5181317		
TCMDC-133097	-6.7788906	TCMDC-125495	-6.5173159		
TCMDC-140313	-6.7788892	TCMDC-139132	-6.5172806		
TCMDC-140942	-6.7785425	TCMDC-134419	-6.5167189		

TCMDC-123568	-6.7782378	TCMDC-124698	-6.5166583		
TCMDC-136167	-6.7777314	TCMDC-132737	-6.5159173		
TCMDC-135554	-6.7776818	TCMDC-125199	-6.5157547		
TCMDC-135118	-6.7776351	TCMDC-131347	-6.5154095		
TCMDC-123891	-6.7774906	TCMDC-136877	-6.515286		
TCMDC-135460	-6.7774305	TCMDC-141500	-6.5152421		
TCMDC-124076	-6.7769885	TCMDC-138209	-6.5150614		
TCMDC-125834	-6.7768145	TCMDC-135994	-6.5148602		
TCMDC-136971	-6.7762346	TCMDC-123755	-6.5147309		
TCMDC-134958	-6.7761021	TCMDC-131954	-6.5142097		
TCMDC-133856	-6.7756281	TCMDC-125259	-6.5137725		
TCMDC-137287	-6.7751942	TCMDC-132803	-6.5127993		
TCMDC-124742	-6.7751484	TCMDC-136536	-6.5124955		
TCMDC-131766	-6.7749419	TCMDC-124210	-6.5115657		
TCMDC-141039	-6.7749085	TCMDC-142051	-6.5112195		
TCMDC-131256	-6.7743983	TCMDC-137301	-6.5110445		
TCMDC-124519	-6.7741418	TCMDC-124292	-6.511024		
TCMDC-133105	-6.7738414	TCMDC-135484	-6.5109882		
TCMDC-133869	-6.7736239	TCMDC-142236	-6.5107675		
TCMDC-125020	-6.7732582	TCMDC-137493	-6.5104885		
TCMDC-139350	-6.7731638	TCMDC-125648	-6.5093279		
TCMDC-139420	-6.772934	TCMDC-142199	-6.5091715		
TCMDC-125794	-6.7725406	TCMDC-124313	-6.5089874		
TCMDC-124114	-6.7723136	TCMDC-124694	-6.5084953		
TCMDC-125194	-6.7721982	TCMDC-125308	-6.5083137		
TCMDC-135022	-6.7712421	TCMDC-141981	-6.5082321		
TCMDC-123709	-6.7710538	TCMDC-124129	-6.507906		
TCMDC-123732	-6.7708359	TCMDC-125064	-6.5065408		
TCMDC-138405	-6.7705083	TCMDC-137015	-6.5065298		
TCMDC-140139	-6.7703414	TCMDC-124331	-6.5063643		
TCMDC-139908	-6.7703147	TCMDC-137882	-6.506125		
TCMDC-141288	-6.7701831	TCMDC-140444	-6.5058236		
TCMDC-135044	-6.7696877	TCMDC-141094	-6.5056567		
TCMDC-134949	-6.7679439	TCMDC-124690	-6.5052357		
TCMDC-135623	-6.7675781	TCMDC-131784	-6.5047908		
TCMDC-133575	-6.767447	TCMDC-134717	-6.5031304		
TCMDC-133755	-6.7668829	TCMDC-136961	-6.5029726		
TCMDC-136688	-6.7666855	TCMDC-123899	-6.5028257		
TCMDC-140386	-6.7663226	TCMDC-142274	-6.5025568		
TCMDC-135637	-6.7663097	TCMDC-136937	-6.5024858		
TCMDC-139123	-6.7655258	TCMDC-141733	-6.5023575		
TCMDC-136004	-6.7652097	TCMDC-136880	-6.5019684		
TCMDC-138449	-6.7651062	TCMDC-141416	-6.5018578		
TCMDC-136872	-6.7647309	TCMDC-139788	-6.5018377		

TCMDC-132464	-6.7643895	TCMDC-140360	-6.5015864		
TCMDC-132886	-6.7643809	TCMDC-131483	-6.5011921		
TCMDC-131791	-6.7643514	TCMDC-136086	-6.5010471		
TCMDC-131442	-6.7640023	TCMDC-125498	-6.5008054		
TCMDC-134037	-6.7639227	TCMDC-123775	-6.5004416		
TCMDC-136496	-6.7638044	TCMDC-136316	-6.5004015		
TCMDC-136032	-6.7637935	TCMDC-125652	-6.4997296		
TCMDC-136025	-6.7636676	TCMDC-131594	-6.49962		
TCMDC-138886	-6.7634082	TCMDC-131360	-6.4985633		
TCMDC-133224	-6.7632232	TCMDC-140467	-6.4982929		
TCMDC-136576	-6.7629266	TCMDC-131703	-6.4974713		
TCMDC-135289	-6.7628813	TCMDC-140795	-6.4971094		
TCMDC-135607	-6.7627497	TCMDC-124524	-6.4967732		
TCMDC-136219	-6.7625918	TCMDC-124017	-6.4961281		
TCMDC-140162	-6.7614841	TCMDC-133710	-6.4956403		
TCMDC-136673	-6.7612629	TCMDC-134835	-6.4950724		
TCMDC-136230	-6.7611971	TCMDC-135254	-6.4949198		
TCMDC-131941	-6.7610416	TCMDC-131842	-6.4947433		
TCMDC-133333	-6.7604084	TCMDC-124343	-6.4943604		
TCMDC-139368	-6.7599931	TCMDC-123893	-6.4942455		
TCMDC-133207	-6.7598152	TCMDC-137644	-6.494173		
TCMDC-136473	-6.7597785	TCMDC-124701	-6.4939203		
TCMDC-139108	-6.7597461	TCMDC-123564	-6.493855		
TCMDC-131500	-6.7596831	TCMDC-133568	-6.4937372		
TCMDC-124789	-6.7596579	TCMDC-138586	-6.4933705		
TCMDC-133554	-6.7592382	TCMDC-139783	-6.4928465		
TCMDC-124927	-6.7590346	TCMDC-131681	-6.4920239		
TCMDC-125447	-6.758862	TCMDC-124528	-6.4918523		
TCMDC-133533	-6.7582421	TCMDC-142299	-6.4916606		
TCMDC-139752	-6.757925	TCMDC-135308	-6.4912801		
TCMDC-124309	-6.7578158	TCMDC-131368	-6.4909639		
TCMDC-138959	-6.7574267	TCMDC-125009	-6.4898996		
TCMDC-141461	-6.7570457	TCMDC-131765	-6.4896593		
TCMDC-139403	-6.7569609	TCMDC-124885	-6.4890108		
TCMDC-133766	-6.7566562	TCMDC-125206	-6.4890041		
TCMDC-131751	-6.7562895	TCMDC-141423	-6.4886208		
TCMDC-134165	-6.7560954	TCMDC-124025	-6.4883695		
TCMDC-125621	-6.756031	TCMDC-133507	-6.4881787		
TCMDC-139713	-6.7556696	TCMDC-133658	-6.4881434		
TCMDC-138404	-6.7553496	TCMDC-136197	-6.4879599		
TCMDC-141746	-6.7551508	TCMDC-140073	-6.4879427		
TCMDC-136710	-6.7549591	TCMDC-140378	-6.4876552		
TCMDC-125183	-6.7546272	TCMDC-140411	-6.4865675		
TCMDC-125363	-6.7544556	TCMDC-123559	-6.4865575		

TCMDC-136962	-6.7540264	TCMDC-139052	-6.4863038		
TCMDC-134555	-6.7538509	TCMDC-124793	-6.4859023		
TCMDC-139347	-6.7538004	TCMDC-139288	-6.4858279		
TCMDC-133485	-6.7536898	TCMDC-125672	-6.4858098		
TCMDC-136006	-6.753037	TCMDC-133400	-6.4856167		
TCMDC-132866	-6.7526956	TCMDC-131653	-6.4852686		
TCMDC-139060	-6.7523193	TCMDC-135582	-6.4840035		
TCMDC-135579	-6.7518687	TCMDC-138597	-6.4830546		
TCMDC-133632	-6.7513852	TCMDC-124702	-6.4830165		
TCMDC-131629	-6.7513342	TCMDC-136495	-6.4826436		
TCMDC-125131	-6.7511268	TCMDC-135513	-6.4825583		
TCMDC-135596	-6.7508225	TCMDC-135861	-6.4824066		
TCMDC-135586	-6.7506666	TCMDC-142321	-6.4821749		
TCMDC-136345	-6.7504244	TCMDC-133483	-6.48209		
TCMDC-133576	-6.7492833	TCMDC-125565	-6.4818645		
TCMDC-135101	-6.7490954	TCMDC-141074	-6.4816804		
TCMDC-134001	-6.7486768	TCMDC-125875	-6.4815278		
TCMDC-133402	-6.7486286	TCMDC-135577	-6.4810066		
TCMDC-124497	-6.748342	TCMDC-123814	-6.4809456		
TCMDC-140257	-6.7482729	TCMDC-125379	-6.4808588		
TCMDC-125102	-6.7482653	TCMDC-135608	-6.4807677		
TCMDC-133794	-6.7480841	TCMDC-123884	-6.4806776		
TCMDC-124384	-6.74787	TCMDC-123914	-6.4801335		
TCMDC-134231	-6.7477932	TCMDC-139401	-6.4796696		
TCMDC-137224	-6.7474494	TCMDC-125421	-6.4794803		
TCMDC-133071	-6.7471566	TCMDC-133668	-6.4791522		
TCMDC-140023	-6.7470589	TCMDC-123687	-6.4791451		
TCMDC-141959	-6.7470312	TCMDC-125217	-6.4786181		
TCMDC-124838	-6.7469449	TCMDC-135813	-6.4785538		
TCMDC-137004	-6.7467885	TCMDC-124791	-6.478229		
TCMDC-132419	-6.7463646	TCMDC-133653	-6.4774175		
TCMDC-141237	-6.7457905	TCMDC-135641	-6.4771953		
TCMDC-140564	-6.7454162	TCMDC-136545	-6.4769464		
TCMDC-124246	-6.7449641	TCMDC-137798	-6.476521		
TCMDC-124382	-6.7448425	TCMDC-131337	-6.4759803		
TCMDC-138335	-6.7446613	TCMDC-139624	-6.4758186		
TCMDC-137587	-6.7440662	TCMDC-124645	-6.4756179		
TCMDC-140402	-6.7438912	TCMDC-123695	-6.4755926		
TCMDC-141143	-6.7429295	TCMDC-140387	-6.4754448		
TCMDC-124642	-6.7428288	TCMDC-137009	-6.4752698		
TCMDC-125613	-6.7428041	TCMDC-123537	-6.4752531		
TCMDC-125204	-6.7427096	TCMDC-131307	-6.4750943		
TCMDC-141942	-6.7426524	TCMDC-131313	-6.4746165		
TCMDC-123617	-6.7425079	TCMDC-135486	-6.4735441		

TCMDC-132201	-6.7424679	TCMDC-133907	-6.473208		
TCMDC-123553	-6.7419147	TCMDC-139101	-6.4731188		
TCMDC-138642	-6.7418513	TCMDC-140223	-6.4724436		
TCMDC-124097	-6.7415261	TCMDC-124345	-6.4723744		
TCMDC-134488	-6.7414427	TCMDC-125763	-6.4721098		
TCMDC-141046	-6.7414198	TCMDC-140437	-6.4712634		
TCMDC-142265	-6.7409668	TCMDC-138988	-6.4710793		
TCMDC-134157	-6.74051	TCMDC-124315	-6.4710569		
TCMDC-131756	-6.740344	TCMDC-141501	-6.4710159		
TCMDC-132647	-6.7399325	TCMDC-139395	-6.4709711		
TCMDC-138670	-6.7389913	TCMDC-135606	-6.4704862		
TCMDC-125018	-6.7386365	TCMDC-136888	-6.469975		
TCMDC-123590	-6.7383132	TCMDC-132998	-6.4699292		
TCMDC-133403	-6.7377758	TCMDC-139782	-6.4697351		
TCMDC-124844	-6.7376928	TCMDC-133579	-6.466784		
TCMDC-134318	-6.7373533	TCMDC-125813	-6.4664545		
TCMDC-123498	-6.7373276	TCMDC-125375	-6.4664106		
TCMDC-136583	-6.7369623	TCMDC-134195	-6.466404		
TCMDC-140131	-6.7367315	TCMDC-140765	-6.4655638		
TCMDC-135126	-6.73669	TCMDC-123970	-6.465416		
TCMDC-135135	-6.7364039	TCMDC-133663	-6.4651747		
TCMDC-124130	-6.736186	TCMDC-137341	-6.4649038		
TCMDC-140409	-6.736167	TCMDC-131754	-6.4648557		
TCMDC-123618	-6.7359447	TCMDC-133945	-6.4639516		
TCMDC-136080	-6.7356248	TCMDC-125058	-6.4638066		
TCMDC-141191	-6.7354565	TCMDC-138117	-6.4633994		
TCMDC-139122	-6.7351723	TCMDC-136879	-6.4633346		
TCMDC-125787	-6.7350569	TCMDC-133470	-6.4632564		
TCMDC-131432	-6.7350416	TCMDC-131329	-6.4625568		
TCMDC-132887	-6.7347145	TCMDC-138011	-6.4624939		
TCMDC-124029	-6.7346706	TCMDC-135877	-6.4622774		
TCMDC-134031	-6.7345243	TCMDC-136791	-6.4617224		
TCMDC-137546	-6.7340055	TCMDC-140441	-6.4617167		
TCMDC-137570	-6.7338915	TCMDC-133406	-6.4614248		
TCMDC-141223	-6.7337551	TCMDC-136530	-6.4613476		
TCMDC-131409	-6.7336969	TCMDC-124468	-6.4609799		
TCMDC-132748	-6.7335267	TCMDC-123510	-6.4600573		
TCMDC-135009	-6.7334228	TCMDC-137789	-6.4600363		
TCMDC-135048	-6.7332344	TCMDC-131249	-6.4598637		
TCMDC-139030	-6.7332311	TCMDC-131884	-6.4596629		
TCMDC-132179	-6.7328033	TCMDC-123705	-6.4583755		
TCMDC-134208	-6.7327085	TCMDC-124161	-6.4581537		
TCMDC-135095	-6.7321315	TCMDC-137772	-6.4581194		
TCMDC-132715	-6.7316527	TCMDC-133458	-6.4580507		

TCMDC-124512	-6.7315683	TCMDC-136462	-6.4579344		
TCMDC-141342	-6.7309885	TCMDC-124562	-6.457643		
TCMDC-139720	-6.730679	TCMDC-138511	-6.4571724		
TCMDC-125553	-6.7306175	TCMDC-134305	-6.4571028		
TCMDC-124009	-6.7305861	TCMDC-132741	-6.4562426		
TCMDC-131389	-6.7302585	TCMDC-133580	-6.4559879		
TCMDC-123958	-6.7300391	TCMDC-135880	-6.4555459		
TCMDC-138619	-6.7299752	TCMDC-124387	-6.4551945		
TCMDC-123790	-6.7298598	TCMDC-136485	-6.4548736		
TCMDC-131320	-6.729353	TCMDC-125041	-6.4546313		
TCMDC-133131	-6.7293162	TCMDC-133661	-6.4544702		
TCMDC-142054	-6.7291961	TCMDC-132113	-6.4542532		
TCMDC-125477	-6.7290535	TCMDC-142203	-6.452539		
TCMDC-137043	-6.7288952	TCMDC-131610	-6.4523911		
TCMDC-135587	-6.7288208	TCMDC-141211	-6.4515853		
TCMDC-132539	-6.7283964	TCMDC-134205	-6.4510512		
TCMDC-124146	-6.7283869	TCMDC-138949	-6.4508219		
TCMDC-135687	-6.7280378	TCMDC-137390	-6.4506526		
TCMDC-133356	-6.7280211	TCMDC-131392	-6.4503365		
TCMDC-124188	-6.7278543	TCMDC-142041	-6.4487863		
TCMDC-135584	-6.7270355	TCMDC-140907	-6.4487371		
TCMDC-133691	-6.7268	TCMDC-139009	-6.4482188		
TCMDC-138591	-6.7267666	TCMDC-124949	-6.4481859		
TCMDC-141953	-6.7257833	TCMDC-133434	-6.4480433		
TCMDC-136460	-6.7257714	TCMDC-136212	-6.4473777		
TCMDC-132521	-6.7257333	TCMDC-124835	-6.4473772		
TCMDC-142258	-6.7256951	TCMDC-124253	-6.4473572		
TCMDC-131525	-6.7255325	TCMDC-125608	-6.4470148		
TCMDC-137557	-6.7254119	TCMDC-125001	-6.446732		
TCMDC-140450	-6.7251973	TCMDC-135515	-6.4455037		
TCMDC-139142	-6.7251687	TCMDC-124627	-6.4447947		
TCMDC-133780	-6.7249689	TCMDC-135600	-6.4447498		
TCMDC-138195	-6.724865	TCMDC-139250	-6.4446301		
TCMDC-124151	-6.7243319	TCMDC-132418	-6.4444141		
TCMDC-133573	-6.7242818	TCMDC-135609	-6.4439192		
TCMDC-131535	-6.7238216	TCMDC-137011	-6.4422946		
TCMDC-135578	-6.7237234	TCMDC-140516	-6.4411364		
TCMDC-123938	-6.7236848	TCMDC-125040	-6.4410996		
TCMDC-133847	-6.7236814	TCMDC-136213	-6.4409146		
TCMDC-135789	-6.723084	TCMDC-138129	-6.440577		
TCMDC-131968	-6.7230644	TCMDC-124490	-6.4402032		
TCMDC-132314	-6.7225132	TCMDC-135576	-6.4389868		
TCMDC-132425	-6.722178	TCMDC-133764	-6.4389014		
TCMDC-135590	-6.7219701	TCMDC-134315	-6.4386649		

TCMDC-140142	-6.7213697	TCMDC-141333	-6.4380817		
TCMDC-136881	-6.7206001	TCMDC-131800	-6.4379096		
TCMDC-131772	-6.7204847	TCMDC-125330	-6.4369378		
TCMDC-138598	-6.720396	TCMDC-125733	-6.4369354		
TCMDC-136527	-6.7202225	TCMDC-141209	-6.436902		
TCMDC-132572	-6.7197189	TCMDC-142089	-6.4366541		
TCMDC-136607	-6.719511	TCMDC-125247	-6.4365668		
TCMDC-135631	-6.7193322	TCMDC-135807	-6.4365439		
TCMDC-131649	-6.7191992	TCMDC-125453	-6.4360819		
TCMDC-125844	-6.7191515	TCMDC-136735	-6.4355588		
TCMDC-133478	-6.7187791	TCMDC-124680	-6.4344583		
TCMDC-125200	-6.7187204	TCMDC-142229	-6.4342518		
TCMDC-123649	-6.7182856	TCMDC-137486	-6.4342237		
TCMDC-135555	-6.7182517	TCMDC-123698	-6.4339452		
TCMDC-140768	-6.7170362	TCMDC-142156	-6.4338236		
TCMDC-134683	-6.7170238	TCMDC-123604	-6.4335251		
TCMDC-142195	-6.7170057	TCMDC-139308	-6.4334092		
TCMDC-140394	-6.716794	TCMDC-131861	-6.433073		
TCMDC-133815	-6.7161756	TCMDC-132805	-6.4326315		
TCMDC-132232	-6.7161407	TCMDC-136894	-6.4325161		
TCMDC-137191	-6.7160769	TCMDC-123956	-6.4319539		
TCMDC-141202	-6.7160363	TCMDC-131517	-6.4316063		
TCMDC-131491	-6.7157745	TCMDC-134583	-6.4311981		
TCMDC-125414	-6.7154298	TCMDC-124360	-6.4311399		
TCMDC-123724	-6.7154188	TCMDC-134550	-6.4311371		
TCMDC-124365	-6.7153158	TCMDC-132098	-6.4310675		
TCMDC-139124	-6.7152634	TCMDC-132352	-6.4307332		
TCMDC-140222	-6.7151556	TCMDC-138924	-6.4307117		
TCMDC-140129	-6.7148509	TCMDC-132582	-6.4307094		
TCMDC-124451	-6.7144475	TCMDC-125561	-6.4302096		
TCMDC-141154	-6.714098	TCMDC-141346	-6.4299688		
TCMDC-133827	-6.7140193	TCMDC-124764	-6.4299083		
TCMDC-142218	-6.7139654	TCMDC-139408	-6.4286604		
TCMDC-141913	-6.7137713	TCMDC-140468	-6.4280624		
TCMDC-134002	-6.7131691	TCMDC-125668	-6.4274969		
TCMDC-139447	-6.7131429	TCMDC-123810	-6.4270101		
TCMDC-124016	-6.7130737	TCMDC-125215	-6.4266415		
TCMDC-135057	-6.7124581	TCMDC-124455	-6.426569		
TCMDC-124406	-6.7123475	TCMDC-138575	-6.4259028		
TCMDC-139138	-6.7122979	TCMDC-136682	-6.4257231		
TCMDC-132072	-6.7120214	TCMDC-134201	-6.4256768		
TCMDC-139455	-6.7118392	TCMDC-131388	-6.4246073		
TCMDC-123578	-6.7109628	TCMDC-138816	-6.424499		
TCMDC-125358	-6.7109408	TCMDC-125568	-6.4240875		

TCMDC-134999	-6.7106504	TCMDC-123897	-6.4237442		
TCMDC-124063	-6.7103462	TCMDC-124425	-6.4237132		
TCMDC-142191	-6.7099504	TCMDC-131732	-6.4237018		
TCMDC-136772	-6.7096019	TCMDC-136842	-6.4233537		
TCMDC-134832	-6.7092814	TCMDC-131485	-6.4217424		
TCMDC-124358	-6.7090397	TCMDC-137996	-6.4216137		
TCMDC-131475	-6.7086039	TCMDC-134034	-6.4213924		
TCMDC-131989	-6.7085738	TCMDC-139731	-6.4193106		
TCMDC-125124	-6.7082906	TCMDC-138943	-6.41927		
TCMDC-124010	-6.7081833	TCMDC-142234	-6.4184747		
TCMDC-137250	-6.7081728	TCMDC-125499	-6.4184508		
TCMDC-133251	-6.7075329	TCMDC-133477	-6.4184289		
TCMDC-139274	-6.7073884	TCMDC-124554	-6.4181809		
TCMDC-139054	-6.7073069	TCMDC-134542	-6.4179344		
TCMDC-138170	-6.706789	TCMDC-131801	-6.4179077		
TCMDC-133990	-6.7062058	TCMDC-131757	-6.4174528		
TCMDC-137479	-6.705925	TCMDC-131898	-6.4169979		
TCMDC-141307	-6.7058501	TCMDC-142076	-6.4168334		
TCMDC-125718	-6.7057943	TCMDC-124260	-6.4168129		
TCMDC-124913	-6.7051911	TCMDC-125526	-6.4167943		
TCMDC-125584	-6.7051792	TCMDC-135132	-6.4166965		
TCMDC-134554	-6.704999	TCMDC-124544	-6.4165621		
TCMDC-141177	-6.7049155	TCMDC-140158	-6.4165225		
TCMDC-138646	-6.7047172	TCMDC-131305	-6.41641		
TCMDC-141650	-6.7045665	TCMDC-136010	-6.4158673		
TCMDC-133719	-6.7045345	TCMDC-131975	-6.4155335		
TCMDC-123596	-6.7043862	TCMDC-123872	-6.415133		
TCMDC-135053	-6.7039638	TCMDC-125023	-6.4149613		
TCMDC-137584	-6.7039328	TCMDC-138482	-6.4148717		
TCMDC-140401	-6.7037578	TCMDC-131490	-6.4147115		
TCMDC-131430	-6.7032447	TCMDC-139487	-6.4143243		
TCMDC-142210	-6.7030554	TCMDC-135161	-6.4142761		
TCMDC-124888	-6.7029376	TCMDC-123570	-6.4141841		
TCMDC-137542	-6.7029324	TCMDC-131397	-6.41398		
TCMDC-138909	-6.7025933	TCMDC-124795	-6.4139619		
TCMDC-125619	-6.7022047	TCMDC-124500	-6.4134827		
TCMDC-123759	-6.7021966	TCMDC-134256	-6.4129572		
TCMDC-138450	-6.7021713	TCMDC-123575	-6.4123445		
TCMDC-131487	-6.7021155	TCMDC-140391	-6.4115171		
TCMDC-139879	-6.7012968	TCMDC-123483	-6.4114699		
TCMDC-124306	-6.7010703	TCMDC-136181	-6.4111905		
TCMDC-140011	-6.7006931	TCMDC-142198	-6.4107356		
TCMDC-140449	-6.7002592	TCMDC-133656	-6.4098563		
TCMDC-136726	-6.7000628	TCMDC-133585	-6.4095736		

TCMDC-140426	-6.6994805	TCMDC-133375	-6.4094186		
TCMDC-141180	-6.699471	TCMDC-137539	-6.4086666		
TCMDC-134343	-6.6993189	TCMDC-125475	-6.4084496		
TCMDC-134258	-6.6989837	TCMDC-135485	-6.4084144		
TCMDC-124427	-6.6987972	TCMDC-135303	-6.4079585		
TCMDC-139305	-6.6986394	TCMDC-124375	-6.4075203		
TCMDC-140663	-6.6985159	TCMDC-131713	-6.4066725		
TCMDC-124675	-6.69803	TCMDC-138207	-6.405489		
TCMDC-136387	-6.697957	TCMDC-131426	-6.4046392		
TCMDC-142242	-6.6975398	TCMDC-133482	-6.4043646		
TCMDC-131326	-6.6973958	TCMDC-134634	-6.4040852		
TCMDC-141110	-6.6973667	TCMDC-141270	-6.4037724		
TCMDC-124511	-6.697288	TCMDC-136068	-6.403204		
TCMDC-141130	-6.697269	TCMDC-139241	-6.4029217		
TCMDC-141017	-6.6967883	TCMDC-134576	-6.4025345		
TCMDC-140442	-6.6957812	TCMDC-123647	-6.4020758		
TCMDC-132693	-6.6956406	TCMDC-133349	-6.4018836		
TCMDC-134946	-6.6954446	TCMDC-138027	-6.4016576		
TCMDC-131505	-6.6954188	TCMDC-125303	-6.4014778		
TCMDC-131494	-6.6950598	TCMDC-137807	-6.4008355		
TCMDC-139704	-6.6947794	TCMDC-124914	-6.4002867		
TCMDC-124431	-6.6946807	TCMDC-138782	-6.4002347		
TCMDC-137056	-6.6935086	TCMDC-124557	-6.4000945		
TCMDC-135186	-6.6933379	TCMDC-125602	-6.3995748		
TCMDC-124575	-6.693336	TCMDC-134530	-6.3995538		
TCMDC-125710	-6.6931767	TCMDC-141668	-6.3983335		
TCMDC-135386	-6.6929965	TCMDC-124180	-6.3982062		
TCMDC-123602	-6.6928515	TCMDC-138639	-6.3979754		
TCMDC-131558	-6.6925621	TCMDC-138047	-6.3977933		
TCMDC-125765	-6.6922207	TCMDC-132538	-6.3977561		
TCMDC-133577	-6.6918073	TCMDC-136005	-6.3971119		
TCMDC-124733	-6.6917629	TCMDC-141748	-6.3968496		
TCMDC-142040	-6.6910849	TCMDC-134175	-6.396791		
TCMDC-124317	-6.6908975	TCMDC-134666	-6.3966074		
TCMDC-141657	-6.6906695	TCMDC-123635	-6.3964353		
TCMDC-124205	-6.6906266	TCMDC-136379	-6.3961201		
TCMDC-136905	-6.6905379	TCMDC-125728	-6.396029		
TCMDC-139396	-6.6905012	TCMDC-131433	-6.3956251		
TCMDC-136562	-6.6900606	TCMDC-131996	-6.395093		
TCMDC-136211	-6.6889982	TCMDC-134503	-6.3949828		
TCMDC-124527	-6.6889358	TCMDC-133221	-6.3949804		
TCMDC-132674	-6.6887851	TCMDC-142217	-6.3946018		
TCMDC-140563	-6.6886911	TCMDC-133343	-6.3943386		
TCMDC-124863	-6.6883121	TCMDC-125566	-6.3940897		

TCMDC-137723	-6.6881714	TCMDC-125736	-6.3940105		
TCMDC-135819	-6.6879411	TCMDC-136360	-6.3938999		
TCMDC-132700	-6.6875243	TCMDC-141238	-6.3936749		
TCMDC-132529	-6.6874642	TCMDC-135788	-6.3936658		
TCMDC-134702	-6.6867342	TCMDC-136362	-6.393332		
TCMDC-131984	-6.6866031	TCMDC-141378	-6.393332		
TCMDC-134004	-6.6862688	TCMDC-133655	-6.3932314		
TCMDC-141673	-6.6859083	TCMDC-137588	-6.3929262		
TCMDC-125599	-6.6855783	TCMDC-124787	-6.3928881		
TCMDC-133647	-6.6852517	TCMDC-124403	-6.3919697		
TCMDC-140975	-6.6844854	TCMDC-124366	-6.3918571		
TCMDC-123906	-6.6842217	TCMDC-138233	-6.3917117		
TCMDC-134356	-6.6833496	TCMDC-137753	-6.3910198		
TCMDC-138793	-6.6832995	TCMDC-140066	-6.3907089		
TCMDC-137551	-6.6830187	TCMDC-142284	-6.3903241		
TCMDC-138130	-6.6829772	TCMDC-137435	-6.3899746		
TCMDC-125480	-6.6827178	TCMDC-124881	-6.3897476		
TCMDC-125402	-6.6816244	TCMDC-124485	-6.3895922		
TCMDC-135227	-6.6815009	TCMDC-131690	-6.3893051		
TCMDC-141151	-6.6810322	TCMDC-142211	-6.3892331		
TCMDC-133100	-6.6809859	TCMDC-138970	-6.389101		
TCMDC-123460	-6.6808343	TCMDC-133726	-6.3887739		
TCMDC-124228	-6.6805558	TCMDC-133651	-6.3885889		
TCMDC-132057	-6.6805348	TCMDC-131761	-6.3879447		
TCMDC-125809	-6.6791139	TCMDC-135514	-6.3877807		
TCMDC-124225	-6.6789603	TCMDC-134298	-6.3877788		
TCMDC-137080	-6.6789188	TCMDC-142202	-6.3876615		
TCMDC-138370	-6.6783547	TCMDC-131306	-6.3875785		
TCMDC-136623	-6.6782045	TCMDC-136900	-6.3873982		
TCMDC-124924	-6.6780782	TCMDC-132586	-6.3873577		
TCMDC-123731	-6.6778593	TCMDC-124910	-6.3867393		
TCMDC-133383	-6.6778541	TCMDC-138023	-6.3864207		
TCMDC-132831	-6.6775427	TCMDC-141652	-6.3859916		
TCMDC-125486	-6.6773772	TCMDC-124477	-6.3857284		
TCMDC-124099	-6.6771326	TCMDC-131738	-6.3845315		
TCMDC-140081	-6.6769524	TCMDC-125640	-6.3839912		
TCMDC-124072	-6.6765099	TCMDC-138566	-6.3834567		
TCMDC-131995	-6.6763034	TCMDC-124513	-6.3832059		
TCMDC-123525	-6.6762929	TCMDC-141738	-6.3831191		
TCMDC-137053	-6.676229	TCMDC-131752	-6.3827195		
TCMDC-125573	-6.6761827	TCMDC-136572	-6.3823328		
TCMDC-138106	-6.6756401	TCMDC-142002	-6.3814421		
TCMDC-141415	-6.6755958	TCMDC-141206	-6.3812456		
TCMDC-137581	-6.6751614	TCMDC-134274	-6.3804345		

TCMDC-124558	-6.674274	TCMDC-138826	-6.379149		
TCMDC-139755	-6.6741376	TCMDC-133906	-6.3788319		
TCMDC-131843	-6.6738858	TCMDC-141736	-6.3780985		
TCMDC-135796	-6.673872	TCMDC-125814	-6.3778472		
TCMDC-134584	-6.6736059	TCMDC-137208	-6.3777499		
TCMDC-133218	-6.6734953	TCMDC-125397	-6.3770027		
TCMDC-140106	-6.6728859	TCMDC-137006	-6.3760409		
TCMDC-125632	-6.6726489	TCMDC-135918	-6.3757982		
TCMDC-134646	-6.6722798	TCMDC-137675	-6.3753891		
TCMDC-124177	-6.6721058	TCMDC-142048	-6.3746781		
TCMDC-133864	-6.6716413	TCMDC-140225	-6.3742595		
TCMDC-137822	-6.6715355	TCMDC-135522	-6.3739438		
TCMDC-131341	-6.6714916	TCMDC-139423	-6.3736606		
TCMDC-124905	-6.6714258	TCMDC-141665	-6.3736038		
TCMDC-138095	-6.6709785	TCMDC-123901	-6.3735733		
TCMDC-132353	-6.6708503	TCMDC-125365	-6.3734879		
TCMDC-124342	-6.6708007	TCMDC-125380	-6.3730993		
TCMDC-124108	-6.6697292	TCMDC-138697	-6.3728528		
TCMDC-138190	-6.6694536	TCMDC-137886	-6.3721857		
TCMDC-137571	-6.6693959	TCMDC-125110	-6.3718872		
TCMDC-134831	-6.6690803	TCMDC-139146	-6.3715754		
TCMDC-140974	-6.6690307	TCMDC-137585	-6.3715281		
TCMDC-141400	-6.6690145	TCMDC-131366	-6.371439		
TCMDC-124136	-6.6687503	TCMDC-134539	-6.3709321		
TCMDC-132300	-6.6681786	TCMDC-125403	-6.3708515		
TCMDC-134292	-6.6680617	TCMDC-139874	-6.3708134		
TCMDC-137194	-6.6677828	TCMDC-136165	-6.3705139		
TCMDC-138784	-6.6675491	TCMDC-124436	-6.3702602		
TCMDC-133446	-6.6673884	TCMDC-135654	-6.370151		
TCMDC-124843	-6.666914	TCMDC-123995	-6.3699789		
TCMDC-137065	-6.6668196	TCMDC-138964	-6.3693876		
TCMDC-135222	-6.6658707	TCMDC-137748	-6.3685608		
TCMDC-131462	-6.6652098	TCMDC-131374	-6.3683324		
TCMDC-124465	-6.6648517	TCMDC-135271	-6.3681126		
TCMDC-136494	-6.6646075	TCMDC-141335	-6.3680391		
TCMDC-137193	-6.6642904	TCMDC-124828	-6.3679786		
TCMDC-140398	-6.6642885	TCMDC-131674	-6.3678365		
TCMDC-124747	-6.6642466	TCMDC-137732	-6.3676519		
TCMDC-139717	-6.6642323	TCMDC-140422	-6.3674674		
TCMDC-124605	-6.6634188	TCMDC-139326	-6.3671293		
TCMDC-131588	-6.6633573	TCMDC-125571	-6.3666325		
TCMDC-136043	-6.6631274	TCMDC-123877	-6.3665009		
TCMDC-131257	-6.6630239	TCMDC-124832	-6.3664498		
TCMDC-141057	-6.6629386	TCMDC-137937	-6.3659744		

TCMDC-141329	-6.662817	TCMDC-125310	-6.3657708		
TCMDC-123699	-6.6627507	TCMDC-137381	-6.3652539		
TCMDC-133520	-6.6627502	TCMDC-137378	-6.3650804		
TCMDC-133287	-6.6623387	TCMDC-132706	-6.3650117		
TCMDC-123580	-6.6609735	TCMDC-135595	-6.3642311		
TCMDC-123788	-6.6604133	TCMDC-139114	-6.3640552		
TCMDC-125369	-6.659771	TCMDC-123682	-6.3629007		
TCMDC-139485	-6.6597557	TCMDC-131790	-6.3627591		
TCMDC-133474	-6.659564	TCMDC-124849	-6.3623748		
TCMDC-124222	-6.6594748	TCMDC-137500	-6.362289		
TCMDC-131864	-6.659328	TCMDC-131520	-6.3621707		
TCMDC-138731	-6.6587958	TCMDC-124239	-6.3619194		
TCMDC-135593	-6.6587672	TCMDC-136051	-6.3612852		
TCMDC-133279	-6.658596	TCMDC-131799	-6.3604808		
TCMDC-133669	-6.6585517	TCMDC-142206	-6.3603597		
TCMDC-135012	-6.6584687	TCMDC-123972	-6.3602571		
TCMDC-139426	-6.6582026	TCMDC-139477	-6.359642		
TCMDC-125367	-6.6580653	TCMDC-138542	-6.3595767		
TCMDC-133819	-6.6580424	TCMDC-134306	-6.3594251		
TCMDC-133838	-6.6579361	TCMDC-139458	-6.3590002		
TCMDC-124492	-6.6578722	TCMDC-138138	-6.3581939		
TCMDC-124530	-6.6574655	TCMDC-124432	-6.3573413		
TCMDC-125564	-6.657095	TCMDC-131903	-6.3572698		
TCMDC-137574	-6.657064	TCMDC-141171	-6.3571992		
TCMDC-124867	-6.6565723	TCMDC-125305	-6.3571901		
TCMDC-131605	-6.6565342	TCMDC-124274	-6.3567147		
TCMDC-125221	-6.6564517	TCMDC-123887	-6.3564701		
TCMDC-137900	-6.656198	TCMDC-134154	-6.3564215		
TCMDC-123645	-6.6557446	TCMDC-125354	-6.3561206		
TCMDC-132730	-6.6556044	TCMDC-137813	-6.3560586		
TCMDC-131423	-6.6553149	TCMDC-137682	-6.3558111		
TCMDC-137218	-6.6548085	TCMDC-137859	-6.3554621		
TCMDC-134338	-6.6546121	TCMDC-140762	-6.3552899		
TCMDC-131613	-6.6545067	TCMDC-135164	-6.3552394		
TCMDC-134582	-6.6544466	TCMDC-131537	-6.3546662		
TCMDC-124688	-6.6541171	TCMDC-125419	-6.3542452		
TCMDC-124723	-6.6538148	TCMDC-125489	-6.3539915		
TCMDC-132988	-6.6538091	TCMDC-138199	-6.3536692		
TCMDC-136661	-6.6537008	TCMDC-125801	-6.3526468		
TCMDC-133282	-6.6535296	TCMDC-138995	-6.3521018		
TCMDC-124753	-6.6534023	TCMDC-133479	-6.3520508		
TCMDC-125678	-6.6532702	TCMDC-125182	-6.3519883		
TCMDC-135580	-6.6529822	TCMDC-124328	-6.3519068		
TCMDC-124827	-6.6515369	TCMDC-125818	-6.3517585		

TCMDC-131758	-6.6515226	TCMDC-142047	-6.351594		
TCMDC-123925	-6.6515069	TCMDC-140057	-6.3514681		
TCMDC-125609	-6.6514964	TCMDC-125004	-6.351306		
TCMDC-135272	-6.651269	TCMDC-131637	-6.3512526		
TCMDC-139719	-6.6511974	TCMDC-137707	-6.3510876		
TCMDC-139039	-6.6511765	TCMDC-131763	-6.3510475		
TCMDC-140322	-6.651031	TCMDC-138790	-6.3509312		
TCMDC-136801	-6.6509771	TCMDC-141347	-6.3507228		
TCMDC-134585	-6.6503701	TCMDC-134540	-6.3506732		
TCMDC-134830	-6.6502609	TCMDC-137249	-6.3490081		
TCMDC-132832	-6.6498318	TCMDC-139957	-6.3486767		
TCMDC-136686	-6.6498094	TCMDC-136015	-6.3485489		
TCMDC-132725	-6.6494856	TCMDC-142254	-6.3484273		
TCMDC-125024	-6.6490002	TCMDC-139801	-6.3481398		
TCMDC-137389	-6.6489139	TCMDC-131676	-6.3479266		
TCMDC-133404	-6.6486506	TCMDC-123546	-6.3471408		
TCMDC-136363	-6.6485205	TCMDC-136878	-6.3467703		
TCMDC-139013	-6.6484232	TCMDC-137979	-6.3451643		
TCMDC-123592	-6.6484137	TCMDC-139415	-6.3442626		
TCMDC-133544	-6.6479731	TCMDC-135519	-6.3441601		
TCMDC-125213	-6.6477022	TCMDC-134050	-6.3440142		
TCMDC-125355	-6.6476264	TCMDC-131590	-6.3439436		
TCMDC-133407	-6.6471653	TCMDC-134611	-6.3434896		
TCMDC-134345	-6.6466355	TCMDC-125730	-6.3431649		
TCMDC-137164	-6.6463571	TCMDC-124111	-6.3428135		
TCMDC-133995	-6.6462817	TCMDC-140108	-6.3419123		
TCMDC-123641	-6.6460648	TCMDC-131764	-6.3418384		
TCMDC-140373	-6.6459627	TCMDC-138012	-6.341804		
TCMDC-140457	-6.645762	TCMDC-141234	-6.3409653		
TCMDC-124409	-6.6457534	TCMDC-134661	-6.3409348		
TCMDC-139915	-6.6455441	TCMDC-131463	-6.3408394		
TCMDC-133484	-6.64467	TCMDC-123488	-6.3408127		
TCMDC-137736	-6.6446662	TCMDC-136578	-6.3407102		
TCMDC-123890	-6.644444	TCMDC-133410	-6.3407006		
TCMDC-133569	-6.6439886	TCMDC-137449	-6.340518		
TCMDC-132384	-6.6438642	TCMDC-135909	-6.3405094		
TCMDC-136009	-6.6433334	TCMDC-134720	-6.3402162		
TCMDC-139498	-6.6433196	TCMDC-140070	-6.3399262		
TCMDC-138587	-6.6428986	TCMDC-124133	-6.3397722		
TCMDC-133729	-6.6426573	TCMDC-133587	-6.3394518		
TCMDC-132121	-6.6424446	TCMDC-134695	-6.3393092		
TCMDC-131403	-6.6423178	TCMDC-137246	-6.3392453		
TCMDC-138627	-6.6422982	TCMDC-124889	-6.3390794		
TCMDC-139312	-6.6422801	TCMDC-135160	-6.3381972		

TCMDC-141424	-6.6421194	TCMDC-138919	-6.3376117		
TCMDC-140734	-6.6421127	TCMDC-125673	-6.3367329		
TCMDC-124374	-6.6417551	TCMDC-125118	-6.3363605		
TCMDC-125011	-6.6413603	TCMDC-125051	-6.3359952		
TCMDC-136199	-6.6412268	TCMDC-124531	-6.3355589		
TCMDC-136683	-6.6410413	TCMDC-124883	-6.3354874		
TCMDC-141268	-6.6409726	TCMDC-124594	-6.335381		
TCMDC-124363	-6.6409469	TCMDC-138875	-6.3353758		
TCMDC-124735	-6.640759	TCMDC-124160	-6.3353758		
TCMDC-125384	-6.6405315	TCMDC-137013	-6.3350458		
TCMDC-125071	-6.640192	TCMDC-131345	-6.3350387		
TCMDC-124587	-6.6399679	TCMDC-131777	-6.3345838		
TCMDC-132423	-6.6397648	TCMDC-137765	-6.3344359		
TCMDC-139463	-6.639637	TCMDC-134833	-6.3342395		
TCMDC-123733	-6.6395454	TCMDC-131468	-6.3342314		
TCMDC-131735	-6.639195	TCMDC-134625	-6.3342233		
TCMDC-137880	-6.6387248	TCMDC-134211	-6.3339562		
TCMDC-124876	-6.6387234	TCMDC-136680	-6.3332753		
TCMDC-136071	-6.638278	TCMDC-135423	-6.3327646		
TCMDC-137387	-6.6376672	TCMDC-135130	-6.3322062		
TCMDC-136498	-6.6376238	TCMDC-136693	-6.3307867		
TCMDC-125253	-6.6374993	TCMDC-139070	-6.3307743		
TCMDC-140549	-6.6374817	TCMDC-133717	-6.32972		
TCMDC-125413	-6.6374002	TCMDC-125313	-6.329567		
TCMDC-135610	-6.637383	TCMDC-123547	-6.3294272		
TCMDC-137873	-6.6372194	TCMDC-124882	-6.3292937		
TCMDC-133828	-6.6369367	TCMDC-136771	-6.3284755		
TCMDC-124325	-6.6365962	TCMDC-135644	-6.3284335		
TCMDC-131503	-6.635663	TCMDC-134670	-6.3283215		
TCMDC-134366	-6.6352015	TCMDC-125126	-6.3278399		
TCMDC-134657	-6.6350942	TCMDC-133149	-6.3268604		
TCMDC-140908	-6.6350417	TCMDC-131636	-6.3266168		
TCMDC-131892	-6.6346903	TCMDC-124217	-6.3259172		
TCMDC-141801	-6.6344504	TCMDC-124135	-6.3239546		
TCMDC-124614	-6.6336927	TCMDC-124015	-6.3236551		
TCMDC-124934	-6.6333971	TCMDC-137007	-6.3233566		
TCMDC-125212	-6.6333227	TCMDC-125066	-6.3233042		
TCMDC-142315	-6.6332784	TCMDC-139337	-6.3232512		
TCMDC-132104	-6.6331048	TCMDC-125278	-6.3232436		
TCMDC-124494	-6.6329727	TCMDC-131836	-6.3227468		
TCMDC-139088	-6.6324172	TCMDC-133518	-6.3226981		
TCMDC-131532	-6.6302118	TCMDC-136492	-6.3226681		
TCMDC-141595	-6.6300278	TCMDC-138073	-6.3224874		
TCMDC-134314	-6.6300097	TCMDC-139821	-6.322423		

TCMDC-136640	-6.6298876	TCMDC-134216	-6.3218489		
TCMDC-136061	-6.6296406	TCMDC-139418	-6.3217096		
TCMDC-134272	-6.629344	TCMDC-136296	-6.3200889		
TCMDC-140306	-6.6292443	TCMDC-138353	-6.3199258		
TCMDC-124936	-6.6292272	TCMDC-142289	-6.3199072		
TCMDC-132915	-6.6289639	TCMDC-141655	-6.3198957		
TCMDC-133797	-6.6283398	TCMDC-125109	-6.319828		
TCMDC-133854	-6.6283269	TCMDC-134719	-6.319097		
TCMDC-139627	-6.6279583	TCMDC-135052	-6.3190351		
TCMDC-134083	-6.6278481	TCMDC-142235	-6.3177633		
TCMDC-124655	-6.62678	TCMDC-135430	-6.3176041		
TCMDC-140740	-6.62676	TCMDC-123774	-6.3170333		
TCMDC-131883	-6.6265349	TCMDC-125837	-6.3165402		
TCMDC-125195	-6.6264596	TCMDC-133584	-6.3165264		
TCMDC-136325	-6.6259112	TCMDC-131672	-6.3163652		
TCMDC-135142	-6.6257663	TCMDC-123526	-6.3162894		
TCMDC-139504	-6.6253972	TCMDC-134266	-6.316205		
TCMDC-124572	-6.6251016	TCMDC-138635	-6.3156123		
TCMDC-135946	-6.6250939	TCMDC-142253	-6.315196		
TCMDC-131916	-6.6246653	TCMDC-139055	-6.3150234		
TCMDC-125038	-6.6243591	TCMDC-125378	-6.3139133		
TCMDC-125377	-6.6243277	TCMDC-131891	-6.3136535		
TCMDC-136694	-6.6240635	TCMDC-141743	-6.3129482		
TCMDC-140774	-6.6236634	TCMDC-125323	-6.3128514		
TCMDC-136029	-6.6235886	TCMDC-131696	-6.312005		
TCMDC-124541	-6.6227789	TCMDC-134607	-6.311573		
TCMDC-137897	-6.6227684	TCMDC-131507	-6.3108344		
TCMDC-133398	-6.6227016	TCMDC-123664	-6.3102527		
TCMDC-135658	-6.6224532	TCMDC-123600	-6.3097649		
TCMDC-141412	-6.6221519	TCMDC-125476	-6.3091927		
TCMDC-133648	-6.6211863	TCMDC-131983	-6.3085384		
TCMDC-135545	-6.6207299	TCMDC-124410	-6.308495		
TCMDC-133125	-6.6203742	TCMDC-139397	-6.3079481		
TCMDC-133491	-6.6202149	TCMDC-134268	-6.3078394		
TCMDC-133399	-6.6200399	TCMDC-135518	-6.3077836		
TCMDC-134084	-6.6199503	TCMDC-124898	-6.3073368		
TCMDC-133662	-6.6192546	TCMDC-124402	-6.3069024		
TCMDC-140067	-6.6189609	TCMDC-124110	-6.3068137		
TCMDC-136310	-6.6188951	TCMDC-124119	-6.306284		
TCMDC-136903	-6.6187363	TCMDC-138777	-6.3061476		
TCMDC-125855	-6.6184006	TCMDC-136669	-6.3059602		
TCMDC-138373	-6.6183934	TCMDC-125292	-6.3059492		
TCMDC-134028	-6.6183167	TCMDC-134721	-6.3058734		
TCMDC-138436	-6.6180649	TCMDC-131945	-6.3057823		

TCMDC-124648	-6.6180243	TCMDC-131304	-6.3057775		
TCMDC-136533	-6.6179924	TCMDC-138136	-6.3050904		
TCMDC-137846	-6.6169672	TCMDC-135413	-6.3049231		
TCMDC-140794	-6.6167789	TCMDC-136671	-6.3047047		
TCMDC-125273	-6.6167126	TCMDC-141495	-6.3042026		
TCMDC-134108	-6.6166091	TCMDC-125782	-6.3037949		
TCMDC-137609	-6.6162658	TCMDC-141994	-6.3036089		
TCMDC-138144	-6.6158972	TCMDC-131382	-6.3031797		
TCMDC-132938	-6.6158113	TCMDC-138951	-6.3027415		
TCMDC-137230	-6.6157866	TCMDC-133465	-6.3019471		
TCMDC-124699	-6.6151762	TCMDC-142239	-6.3018141		
TCMDC-139417	-6.6149669	TCMDC-137400	-6.3014812		
TCMDC-138178	-6.6145372	TCMDC-136814	-6.3014517		
TCMDC-124802	-6.6144824	TCMDC-134534	-6.3013425		
TCMDC-136585	-6.6140571	TCMDC-138792	-6.3009844		
TCMDC-124891	-6.613791	TCMDC-135848	-6.3007936		
TCMDC-136058	-6.6134701	TCMDC-131365	-6.2990584		
TCMDC-137677	-6.6132193	TCMDC-136358	-6.2988176		
TCMDC-132043	-6.6131587	TCMDC-142192	-6.2987142		
TCMDC-136679	-6.6129265	TCMDC-125013	-6.2985387		
TCMDC-131464	-6.6126513	TCMDC-134277	-6.2977123		
TCMDC-139311	-6.6126218	TCMDC-131265	-6.2973146		
TCMDC-124467	-6.6123981	TCMDC-139099	-6.2970362		
TCMDC-125008	-6.6123037	TCMDC-138948	-6.2967448		
TCMDC-137216	-6.6122656	TCMDC-132122	-6.2961516		
TCMDC-137005	-6.6122007	TCMDC-124311	-6.2961402		
TCMDC-123651	-6.6119957	TCMDC-125224	-6.2957654		
TCMDC-140443	-6.611762	TCMDC-131792	-6.2951713		
TCMDC-141219	-6.6111975	TCMDC-125231	-6.2938657		
TCMDC-131248	-6.6102529	TCMDC-140333	-6.2918787		
TCMDC-133364	-6.6100726	TCMDC-125464	-6.2912474		
TCMDC-131926	-6.6096325	TCMDC-142337	-6.2911987		
TCMDC-140462	-6.6095576	TCMDC-125340	-6.2911248		
TCMDC-123915	-6.6095166	TCMDC-141201	-6.2908225		
TCMDC-133570	-6.6089091	TCMDC-139381	-6.2902999		
TCMDC-132598	-6.6088748	TCMDC-133074	-6.29006		
TCMDC-131642	-6.6088552	TCMDC-124214	-6.2899833		
TCMDC-131826	-6.6086779	TCMDC-124079	-6.2894664		
TCMDC-136964	-6.6085768	TCMDC-140685	-6.2893066		
TCMDC-137049	-6.607935	TCMDC-141480	-6.289289		
TCMDC-142264	-6.60747	TCMDC-135605	-6.2883387		
TCMDC-123626	-6.6070833	TCMDC-138111	-6.2880564		
TCMDC-131309	-6.6070485	TCMDC-125342	-6.2878962		
TCMDC-131630	-6.6070051	TCMDC-142042	-6.2878466		

TCMDC-131322	-6.6069908	TCMDC-124172	-6.2872643		
TCMDC-135110	-6.6068988	TCMDC-137264	-6.2869625		
TCMDC-134998	-6.6067996	TCMDC-124411	-6.2869158		
TCMDC-139445	-6.6062288	TCMDC-138471	-6.2860103		
TCMDC-136681	-6.6062036	TCMDC-124165	-6.2850032		
TCMDC-134599	-6.60606	TCMDC-124078	-6.2848787		
TCMDC-125832	-6.6052256	TCMDC-139446	-6.2846069		
TCMDC-133829	-6.6051979	TCMDC-133868	-6.2844682		
TCMDC-123612	-6.6045856	TCMDC-131671	-6.2844114		
TCMDC-141285	-6.6045609	TCMDC-131459	-6.2835345		
TCMDC-123952	-6.6035242	TCMDC-142185	-6.2834601		
TCMDC-141341	-6.6028152	TCMDC-137268	-6.2833376		
TCMDC-125209	-6.6013646	TCMDC-123487	-6.2821293		
TCMDC-124423	-6.6007056	TCMDC-139362	-6.2818685		
TCMDC-131833	-6.6004667	TCMDC-134591	-6.2818265		
TCMDC-123924	-6.600441	TCMDC-137409	-6.2814717		
TCMDC-135144	-6.6004262	TCMDC-142109	-6.2811804		
TCMDC-140518	-6.6004114	TCMDC-125551	-6.2811146		
TCMDC-137553	-6.6001306	TCMDC-137593	-6.2809024		
TCMDC-124379	-6.5999575	TCMDC-134420	-6.2798204		
TCMDC-141330	-6.5999231	TCMDC-125857	-6.2797723		
TCMDC-123717	-6.5998797	TCMDC-131346	-6.2795296		
TCMDC-140418	-6.5997195	TCMDC-137695	-6.2792282		
TCMDC-136687	-6.5996213	TCMDC-141737	-6.2789993		
TCMDC-133397	-6.5993028	TCMDC-137339	-6.278801		
TCMDC-132740	-6.5992484	TCMDC-131759	-6.2787519		
TCMDC-137029	-6.5992451	TCMDC-142050	-6.2787457		
TCMDC-125560	-6.5987968	TCMDC-133219	-6.2786965		
TCMDC-131662	-6.5985155	TCMDC-131402	-6.2784653		
TCMDC-139856	-6.5985055	TCMDC-137883	-6.2782931		
TCMDC-141075	-6.5984879	TCMDC-137331	-6.2779565		
TCMDC-137010	-6.5983214	TCMDC-137401	-6.2777133		
TCMDC-134147	-6.5983191	TCMDC-131755	-6.2775459		
TCMDC-131555	-6.5982361	TCMDC-133728	-6.277504		
TCMDC-124167	-6.5982189	TCMDC-141667	-6.2766223		
TCMDC-137692	-6.5980129	TCMDC-142096	-6.2762694		
TCMDC-124842	-6.5967703	TCMDC-135653	-6.276238		
TCMDC-134644	-6.5967283	TCMDC-137556	-6.2759528		
TCMDC-133659	-6.5963521	TCMDC-140163	-6.2756944		
TCMDC-139382	-6.5962987	TCMDC-125144	-6.2756777		
TCMDC-133665	-6.5956936	TCMDC-131639	-6.275568		
TCMDC-141960	-6.5956483	TCMDC-131646	-6.2753005		
TCMDC-138000	-6.5956316	TCMDC-124438	-6.2752771		
TCMDC-124252	-6.5956159	TCMDC-142193	-6.2751088		

TCMDC-138763	-6.5953307	TCMDC-124884	-6.2736545		
TCMDC-125711	-6.5949636	TCMDC-124419	-6.2733712		
TCMDC-132744	-6.5947504	TCMDC-131460	-6.2707214		
TCMDC-142277	-6.5942941	TCMDC-138046	-6.2704039		
TCMDC-140100	-6.5942388	TCMDC-131623	-6.2695575		
TCMDC-124117	-6.593935	TCMDC-135234	-6.2693963		
TCMDC-123477	-6.5939293	TCMDC-124848	-6.2693524		
TCMDC-139749	-6.5939112	TCMDC-124321	-6.2692871		
TCMDC-136461	-6.5938954	TCMDC-137159	-6.2690759		
TCMDC-131998	-6.5937047	TCMDC-137967	-6.2682419		
TCMDC-136561	-6.5933867	TCMDC-140012	-6.2680936		
TCMDC-139424	-6.5926232	TCMDC-139072	-6.2677469		
TCMDC-123657	-6.5915713	TCMDC-125010	-6.2665296		
TCMDC-123743	-6.591238	TCMDC-131504	-6.2664165		
TCMDC-141995	-6.5910902	TCMDC-138928	-6.2661653		
TCMDC-123737	-6.5910306	TCMDC-133438	-6.2652311		
TCMDC-125138	-6.5908494	TCMDC-125069	-6.2648511		
TCMDC-133471	-6.5908451	TCMDC-123527	-6.2643671		
TCMDC-124362	-6.5907941	TCMDC-139377	-6.2641678		
TCMDC-124061	-6.5902429	TCMDC-132206	-6.2641644		
TCMDC-124044	-6.5902276	TCMDC-139051	-6.2640562		
TCMDC-135585	-6.5899448	TCMDC-124792	-6.2636852		
TCMDC-125357	-6.5898194	TCMDC-125420	-6.2632589		
TCMDC-131726	-6.5896692	TCMDC-141380	-6.2625594		
TCMDC-133915	-6.5894752	TCMDC-137211	-6.2621698		
TCMDC-132643	-6.5893416	TCMDC-142216	-6.2620912		
TCMDC-137770	-6.5892124	TCMDC-134996	-6.2601819		
TCMDC-135117	-6.5890889	TCMDC-125309	-6.2601352		
TCMDC-138334	-6.5890398	TCMDC-124693	-6.260087		
TCMDC-136240	-6.5888438	TCMDC-124805	-6.2597103		
TCMDC-136793	-6.5886288	TCMDC-139297	-6.2591648		
TCMDC-133997	-6.5882263	TCMDC-138791	-6.2590599		
TCMDC-135255	-6.5881963	TCMDC-125134	-6.2583051		
TCMDC-138481	-6.5880055	TCMDC-142241	-6.2576718		
TCMDC-124059	-6.5879154	TCMDC-132895	-6.2568021		
TCMDC-131252	-6.587502	TCMDC-138977	-6.256042		
TCMDC-139421	-6.5870795	TCMDC-132123	-6.2556314		
TCMDC-132879	-6.5870471	TCMDC-136185	-6.2555537		
TCMDC-134473	-6.5870385	TCMDC-123722	-6.2552433		
TCMDC-133462	-6.5868168	TCMDC-124517	-6.2551384		
TCMDC-131626	-6.5866761	TCMDC-134645	-6.2539105		
TCMDC-124516	-6.586585	TCMDC-123871	-6.2538419		
TCMDC-135973	-6.5864377	TCMDC-135642	-6.2537055		
TCMDC-123980	-6.5864325	TCMDC-123792	-6.2535949		

TCMDC-125556	-6.5863991	TCMDC-123840	-6.2527981		
TCMDC-137913	-6.586338	TCMDC-136566	-6.2527709		
TCMDC-136456	-6.5862479	TCMDC-125825	-6.2523088		
TCMDC-132834	-6.5860367	TCMDC-134606	-6.2522473		
TCMDC-124576	-6.5857954	TCMDC-139065	-6.2520442		
TCMDC-124014	-6.5854445	TCMDC-139732	-6.2520108		
TCMDC-132235	-6.585393	TCMDC-134009	-6.2515812		
TCMDC-139393	-6.5848274	TCMDC-131652	-6.2504668		
TCMDC-123683	-6.5844126	TCMDC-131844	-6.2501068		
TCMDC-141269	-6.5839362	TCMDC-125518	-6.2496648		
TCMDC-139778	-6.5836558	TCMDC-137688	-6.248579		
TCMDC-125457	-6.5830431	TCMDC-138266	-6.2484818		
TCMDC-131750	-6.5825353	TCMDC-124893	-6.2475052		
TCMDC-140104	-6.582027	TCMDC-131684	-6.247263		
TCMDC-142328	-6.5819178	TCMDC-142184	-6.2471514		
TCMDC-123667	-6.5816827	TCMDC-125743	-6.247077		
TCMDC-139480	-6.5816083	TCMDC-123499	-6.2470064		
TCMDC-137440	-6.5813422	TCMDC-125807	-6.2466855		
TCMDC-124992	-6.5810628	TCMDC-137747	-6.2465849		
TCMDC-124734	-6.5808182	TCMDC-124754	-6.2464323		
TCMDC-137476	-6.5806394	TCMDC-123530	-6.2462254		
TCMDC-125601	-6.5802116	TCMDC-139723	-6.2461295		
TCMDC-133725	-6.5797801	TCMDC-135253	-6.2460542		
TCMDC-124461	-6.5796237	TCMDC-131514	-6.24473		
TCMDC-123834	-6.5794935	TCMDC-124812	-6.2446418		
TCMDC-132069	-6.5786214	TCMDC-134013	-6.2444115		
TCMDC-142049	-6.578578	TCMDC-135688	-6.244267		
TCMDC-134194	-6.5784826	TCMDC-142323	-6.2439685		
TCMDC-124563	-6.5780325	TCMDC-135853	-6.2438107		
TCMDC-125466	-6.5778246	TCMDC-123864	-6.2433877		
TCMDC-137573	-6.5777879	TCMDC-140395	-6.2430663		
TCMDC-123823	-6.5777445	TCMDC-131628	-6.2428985		
TCMDC-137266	-6.5774374	TCMDC-137921	-6.2421627		
TCMDC-136592	-6.5772204	TCMDC-138684	-6.2417336		
TCMDC-139011	-6.5768323	TCMDC-142091	-6.2413249		
TCMDC-124401	-6.5762625	TCMDC-131739	-6.2406125		
TCMDC-123750	-6.5760102	TCMDC-141212	-6.2392588		
TCMDC-133353	-6.5757985	TCMDC-125356	-6.2387695		
TCMDC-132037	-6.5757346	TCMDC-142286	-6.2376556		
TCMDC-134180	-6.575449	TCMDC-134594	-6.23738		
TCMDC-123994	-6.575387	TCMDC-138565	-6.2371578		
TCMDC-139967	-6.5746026	TCMDC-125664	-6.2355261		
TCMDC-133996	-6.5745649	TCMDC-131727	-6.2348266		
TCMDC-134541	-6.5743804	TCMDC-123586	-6.2347918		

TCMDC-137938	-6.5743389	TCMDC-123851	-6.2344975		
TCMDC-137875	-6.5743051	TCMDC-141131	-6.2342558		
TCMDC-123799	-6.5742497	TCMDC-124917	-6.2329645		
TCMDC-131336	-6.5740867	TCMDC-131882	-6.2328696		
TCMDC-141374	-6.5732574	TCMDC-125415	-6.232666		
TCMDC-125286	-6.5727129	TCMDC-141379	-6.2319312		
TCMDC-125114	-6.5722847	TCMDC-140304	-6.2317953		
TCMDC-135256	-6.5719824	TCMDC-125258	-6.231462		
TCMDC-141366	-6.5719166	TCMDC-134635	-6.2291346		
TCMDC-132577	-6.571353	TCMDC-131970	-6.2281933		
TCMDC-142222	-6.5710654	TCMDC-124357	-6.2280421		
TCMDC-136847	-6.5710511	TCMDC-131793	-6.2275791		
TCMDC-136598	-6.5709939	TCMDC-131440	-6.227447		
TCMDC-131338	-6.5709934	TCMDC-134544	-6.2267227		
TCMDC-131513	-6.5705881	TCMDC-124240	-6.2266068		
TCMDC-125580	-6.569674	TCMDC-131441	-6.2264223		
TCMDC-123902	-6.5695868	TCMDC-139802	-6.225976		
TCMDC-141200	-6.5695076	TCMDC-124090	-6.2259202		
TCMDC-136768	-6.5683117	TCMDC-136672	-6.2243261		
TCMDC-140307	-6.5680923	TCMDC-123544	-6.2242799		
TCMDC-136332	-6.567975	TCMDC-142291	-6.223937		
TCMDC-132568	-6.5678797	TCMDC-139820	-6.2239261		
TCMDC-125563	-6.5674777	TCMDC-124506	-6.2227225		
TCMDC-124088	-6.5674052	TCMDC-124599	-6.2226992		
TCMDC-134260	-6.5671401	TCMDC-123556	-6.2202539		
TCMDC-136532	-6.5671124	TCMDC-131465	-6.2199311		
TCMDC-131443	-6.5664983	TCMDC-125321	-6.2187457		
TCMDC-137492	-6.566236	TCMDC-140767	-6.2184448		
TCMDC-141675	-6.5658917	TCMDC-124637	-6.2183881		
TCMDC-136321	-6.5651903	TCMDC-141348	-6.2178922		
TCMDC-124501	-6.5650311	TCMDC-138287	-6.217793		
TCMDC-134565	-6.5650196	TCMDC-131327	-6.2174358		
TCMDC-135103	-6.5647492	TCMDC-141205	-6.2171435		
TCMDC-125234	-6.5646925	TCMDC-139149	-6.216754		
TCMDC-135574	-6.5643749	TCMDC-134843	-6.2150769		
TCMDC-134601	-6.5641818	TCMDC-142053	-6.2150135		
TCMDC-139451	-6.5638142	TCMDC-141479	-6.2148156		
TCMDC-139547	-6.5636587	TCMDC-125345	-6.2147861		
TCMDC-137580	-6.5636344	TCMDC-123688	-6.2135963		
TCMDC-136082	-6.5635509	TCMDC-133727	-6.2135267		
TCMDC-131543	-6.5632935	TCMDC-123886	-6.2132049		
TCMDC-123691	-6.5632863	TCMDC-125600	-6.2131014		
TCMDC-134177	-6.5632124	TCMDC-125653	-6.2128401		
TCMDC-133578	-6.5620275	TCMDC-125586	-6.2122593		

TCMDC-135656	-6.5617862	TCMDC-137295	-6.2118101		
TCMDC-133872	-6.5616159	TCMDC-136504	-6.2114463		
TCMDC-134533	-6.5614371	TCMDC-133432	-6.2107897		
TCMDC-141572	-6.561286	TCMDC-134578	-6.2107477		
TCMDC-136288	-6.5611544	TCMDC-123726	-6.2104297		
TCMDC-135873	-6.5607209	TCMDC-124829	-6.2103772		
TCMDC-139057	-6.5603952	TCMDC-131367	-6.2100463		
TCMDC-133124	-6.5603814	TCMDC-125501	-6.2094283		
TCMDC-131731	-6.5601659	TCMDC-139148	-6.2068048		
TCMDC-136596	-6.5600581	TCMDC-142298	-6.2059979		
TCMDC-135094	-6.5596962	TCMDC-131831	-6.2054844		
TCMDC-142186	-6.5596004	TCMDC-139315	-6.2054229		
TCMDC-132701	-6.5595646	TCMDC-133733	-6.2053232		
TCMDC-138001	-6.5591607	TCMDC-124998	-6.2052007		
TCMDC-125268	-6.5586057	TCMDC-125735	-6.2037435		
TCMDC-131473	-6.5585971	TCMDC-123535	-6.2031817		
TCMDC-134036	-6.5585518	TCMDC-124794	-6.2031093		
TCMDC-125364	-6.5578194	TCMDC-141325	-6.2023573		
TCMDC-131391	-6.557693	TCMDC-131722	-6.2022691		
TCMDC-136182	-6.5573606	TCMDC-125104	-6.2017331		
TCMDC-136019	-6.5571108	TCMDC-134570	-6.2016993		
TCMDC-123955	-6.556251	TCMDC-138717	-6.2014341		
TCMDC-140674	-6.5561795	TCMDC-134633	-6.2011099		
TCMDC-133902	-6.5561047	TCMDC-138096	-6.2007332		
TCMDC-133526	-6.5560837	TCMDC-123637	-6.2003202		
TCMDC-124928	-6.5560532	TCMDC-139727	-6.1996527		
TCMDC-131728	-6.5560298	TCMDC-132415	-6.1993332		
TCMDC-136957	-6.5558257	TCMDC-135297	-6.1986737		
TCMDC-137363	-6.5553756	TCMDC-125344	-6.1979194		
TCMDC-139313	-6.5552263	TCMDC-138956	-6.1976309		
TCMDC-136786	-6.5550861	TCMDC-139981	-6.1974831		
TCMDC-125186	-6.5541248	TCMDC-137640	-6.1969891		
TCMDC-135520	-6.5536985	TCMDC-125517	-6.1969795		
TCMDC-140434	-6.5534449	TCMDC-138498	-6.1966419		
TCMDC-124833	-6.553237	TCMDC-132040	-6.1966333		
TCMDC-134032	-6.553185	TCMDC-137993	-6.1958265		
TCMDC-141651	-6.5529108	TCMDC-141231	-6.1956458		
TCMDC-125416	-6.5525184	TCMDC-135516	-6.1950054		
TCMDC-131358	-6.5525017	TCMDC-123987	-6.1947169		
TCMDC-124878	-6.552094	TCMDC-142138	-6.1943111		
TCMDC-140414	-6.5520616	TCMDC-134199	-6.1941171		
TCMDC-133574	-6.5520358	TCMDC-139459	-6.1938848		
TCMDC-133824	-6.5514622	TCMDC-131509	-6.193294		
TCMDC-125812	-6.5512037	TCMDC-124845	-6.192627		

TCMDC-139365	-6.5509763	TCMDC-141236	-6.1918807		
TCMDC-136575	-6.550561	TCMDC-137422	-6.1917996		
TCMDC-125383	-6.5503674	TCMDC-135244	-6.1915154		
TCMDC-140796	-6.549757	TCMDC-124672	-6.1913195		
TCMDC-141232	-6.5495906	TCMDC-142145	-6.1911449		
TCMDC-124703	-6.5491815	TCMDC-135220	-6.1909585		
TCMDC-123555	-6.548367	TCMDC-139336	-6.1899281		
TCMDC-142204	-6.5482459	TCMDC-131797	-6.1897373		
TCMDC-123601	-6.5481405	TCMDC-142326	-6.1895676		
TCMDC-131730	-6.5478163	TCMDC-131658	-6.1889224		
TCMDC-132804	-6.5477142	TCMDC-142146	-6.1887889		
TCMDC-125091	-6.5456843	TCMDC-142088	-6.188664		
TCMDC-139061	-6.54456	TCMDC-139826	-6.1883388		
TCMDC-124310	-6.5445147	TCMDC-135457	-6.1881213		
TCMDC-124038	-6.5442681	TCMDC-135292	-6.1873631		
TCMDC-131881	-6.5438414	TCMDC-134537	-6.1873055		
TCMDC-137214	-6.5438304	TCMDC-138296	-6.1868706		
TCMDC-125362	-6.5433903	TCMDC-141210	-6.1867595		
TCMDC-131469	-6.5433841	TCMDC-125360	-6.1864958		
TCMDC-132838	-6.5432119	TCMDC-135816	-6.1860857		
TCMDC-136014	-6.5424838	TCMDC-142187	-6.1853456		
TCMDC-124798	-6.5422907	TCMDC-134170	-6.1851916		
TCMDC-132632	-6.5420437	TCMDC-125595	-6.1851845		
TCMDC-123813	-6.541924	TCMDC-131355	-6.1850142		
TCMDC-125187	-6.5419183	TCMDC-137917	-6.1848507		
TCMDC-138018	-6.5414658	TCMDC-139534	-6.1843452		
TCMDC-131666	-6.5412955	TCMDC-142080	-6.1838746		
TCMDC-123536	-6.5412579	TCMDC-138821	-6.183754		
TCMDC-137388	-6.5411992	TCMDC-140924	-6.1834292		
TCMDC-139551	-6.5397425	TCMDC-125312	-6.1834121		
TCMDC-125037	-6.5396948	TCMDC-135178	-6.1822472		
TCMDC-141345	-6.5396461	TCMDC-137414	-6.1816301		
TCMDC-124732	-6.5395837	TCMDC-141204	-6.1814284		
TCMDC-141323	-6.5394735	TCMDC-142197	-6.1813903		
TCMDC-142287	-6.5393267	TCMDC-135517	-6.1812282		
TCMDC-125762	-6.5389624	TCMDC-137725	-6.1809821		
TCMDC-124943	-6.5388489	TCMDC-124054	-6.1807323		
TCMDC-140226	-6.5386829	TCMDC-138957	-6.1806579		
TCMDC-138247	-6.5385456	TCMDC-125623	-6.1804204		
TCMDC-139407	-6.5385427	TCMDC-137977	-6.179369		
TCMDC-134167	-6.5374579	TCMDC-135305	-6.1790347		
TCMDC-137881	-6.5370331	TCMDC-137850	-6.1789293		
TCMDC-123560	-6.5367098	TCMDC-141982	-6.1787424		
TCMDC-136870	-6.5365562	TCMDC-124006	-6.1786819		

TCMDC-131621	-6.5364389	TCMDC-138291	-6.1784277		
TCMDC-138203	-6.5364075	TCMDC-124303	-6.1766868		
TCMDC-133814	-6.5361786	TCMDC-123616	-6.1766019		
TCMDC-124164	-6.5360489	TCMDC-131461	-6.1754017		
TCMDC-138946	-6.5357327	TCMDC-137894	-6.1747866		
TCMDC-123730	-6.5354495	TCMDC-142215	-6.1742611		
TCMDC-124255	-6.5353665	TCMDC-131497	-6.1739178		
TCMDC-138942	-6.5352688	TCMDC-124137	-6.1722775		
TCMDC-134003	-6.5352468	TCMDC-131591	-6.1717401		
TCMDC-124790	-6.5348477	TCMDC-139335	-6.1711602		
TCMDC-133427	-6.534555	TCMDC-138176	-6.1704607		
TCMDC-134718	-6.534379	TCMDC-138502	-6.1700125		
TCMDC-141653	-6.1690302	TCMDC-141653	-6.1690302		
TCMDC-142228	-6.1689725	TCMDC-142228	-6.1689725		
TCMDC-125113	-6.1687932	TCMDC-125113	-6.1687932		
TCMDC-137170	-6.1684752	TCMDC-137170	-6.1684752		
TCMDC-124752	-6.1680999	TCMDC-124752	-6.1680999		
TCMDC-131774	-6.16715	TCMDC-131774	-6.16715		
TCMDC-131240	-6.1666222	TCMDC-131240	-6.1666222		
TCMDC-131445	-6.1658416	TCMDC-131445	-6.1658416		
TCMDC-131331	-6.1655078	TCMDC-131331	-6.1655078		
TCMDC-125028	-6.1654525	TCMDC-125028	-6.1654525		
TCMDC-136505	-6.1653285	TCMDC-136505	-6.1653285		
TCMDC-124823	-6.1638641	TCMDC-124823	-6.1638641		
TCMDC-138180	-6.1631722	TCMDC-138180	-6.1631722		
TCMDC-139267	-6.163094	TCMDC-139267	-6.163094		
TCMDC-124904	-6.1628547	TCMDC-124904	-6.1628547		
TCMDC-139378	-6.1627617	TCMDC-139378	-6.1627617		
TCMDC-134186	-6.162077	TCMDC-134186	-6.162077		
TCMDC-138078	-6.161942	TCMDC-138078	-6.161942		
TCMDC-125458	-6.1617665	TCMDC-125458	-6.1617665		
TCMDC-125080	-6.1617417	TCMDC-125080	-6.1617417		
TCMDC-125627	-6.1595521	TCMDC-125627	-6.1595521		
TCMDC-124683	-6.1593599	TCMDC-124683	-6.1593599		
TCMDC-131702	-6.1591048	TCMDC-131702	-6.1591048		
TCMDC-125606	-6.1590199	TCMDC-125606	-6.1590199		
TCMDC-125376	-6.1589856	TCMDC-125376	-6.1589856		
TCMDC-131909	-6.1589637	TCMDC-131909	-6.1589637		
TCMDC-141979	-6.1583781	TCMDC-141979	-6.1583781		
TCMDC-137334	-6.158287	TCMDC-137334	-6.158287		
TCMDC-139298	-6.1578884	TCMDC-139298	-6.1578884		
TCMDC-135602	-6.1574516	TCMDC-135602	-6.1574516		
TCMDC-136493	-6.1571193	TCMDC-136493	-6.1571193		
TCMDC-137003	-6.1567655	TCMDC-137003	-6.1567655		

TCMDC-138248	-6.1559372	TCMDC-138248	-6.1559372		
TCMDC-139845	-6.155426	TCMDC-139845	-6.155426		
TCMDC-131839	-6.1548829	TCMDC-131839	-6.1548829		
TCMDC-123634	-6.1546583	TCMDC-123634	-6.1546583		
TCMDC-123581	-6.1539097	TCMDC-123581	-6.1539097		
TCMDC-138969	-6.1536536	TCMDC-138969	-6.1536536		
TCMDC-132306	-6.152885	TCMDC-132306	-6.152885		
TCMDC-131446	-6.1524663	TCMDC-131446	-6.1524663		
TCMDC-125831	-6.152288	TCMDC-125831	-6.152288		
TCMDC-133420	-6.1517239	TCMDC-133420	-6.1517239		
TCMDC-138196	-6.1513853	TCMDC-138196	-6.1513853		
TCMDC-138550	-6.1509843	TCMDC-138550	-6.1509843		
TCMDC-124560	-6.15061	TCMDC-124560	-6.15061		
TCMDC-137634	-6.1503491	TCMDC-137634	-6.1503491		
TCMDC-131622	-6.1502986	TCMDC-131622	-6.1502986		
TCMDC-135463	-6.1490006	TCMDC-135463	-6.1490006		
TCMDC-135202	-6.148983	TCMDC-135202	-6.148983		
TCMDC-134693	-6.1475835	TCMDC-134693	-6.1475835		
TCMDC-123764	-6.1474895	TCMDC-123764	-6.1474895		
TCMDC-137392	-6.1466994	TCMDC-137392	-6.1466994		
TCMDC-137664	-6.1466246	TCMDC-137664	-6.1466246		
TCMDC-137220	-6.1465039	TCMDC-137220	-6.1465039		
TCMDC-131310	-6.14535	TCMDC-131310	-6.14535		
TCMDC-131720	-6.1453261	TCMDC-131720	-6.1453261		
TCMDC-131247	-6.1442571	TCMDC-131247	-6.1442571		
TCMDC-135546	-6.1440454	TCMDC-135546	-6.1440454		
TCMDC-125454	-6.1439295	TCMDC-125454	-6.1439295		
TCMDC-123808	-6.1439285	TCMDC-123808	-6.1439285		
TCMDC-141118	-6.1436391	TCMDC-141118	-6.1436391		
TCMDC-142069	-6.1435394	TCMDC-142069	-6.1435394		
TCMDC-125232	-6.1434889	TCMDC-125232	-6.1434889		
TCMDC-138966	-6.1426077	TCMDC-138966	-6.1426077		
TCMDC-131934	-6.1420431	TCMDC-131934	-6.1420431		
TCMDC-124055	-6.1413198	TCMDC-124055	-6.1413198		
TCMDC-131587	-6.1400962	TCMDC-131587	-6.1400962		
TCMDC-136798	-6.1395049	TCMDC-136798	-6.1395049		
TCMDC-131762	-6.1394515	TCMDC-131762	-6.1394515		
TCMDC-123751	-6.1394086	TCMDC-123751	-6.1394086		
TCMDC-133350	-6.1390071	TCMDC-133350	-6.1390071		
TCMDC-137676	-6.1389852	TCMDC-137676	-6.1389852		
TCMDC-125786	-6.1387372	TCMDC-125786	-6.1387372		
TCMDC-123521	-6.1386957	TCMDC-123521	-6.1386957		
TCMDC-131609	-6.1385498	TCMDC-131609	-6.1385498		
TCMDC-124796	-6.1384587	TCMDC-124796	-6.1384587		

TCMDC-133508	-6.1382828	TCMDC-133508	-6.1382828		
TCMDC-137358	-6.1377478	TCMDC-137358	-6.1377478		
TCMDC-142142	-6.1374416	TCMDC-142142	-6.1374416		
TCMDC-137891	-6.1373367	TCMDC-137891	-6.1373367		
TCMDC-125841	-6.137135	TCMDC-125841	-6.137135		
TCMDC-142043	-6.1366677	TCMDC-142043	-6.1366677		
TCMDC-123916	-6.1363497	TCMDC-123916	-6.1363497		
TCMDC-137391	-6.1359844	TCMDC-137391	-6.1359844		
TCMDC-125596	-6.1353602	TCMDC-125596	-6.1353602		
TCMDC-131589	-6.1332541	TCMDC-131589	-6.1332541		
TCMDC-131364	-6.1330218	TCMDC-131364	-6.1330218		
TCMDC-123550	-6.1329093	TCMDC-123550	-6.1329093		
TCMDC-142157	-6.1312275	TCMDC-142157	-6.1312275		
TCMDC-142072	-6.1300921	TCMDC-142072	-6.1300921		
TCMDC-137229	-6.1297898	TCMDC-137229	-6.1297898		
TCMDC-138034	-6.1295686	TCMDC-138034	-6.1295686		
TCMDC-123862	-6.1292429	TCMDC-123862	-6.1292429		
TCMDC-137434	-6.1291871	TCMDC-137434	-6.1291871		
TCMDC-137625	-6.1285057	TCMDC-137625	-6.1285057		
TCMDC-131352	-6.1284781	TCMDC-131352	-6.1284781		
TCMDC-137405	-6.1282387	TCMDC-137405	-6.1282387		
TCMDC-125385	-6.1277423	TCMDC-125385	-6.1277423		
TCMDC-131541	-6.127461	TCMDC-131541	-6.127461		
TCMDC-133731	-6.127429	TCMDC-133731	-6.127429		
TCMDC-142087	-6.1269822	TCMDC-142087	-6.1269822		
TCMDC-131319	-6.1260147	TCMDC-131319	-6.1260147		
TCMDC-136813	-6.1245952	TCMDC-136813	-6.1245952		
TCMDC-131344	-6.1236348	TCMDC-131344	-6.1236348		
TCMDC-142035	-6.1235013	TCMDC-142035	-6.1235013		
TCMDC-131679	-6.123035	TCMDC-131679	-6.123035		
TCMDC-124100	-6.1223803	TCMDC-124100	-6.1223803		
TCMDC-125748	-6.1218228	TCMDC-125748	-6.1218228		
TCMDC-131437	-6.1216097	TCMDC-131437	-6.1216097		
TCMDC-131723	-6.1213012	TCMDC-131723	-6.1213012		
TCMDC-135879	-6.1211014	TCMDC-135879	-6.1211014		
TCMDC-132089	-6.1205363	TCMDC-132089	-6.1205363		
TCMDC-136134	-6.1204767	TCMDC-136134	-6.1204767		
TCMDC-138953	-6.120306	TCMDC-138953	-6.120306		
TCMDC-135860	-6.1202106	TCMDC-135860	-6.1202106		
TCMDC-131721	-6.1201696	TCMDC-131721	-6.1201696		
TCMDC-124145	-6.119472	TCMDC-124145	-6.119472		
TCMDC-131498	-6.1192131	TCMDC-131498	-6.1192131		
TCMDC-142327	-6.1189733	TCMDC-142327	-6.1189733		
TCMDC-124534	-6.118628	TCMDC-124534	-6.118628		

TCMDC-124456	-6.1179543	TCMDC-124456	-6.1179543		
TCMDC-131288	-6.1173224	TCMDC-131288	-6.1173224		
TCMDC-135808	-6.1167932	TCMDC-135808	-6.1167932		
TCMDC-139354	-6.1166391	TCMDC-139354	-6.1166391		
TCMDC-124196	-6.1162224	TCMDC-124196	-6.1162224		
TCMDC-134535	-6.1160583	TCMDC-134535	-6.1160583		
TCMDC-137989	-6.1160097	TCMDC-137989	-6.1160097		
TCMDC-141660	-6.1141777	TCMDC-141660	-6.1141777		
TCMDC-123827	-6.113678	TCMDC-123827	-6.113678		
TCMDC-124918	-6.1135707	TCMDC-124918	-6.1135707		
TCMDC-139100	-6.1130295	TCMDC-139100	-6.1130295		
TCMDC-123844	-6.1127071	TCMDC-123844	-6.1127071		
TCMDC-124788	-6.1125469	TCMDC-124788	-6.1125469		
TCMDC-141344	-6.112288	TCMDC-141344	-6.112288		
TCMDC-135368	-6.1116743	TCMDC-135368	-6.1116743		
TCMDC-134609	-6.1112094	TCMDC-134609	-6.1112094		
TCMDC-137649	-6.1111465	TCMDC-137649	-6.1111465		
TCMDC-140369	-6.1111116	TCMDC-140369	-6.1111116		
TCMDC-137812	-6.110785	TCMDC-137812	-6.110785		
TCMDC-123772	-6.1106634	TCMDC-123772	-6.1106634		
TCMDC-125472	-6.1092987	TCMDC-125472	-6.1092987		
TCMDC-138971	-6.1089253	TCMDC-138971	-6.1089253		
TCMDC-138955	-6.1083989	TCMDC-138955	-6.1083989		
TCMDC-142004	-6.1083694	TCMDC-142004	-6.1083694		
TCMDC-125512	-6.1074843	TCMDC-125512	-6.1074843		
TCMDC-124478	-6.1073136	TCMDC-124478	-6.1073136		
TCMDC-142220	-6.1073012	TCMDC-142220	-6.1073012		
TCMDC-138783	-6.1069355	TCMDC-138783	-6.1069355		
TCMDC-125188	-6.1067777	TCMDC-125188	-6.1067777		
TCMDC-125473	-6.1063995	TCMDC-125473	-6.1063995		
TCMDC-138045	-6.1063967	TCMDC-138045	-6.1063967		
TCMDC-124600	-6.1062746	TCMDC-124600	-6.1062746		
TCMDC-135678	-6.1060767	TCMDC-135678	-6.1060767		
TCMDC-136161	-6.1055069	TCMDC-136161	-6.1055069		
TCMDC-131704	-6.105371	TCMDC-131704	-6.105371		
TCMDC-125270	-6.1046906	TCMDC-125270	-6.1046906		
TCMDC-125474	-6.1045847	TCMDC-125474	-6.1045847		
TCMDC-131650	-6.1040807	TCMDC-131650	-6.1040807		
TCMDC-142108	-6.1037021	TCMDC-142108	-6.1037021		
TCMDC-134395	-6.1033211	TCMDC-134395	-6.1033211		
TCMDC-124561	-6.1028628	TCMDC-124561	-6.1028628		
TCMDC-142309	-6.1022625	TCMDC-142309	-6.1022625		
TCMDC-131615	-6.1021252	TCMDC-131615	-6.1021252		
TCMDC-123566	-6.1018968	TCMDC-123566	-6.1018968		

TCMDC-139394	-6.1016502	TCMDC-139394	-6.1016502		
TCMDC-123758	-6.10147	TCMDC-123758	-6.10147		
TCMDC-138516	-6.1006327	TCMDC-138516	-6.1006327		
TCMDC-125002	-6.1002822	TCMDC-125002	-6.1002822		

Appendix 2-ADME Analysis of Top Binding Compounds

ChEMBL_NTD_ID	logP	MW	HBD	Rotatable Bonds	HBA	TPSA
TCMDC-131406	1.529	239.2	2	7	6	84.86
SJ000111238	0.8721	163.2	2	3	5	87.48
TCMDC-141973	1.485	231.3	1	5	4	62.76
TCMDC-123981	1.399	209.2	2	4	7	107.5
TCMDC-131967	0.7346	167.1	1	2	6	91.3
TCMDC-123468	0.5473	150.1	2	2	5	81.83
TCMDC-131398	1.756	217.2	1	2	5	83.46
TCMDC-131398	1.756	217.2	1	2	5	83.46
TCMDC-131601	0.9787	176.2	3	2	5	83.8
TCMDC-131644	0.6055	180.2	2	4	5	85.33
TCMDC-124295	2.39	247.1	4	4	5	91
TCMDC-125535	0.9339	205.2	2	4	5	67.01
TCMDC-137470	1.658	226.7	3	3	5	93.5
TCMDC-137879	1.153	239.3	3	4	5	68.09
TCMDC-131778	1.206	275.3	1	6	6	85.61
TCMDC-131646	1.234	272.3	2	7	5	67.43
TCMDC-125514	1.718	279.3	1	5	5	74.68
TCMDC-137472	1.166	239.7	4	5	6	103.4
TCMDC-137907	1.493	266.4	2	8	5	58.54
TCMDC-137562	1.127	284.1	4	5	6	103.4
TCMDC-131647	1.148	254.7	2	7	4	58.2
TCMDC-131370	1.561	258.3	0	7	6	78.38
TCMDC-124231	1.716	265.4	0	3	5	52.98
TCMDC-139220	1.203	240.3	1	3	4	71.44
TCMDC-124231	1.716	265.4	0	3	5	52.98

TCMDC-137466	1.787	274.1	4	5	6	103.4
SJ000291458	1.543	231.3	2	2	6	99.41
TCMDC-123475	1.091	208.3	2	4	4	49.31
TCMDC-131748	0.7613	182.2	2	2	4	49.31
TCMDC-137662	1.731	236.3	3	2	4	74.26
TCMDC-125851	0.7672	195.2	2	4	4	58.56
TCMDC-125862	1.676	239.7	1	2	4	57.61
TCMDC-123844	1.322	275.3	2	8	5	61.44
SJ000148003	1.602	231.3	2	2	6	99.41
TCMDC-124155	1.858	180.1	1	2	3	50.44
TCMDC-124155	1.858	180.1	1	2	3	50.44
TCMDC-137564	1.585	288.1	3	4	6	105.9
TCMDC-131556	1.521	303.4	2	5	6	85.59
TCMDC-131332	1.239	209.1	1	1	5	83.12
TCMDC-124268	1.073	251.7	3	2	5	74.8
TCMDC-137360	2.105	250.3	3	3	4	74.26
TCMDC-137521	0.7655	233.3	3	5	6	105.9
TCMDC-141971	1.096	242.3	4	5	6	99.71
TCMDC-131394	1.554	172.2	2	2	4	64.5
TCMDC-131690	1.01	273.3	3	5	6	84.03
TCMDC-137510	2.448	309.5	4	4	5	91
TCMDC-123474	1.769	167.2	1	5	3	44.48
SJ000251874	1.685	276.3	2	5	6	88
TCMDC-125870	0.3888	224.2	2	4	6	91.76
TCMDC-137562	1.127	284.1	4	5	6	103.4
TCMDC-131647	1.148	254.7	2	7	4	58.2
TCMDC-131370	1.561	258.3	0	7	6	78.38
TCMDC-124231	1.716	265.4	0	3	5	52.98
TCMDC-139220	1.203	240.3	1	3	4	71.44
TCMDC-124231	1.716	265.4	0	3	5	52.98
TCMDC-137466	1.787	274.1	4	5	6	103.4
SJ000291458	1.543	231.3	2	2	6	99.41

TCMDC-123475	1.091	208.3	2	4	4	49.31
TCMDC-131748	0.7613	182.2	2	2	4	49.31
TCMDC-137662	1.731	236.3	3	2	4	74.26
TCMDC-125851	0.7672	195.2	2	4	4	58.56
TCMDC-125862	1.676	239.7	1	2	4	57.61
TCMDC-123844	1.322	275.3	2	8	5	61.44
SJ000148003	1.602	231.3	2	2	6	99.41
TCMDC-124155	1.858	180.1	1	2	3	50.44
TCMDC-124155	1.858	180.1	1	2	3	50.44
TCMDC-137564	1.585	288.1	3	4	6	105.9
TCMDC-131556	1.521	303.4	2	5	6	85.59
TCMDC-131332	1.239	209.1	1	1	5	83.12
TCMDC-124268	1.073	251.7	3	2	5	74.8
TCMDC-137360	2.105	250.3	3	3	4	74.26
TCMDC-137521	0.7655	233.3	3	5	6	105.9
TCMDC-141971	1.096	242.3	4	5	6	99.71
TCMDC-131394	1.554	172.2	2	2	4	64.5
TCMDC-131690	1.01	273.3	3	5	6	84.03
TCMDC-137510	2.448	309.5	4	4	5	91
TCMDC-123474	1.769	167.2	1	5	3	44.48
SJ000251874	1.685	276.3	2	5	6	88
TC MDC-125870	0.3888	224.2	2	4	6	91.76
TCMDC-137562	1.127	284.1	4	5	6	103.4
TCMDC-131647	1.148	254.7	2	7	4	58.2
TCMDC-131370	1.561	258.3	0	7	6	78.38
TCMDC-124231	1.716	265.4	0	3	5	52.98
TCMDC-139220	1.203	240.3	1	3	4	71.44
TCMDC-124231	1.716	265.4	0	3	5	52.98
TCMDC-137466	1.787	274.1	4	5	6	103.4
SJ000291458	1.543	231.3	2	2	6	99.41
TCMDC-123475	1.091	208.3	2	4	4	49.31
TCMDC-131748	0.7613	182.2	2	2	4	49.31

TCMDC-137662	1.731	236.3	3	2	4	74.26
TCMDC-125851	0.7672	195.2	2	4	4	58.56
TCMDC-125862	1.676	239.7	1	2	4	57.61
TCMDC-123844	1.322	275.3	2	8	5	61.44
SJ000148003	1.602	231.3	2	2	6	99.41
TCMDC-124155	1.858	180.1	1	2	3	50.44
TCMDC-124155	1.858	180.1	1	2	3	50.44
TCMDC-137564	1.585	288.1	3	4	6	105.9
TCMDC-131556	1.521	303.4	2	5	6	85.59
TCMDC-131332	1.239	209.1	1	1	5	83.12
TCMDC-124268	1.073	251.7	3	2	5	74.8
TCMDC-137360	2.105	250.3	3	3	4	74.26
TCMDC-137521	0.7655	233.3	3	5	6	105.9
TCMDC-141971	1.096	242.3	4	5	6	99.71
TCMDC-131394	1.554	172.2	2	2	4	64.5
TCMDC-131690	1.01	273.3	3	5	6	84.03
TCMDC-137510	2.448	309.5	4	4	5	91
TCMDC-123474	1.769	167.2	1	5	3	44.48
SJ000251874	1.685	276.3	2	5	6	88
TCMDC-125870	0.3888	224.2	2	4	6	91.76
TCMDC-137562	1.127	284.1	4	5	6	103.4
TCMDC-131647	1.148	254.7	2	7	4	58.2
TCMDC-131370	1.561	258.3	0	7	6	78.38
TCMDC-124231	1.716	265.4	0	3	5	52.98
TCMDC-139220	1.203	240.3	1	3	4	71.44
TCMDC-124231	1.716	265.4	0	3	5	52.98
TCMDC-137466	1.787	274.1	4	5	6	103.4
SJ000291458	1.543	231.3	2	2	6	99.41
TCMDC-123475	1.091	208.3	2	4	4	49.31
TCMDC-131748	0.7613	182.2	2	2	4	49.31
TCMDC-137662	1.731	236.3	3	2	4	74.26
TCMDC-125851	0.7672	195.2	2	4	4	58.56

TCMDC-125862	1.676	239.7	1	2	4	57.61
TCMDC-123844	1.322	275.3	2	8	5	61.44
SJ000148003	1.602	231.3	2	2	6	99.41
TCMDC-124155	1.858	180.1	1	2	3	50.44
TCMDC-124155	1.858	180.1	1	2	3	50.44
TCMDC-137564	1.585	288.1	3	4	6	105.9
TCMDC-131556	1.521	303.4	2	5	6	85.59
TCMDC-131332	1.239	209.1	1	1	5	83.12
TCMDC-124268	1.073	251.7	3	2	5	74.8
TCMDC-137360	2.105	250.3	3	3	4	74.26
TCMDC-137521	0.7655	233.3	3	5	6	105.9
TCMDC-141971	1.096	242.3	4	5	6	99.71
TCMDC-131394	1.554	172.2	2	2	4	64.5
TCMDC-131690	1.01	273.3	3	5	6	84.03
TCMDC-137510	2.448	309.5	4	4	5	91
TCMDC-123474	1.769	167.2	1	5	3	44.48
SJ000251874	1.685	276.3	2	5	6	88
TCMDC-125870	0.3888	224.2	2	4	6	91.76
TCMDC-137562	1.127	284.1	4	5	6	103.4
TCMDC-131647	1.148	254.7	2	7	4	58.2
TCMDC-131370	1.561	258.3	0	7	6	78.38
TCMDC-124231	1.716	265.4	0	3	5	52.98
TCMDC-139220	1.203	240.3	1	3	4	71.44
TCMDC-124231	1.716	265.4	0	3	5	52.98
TCMDC-137466	1.787	274.1	4	5	6	103.4
SJ000291458	1.543	231.3	2	2	6	99.41
TCMDC-123475	1.091	208.3	2	4	4	49.31
TCMDC-131748	0.7613	182.2	2	2	4	49.31
TCMDC-136889	1.767	249.3	2	2	3	64.93
TCMDC-124296	1.824	214.3	2	2	4	77.82
TCMDC-131744	1.909	304.3	2	6	7	105.5

TCMDC-137296	1.74	238.6	2	1	4	77.82
TCMDC-137386	1.981	284.1	3	1	5	103.8
TCMDC-124299	2.034	247.2	0	5	5	57.01
TCMDC-137376	2.05	250.7	2	2	5	87.05
TCMDC-125771	2.047	266.3	1	3	6	69.68
TCMDC-123458	1.874	277.3	5	3	5	115.5
TCMDC-137177	1.863	226.2	2	1	5	90.96
TCMDC-137561	1.951	307.7	4	6	6	103.4
TCMDC-124916	1.685	218.3	0	3	4	44.12
TCMDC-142030	1.976	278.3	1	4	5	59.4
TCMDC-133421	1.776	237.3	2	1	5	90.71
TCMDC-136517	1.938	237.3	1	2	4	61.03
TCMDC-142029	1.976	278.3	1	4	5	59.4
TCMDC-137725	2.04	310.4	1	8	4	55.56
TCMDC-142028	1.976	278.3	1	4	5	59.4
TCMDC-137923	1.95	217.3	2	2	5	90.71
TCMDC-124304	1.705	348.4	4	6	7	89.91
TCMDC-135294	1.748	306.4	2	2	6	112
TCMDC-123842	2.043	271.3	2	6	4	54.02
TCMDC-131255	1.962	234.1	2	3	2	32.26
TCMDC-142032	2.068	278.3	1	4	5	59.4
TCMDC-142033	2.068	278.3	1	4	5	59.4
TCMDC-135191	2.027	268.7	0	2	4	59.92
TCMDC-131981	1.9	198.3	0	4	3	35.53
TCMDC-137860	1.778	231.3	2	3	5	81.06
TCMDC-125874	1.894	228.3	0	1	3	34.89
TCMDC-124503	1.732	320.6	2	1	5	80
TCMDC-136756	1.877	301.3	2	2	6	106.2
TCMDC-137947	2.059	206.3	2	1	4	77.82
TCMDC-131290	1.899	327.8	2	4	5	80
TCMDC-124459	1.973	252.3	3	2	5	84.06
TCMDC-123465	1.791	344.4	0	8	6	71.06

TCMDC-124275	1.869	254.3	1	3	4	50.7
TCMDC-123985	1.887	233.3	0	2	3	38.67
TCMDC-125567	2.02	237.3	2	2	4	58.04
TCMDC-124307	2.108	308.3	3	4	6	90.9
TCMDC-124536	1.952	267.3	1	5	5	56.15
TCMDC-125870	0.3888	224.2	2	4	6	91.76